CAMBRIDGE OBSERVING HANDBOOKS FOR RESEARCH ASTRONOMERS 2

Practical Statistics for Astronomers

J. V. Wall and C. R. Jenkins

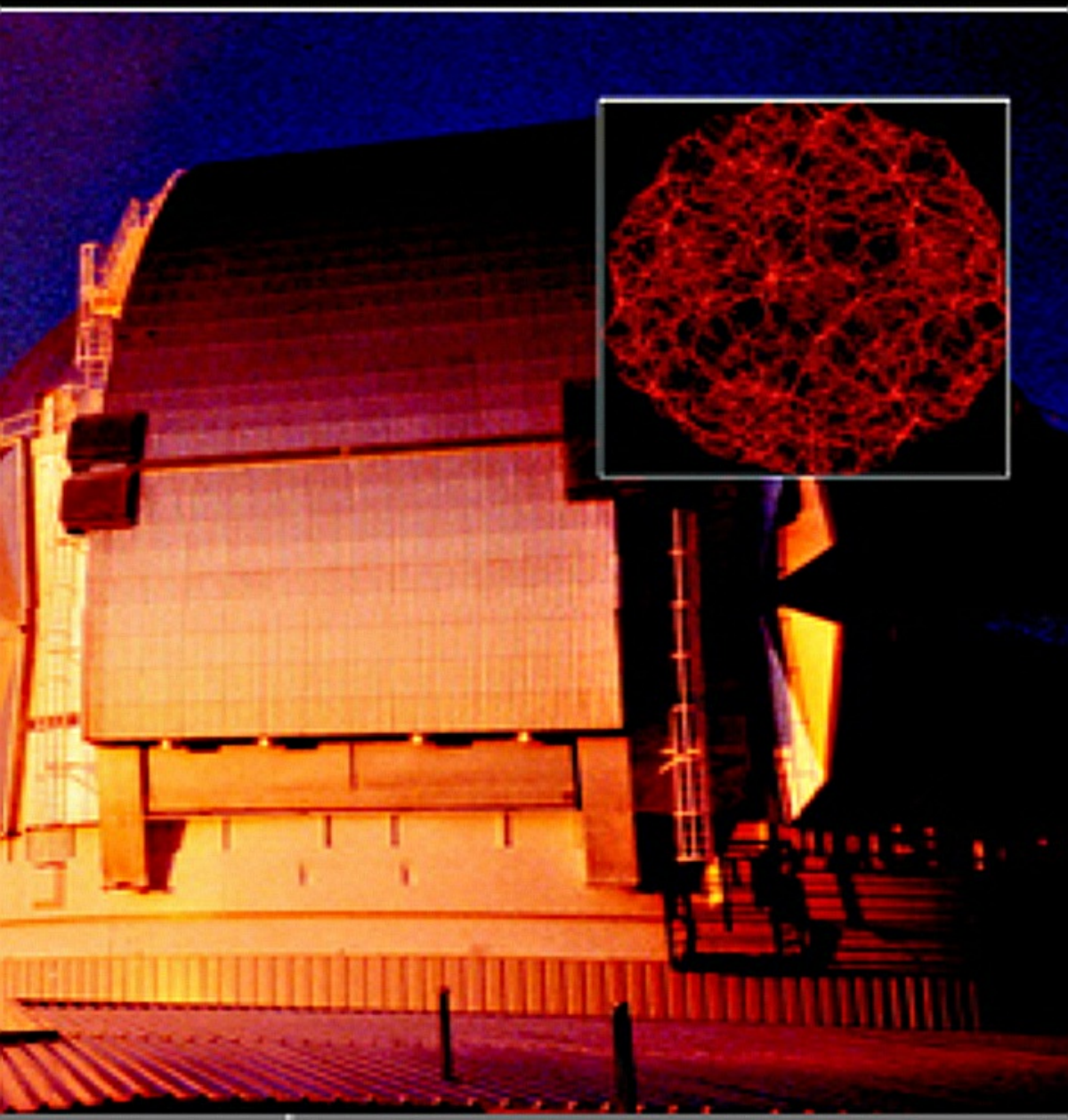

CAMBRIDGE www.cambridge.org/9780521454162

This page intentionally left blank

Practical Statistics for Astronomers

Astronomy, like any experimental subject, needs statistical methods to interpret data reliably. This practical handbook presents the most relevant statistical and probabilistic machinery for use in observational astronomy. Classical parametric and non-parametric methods are covered, but there is a strong emphasis on Bayesian solutions and the importance of probability in experimental inference. Chapters cover basic probability, correlation analysis, hypothesis testing, Bayesian modelling, time series analysis, luminosity functions and clustering. The book avoids the technical language of statistics in favour of demonstrating astronomical relevance and applicability. It contains many worked examples and problems that make use of databases which are available on the Web. It is suitable for self-study at advanced undergraduate or graduate level, as a reference for professional astronomers, and as a textbook basis for courses in statistical methods in astronomy.

JASPER WALL was, to 2003, Visiting Professor of Astrophysics and Director of Graduate Studies in the Department of Astrophysics at the University of Oxford. He obtained his Ph.D. in Astronomy at the Australian National University, Canberra, and has since been Head of Astrophysics at the Royal Greenwich Observatory, Director of the Isaac Newton Group of Telescopes, La Palma, and Director of the Royal Greenwich Observatory. Professor Wall has edited three books and published over 150 scientific articles on extragalactic radio sources, space distribution and cosmology, astronomy instrumentation, and statistics in astronomy.

CHARLES JENKINS has worked at Schlumberger's Cambridge research lab since 1997, where he is a Principal Scientist working on innovations in oilfield telemetry and robotics. He obtained his Ph.D. in the Radio Astronomy group at the Cavendish Laboratory, Cambridge, and was an Astronomer at the Royal Greenwich Observatory for 14 years. Dr Jenkins has been involved in the commissioning of the Isaac Newton and William Herschel Telescopes as Project Scientist for numerous instruments, and latterly headed the New Projects Group and was Project Scientist for the tracking systems of the Gemini 8-m telescopes. His main research interests in astronomy were galaxy dynamics and adaptive optics.

PRACTICAL STATISTICS FOR ASTRONOMERS

J. V. WALL
UNIVERSITY OF OXFORD
C. R. JENKINS
SCHLUMBERGER CAMBRIDGE RESEARCH

CAMBRIDGE
UNIVERSITY PRESS

CAMBRIDGE UNIVERSITY PRESS
Cambridge, New York, Melbourne, Madrid, Cape Town, Singapore, São Paulo

Cambridge University Press
The Edinburgh Building, Cambridge CB2 8RU, UK
Published in the United States of America by Cambridge University Press, New York
www.cambridge.org
Information on this title: www.cambridge.org/9780521454162

First published in print format 2003

ISBN-13 978-0-511-33812-0 eBook (NetLibrary)
ISBN-10 0-511-33812-0 eBook (NetLibrary)

ISBN-13 978-0-521-45416-2 hardback
ISBN-10 0-521-45416-6 hardback

ISBN-13 978-0-521-45616-6 paperback
ISBN-10 0-521-45616-9 paperback

In affectionate memory of Peter Scheuer (1930–2001)
mentor and friend
'$2 + 2 \simeq 5$'

Contents

Preface

Peter Scheuer started this. In 1977 he walked into JVW's office in the Cavendish Lab and quietly asked for advice on what further material should be taught to the new intake of Radio Astronomy graduate students (that year including the hapless CRJ). JVW, wrestling with simple chi-square testing at the time, blurted out 'They know nothing about practical statistics'. Peter left thoughtfully. A day later he returned. '**Good news!** The Management Board has decided that the students are going to have a course on practical statistics.' Can I sit in, JVW asked innocently. '**Better news!** The Management Board has decided that you're going to teach it'.

So, for us, began the notion of practical statistics. A subject that began with gambling is not an arcane academic pursuit, but it is certainly subtle as well. It is fitting that Peter Scheuer was involved at the beginning of this (lengthy) project; his style of science exemplified both subtlety and pragmatism. We hope that we can convey something of both. If an echo of Peter's booming laugh is sometimes heard in these pages, it is because we both learned from him that a useful answer is often much easier – and certainly much more entertaining – than you at first think.

After the initial course, the material for this book grew out of various further courses, journal articles, and the abundant personal experience that results from understanding just a little of any field of knowledge that counts Gauss and Laplace amongst its originators. More recently, the invigorating polemics of Jeffreys and Jaynes, authors of standard works on probability, have been a great stimulus; although we have tried in this book not to engage too much with 'old, unhappy, far-off things / and battles long ago.'

Amongst today's practioners of practical statistics, we have had valued discussions with Mark Birkinshaw, Phil Charles, Eric Feigelson, Pedro Ferreira, Paul Francis, Dave Jauncey, Ofer Lahav, Steve Gull, Tony Lynas-Gray, Donald Lynden-Bell, Robert Laing, Louis Lyons, Andrew Murray, John Peacock, Chris Pritchett, Prasenjit Saha and Adrian Webster. We are very grateful to Chris Blake, whose excellent D.Phil. thesis laid out clearly the interrelation of 2D descriptive statistics; and who has allowed us to borrow extensively from this opus. CRJ particularly acknowledges the Bayesian convictions of the Real Time Decisions group at Schlumberger; Dave Hargreaves, Iain Tuddenham and Tim Jervis. Try betting lives on your interpretation of the Kolmogorov axioms.

JVW is indebted to the Astrophysics Department of the University of Oxford for the enjoyable environment in which much of this was pulled together. The hospitality of the Department Heads – Phil Charles and then Joe Silk – is greatly appreciated; the stimulation, kindness, technical support and advice of colleagues there has been invaluable. Jenny Wall gave total support and encouragement throughout; the writing benefited greatly from the warmth and happiness of her companionship.

CRJ wishes to acknowledge the support of Schlumberger Cambridge Research for the writing of this book, as part of its 'Personal Research Time' initiative. The encouragement of the lab's director, Mike Sheppard, catalysed its completion. Program manager Ashley Johnson created the necessary space in a busy research group. Fiona Hall listened, helped with laughter and wise words through the long period of gestation, and took time out from many pressing matters to support that final burst of writing.

Notation

Here are some of the symbols used in the mathematical parts of this book. The list is not complete, but does include notation of more than localized interest. Some symbols are used with different meanings in different parts of the book, but in context there should be no possibility of confusion.

a_{lm}:	the coefficients of a spherical harmonic expansion.
C:	usually the covariance (or error) matrix, characterizing a multivariate Gaussian.
c_l:	the coefficients of the angular power spectrum.
$\mathrm{cov}[x, y]$:	the covariance of two random variables x and y.
D:	the Kolmogorov-Smirnov test statistic.
$E[X]$:	the expectation or ensemble average. Also denoted $<X>$.
f, F:	Probability density distributions and cumulative probability density distributions, respectively; in Chapter 8, Fourier pairs.
$\mathcal{F}$:	a variable distributed according to the F distribution.
H:	the Hessian matrix.
H_0, H_1:	the null hypothesis and alternative hypothesis.
$\mathcal{K}$:	the Kaplan-Meier estimator.
L:	intrinsic luminosity.
$\mathcal{L}$:	the likelihood.
$N(S)$:	the flux density distribution, or source count.
N, n:	usually the number of data.
$P(N)$:	the counts-in-cells probability of finding N objects in a cell.
P_l:	the Legendre polynomials.

prob(...):	the probability of the indicated event. In the case of a continuous variable, the probability density.
prob($A \mid B$):	the probability of A, given B.
R:	distance.
r:	the product-moment coefficient.
$\mathcal{R}$:	the Rayleigh test statistic.
S:	the mean square deviation of a set of data; in Chapter 7, flux density.
$\mathcal{S}$:	the test statistic for a particular orientation of the principal axis of the orientation matrix.
S_e:	the sample cumulative distribution, as used in the Kolmogorov–Smirnov test.
t:	a variable distributed according to the t distribution.
U:	the Wilcoxon–Mann–Whitney test statistic.
V, $V_{\max}$:	the volume contained within R; the maximum volume, corresponding to the greatest distance consistent with an object still appearing in a catalogue.
var[x]:	the variance of a random variable x.
$w(\theta)$:	the two-point angular correlation function.
$\overline{X}$:	the sample average of a set of data.
$X_1, X_2, \ldots$:	usually a specific set of data; instances of possible data, denoted x. We try to keep to this distinction by using upper case for particular values and lower case for algebraic variables (although not with Greek letters, or statistics like t where lower-case is standard).
y, z:	the excess variance and skewness of clustered counts-in-cells.
Y_{lm}:	the spherical harmonics.
$\vec{\alpha}$:	a vector, usually a vector of parameters.
Γ:	the Gehan test statistic.
η:	the luminosity distribution.
κ:	the Kendall test statistic.
μ, σ:	usually the mean and standard deviation of a Gaussian distribution; μ may also be the parameter of a Poisson distribution.
μ_n:	the nth central moment of a distribution.

ρ:	the covariance coefficient of a bivariate Gaussian; in Chapter 7, the luminosity function.
$\varsigma(\theta, \phi)$:	the surface density of objects on the sky.
$\sigma_{\rm s}$:	the sample standard deviation.
ϕ:	the space distribution.
χ^2:	a variable distributed according to the chi-square distribution.

1
Decision

> If your experiment needs statistics, you ought to have done a better experiment.
>
> *(Ernest Rutherford)*

Science is about decision. Building instruments, collecting data, reducing data, compiling catalogues, classifying, doing theory – all of these are tools, techniques or aspects which are necessary. But we are not doing science unless we are deciding something; only decision counts. Is this hypothesis or theory correct? If not, why not? Are these data self-consistent or consistent with other data? Adequate to answer the question posed? What further experiments do they suggest?

We decide by comparing. We compare by describing properties of an object or sample, because lists of numbers or images do not present us with immediate results enabling us to decide anything. Is the faint smudge on an image a star or a galaxy? We characterize its shape, crudely perhaps, by a property, say the full-width half-maximum, the FWHM, which we compare with the FWHM of the point-spread function. We have represented a dataset, the image of the object, by a statistic, and in so doing we reach a decision.

Statistics are there for decision and because we know a background against which to take a decision. To this end, every measurement we make, and every parameter or value we derive, requires an error estimate, a measure of range (expressed in terms of probability) that encompasses our belief of the true value of the parameter. We are taught this by our masters in the course of interminable undergrad lab experiments. Why? It is because no measured quantity or property is of the slightest use in

decision and therefore in science unless it has a 'range quantity' attached to it.

A *statistic* is a quantity that summarizes data; it is the ultimate data reduction. It is a property of the data and nothing else. It may be a number, a mean for example, but it doesn't have to be. It is a basis for using the data or experimental result to make a decision. We need to know how to treat data with a view to decision, to obtain the right *statistics* to use in drawing *statistical inference*. (It is the latter which is the branch of science; at times the term *statistics* is loosely used to describe both the descriptive values and the science.)

Rutherford's message appears uncompromisingly clear, but it can only hold in some specialized circumstances. For a start, astronomers are not always free to do better experiments. The laboratory is the big stage; the Universe is an experiment we cannot rerun. Attempting to understand astrophysics and cosmology from one freeze-frame in the spacetime continuum requires some reconsideration of the classical scientific method. This scientific method of *repetition* of experimentally reproduced results does not apply. We cannot reroll the dice, and anyway, repetition implies similar conditions. We are never at the same coordinates in spacetime.

There is thus need for a certain rigour in our methodology. The inability to reroll dice has led and still leads astronomers into some of the greatest errors of inference. It becomes tempting to the point of irresistibility *to use the data on which a hypothesis was proposed to verify that hypothesis*.

EXAMPLE *The Black Cloud* (Hoyle 1958). The Black Cloud appears to be heading for the Earth. The scientific team suggests that this proves the cloud has intelligence. Not so, says the dissenting team member. Why? A golf ball lands on a golf course which contains 10^7 blades of grass; it stops on one blade; the chances are 1 in 10^7 of this event occurring by chance. This is not so amazing – the ball had to land somewhere. It would only be amazing if the experiment were repeated to test the newly formulated hypothesis (e.g. the blade being of special attractive character; the golfer of unusual skill) so that the event were repeated. However, the importance of deciding if the Black Cloud knew about the Earth cannot await the next event or the sequence of events, and tempts the rush to judgement in which initial data, hypothesis and test data are combined; so in many instances in astronomy and cosmology.

A second difference for astronomers stems from the first – the remoteness of our objects and the inability to 'rerun our experiments' means that we do not necessarily know the underlying distributions of the variables measured. The essence of classical statistical analysis is (i) the formulation of a hypothesis, (ii) the gathering of hypothesis-test data via experiment, and (iii) the construction of a test statistic. But making a decision on the basis of the test statistic may demand that the sampling distribution or expectation of the statistic must be known before a decision can be made. To calculate this it is frequently essential to know the frequency distribution of the test statistic; how else could we decide if the value we got was normal or abnormal? It may well be the case that no one, physicist, sociologist, botanist, ever does know these underlying distributions exactly; but astronomers are worse off than most because of our necessarily small samples and our inability to control experiments, leading to poor definitions of the underlying distributions.

It is thus the case that astronomers cannot avoid statistics and there are the following reasons at least for this unfortunate situation.

(i) Error (range) assignment – ours, and the errors assigned by others: what do they mean?
(ii) How can data be used best? Or at all?
(iii) Correlation, hypothesis-testing, model fitting; how do we proceed?
(iv) Incomplete samples, samples from an experiment which cannot be rerun, upper limits; how can we use these to best advantage?
(v) Others describe their data and conclusions in statistical terms. We need some self-defence.
(vi) But above all, we must decide. The decision process cannot be done without some methodology, no matter how good the experiment. Rutherford may not have known when he was using statistics.

This is not a book about statistics, the values or the science. It is about how to get results in astronomy, using statistics, data analysis and statistical inference.

Consider first how we do science in order to see at what point 'statistics' enter(s) the process.

1.1 How is science done?

In simplest terms, each experiment goes round a loop which can be characterized by five stages:

(1) Observe: record the data, or obtain the data.
(2) Reduce: clean up the data to remove experimental effects, i.e. flat-field it, calibrate it.
(3) Analyse: obtain the numbers from the clean data – intensities, positions. Produce from these summary descriptors of the data which enable comparison or modelling – descriptors which lead to reaching the decision which governed the design of the experiment; and which are *statistics*.
(4) Conclude: carry through a process to reach a decision. Test the hypothesis; correlate; model, etc.
(5) Reflect: what has been learnt? Is the decision plausible? Is it unexpected? At which experimental stage must re-entry be made to check? What is required to confirm this unexpected result? Or, what was inadequate in the experimental design? How should the next version be defined? Is an extended or new hypothesis suggested? Back to point (1).

This process is a loop and 'experiments' may begin at different points. For instance, we disbelieve someone else's conclusions based on their published dataset. We enter at point (3) or even (4); and we may then go around the data-gathering cycle ourselves as a result. Or we look at an old result in the light of new and complementary ones from other fields – and enter at (5).

All too often we use (3) to set up the tests at (4). This carries the charge of mingling hypothesis and data, as in the Black Cloud example.

Table 1.1 summarizes the process. Points in Table 1.1 at which recourse to statistics or to statistical inference is important have been indicated by *Stats*; a T appears when the issue applies to theorists as well as to experimentalists. Few are the regions in which we can ignore statistics and statistical inference. *Experiment design needs to consider from the start* what statistic or summarized data form is required to achieve the desired outcome. There are then checks throughout the experiment, and finally there is analysis in which the measured statistics are used in inference.

1.2 Probability; probability distributions

The concept of *probability* is crucial in decision processes, and there is a commonly accepted relationship between probability and statistics.

Table 1.1. Stages in astronomy experimentation

Stage	How	Examples	Considerations
Observe	Carefully	Experiment design: calibration, integration time *Stats*	What is wanted? Number of objects *Stats*
Reduce	Algorithms	Flat field Flux calibration	Data integrity Signal-to-noise *T Stats*
Analyse	Parameter estimation, Hypothesis testing *T Stats*	Intensity measurements Positions *T Stats*	Frequentist, Bayesian? *T Stats*
Conclude	Hypothesis-testing *T Stats*	Correlation tests Distribution tests *T Stats*	Believable, Repeatable, Understandable? *T Stats*
Reflect	Carefully	Mission achieved? A better way? 'We need more data'? *T Stats*	The next observations *T Stats*

In a world in which our statistics are derived from finite amounts of data, we need probabilities as a basis for inference. For example, limited data yields only a partial idea of the point-spread function, such as the FWHM; we can only assign probabilities to the range of point-spread functions roughly matching this parameter.

We all have an inbuilt sense of probability. We know for example that the height of adults is anything from say 1.5 to 2.5 metres. We know this from the totality of the population, all adults. But we know what a tall person is – and it is not necessarily somebody who is 2.5 m tall. The distribution is not flat; it peaks at around 1.7 m. The distribution of the heights of all adults, normalized to have an area of 1.0, is the measured probability density function, often called the probability distribution. (We meet them in a more rigorous context in Chapter 2.) The tails contain little area; and it is the tails that give us the decision: we probably call somebody tall when they are taller than 75 per cent of us.

We have made a decision based on a statistic, by relating that statistic to a probability distribution; we have decided that the person in question was tall. Note also what we did – observe, reduce, analyse, conclude, probably all in one glance. We did not do this rigorously in making a quantitative assessment of just how tall, which would have required a detailed knowledge of the distribution of height and a quantitative measurement. And reflect? Context of our observation? Why did we wish to register or decide that the person was tall? What next as a result? How was this person selected from the population? The brain has not only done the five steps but has also set the result into an extensive context; and this in processing the single glance.

This is an example of a probability distribution for which there is unlikely to be a mathematical description, one determined by counting most of the population, or at least so much of it as to leave no doubt that it is well defined. There are distributions for which mathematical description is very precise, such as the Poisson and Gaussian (Normal) distributions, and there are many cases in which we have good reason to believe that these must represent the underlying distributions well.

This is also an example of a 'ruling-out'; here we ruled out the hypothesis that the person is of 'ordinary' height. There is a different type of statistical inference, the 'ruling-in' process, in which we compute the probability of getting a given result, and if it is 'probable', we accept the original hypothesis. It is also an example of 'counting' to find the probabilities, the frequency distribution. There are other ways of assigning probabilities, including opinion and states of knowledge; and in fact there are instances in which we are moderately comfortable with the paradoxical notion of assigning probabilities to unique events. It is essential that our view of statistics and statistical inference be broad enough to take such probability concepts on board.

1.3 Probability and statistics in inference

What is the relationship between these two notions? Statistics, to anticipate later definitions, are combinations of the data that do not depend on any unknown parameters. The average is a common example. When we calculate the average of a set of data, we expect that it will bear some relation to the true, underlying mean of the distribution from which our data were drawn. In the classical tradition, we calculate the sampling distribution of the average, the probabilities of the various values it may assume as we (hypothetically) repeat our experiment many times. We

then know the probability that some range around our single measurement will contain the true mean. This is information that we can use to take decisions.

This is precisely the utility of statistics – they are laboriously discovered combinations of observations which converge, for large sample sizes, to some underlying parameter we want to know (say, the mean). Useful statistics are actually rather few in number.

There is another, radically different way of making inferences – the Bayesian approach. This focuses on the probabilities right away, without the intermediate step of statistics. In the Bayesian tradition, we invert the reasoning just described. The data, we say, are unique and known; it is the mean that is unknown, that should have probability attached to it. Without using statistics, we instead calculate the probability of various values of the mean, given the data we have. This also allows us to make decisions. In fact, as we shall see, this approach comes a great deal closer to answering the questions that scientists actually ask.

1.4 Non-parametric or distribution-free statistical inference

There are four reasons why statistical inference based on known probability distributions does not work, or limits our possibilities severely.

(i) We are measuring in experiments being run out there in the Universe, not by us. The underlying distributions may be far from known or understood; no averaging may be going on to lead us towards the central limit theorem and Gaussian distributions (see Chapter 2); yet we still wish to draw inferences about the underlying population. We only do so safely with *non-parametric statistics*, methods that do not require knowledge of the underlying distributions.

(ii) We may have to deal with small-number samples, such as $N = 3$. Non-parametric techniques have the power to do this.

(iii) The range of observation scales available to us is given in Table 1.2. Each such scale has a formal definition and formal properties. Each has admissible operations. Suffice it to say here that use of scales other than numerical ('interval') requires in most (but not all) cases that we use non-parametric methods. *We may wish to make statistical inference without recourse to numerical scales.*

(iv) Others use such methods to draw inference. We need to understand what they are doing.

Table 1.2. Measurement scales

Scale type	Also called	Example and measurement
Nominal/ Categorical	Bins	Psychiatric types: schizophrenic, paranoid, manic-depressive, neurotic, psychopathic
Ordinal/ Ranking	Order	Army ranks: private, corporal, sergeant, major
Interval	Measures	Temperature: degrees Celsius

Non-parametric methods thus enormously increase the possibilities in decision-making and form an essential part of our process. They are described in the course of this book.

1.5 How to use this book

This is not a textbook of statistical theory, a guide to numerical analysis, or a review of published work. It is a practical manual, which assumes that proofs, numerical methods and citation lists can easily be found elsewhere. This book sets out to tell it from an astronomer's perspective, and our main objective is to help in gaining familiarity with the broad concepts of statistics and probability, to understand their usefulness, and to feel confident in applying them. Work through the examples and exercises; they are drawn from our experience and have been chosen to clarify the text. They vary in difficulty, from one-page calculations to mini-projects. Some need data; this may be simulated. If preferred, example datasets are available on the book's website – as are the solutions to the exercises. Aim to become confident in the use of Monte Carlo simulations to check any calculations, and to try out ideas. Remember, in this subject we can do useful and revealing experiments – in the computer. Don't be ashamed to let simulations guide your mathematical intuition!

For further details on statistical methods and justification of theory, there is no substitute for a proper textbook. None of our topics is arcane and they will be found in the index of any elementary statistics book. We have found several particularly helpful: Mood, Graybill & Boes (1974), Lyons (1986), Barlow (1989), Lee (1997) and Bevington & Robinson (2002). Feigelson & Babu (1992a) and Babu & Feigelson (1996) cover many useful astronomical applications from a more rigorous point of view than we do.

There is little algebra in this book; it would have greatly lengthened and cluttered the presentation to have worked through details. Likewise, we have not explained how various integrals were done or eigenvalues found. These things can be done by computers; packages such as the superb MATHEMATICA, used for many of the calculations in this book, can deal swiftly with more mathematical technology than most of us know. Using these packages frees us all up to think about the problem to hand, rather than searching in vain for missing minus signs or delving into handbooks for integrals which never seem to be there in quite the needed form.

The other source is the indispensable Numerical Recipes (Press et al. 1992), which points the way for numerical solution of an enormous variety of problems, plus providing humorous and wise advice.

We have not attempted exhaustive referencing. Rather, we have given enough key references to provide entry points to the literature. Online bibliographic databases provide excellent cross-referencing, showing who has cited a paper and who it cites; it is the work of minutes to collect a comprehensive reading list on any topic. The lecture notes for many excellent university courses are now on the Web; a well-phrased search may yield useful material to help with whatever is puzzling you.

Finally, use this book as you need it. It can be read from front to back, or dipped into. Of course, no interesting topic is self-contained, but we hope the cross-referencing will connect all the technology needed to explore a particular topic.

Exercises

1.1 At first sight, discovery of a new phenomenon may not read as an experiment as described in section 1.1. But it is. Describe the discovery of pulsars (Hewish et al. 1968) in terms of the five experimental stages.

1.2 The significance of a certain conclusion depends very strongly on whether the most luminous known quasar is included in the dataset. The object is legitimately in the dataset in terms of prestated selection criteria. Is the conclusion robust? Believable?

2
Probability

God does not play dice with the Universe.
(Albert Einstein)

Whether He does or not, the concepts of probability are important in astronomy for two reasons.

(1) Astronomical measurements are subject to random measurement error, perhaps more so than most physical sciences because of our inability to rerun experiments and our perpetual wish to observe at the extreme limit of instrumental capability. We have to express these errors as precisely and usefully as we can. Thus when we say 'an interval of 10^{-6} units, centred on the measured mass of the Moon, has a 95 per cent chance of containing the true value', it is a much more quantitative statement than 'the mass of the Moon is 1 ± 10^{-6} units'. The second statement really only means anything because of some unspoken assumption about the distribution of errors. Knowing the error distribution allows us to assign a probability, or measure of confidence, to the answer.

(2) The inability to do experiments on our subject matter leads us to draw conclusions by contrasting properties of controlled samples. These samples are often small and subject to uncertainty in the same way that a Gallup poll is subject to 'sampling error'. In astronomy we draw conclusions such as 'the distributions of luminosity in X-ray-selected Type I and Type II objects differ at the 95 per cent level of significance'. Very often the strength of this conclusion is dominated by the number of objects in the sample and is virtually unaffected by observational error.

This chapter begins with a discussion of what probability is, and proceeds to introduce the concepts of conditionality and independence, providing a basis for the consequent discussion of Bayes' theorem, with

prior and posterior probabilities. Only at this point is it safe to consider the concept of probability distributions; some common probability distributions are compared and contrasted. This sets the stage for the following chapter, dealing with statistics themselves, the penultimate product of data reduction – if conclusions/discoveries are considered as the ultimate product. The issues of expectation and errors, dependent on the distributions and statistics, are discussed in the final section of the following chapter.

2.1 What is probability?

For a fascinating historical study of probability, see the books by Hald (1990; 1998). The ideas in this chapter draw heavily on the writings of Jaynes (1976; 1983; 2003). Another fundamental reference, rather heavy going, is Jeffreys (1961).

The study of probability began with the analysis of games of chance involving cards or dice. Because of this background we often think of probabilities as a kind of limiting case of a frequency. Many textbook problems are still about dice, hands of cards, or coloured balls drawn from urns; in these cases it seems obvious to take the probabilities of certain events according to the ratio

$$\frac{\text{number of favourable events}}{\text{total number of events}}$$

and the probability of throwing a six with one roll of the dice is 'obviously' 1/6.

This probability derives from what Laplace called the 'principle of indifference', which in effect tells us to assign equal probabilities to events unless we have any information distinguishing them. In effect we have done the following calculation:

$$\begin{aligned}\text{probability of one spot} &= x\\ \text{probability of two spots} &= x\\ \text{probability of three spots} &= x\end{aligned}$$

and so on; this is the principle of indifference step. Further, we believe that we have identified all the cases; with the convention that the probability of a certain event (anything between one and six spots) is unity, we have

$$6x = 1.$$

This calculation, apparently trivial as it is, shows a vitally important feature: we cannot usefully define probability by this kind of ratio. We have had to assume that each face of the die is equally probable to start with – thus the definition of probability becomes circular.

If we can *identify* equally likely cases, then *calculating* probabilities amounts simply to enumerating cases – not always easy, but straightforward in principle. However, identifying equally likely cases requires more thought.

Many interesting and useful calculations can be done using the principle of indifference, either directly or by exploiting its applicability to aspects of the problem. For example, we may know that a die is biased, the faces are not 'equally likely'. However, given some details of, say, the mass distribution of the die, we may be able to calculate the probabilities of the faces using an assumption that the initial direction of the throw is isotropic – in which case the principle of indifference applies to throw-directions.

Sometimes we estimate probabilities from data. The probability of our precious observing run being clouded out is estimated by

$$\frac{\text{number of cloudy nights last year}}{365}$$

but two issues arise. One is the limited data – we suspect that 10 years' worth of data would give a different, more accurate result. The second issue is simply the identification of the 'equally likely' cases. Not all nights are equally likely to be cloudy, some student of these matters tells us; it's much more likely to be cloudy in winter. What is 'winter', then? A set of nights equally likely to be cloudy?

We can only estimate the probabilities correctly once we have identified the equally likely cases, and this identification is the subjective, intuitive step that is built into our reasoning about data from apparently malevolent instrumentation in an increasingly uncertain world.

It is common to define probabilities as empirical statements about frequencies, in the limit of large numbers of cases – our 10 years' worth of data. But, as we have seen, this definition must be circular because selecting the data depends on knowing which cases are equally likely. Defining probabilities in this way is sometimes called 'frequentist'. It is sometimes the only way; but the risks must be recognized.

So what is probability? The notion we adopt for the present is that probability is *a numerical formalization of our degree or intensity of*

belief. In everyday speech we often refer to the probability of unique events, showers of rain or election results. In the desiccated example of throwing dice, x measures the strength of our belief that any face will turn up. Provided that the die is not loaded, this belief is 1/6, the same for each face.

Ascribing an apparently subjective meaning to probability in this way needs careful justification. After all, one person's degree of belief is another person's certainty, depending on what is known. We can only reason as best we can with the information we have; if our probabilities turn out to be wrong, the deficiency is in what we know, not the definition of probability. We just need to be sure that two people with the same information will arrive at the same probabilities. It turns out that this constraint, properly expressed, is enough to develop a theory of probability which is mathematically identical to the one often interpreted in frequentist terms.

A useful set of properties of probability can be deduced by formalizing the 'measure of belief' idea. The argument is originally due to Cox (1946) and goes as follows: if A, B and C are three events and we wish to have some measure of how strongly we think each is likely to happen, then for consistent reasoning we should at least apply the rule if A is more likely than B, and B is more likely than C, then A is more likely than C. Remarkably, this is sufficient to put constraints on the probability function which are identical to the Kolmogorov axioms of probability, proposed some years before Cox's paper:

- Any random event A has a probability prob(A) between zero and one.
- The sure event has prob(A) = 1.
- If A and B are exclusive events, then prob(A or B) = prob(A) + prob(B).

The Kolmogorov axioms are a sufficient foundation for the entire development of mathematical probability theory, by which we mean the apparatus for manipulating probabilities once we have assigned them.

EXAMPLE Before 1987, four naked-eye supernovae had been recorded in ten centuries. What, before 1987, was the probability of a bright supernova happening in the twentieth century?

There are three possible answers.

(1) Probability is meaningless in this context. Supernovae are physically determined events and when they are going to happen can, in principle, be accurately calculated. They are not random events.

From this God's-eye viewpoint, probability is indeed meaningless; events are either certain or forbidden. 'God does not play dice ...'

(2) From a frequentist point of view our best estimate of the probability is 4/10, although it is obviously not very well determined.

This assumes supernovae were equally likely to be reported throughout 10 centuries, which may well not be true. Eventually some degree of belief about detection e ciency will have to be made explicit in this kind of assignment.

(3) We could try an a-priori assignment. In principle we might know the stellar mass function, the fate and lifetime as a function of mass, and the stellar birth rate. We would also need a detection efficiency. From this we could calculate the mean number of supernovae expected in 1987, and we would put some error bars around this number to reflect the fact that there will be variation caused by factors we do not know about – metallicity, perhaps, or location behind a dust cloud, and so on.

The belief-measure structure is more complicated in this detailed m odel but it is still there. The model deals in populations, not individual stars, and assumes that certain groups of stars can be identified which are equally likely to explode at a certain time.

Suppose now that we sight supernova 1987A. Is the probability of there being a supernova later in the twentieth century affected by this event?

Approach (1) would say no – one supernova does not affect another. Approach (2), in which the probability simply reflects what we know, would revise the probability upward to 5/10. Approach (3) might need to adjust some aspects of its models in the light of fresh data; predicted probabilities would change.

Probabilities reflect what we know – they are not things with an existence all of their own. Even if we could define 'random events' (approach 1), we should not regard the probabilities as being properties of supernovae.

2.2 Conditionality and independence

Two events A and B are said to be independent if the probability of one is unaffected by what we may know about the other. In this case, it follows (not trivially!) from the Kolmogorov axioms that

$$\text{prob}(A \text{ and } B) = \text{prob}(A)\text{prob}(B). \tag{2.1}$$

Sometimes independence does not hold, so that we would also like to know the conditional probability: the probability of A, given that we know B. The definition is

$$\text{prob}(A \mid B) = \frac{\text{prob}(A \text{ and } B)}{\text{prob}(B)}. \tag{2.2}$$

If A and B are independent, knowing that B has happened should not affect our beliefs about the probability of A. Hence $\text{prob}(A \mid B) = \text{prob}(A)$ and the definition reduces to $\text{prob}(A \text{ and } B) = \text{prob}(A)\text{prob}(B)$ again.

If there are several possibilities for event B (label them $B_1, B_2, \ldots$) then we have that

$$\text{prob}(A) = \sum_i \text{prob}(A \mid B_i)\text{prob}(B_i). \tag{2.3}$$

A might be a cosmological parameter of interest, while the Bs are not of interest. They might be instrumental parameters, for example. Knowing the probabilities $\text{prob}(B_i)$ we can get rid of these 'nuisance parameters' by a summation (or integration). This is called marginalization.

EXAMPLE Take the familiar case in astronomy where some 'remarkable' event is observed, for example two quasars of very different redshifts close together on the sky. The temptation is to calculate an a-priori probability, based on surface densities, of two specified objects being so close. However, the probability of the two quasars being close together is conditional on having noticed this fact in the first place. Thus the probability of the full event is simply $\text{prob}(A \mid A) = 1$, consistent with how we should expect to measure our belief in something that we

already know. We can say nothing further, although we might be able to formulate a hypothesis to carry out an experiment.

Consider now the very different case in which we wish to know the probability of finding two objects of different types, say a galaxy and a quasar, within a specified angular distance r of each other. To be specific, we plan to search some fixed solid angle Ω. The surface densities in question are ς_{G} and ς_{Q}. On finding a galaxy, we will search around it for a quasar. We need

$$\begin{aligned}&\mathrm{prob}(\mathrm{G\ in\ field\ and\ Q\ within}\ r)\\ &\quad = \mathrm{prob}(\mathrm{Q\ within}\ r \mid \mathrm{G\ in\ field})\mathrm{prob}(\mathrm{G\ in\ field}).\end{aligned}$$

This assumes that the probabilities are independent, obviously what we would like to test. A suitable model for the probabilities is the Poisson distribution (Section 2.4.2.2), and in the interesting case where the probabilities are small we have

$$\mathrm{prob}(\mathrm{G\ in\ field}) = \varsigma_{\mathrm{G}}\Omega$$

and

$$\mathrm{prob}(\mathrm{Q\ within}\ r) = \pi r^2 \varsigma_{\mathrm{Q}}.$$

The answer we require is therefore

$$\mathrm{prob}(\mathrm{G\ in\ field\ and\ Q\ within}\ r) = \varsigma_{\mathrm{G}}\varsigma_{\mathrm{Q}}\Omega\pi r^2.$$

This is symmetrical in the quasar and galaxy surface densities as we would expect; it should not matter whether we searched first for a galaxy or for a quasar. Note the strong dependence on the search area that is specified before the experiment; if there is obscurity about this then the probabilities are not well determined.

As an extension of this example, it is possible to calculate the probability of finding triples of objects aligned to some small tolerance (Edmunds & George 1985). If the objects are all the same, the probability of a linear triple depends on the cube of the surface density and search area.

2.3 ... and Bayes' theorem

Bayes'[1] theorem is a simple equality, derived by equating prob (A and B) with prob (B and A). This gives the 'theorem':

$$\text{prob}(B \mid A) = \frac{\text{prob}(A \mid B)\text{prob}(B)}{\text{prob}(A)}. \tag{2.4}$$

In this, the denominator is a normalizing factor. The theorem is particularly useful when interpreted as a rule for induction; the data, the event A, are regarded as succeeding B, the state of belief preceding the experiment. Thus prob(B) is the prior probability which will be modified by experience. This experience is expressed by the likelihood prob($A \mid B$). Finally prob($B \mid A$) is the posterior probability, the state of belief after the data have been analysed.

Bayes' theorem by itself is a perfectly innocent identity, a mathematical truism. It acquires its force from its interpretation. To see what this force is, we return to the familiar and simple problem of drawing those coloured balls from urns. It is clear, even automatic, what to calculate; if there are M red balls and N white balls, the probability of drawing three red balls and two white ones is ...

As a series of brilliant scientists realized, and as a series of brilliant scientists did not, this is generally not the problem we face. As scientists, we more often have a datum (three red balls, two white ones) and we are trying to infer something about the contents of the urn. This is sometimes called the problem of 'inverse probability'. How does Bayes' theorem help? We interpret it to be saying

$$\text{prob}(\text{contents of urn} \mid \text{data}) \propto \text{prob}(\text{data} \mid \text{contents of urn})$$

and of course we can calculate the right-hand side, given some assumptions.

The urn example illustrates the principles involved; these are far more interesting than coloured balls.

[1] Who was Bayes? Thomas Bayes (1702–61) was an English vicar, mathematician and statistician. His bibliography consisted of three works: one (by the vicar) on divine providence, the second (by the mathematician) a defence of the logical bases of Newton's calculus against the attacks of Bishop Berkeley, and the third (by the statistician and published posthumously) the famous *Essay Towards Solving a Problem in the Doctrine of Chances*. There is speculation that it was published posthumously because of the controversy which Bayes believed would ensue. This must be an a-posteriori judgement. Surely Bayes could never have imagined the extent of this controversy without envisaging the nature and extent of modern scientific data.

EXAMPLE There are N red balls and M white balls in an urn; we know the total $N + M = 10$, say. We draw $T = 3$ times (putting the balls back after drawing them) and get $R = 2$ red balls. How many red balls are there in the urn?

Our model (hypothesis) is that the probability of a red ball is

$$\frac{N}{N+M}.$$

We assume that the balls are not stratified, arranged in pairs, or anything else 'peculiar'. The probability of getting R red balls, the likelihood, is

$$\binom{T}{R}\left(\frac{N}{N+M}\right)^{R}\left(\frac{M}{N+M}\right)^{T-R}.$$

This is the number of permutations of the R red balls amongst the T draws, multiplied by the probability that R balls will be red and $T - R$ will not be red. (This is a `Binomial` distribution; see section 2.4.2.1.)

Thus we have the `probability (data, given the model)` part of the right-hand side of Bayes' theorem. We also need `probability (model)`, or the prior. We assume that the only uncertain bit of the model is N, which to start with we take as being uniformly likely between zero and $N+M$. Without bothering with the details at the moment, we plot up the left-hand side of Bayes' theorem (the posterior probability) as a function of N – see Fig. 2.1. For a draw of, say, three red balls in five tries, the posterior probability peaks at 6; for 30 out of 50, the peak is still at 6 but other possibilities are much less likely.

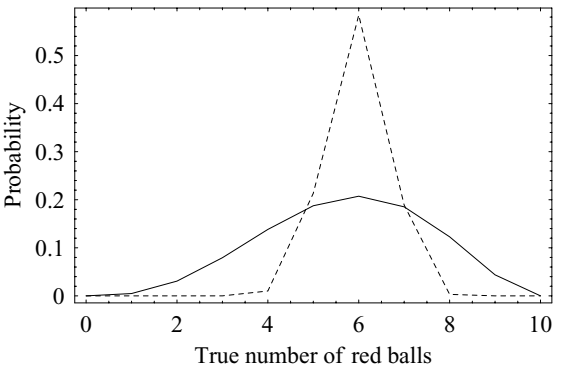

Fig. 2.1. The probability distribution of the number of red balls in the urn, for five (solid curve) and 50 drawings (dashed curve).

This seems unsurprising and in accord with common sense – but notice that we are speaking now of the probability of there being 1, 2, 3, ... red balls in a unique urn that is the subject of our experiment. We are describing our state of belief about the contents of the urn, given what we know (the data, and our prior information).

The key point of this example is that we have succeeded in answering our scientific question: we have made an inference about the contents of the urn, and can make probabilistic statements about this inference. For example, the probability of the urn containing three or fewer red balls is 11 per cent. We are assigning probabilities to these statements to N because we are using probability to reflect our degree of certainty. Our concern, as experimental scientists, is with what we can infer about the world from what we know.

Bayes' theorem allows us to make inferences from data, rather than compute the data we would get if we happened to know all the relevant information about our problem.

This may seem academic; but suppose we had data from two populations and wanted to know if the means were different. Many chapters of statistics textbooks answer the opposite question for us: given populations with two different means, what data would you get? The combination of interpreting probability as a consistent measure of belief, plus Bayes' theorem, allows us to answer the question we wish to pose: given the data, what are the probabilities of the parameters contained in our statistical model?

Another very significant point about this example is the use of prior information; again, we assigned probabilities to N to reflect what we know. Notice that although the word 'prior' suggests 'before the experiment' it really means 'what we know apart from the data'. Sometimes this can have a dramatic, even disconcerting effect on our inferences:

EXAMPLE Suppose we make an observation with a radio telescope at a randomly selected position in the sky. Our model of the data (an event labelled D, consisting of the single measured flux density f) is that it is distributed in a Gaussian way (Section 2.4.2.3) about the true flux density S with a variance (Section 2.4.2) σ^2. The extensive body of radio source counts also tells us the a-priori distribution of S; for the purposes of this example, we approximate this information by the simple prior

$$\text{prob}(S) = KS^{-5/2}$$

describing our prior state of knowledge. K normalizes the counts to unity; there is presumed to be one source in the beam at some flux-density level. The probability of observing f when the true value is S we take to be

$$\exp\left[-\frac{1}{2\sigma^2}(f-S)^2\right].$$

Bayes' theorem then tells us

$$\text{prob}(S \mid D) = K' \exp\left[-\frac{1}{2\sigma^2}(f-S)^2\right] S^{-5/2},$$

with the normalizations condensed into the single parameter K'. If we were able to obtain n independent flux measurements f_i then the result would be

$$\text{prob}(S \mid D) = K'' \exp\left[-\frac{1}{2\sigma^2}\sum_{i=1}^{n}(f_i-S)^2\right] S^{-5/2}.$$

Suppose, for specific example, that the source counts were known to extend from 1 to 100 units, the noise level was $\sigma = 1$, and the data were 2, 1.3, 3, 1.5, 2 and 1.8. In Fig. 2.2 are the posterior probabilities for the first two, then four, then six measurements. The increase in data gradually overwhelms the prior but the prior affects conclusions markedly (as it should) when there are few measurements.

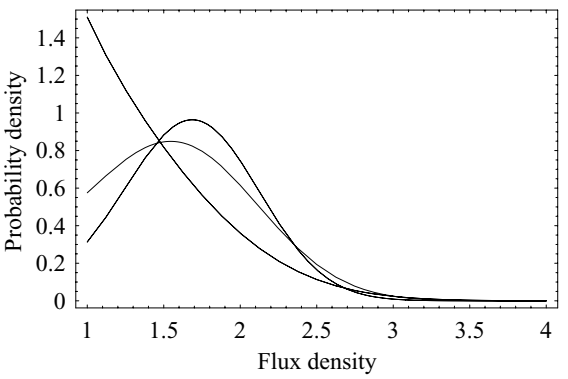

Fig. 2.2. Measurement of flux density given a power-law prior (source count) and a Gaussian error distribution. The posterior probability distribution for flux density is plotted for two, four and then six of the measurements listed in the text; the form of the curve approaches Gaussian as numbers increase.

If subsequently we looked at a survey plate of the region we had observed, and found that the radio emission was from some category of object (say, a quasar) with different source counts, our prior would change and so would the posterior probability. In turn, our idea of the most probable flux density would also change.

In this example, the prior seems to be well determined. However, in some cases we wish to estimate quantities where the argument is not so straightforward. What would we take as the prior in the previous example if we were making the first ever radio measurements? Or if we needed an estimate of the mean of a Gaussian, then we have to ask how we interpret the prior probability of the mean. Sometimes we even need a probability of a probability:

EXAMPLE Return to the question of supernova rate per century and consider how to estimate this; call this ρ. Our data are four supernovae in ten centuries. Our prior on ρ, expressing our total ignorance, is uniform between 0 and 1; we have no preconceptions or information about ρ. A suitable model for prob(data | ρ) is the Binomial distribution (Section 2.4.2.1), because in any century we either get a supernova or we do not (neglecting here the possibility of two supernovae in a century). Our posterior probability is then

$$\text{prob}(\rho \mid \text{data}) \propto \binom{10}{4} \rho^4 (1-\rho)^6 \times \text{prior on } \rho.$$

We follow Bayes and Laplace in taking the prior to be uniform in the range 0 to 1. Then, to normalize the posterior probability properly we need

$$\int_0^1 \text{prob}(\rho \mid \text{data})\, \mathrm{d}\rho = 1,$$

resulting in the normalizing constant

$$\int_0^1 \binom{10}{4} \rho^4 (1-\rho)^6 \, \mathrm{d}\rho,$$

which happens to be

$$\frac{\Gamma(10)\Gamma(4)}{\Gamma(14)} = B[5,7],$$

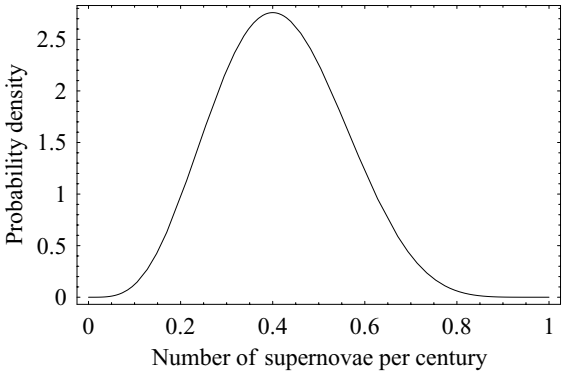

Fig. 2.3. The posterior probability distribution for ρ, given that we have four supernovae in ten centuries.

where B is the (tabulated) beta function. In general, for n supernovae in m centuries, the distribution is

$$\text{prob}(\rho \mid \text{data}) = \frac{\rho^n (1-\rho)^{m-n}}{B[n+1, m-n+1]}.$$

Our distribution ($n = 4,\ m = 10$) peaks – unsurprisingly – at 4/10, as shown in Fig. 2.3.

As the sample size increases the distribution becomes narrower so that the peak posterior probability is more and more closely defined by the ratio of successes (supernovae, in our example) to sample size. This result is sometimes called the law of large numbers, expressing as it does the frequentist idea of a large number of repetitions resulting in a converging estimate of probability.

The key step in this example is ascribing a probability distribution to ρ, *in itself a probability*. This makes no sense in a frequentist approach, nor indeed in any interpretation of probabilities as objective. Even if we are prepared to leap this metaphysical hurdle, in very many cases the assignment of a prior probability is much more difficult than in this example. Indeed, it is certain that the assignment of priors in the current example has been greatly oversimplified.

Both Jeffreys (1961) and Jaynes (1968) discuss the prior on ρ, arguing that in many cases a uniform prior is far too agnostic. By intricate

arguments, they arrive at other possibilities:

$$\text{prob}(\rho) = \frac{1}{\rho(1-\rho)}$$

and the 'Haldane prior'

$$\text{prob}(\rho) = \frac{1}{\sqrt{\rho(1-\rho)}}.$$

These are intended to reflect the fact that in most experiments we are expecting a yes or no answer.

Assigning priors when our knowledge is rather vague can be quite difficult, and there has been a long debate about this. Some 'obvious' priors (such as the one we might use for location, simply uniform from $-\infty$ to ∞) are not normalizable and can sometimes get us into trouble. Out of the enormous literature on this subject, try Lee (1997) for an introduction, and Jaynes's writings for some fascinating arguments. One of the ways of determining a prior is the maximum entropy principle; we will see an example of such a prior later (Section 6.7). A common prior for a scale factor σ is Jeffrey's prior, uniform in $\log\sigma$.

EXAMPLE Finally, the use of Bayes' theorem as a method of induction can be neatly illustrated by our supernova example. For simplicity, imagine that we establish our posterior distribution at the end of the nineteenth century, so that it is $\rho^4(1-\rho)^6/B[5,7]$, as shown earlier. At this stage, our data are four supernovae in ten centuries. Reviewing the situation at the end of the twentieth century, we take this as our prior. The available new data consist of one supernova, so that the likelihood is simply the probability of observing exactly one event of probability ρ, namely ρ. The updated posterior distribution is

$$\text{prob}(\rho \mid \text{data}) = \frac{\rho^5(1-\rho)^6}{B[6,7]}$$

which peaks at $\rho = 5/11$ as we might expect.

In these examples we have focused on the peak of the posterior probability distribution. This is one way amongst many of attempting to characterize the distribution by a single number. Another choice is the

posterior mean, defined by

$$< \rho > = \int_0^1 \rho \, \mathrm{prob}(\rho \mid \mathrm{data}) \, \mathrm{d}\rho. \tag{2.5}$$

If we have had N successes and M failures, the posterior mean is given by a famous result called Laplace's rule of succession:

$$< \rho > = \frac{N+1}{N+M+2}.$$

In our example, at the end of the nineteenth century Laplace's rule would give 5/12 as an estimate of the probability of a supernova during the twentieth century. This differs from the 4/10 derived from the peak of the posterior probability, and it will do so in general.

Unless posterior distributions are very narrow, attempting to characterize them by a single number is frequently misleading. How best to characterize the distribution depends on what is to be done with the answer, which in turn depends on having a carefully posed question in the first place.

2.4 Probability distributions

2.4.1 Concept

We have referred several times to probability distributions. The basic idea is intuitive; here is a little more detail.

Consider the fascinating experiment in which we toss four 'fair' coins. The probability of no heads is $(1/2)^4$; of one head $4\times(1/2)^4$; of two heads $6 \times (1/2)^4$, etc. The sum of the possibilities for getting no heads to four heads is readily seen to be 1.0. If x is the number of heads $(0, 1, 2, 3, 4)$, we have a set of probabilities $\mathrm{prob}(x) = (1/16, 1/4, 3/8, 1/4, 1/16)$; we have a probability distribution, describing the expectation of occurrence of event x. This probability distribution is discrete; there is a discrete set of outcomes and so a discrete set of probabilities for those outcomes.

In this sort of case we have a mapping between the outcomes of the experiment and a set of integers. Sometimes the set of outcomes maps onto real numbers instead, the set of outcomes no longer containing discrete elements. We deal with this by the contrivance of discretizing the range of real numbers into little ranges within which we assume the probability does not change. Thus if x is the real number that indexes outcomes, we associate with it a probability density $f(x)$; the

probability that we will get a number 'near' x, say within a tiny range δx, is $\text{prob}(x)\,\delta x$. We loosely refer to probability 'distributions' whether we are dealing with discrete outcomes or not.

Formally: if x is a continuous random variable, then $f(x)$ is its probability density function, commonly termed probability distribution, when

(i) $\text{prob}(a < x < b) = \int_a^b f(x)\,\mathrm{d}x$,
(ii) $\int_{-\infty}^{\infty} f(x)\,\mathrm{d}x = 1$, and
(iii) $f(x)$ is a single-valued non-negative number for all real x.

The corresponding cumulative distribution function is $F(x) = \int_{-\infty}^{x} f(y)\,\mathrm{d}y$. Probability distributions and distribution functions may be similarly defined for sets of discrete values of x; and distributions may be multivariate, functions of more than one variable.

2.4.2 Some common distributions

The better-known probability density functions appear in Table 2.1 together with location (where is the 'centre'?) and dispersion (what is the 'spread'?) quantifiers. These quantifiers can be given by the first two moments of the distributions (Section 3.1):

$$\mu_1(\text{mean}) = \mu = \int_{-\infty}^{\infty} x f(x)\,\mathrm{d}x \tag{2.6}$$

$$\mu_2(\text{variance}) = \sigma^2 = \int_{-\infty}^{\infty} (x-\mu_1)^2 f(x)\,\mathrm{d}x. \tag{2.7}$$

σ is known as the standard deviation. Three of them are of prime importance, the Binomial, Poisson, and Gaussian or Normal, and we discuss these in turn.

2.4.2.1 Binomial distribution

There are two outcomes – 'success' or 'failure'. This common distribution gives the chance of n successes in N trials, where the probability of a success at each trial is the same, namely ρ, and successive trials are independent. This probability is then

$$\text{prob}(n) = \binom{N}{n} \rho^n (1-\rho)^{N-n}. \tag{2.8}$$

Table 2.1. The common probability density functions

Distribution	Density function	Mean	Variance	*Raison d'être*
Uniform	$f(x;a,b) = 1/(b-a)\ a < x < b$ $= 0, \quad x < a, x > b$	$(a+b)/2$	$(b-a)/12$	In the study of rounding errors; as a tool in studies of other continuous distributions.
Binomial	$f(x;p,q) = \frac{n!}{x!(n-x)!} p^x q^{n-x}$	np	npq	x is the number of 'successes' in an experiment with two possible outcomes, one ('success') of probability p, and the other ('failure') of probability $q = 1-p$. Becomes a Normal distribution as $n \to \infty$.
Poisson	$f(x;\mu) = \frac{\mathrm{e}^{-\mu}\mu^x}{x!}$	μ	μ	The limit for the Binomial distribution as $p \ll 1$, setting $\mu \equiv np$. It is the 'count-rate' distribution, e.g. take a star from which an average of μ photons are received per Δt (out of a total of n emitted; hence $p \ll 1$); the probability of receiving x photons in Δt is $f(x;\mu)$. Tends to the Normal distribution as $\mu \to \infty$.
Normal (Gaussian)	$f(x;\mu,\sigma) = \frac{1}{\sigma\sqrt{2\pi}} \exp\left[-\frac{(x-\mu)^2}{2\sigma^2}\right]$	μ	σ^2	The essential distribution; see text. The central limit theorem ensures that the majority of 'scattered things' are dispersed according to $f(x;\mu,\sigma)$.
Chi-square	$f(\chi^2;\nu) = \frac{\chi^{2(\nu/2-1)}}{2^{\nu/2}\Gamma(v/2)} \exp(-\frac{1}{2}\chi^2)$	ν	2ν	Vital in the comparison of samples, model testing; characterizes the dispersion of observed samples from the expected dispersion, because if x_i is a sample of ν variables Normally and independently distributed with means μ_i and variances σ_i^2, then $\chi^2 = \Sigma_{i=1}^{N}(x_i-\mu_i)^2/\sigma_i^2$ obeys $f(\chi^2;\nu)$. Invariably tabulated and used in integral form. Tends to the Normal distribution as $\nu \to \infty$.
Student t	$f(t;\nu) = \Gamma[(\nu+1)/2]\frac{(1+t^2/\nu)^{-[(\nu+1)/2]}}{\sqrt{\pi\nu}\Gamma(\nu/2)}$	0	$\nu/(\nu-2)$ (for $\nu > 2$)	For comparison of means, Normally distributed populations; if n x_i's are taken from a Normal population (μ,σ), and if x_s and σ_s are determined, then $t = \sqrt{n}(\overline{x}_s - \mu)/\sigma_s$ is distributed as $f(t,\nu)$ where the 'degrees of freedom' $\nu = n-1$. The statistic t can also be formulated to compare means for samples from Normal populations with the same σ, different μ. Tends to Normal as $\nu \to \infty$.

The leading term, the combinatorial coefficient, gives the number of distinct ways of choosing n items out of N:

$$\binom{N}{n} = \frac{N!}{n!(N-n)!}. \tag{2.9}$$

This coefficient can be derived in the following way. There are $N!$ equivalent ways of arranging the N trials. However there are $n!$ permutations of the successes, and $(N-n)!$ permutations of the failures, which correspond to the same result – namely, exactly n successes, arrangement unspecified. Since we require not just n successes (probability p^n) but exactly n successes, we need exactly $N-n$ failures, probability $(1-p)^{(N-n)}$ as well. The Binomial distribution follows from this argument. The Binomial distribution has a mean value given by

$$\sum_{n=0}^{N} n\,\mathrm{prob}(n) = Np$$

and a variance or mean square value of

$$\sum_{n=0}^{N} (n-Np)^2 \mathrm{prob}(n) = Np(1-p).$$

EXAMPLE Suppose we know, from a sample of 100 galaxy clusters selected by automatic pattern-recognition techniques, that ten contain a dominant central galaxy. We plan to check a different sample of 30 clusters, now selected by X-ray emission. How many of these clusters do we expect to have a dominant central galaxy?

If we assume that the 10 per cent probability holds for the X-ray sample, then the chance of getting n dominant central galaxies is

$$\mathrm{prob}(n) = \binom{30}{n} 0.1^n 0.9^{30-n}.$$

For example, the chance of getting 10 is about 1 per cent; if we found this many we would be suspicious that the X-ray cluster population differed from the general population.

Suppose we made these observations and did find 10 centrally dominated clusters. What can we do with this information?

The Bayesian thing to do is a calculation that parallels the supernova example. Assuming the X-ray galaxies are a homogeneous set, we can

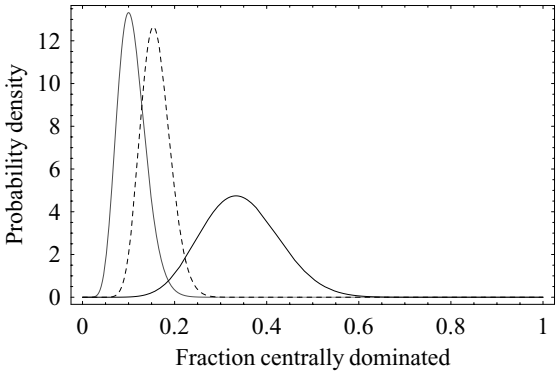

Fig. 2.4. The posterior probability distribution for the fraction of X-ray-selected clusters that are centrally dominated. The black line uses a uniform prior distribution for the fraction; the dashed line uses the prior derived from an assumed previous sample in which 10 out of 100 clusters had dominant central members. The light curve shows the distribution for this earlier sample.

deduce the probability distribution for the fraction of these galaxies that have a dominant central galaxy. A relevant prior would be the results for the original larger survey. Figure 2.4 shows the results, making clear that the data are not really sufficient to alter our prior very much. For example, there is only a 10 per cent chance that the centrally dominant fraction exceeds even 0.2; and indeed Fig. 2.4 shows that the possibility of it being as high as 33 per cent is completely negligible. Our X-ray clusters have a different prior from the general population.

The Binomial distribution is the parent of two other famous distributions, the Poisson and the Gaussian.

2.4.2.2 Poisson distribution

The Poisson distribution derives from the Binomial in the limiting case of very rare events and a large number of trials, so that although $p \to 0$, $Np \to$ a finite value. Calling the finite mean value $\mu_1 = \mu$, the Poisson distribution is

$$\text{prob}(n) = \frac{\mu^n}{n!} e^{-\mu}. \tag{2.10}$$

The variance of the Poisson distribution, μ_2, is also μ.

EXAMPLE A familiar example of a process obeying Poisson statistics is the number of photons arriving during an integration. The probability of a photon arriving in a fixed interval of time is (often) small. The arrivals of successive photons are independent (apart from small correlations arising because photons obey Bose–Einstein statistics, negligible for our purposes). Thus the conditions necessary for the Poisson distribution are met. Hence, if the integration over time t of photons arriving at a rate λ has a mean of $\mu = \lambda t$ photons, then the fluctuation on this number will be $\sigma = \sqrt{\mu}$. (In practice we usually only know the number of photons in a single exposure, rather than the mean number; obviously we can then only estimate the μ. This case is the subject of an exercise in the next chapter.)

For photon-limited observations, such as CCD images or spectra, $\mu = \lambda t$ while $\sigma = \sqrt{\lambda t}$. If we 'integrate' more,

$$\sigma \propto \sqrt{t}, \quad \text{while signal} \propto t.$$

Thus Signal/Noise $\propto \sqrt{t}$, the sky-limited case.
There are the following further cases:

(i) Photon-limited, e.g. CCD observations of faint objects:

$$S/N \propto \frac{\mu}{\sqrt{\mu}}, \quad \text{or} \quad \propto \sqrt{t}.$$

(ii) Readout-limited, e.g. CCD observations of bright objects:

$$S/N \propto \frac{\mu}{\sigma_{\text{ccd}}}, \quad \text{or} \quad \propto t$$

for CCD of readout noise σ_{ccd}.

(iii) Receiver-limited, e.g. radio astronomy:

$$S/N \propto \frac{S}{\sigma_{\text{rec}}/\sqrt{t}}, \quad \text{or} \quad \propto \sqrt{t}$$

for a receiver of thermal noise σ_{rec}.

2.4.2.3 Gaussian (Normal) distribution

Both the Binomial and the Poisson distributions tend to the Gaussian distribution (Fig. 2.5), large N in the case of the Binomial, large μ in

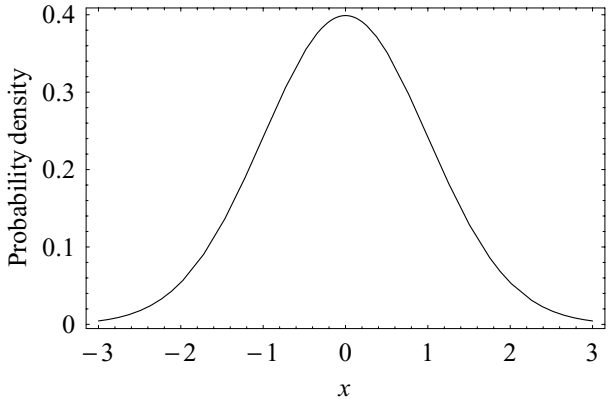

Fig. 2.5. The Normal (Gaussian) distribution. The area under the curve is 1.00; the area between $\pm 1\sigma$ is 0.68; between $\pm 2\sigma$ is 0.95; and between $\pm 3\sigma$ is 0.997.

the case of the Poisson. The (univariate) Gaussian (Normal) distribution is

$$\text{prob}(x) = \frac{1}{\sigma\sqrt{2\pi}} \exp\left[-\frac{1}{2\sigma^2}(x-\mu)^2\right] \tag{2.11}$$

from which it is easy to show that the mean is μ and the variance is σ^2 (Section 3.1). How this comes about for the Binomial distribution is the subject of an exercise.

For the Binomial when the sample size is very large, the discrete distribution tends to a continuous probability density

$$\text{prob}(n) = \frac{1}{\sigma\sqrt{2\pi}} \exp\left[-\frac{1}{2\sigma^2}(n-\mu)^2\right]$$

in which the mean $\mu = Np$ and variance $\sigma^2 = Np(1-p)$ are still given by the parent formulae for the Binomial distribution. Here is an instance of the discrete changing to the continuous distribution: in this approximation we can treat n as a continuous variable (because n changes by one unit at a time, being an integer, and so the fractional change $1/n$ is small).

The true importance of the Gaussian distribution and its dominant position in experimental science, however, stems from the central limit theorem. A non-rigorous statement of this is as follows.

Form averages M_n from repeatedly drawing n samples from a population with finite mean μ, variance σ^2. Then the distribution of

$$\left[\frac{(M_n - \mu)}{\sigma/\sqrt{n}}\right] \rightarrow \text{Gaussian distribution}$$

with mean 0, variance 1, as $n \rightarrow \infty$.

This is a remarkable theorem. What it says is that provided certain conditions are met – and they are in almost all physical situations – a little bit of averaging will produce a Gaussian distribution of results no matter what the shape of the distribution from which the sample is drawn. Even eyeball integration counts. It means that errors on averaged samples will always look 'Gaussian'. The reliance on Gaussian distributions, made valid by the unsung hero of statistical theory and indeed experimentation, the central limit theorem, shapes our entire view of experimentation. It is this theorem which leads us to describe our errors in the universal language of sigmas, and indeed to argue our results in terms of sigmas as well, which we explicitly or implicitly recognize as describing our place within or at the extremities of the Gaussian distribution. Figure 2.6 demonstrates the compelling power of the central limit theorem. Here we have brutally truncated an exponential, clearly an extremely non-Gaussian distribution. The histogram obtained in drawing 200 random samples from the distribution follows it closely. When 200 values resulting from averaging just four values have been formed, the distribution is already becoming symmetrical; by the time 200 values of 16 long averages have been formed, it is virtually Gaussian.

Before leaving the central limit miracle and Gaussian distributions, it is important to emphasize how tight the tails of the Gaussian distribution are (Table A2.2). The range $\pm 2\sigma$ encompasses 95.45 per cent of the area. Thus the infamous 2σ result has a less than 5 per cent chance of occurring by chance. But we scoff – because the error estimates are difficult to make, and observers are optimistic. Things upset the distribution; there are outlying points. Thus astronomers feel it necessary to quote results in the range 3σ to even 10σ, casting inevitable doubt on belief in their own error estimates. In fact, experimentalists are aware of another key feature of the central limit theorem: the convergence to a Gaussian happens fastest at the centre of the distribution, but the wings may converge much more slowly to a Gaussian form. Interesting results (the 10σ ones) of course acquire their probabilistic interpretation from knowing the shape of the tails to high accuracy.

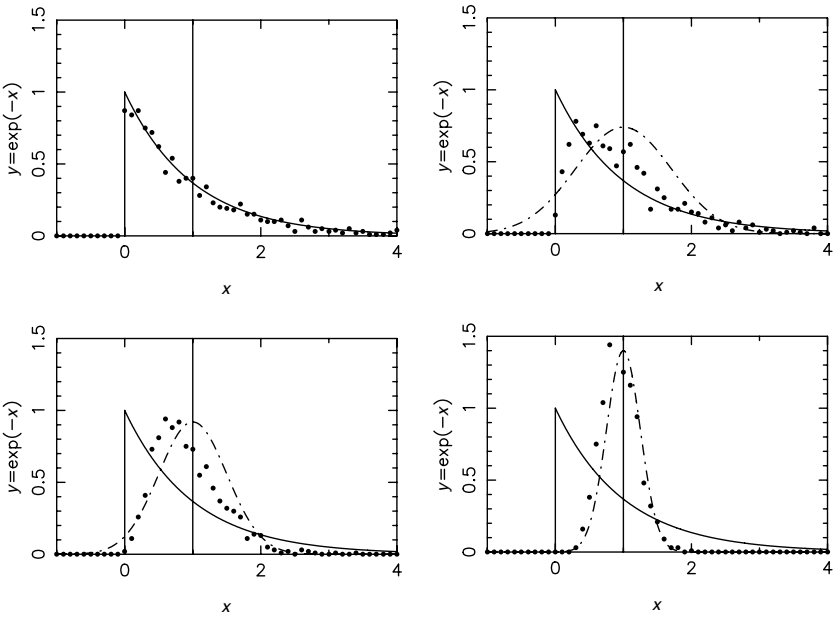

Fig. 2.6. An indication of the power of the central limit theorem. The panels show successive amounts of 'integration': in the upper left panel, a single value has been drawn; in the upper right, 200 values have been formed from an average of two values; lower left, 200 values from an average of four; lower right, 200 values from an average of 16.

2.5 Inferences with probability

What can we do with Bayesian probability calculations? We will use these many times in the rest of this book, but here is a summary of the method.

First, we may estimate parameters. This is closely related to the field of data modelling (Section 6.1). We have a probability distribution $f(\text{data} \mid \vec{\alpha})$ and we wish to know the parameter vector $\vec{\alpha}$. The Bayesian route is clear; compute the posterior distribution of $\vec{\alpha}$, as we have shown in several examples in this chapter.

EXAMPLE Suppose we have N data X_i, drawn from a Gaussian of known variance σ^2 but unknown mean μ. The parameter we want is μ. To proceed, we need a prior on μ; we take the so-called 'diffuse' prior,

where

$$\text{prob}(\mu) = \text{constant}$$

over some wide range of μ, the range defined by our knowledge of the problem. Of course we might have more precise information available.

From Bayes, the posterior distribution follows at once:

$$f(\mu \mid \text{data}) \propto \exp\left[-\frac{\sum_{i=1}^{N}(X_i - \mu)^2}{2\sigma^2}\right]$$

and with some simplification we get

$$f(\mu \mid \text{data}) \propto \exp\left[-\frac{\frac{1}{N}\sum_{i=1}^{N}(X_i - \mu)^2}{2\frac{\sigma^2}{N}}\right]$$

so that the average of the data is distributed around μ, with variance σ^2/N. One of the exercises is to find the distribution of the variance, knowing the mean.

This method is related to the classical technique of maximum likelihood. If the prior is 'diffuse', as in the example, then the posterior probability is proportional to the likelihood term $f(\text{data} \mid \vec{\alpha})$. Maximum likelihood picks out the mode of the posterior, the value of $\vec{\alpha}$ which maximizes the likelihood. This amounts to characterizing the posterior by one number, an approach which is often useful because of powerful theorems on maximum likelihood. We consider this in more detail in Section 6.1; some exercises at the end of this chapter illustrate the procedure.

Often knowing the posterior distribution of the parameter of interest is enough; we might be making a comparison with an exactly known quantity, perhaps derived from some theory. However we may wish to compare with an experimental determination of some other parameter $\vec{\beta}$. A typical case, for scalar parameters α and β, would be to ask for the probability that, say, α is bigger than β.

Suppose therefore we have derived two distributions $\text{prob}(\alpha) = p_A(\alpha)$ and $\text{prob}(\beta) = p_B(\beta)$ from independent samples. The probability that α is larger than β is

$$p(\alpha > \beta) = \int_{-\infty}^{\infty} p_B(y)\,\mathrm{d}y \int_{y}^{\infty} p_A(x)\,\mathrm{d}x$$

and the double integral simplifies to

$$p(\alpha > \beta) = \int_{-\infty}^{\infty} (1 - C_A(x) p_B(x)\ \mathrm{d}x$$

in which C_A is the cumulative distribution corresponding to p_A. If p_A and p_B are the same distribution, this becomes $p(\alpha > \beta) = 1/2$, as expected. Usually these integrals have to be done numerically case by case, but are worth the effort.

We may express posterior probabilities by using the notion of odds, a handy way of expressing probabilities when we have only two possibilities. The odds on event A are just

$$\frac{\mathrm{prob}(A)}{\mathrm{prob}(\mathrm{not}\, A)}.$$

For instance, the odds on throwing a 6 with a fair die are 5 to 1 (probability of 1/6 for throwing a six, 5/6 for anything else). From a betting point of view, the odds on a bet give the profit that might be made on a stake; in the case of our example with dice, being offered 5 to 1 odds for a 6 means we would get \$5 profit (\$6 payout) on a stake of \$1, if a 6 comes up. Of course a bookie will offer slightly different odds, to be sure of a profit in the long run. If we have two exclusive possibilities for a prior, say A and not A, then the posterior odds are given by the ratio of the posterior probabilities with each prior, and give an indication of which prior to bet on, given the available data.

Exercises

2.1 **A warm-up on coin-tossing.** This is not an astronomical problem but does provide a warm-up exercise on probability and random numbers. Every computer has a way of producing a random number between zero and one. Use this to simulate a simple coin-tossing game where player A gets a point for heads, player B a point for tails. Guess how often in a game of N tosses the lead will change; if A is in the lead at toss N, when was the previous change of lead most likely to be? And by how much is a player typically in the lead? Try to back these guesses up with calculations, and then simulate the game. For many more game-based illustrations of probability, see Haigh (1999).

2.2 **Efficient choosing.** Imagine you are on a 10-night observing run with a colleague, in settled weather. You have an agreement that one of the nights, of your choosing, will be for your exclusive use. Show that, if you wait for five nights and then choose the first night that is better than any of the five, you have about a 25 per cent chance of getting the best night of the ten. For a somewhat harder challenge, find the optimum length of the 'training sample'.

2.3 **Bayesian inference.** Consider the proverbial bad penny, for which prior information has indicated that there is a probability of 0.99 that it is unbiased ('ok'); or a probability of 0.01 that it is double-headed ('dh'). What is the (Bayesian) posterior probability, given this information, of obtaining seven heads in a row? In such a circumstance, how might we consider the fairness of the coin? Or of the experimenter who provided us with the prior information? What are the odds on the penny being fair?

2.4 **Laplace's rule and priors.** Laplace's rule (Section 2.3) $\overline{\rho} = (N + 1)/(N + M + 2)$ depends on our prior for ρ. If we have one success and no failures, consider what the rule implies, and discuss why this is odd. How is the rule changed for alternative priors, for example Haldane's?

2.5 **Bayesian reasoning in an everyday situation.** The probability of a certain medical test being positive is 90 per cent, if the patient has disease D. If your doctor tells you the test is positive, what are your chances of having the disease? If your doctor also tells you that 1 per cent of the population have the disease, and that the test will record a false positive 10 per cent of the time, use Bayes' theorem to calculate the chance of having D if the test is positive.

2.6 **Inverse Chi-squared statistic.** For a Gaussian of known mean (say zero), show that the posterior distribution for the variance is "inverse" χ^2. Use the 'Jeffreys prior' for the variance: $\text{prob}(\sigma) = 1/\sigma$. Comment on the differences between this result, and the one obtained by using a uniform prior on σ.

2.7 **Maximum likelihood and the Poisson distribution.** Suppose we have data which obey a Poisson distribution with parameter μ, and in successive identical intervals we observe n_1, $n_2, \ldots$ events. Form the likelihood function by taking the product

of the distributions for each n_i, and differentiate to find the maximum-likelihood estimate of μ. Is it what you expect?

2.8 **Maximum likelihood and the exponential distribution.** Suppose we have data $X_1, X_2, \ldots$ from the distribution $1/2a \exp(-|x|/a)$. Compute the posterior distribution of a for a uniform prior, and Jeffreys's prior $\text{prob}(a) \propto 1/a$. Do the differences seem reasonable? Which prior would you choose? If a were known, but the location μ was to be found, what would be the maximum-likelihood estimate?

2.9 **Birth control.** Imagine a society where boys and girls were (biologically) equally likely to be born, but families cease producing children after the birth of the first boy. Are there more males than females in the population? Attack the problem in three ways: pure thought, by a simulation, and by an analytic calculation.

3

Statistics and expectations

> Lies, damned lies and statistics.
> *(Benjamin Disraeli)*

In embarking on statistics we are entering a vast area, enormously developed for the Gaussian distribution in particular. This is classical territory; historically, statistics were developed because the approach now called Bayesian had fallen out of favour. Hence direct probabilistic inferences were superseded by the indirect and conceptually different route, going through statistics and intimately linked to hypothesis testing. The use of statistics is not particularly easy. The alternatives to Bayesian methods are subtle and not very obvious; they are also associated with some fairly formidable mathematical machinery. We will avoid this, presenting only results and showing the use of statistics, while trying to make clear the conceptual foundations.

3.1 Statistics

Statistics are designed to summarize, reduce or describe data. The formal definition of a `statistic` is that it is some function of the data alone. For a set of data $X_1, X_2, \ldots$, some examples of statistics might be the average, the maximum value or the average of the cosines. Statistics are therefore combinations of finite amounts of data. In the following discussion, and indeed throughout, we try to distinguish particular fixed values of the data, and functions of the data alone, by upper case (except for Greek letters). Possible values, being variables, we will denote in the usual algebraic spirit by lower case.

The summarizing aspect of statistics is exemplified by those describing (1) location and (2) spread or scatter.

(1) The location of the data can be indicated by various combinations:

Average, denoted by overlining: $\overline{X} = 1/N \sum_{i=1}^{N} X_i$.

Median: arrange X_i according to size; renumber. Then $X_{\rm med} = X_j$ where $j = N/2 + 0.5$, N odd, $X_{\rm med} = 0.5(X_j + X_{j+1})$ where $j = N/2$, N even.

Mode: $X_{\rm mode}$ is the value of x_i occurring most frequently; it is the location of the peak in the histogram of X_i.

(2) Statistics indicating the scale or amount of scatter in the data are, for example,

Mean deviation: $\overline{\Delta X} = (1/N) \sum_{i=1}^{N} |X_i - \overline{X}|$.

Mean square deviation: $S^2 = (1/N) \sum_{i=1}^{N} (X_i - \overline{X})^2$.

Root mean square deviation: rms $= S$.

We are so familiar with statistics like these that a result such as 'D $= 8.3 \pm 0.1$ Mpc' provokes no questions. But what does it mean? It does not tell us the probability that the true value of D is between 8.2 and 8.4. We usually assume that a Gaussian distribution applies, placing our faith in the central limit theorem. Knowing the distribution of the errors allows us to make probabilistic statements, which are what we need. After all, if there were only a 1 per cent chance that the interval $[8.2, 8.4]$ contained the true value of D, we might not regard the stated error as being very useful.

So this is one key aspect of statistics; they are associated with distributions. In fact they are most useful when they are estimators of the parameters of distributions. In quoting our measurement of D, we are hoping that 8.3 is an estimate of the parameter μ of some Gaussian, while 0.1 is an estimate of σ.

The other key aspect of statistics is that they are to be interpreted in a classical, not Bayesian framework. We need to look carefully at this distinction; it parallels our discussion of those coloured balls in the urn. Assuming a true distance D_0, a classical analysis tells us that D is (say) Normally distributed around D_0, with a standard deviation of 0.1. So we are to imagine many repetitions of our experiment, each yielding a value of the estimate D which dances around D_0. We might form a confidence interval (such as $[8.2, 8.4]$) which will also dance around randomly, but will contain D_0 with a probability we can calculate. Just as in the case of the coloured balls, this approach assumes the thing we want to know, and tells us how the data will behave.

A Bayesian approach circumvents all this; it deduces directly the probability distribution of D_0 from the data. It assumes the data, and tells us the thing we want to know. There are no imagined repetitions of the experiment. Conceptually it is clearer than classical methods, but these are so well developed and established (particularly for the Gaussian) that we will give some explanation of classical statistics now, and indeed use classical results in many places in this book.

It is worth remembering, however, that statistics of known usefulness are quite rare; the intensive development of statistics based on the Gaussian should not blind us to this fact. In many cases of astronomical interest we may need to derive useful statistics for ourselves. By far the easiest method for doing this is maximum likelihood (Section 6.1) and this is so close to a Bayesian method that we may expect to be doing Bayesian, not classical, inference in any new case where we cannot draw immediately on classical results.

To repeat, statistics are properties of the data and only of the data; they summarize, reduce, or describe the data. Variables such as μ and σ of the Poisson and Gaussian distributions define these distribution functions and are not statistics. But we may anticipate that our data do follow these or other distributions and we may therefore wish to relate statistics from the data to parameters describing the distributions.

This is done through expectations or expectation values, long-run average properties depending on distribution functions. The expectation $E[f(x)]$ of some function f of a random variable x, with distribution function g, is defined as

$$E[f(x)] = \int f(x)g(x)\,\mathrm{d}x \tag{3.1}$$

i.e. the sum of all possible values of f, weighted by the probability of their occurrence. We can think of the expectation as being the result of repeating an experiment many times, and averaging the results. We might, for example, compute an average $\overline{X}$; if we repeat the experiment many times, we will find that the average of $\overline{X}$ will converge to the true mean value, the expectation of the function $f(x) = x$:

$$E[x] = \int xg(x)\,\mathrm{d}x. \tag{3.2}$$

Note that the expectation is not to be understood as referring to a very large sample; we can ask for the expectation value of a combination of a finite number of data.

The statistic S^2 should likewise converge to the variance, defined by

$$\begin{aligned} \mathrm{var}[x] &= E[(x-\mu)^2] && (3.3)\\ &= \int (x-\mu)^2 g(x)\,\mathrm{d}x. && (3.4) \end{aligned}$$

However, as we shall see, we do have to take some care that the integrals actually exist.

EXAMPLE Take our favourite distribution, the Gaussian. The probability density of getting a datum x near μ is

$$g(x \mid \mu, \sigma) = \frac{1}{\sqrt{2\pi}\sigma} \exp\left[\frac{-(x-\mu)^2}{2\sigma^2}\right]$$

but what are these parameters μ and σ? It's not difficult to show (changing variables and using standard identities) that

$$E[x] = \int x g(x \mid \mu, \sigma)\,\mathrm{d}x = \mu, \tag{3.5}$$

and

$$E[(x-\mu)^2] = \int (x-\mu)^2 g(x \mid \mu, \sigma)\,\mathrm{d}x = \sigma^2. \tag{3.6}$$

We would therefore expect that the average $\overline{X}$ and mean square deviation S^2 would be related to μ and σ^2. As any statistics text will show, indeed $\overline{X}$ and S^2, although they are functions only of the data and therefore show random variation, will converge to μ and σ^2 when we have a lot of data.

Other distributions give different results. Take the exponential distribution

$$f(x) = \frac{1}{2a} \exp\left(-\frac{|x|}{a}\right)$$

where the expectation of $|x|$ is the width parameter a.

The pathological Cauchy distribution

$$f(x) = \frac{1}{\pi(1+x^2)}$$

has the alarming property that the expectation of the average of N data is, again, the same Cauchy distribution; the location can apparently just

as well be estimated with one datum. The difficulty arises because the distribution has such wide wings. In astronomy, broad or even open-ended (power-law) distributions are common. It is worth checking any piece of remembered statistics, as it is almost certain to be based on the Gaussian distribution.

Other expectations of theoretical importance are known as the *n*th central moments:

$$\mu_n = \int (x - \mu)^n g(x)\, \mathrm{d}x \tag{3.7}$$

where g is some probability distribution. They are estimated analogously by suitable averages to the way in which mean and variance were estimated in the previous example. They are sometimes useful for characterizing the shape of distributions, although they are very sensitive to outliers. Two descriptors using moments are common: skewness, $\beta_1 = \mu_3^2$, indicates deviation from symmetry (= 0 for symmetry about μ); and kurtosis, $\beta_2 = \mu_4/\mu_2^3$, indicates degree of peakiness (= 3 for the Gaussian distribution).

The Chebyshev inequality is sometimes useful: for any positive integer n, and data X drawn from a distribution of mean μ and variance σ^2,

$$\mathrm{prob}[|X - \mu| > n\sigma] \leq \frac{1}{n}. \tag{3.8}$$

This is very conservative but is sometimes better than nothing as an estimate.

3.2 What should we expect of our statistics?

We have but a few of the data X_i but we want to know how all of them are organized; we want their probability or frequency distribution and we want it for as little effort as we can get away with (efficiently) and as accurately as possible (robustly). Suppose, for instance, that we are drawing samples from a population obeying a Gaussian defined by $\mu = 0$, $\sigma = 1$. Figure 3.1 conveys some indication of how the size of sample would affect estimates of these parameters.

There are, then, at least four requirements for statistics.

(i) They should be unbiased, meaning that the expectation value of the statistic turns out to be the true value. For the Gaussian

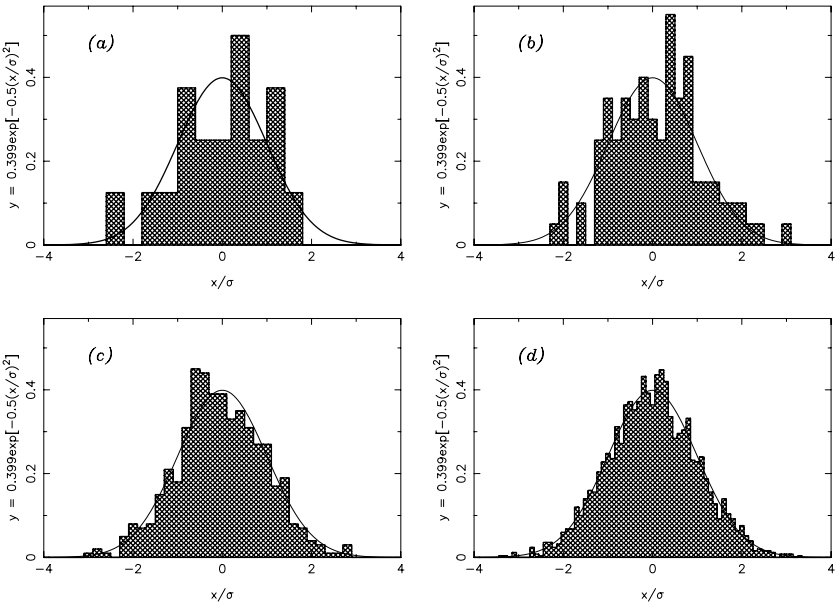

Fig. 3.1. X_i drawn at random from a Gaussian distribution of $\sigma = 1$: (a) 20 values, (b) 100 values, (c) 500 values, (d) 2500 values. The average values of x_i are 0.003, 0.080, −0.032 and −0.005; the median values 0.121, 0.058, −0.069 and −0.003; and the rms values 0.968, 1.017, 0.986, and 1.001. Solid curves represent Gaussians of unit area and standard deviation.

distribution (Section 2.4.2.3), for data X_i, $\overline{X}$ is indeed an unbiased estimate of the mean μ, but the unbiased estimate of the variance σ^2 is

$$\sigma_{\mathrm{s}}^2 = \frac{1}{N-1}\sum_{i=1}^{N}(X_i - \overline{X})^2$$

which differs from the expectation value of S^2 by the factor $N/(N-1)$. The factor is confusing: σ_{s}^2, sometimes referred to as the sample variance, is the estimator for the population variance σ^2. (The difference is understandable as follows. The X_i of our sample are first used to get $\overline{X}$, an estimate of μ, and although this is an unbiased estimate of μ it is the estimate which yields a minimum value from the sum of the squares of the deviations of the sample, and thus a low estimate of the variance. The theory provides the appropriate correction factor $N/(N-1)$; of course the difference disappears as $N \to \infty$.)

(ii) They should be consistent, the case if the descriptor for an arbitrarily large sample size gives the true answer. As we have seen, the rms is a consistent measure of the standard deviation of a Gaussian distribution in that it gives the right answer for large N; but it is a biased estimator for small N unless modified by the factors just discussed.

(iii) The statistic should obey closeness, yielding the smallest possible deviation from the truth. The Cauchy distribution (Section 3.1) looks innocent enough, somewhat similar to a Gaussian, even. But with infinite variance, trying to estimate dispersion via the standard deviation would yield massive scatter and little information.

(iv) The statistic should be robust. For example, if we have a fundamentally symmetric distribution of data but a few experimental errors creep in, outliers appearing at the ends of the distribution, then as a measure of central location the median is far more robust than the average – it is less affected by the outliers.

3.3 Simple error analysis

3.3.1 Random or systematic?

The average is a very common statistic; it is what we are doing all the time, for example, in 'integrating' on a faint object. The variance on the average is

$$S_{\rm m}^2 = E\left[\left(\frac{1}{N}\sum_{i=1}^{N} X_i - \mu\right)^2\right]$$

which, after some manipulation, is

$$S_{\rm m}^2 = \frac{\sigma^2}{N} + \frac{1}{N^2}\sum_{i\neq j} E[(X_i-\mu)(X_j-\mu)]. \tag{3.9}$$

Neglecting the last term for the moment, the first term expresses generally held belief – the error on the mean of some data diminishes, like $\sqrt{N}$, as the amount of data is increased. This is one of the most important tenets of observational astronomy.

Now for the last term: apart from infinite variances (e.g. the Cauchy distribution), the familiar and comforting $\sqrt{N}$ result holds only when this last term is zero. The term contains the covariance, defined as

$$\mathrm{cov}[X_i, X_j] = E[(X_i-\mu_i)(X_j-\mu_j)]; \tag{3.10}$$

it is closely related to the correlation coefficient between x_i and x_j (Section 4.2). We are keeping the subscripts now because of the possibility that the data from the ith pixel, spectral channel, or time slot, are not independent of the data from the jth position. In the simplest cases, the data are independent and identically distributed (probability of X_i and X_j = probability of X_i × probability of X_j) and then the covariance is zero. This is a condition (probably the likeliest) for the familiar $\sqrt{N}$ averaging away of noise; our assumption is that noise from one datum to the next or one pixel to the next is independent.

EXAMPLE Suppose we had a time series, say of photometric measurements X_i. Here the i's index time of observation. It might be a reasonable assumption that the measurements were identically distributed and independent of each other. In this case, the probability distribution would be the same for each time, and so can just be written $g(x \mid \text{parameters})$. The covariance term is then just

$$\begin{aligned} \operatorname{cov}[X_i, X_j] &= E[(X_i - \mu_i)(X_j - \mu_j)] \\ &= \int (x_i - \mu_i) g(x_i \mid \ldots)\, \mathrm{d}x_i \int (x_j - \mu_j) g(x_j \mid \ldots)\, \mathrm{d}x_j \\ &= 0 \end{aligned} \tag{3.11}$$

because, by definition of μ, each integral must separately be zero.

Often this simple situation does not apply. One possibility is that $\operatorname{cov}[x_i, x_j]$ depends only on a 'distance' $(i - j)$. If the data are indexed in some meaningful way, for example as a time series, the data are called **stationary**. As a second possibility, in photometric work it is quite likely that if one measurement is low, because of cloud, then the next few will be low too. (We speak of the dreaded $1/f$ noise; more of this in Section 8.8.) Then the probability distribution becomes multivariate and the simple factorizations do not apply:

$$E[(X_i - \mu_i)(X_j - \mu_j)] = \int\int (x_i - \mu_i)(x_j - \mu_j) g(x_i, x_j \mid \ldots)\, \mathrm{d}x_i\, \mathrm{d}x_j$$

so that we need to know more about the observational errors – in other words, how to write down $g(x_i, x_j \mid \ldots)$ – before we can assess how the

average of the data will behave. In these more complicated cases, the averaging away is almost certain to be slower than $\sqrt{N}$.

A common distinction is made in experimental subjects between random and systematic errors, random errors being considered as those showing the $\sqrt{N}$ diminution. In reality there is a continuum, with the covariance frequently non-zero. At the other far extreme, systematic errors persist no matter how much data are collected. If you are observing Arcturus when you should be observing Vega, the errors will never average away no matter how persistent you are. Systematic errors can only be reduced by thorough understanding of the experimental equipment and circumstances; 'random' errors may be more or less random, depending on how correlated they are with each other.

3.3.2 Error propagation

Often the thing we need to know is some more or less complicated function of the measured data. Knowing data error, how do we estimate error in the desired quantity?

If the errors are small, by far the easiest way is to use a Taylor expansion. Suppose we measure variables $x, y, z, \ldots$ with independent errors $\delta X, \delta Y, \delta Z, \ldots$ and we are interested in some function $f(x, y, z, \ldots)$. The change in f caused by the errors is, to first order,

$$\delta F = \left.\frac{\partial f}{\partial x}\right|_{x=X} \delta X + \left.\frac{\partial f}{\partial y}\right|_{y=Y} \delta Y + \left.\frac{\partial f}{\partial z}\right|_{z=Z} \delta Z + \cdots$$

The variance on a sum is the sum of the variances of the individual terms (because the errors are assumed to be independent) so we get

$$\mathrm{var}[f] = \left.\left(\frac{\partial f}{\partial x}\right)^2\right|_{x=X} \sigma_x^2 + \left.\left(\frac{\partial f}{\partial y}\right)^2\right|_{y=Y} \sigma_y^2 + \left.\left(\frac{\partial f}{\partial z}\right)^2\right|_{z=Z} \sigma_z^2 + \cdots \tag{3.12}$$

where the σ represent the variances in each of the variables.

These considerations lead to a well-known result for combining measurements: if we have n independent estimates, say X_j, each having an associated error σ_j, the best combined estimate is the weighted mean,

$$\overline{X}_{\mathrm{w}} = \frac{\sum_{j=1}^{n} w_j \overline{X}_j}{\sum_{j=1}^{n} w_j}$$

where the weights are given by $w_j = 1/\sigma_j^2$, the reciprocals of the sample

variances. The best estimate of the variance of $\overline{X}_{\rm w}$ is

$$\sigma_{\rm w}^2 = \frac{1}{\sum_{j=1}^{n} 1/\sigma_j^2}.$$

EXAMPLES Suppose (i) $f(x, y) = x/y$. Then the rule gives us immediately

$$\frac{\mathrm{var}[f]}{f^2} = \left(\frac{\sigma_x}{x}\right)^2 + \left(\frac{\sigma_y}{y}\right)^2;$$

we simply add up the relative errors in quadrature. If (ii) $f(x) = \log x$ then the rule gives

$$\mathrm{var}[f] = \left(\frac{\sigma_x}{x}\right)^2$$

and the error in the log is just the relative error in the quantity we have measured.

3.3.3 Combining distributions

Often this method is not good enough – we may need to know details of the probability distribution of the derived quantity. The simplest case is a transformation from the measured x, with probability distribution g, to some derived quantity $f(x)$ with probability distribution h. Since probability is conserved, we have the requirement that

$$h(f)\,\mathrm{d}f = g(x)\,\mathrm{d}x \tag{3.13}$$

so that h involves the derivative $\mathrm{d}f/\mathrm{d}x$. Some care may be needed in applying this simple rule if the function f is not monotonic.

EXAMPLE Suppose we are taking the logarithm of some exponentially distributed data. Here $g(x) = \exp(-x)$ for positive x, and $f(x) = \log(x)$. Applying our rule gives

$$h(f) = \exp(-\exp(f))\exp(f)$$

which, as we might expect (Fig. 3.2) has a pronounced tail to negative values and is correctly normalized to unity. Our simpler methods would give us $\delta h = \delta x/x$, which evidently cannot give a good representation of the asymmetry of h. Quoting '$h \pm \delta h$' is clearly not very informative.

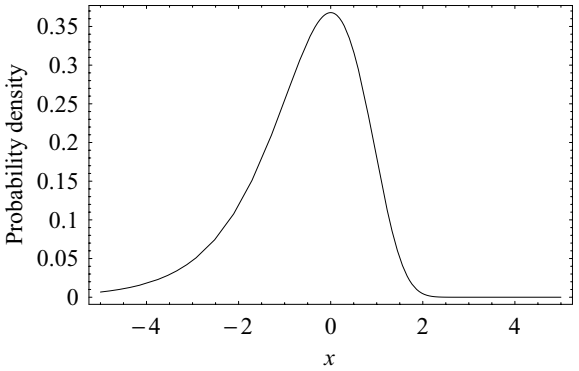

Fig. 3.2. The probability distribution of the logarithm of data drawn from an exponential distribution.

This technique rapidly becomes difficult to apply for more than one variable, but results for some useful cases are as follows.

(1) Suppose we have two identically distributed independent variables x and y, both with distribution function g. What is the distribution of their sum $z = x + y$? For each x, we have to add up the probabilities of all the numbers $y = z - x$ that yield the z we are interested in. The probability distribution $h(z)$ is therefore

$$h(z) = \int g(z - x)g(x)\,\mathrm{d}x \tag{3.14}$$

where the probabilities are simply multiplied because of the assumption of independence. h is therefore the autocorrelation (Section 8.2) of g. The result generalizes to the sum of many variables, and is often best calculated with the aid of the Fourier transform (Section 8.2) of the distribution g. This transform is sometimes called the characteristic function.

(2) Quite often we need the distribution of the product or quotient of two variables. Without details, the results are as follows. For $z = xy$, the distribution of z is

$$h(z) = \int \frac{1}{|x|} g(x)g(z/x)\,\mathrm{d}x \tag{3.15}$$

and of $z = x/y$ is

$$h(z) = \int |x|g(x)g(zx)\,\mathrm{d}x. \tag{3.16}$$

In almost any case of interest, these integrals are too hard to do analytically.

EXAMPLES One exception of interest is the product of two Gaussian variables of zero mean; this has applicability for a radio-astronomical correlator, for instance. Leaving out the mathematical details, the result emerges in the form of a modified Bessel function. The input Gaussians are of zero mean and variance σ^2. The distribution of the product is

$$h(z) = \frac{2}{\pi\sigma^2} K_0\left(\frac{|z|}{\sigma^2}\right)$$

which as Fig. 3.3 shows is quite unlike a Gaussian. It has a logarithmic singularity at zero but is normalized to unity.

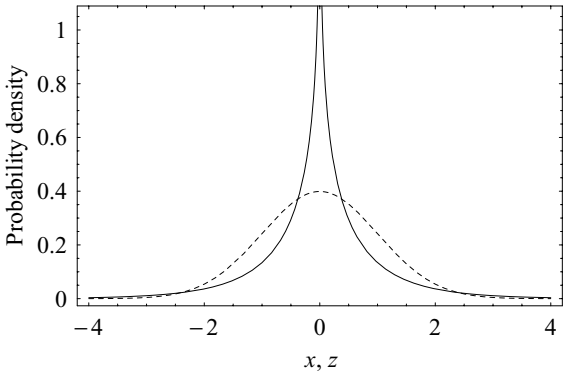

Fig. 3.3. The probability distribution of the product of two identical Gaussians – the original Gaussian is the dashed curve.

The case of the ratio is equally instructive. Here we get

$$h(z) = \frac{1}{\pi}\frac{1}{1+z^2},$$

a Cauchy distribution. It has infinite variance and, as we see in Fig. 3.4, the variance of the original Gaussian surprisingly does not appear in the answer.

This is a somewhat unrealistic case – it corresponds to forming the ratio of data of zero signal-to-noise ratio – but illustrates that ratios involving low signal-to-noise are likely to have very broad wings. The Bessel function distribution will, on average, succumb to the central limit theorem; this is not the case for the Cauchy distribution. In general, deviations from Normality will occur in the tails of distributions, the outliers that are so well known to all experimentalists.

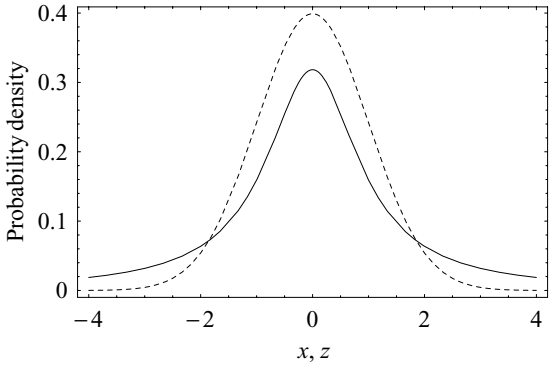

Fig. 3.4. The probability distribution of the ratio of two identical Gaussian variables the original Gaussian is the dashed curve.

3.4 Some statistics, and their distributions

For N data X_i, some useful statistics are the average, the sample variance, and the order statistics. We have already met the first two; they acquire their importance because of their relationship to the parameters of the Gaussian. If the X_i are independent and identically distributed Gaussian variables, where the original Gaussian has mean μ and variance σ^2, then:

(i) The average $\overline{X}$ obeys a Gaussian distribution around μ, with variance σ^2/N. We have met this result before (Section 2.5).

(ii) The sample variance $\sigma_{\rm s}^2$ is distributed like $\sigma^2\chi^2/(N-1)$, where the chi-square variable has $N-1$ degrees of freedom (Table A2.6).

(iii) The ratio

$$\frac{\sqrt{N}(\overline{X}-\mu)}{\sigma_{\rm s}^2}$$

is distributed like the t statistic, with $N-1$ degrees of freedom. This ratio has an obvious usefulness, telling us how far our average might be from the true mean (Table A2.3).

(iv) If we have two samples (size N and M) drawn from the same Gaussian distribution, then the ratio of the sample variances $\sigma_{\rm s_1}^2$ and $\sigma_{\rm s_2}^2$ follows an F distribution. This allows us to check if the data were indeed drawn from Gaussians of the same width (Section 5.2 and Table A2.4).

The order statistics are simply the result of arranging the data X_i in order of size, relabelled as $Y_1, Y_2, \ldots$ So Y_1 is the smallest value of X, and Y_N the largest. Maximum values are often of interest, and the median $Y_{N/2}$ (N even) is a useful robust indicator of location. We might also form robust estimates of widths by using order statistics to find the range containing, say, 50 per cent of the data. Both the density and the cumulative distribution are therefore of interest.

Suppose the distribution of x is $f(x)$, with cumulative distribution $F(x)$. Then the distribution g_n of the nth order statistic is

$$g_n(y) = \frac{N!}{(n-1)!(N-n)!}[F(y)]^{n-1}[1-F(y)]^{N-n}f(y) \qquad (3.17)$$

and the cumulative distribution is

$$G_n(y) = \sum_{j=n}^{N} \binom{N}{j} [F(y)]^j [1-F(y)]^{N-j}. \qquad (3.18)$$

EXAMPLE The Schechter luminosity function $x^\gamma \exp(-x/x^*)$ is a useful model of the luminosity function for field galaxies. The observed value of γ is close to unity, but we will take $\gamma = 1/2$ for convenience in ensuring the distribution can be normalized over the range zero to infinity; we also take $x^* = 1$. If we select 10 galaxies from this distribution, the maximum of the 10 will follow the distribution shown in Fig. 3.5. We

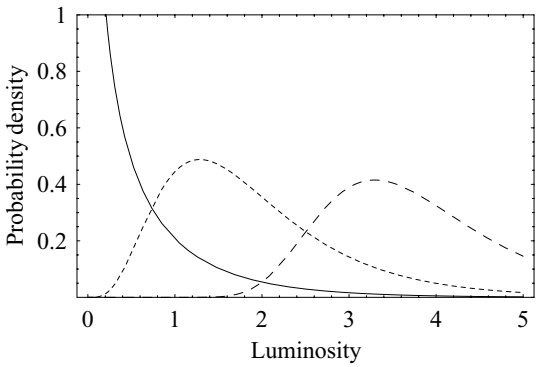

Fig. 3.5. The Schechter luminosity function (solid curve) and the distribution of the maximum of 10 and 100 samples from the distribution, plotted as short- and long-dash curves respectively.

see that the distribution is quite different from the Schechter function, with a peak quite close to x^*. If we choose 100 galaxies, then of course the distribution moves to brighter values.

3.5 Uses of statistics

So far, we have concentrated on defining statistics and noticing that they (a) may estimate parameters of distributions and (b) will be distributed in some more or less complicated way themselves. Their use then parallels the Bayesian method.

First, we may use them to estimate parameters; but the way in which they do this is more subtle than the Bayesian case. We do not get a probability distribution for the parameter of interest, but a distribution of the statistic, given the parameter. As noted in the introductory section of this chapter, the confidence interval is the usual way of making use of a statistic as an estimator.

Second, we may test hypotheses. This again parallels the Bayesian case, but the methods are much further apart conceptually. Recall the case discussed in Section 2.5, where we have estimated parameters α and β. Using statistics, we would have two data combinations A (estimating α) and B (estimating β). How would we answer a question like 'is $\alpha > \beta$' in this approach? The classical method entails finding some new combination, say $t = A - B$, and then computing its distribution on the hypothesis that $\alpha - \beta = 0$. We then find the probability of the observed value of t, or bigger, occurring on this hypothesis; and if the probability is small, we would conclude that the data were unlikely to have occurred by chance. The hint, of course, is that indeed $\alpha > \beta$, but we do not know the probability of this.

This classical approach is the basis of numerous useful tests, and we discuss some of them in detail in later Chapters 4 and 5. However, there is no doubt that the method does not quite seem to answer the question we had in mind, although often its results are indistinguishable from the more intelligible Bayesian approach. The same decisions get taken.

Perhaps the most difficult part of this testing procedure is the implicit use of data corresponding to events that did not occur – the 'observed value of t, or bigger' referred to. Jeffreys (1961) wrote '...a

hypothesis that may be true may be rejected because it has predicted observable results that have not occurred. This seems a remarkable procedure.'

However, using large but unobserved values of the test statistic usually does not matter much; in cases of interest, our statistic will be unlikely anyway, and larger values will be even less likely.

Exercises

3.1 **Means and variances.** Find the mean and variance of a Poisson distribution and of a power law; find the variance ($= \infty$) of a Cauchy distribution.

3.2 **Simple error analysis.** Derive the well-known results for error combining, for two products, and the sum and difference of two quantities, from the Taylor expansion of Section 3.3.2.

3.3 **Combining Gaussian variables.** Use the result of Section 3.3.2 for errors on z when $z = x + y$ to find the distribution of the sum of two Gaussian variables.

3.4 **Average of Cauchy variables.** Show that the average value of Cauchy-distributed variables has the same distribution as the original data. Use characteristic functions and the convolution theorem. Find a better location estimator.

3.5 **Poisson statistics.** Draw random numbers from Poisson distributions (Section 6.5) with $\mu = 10$ and $\mu = 100$. Take 10 or 100 samples, find the average and the rms scatter. How close is the scatter to $\sqrt{\text{average}}$?

3.6 **Robust statistics.** Make a Gaussian with outliers by combining two Gaussians, one of unit variance, one three times wider. Leave the relative weight of the wide Gaussian as a parameter. Compare the mean deviation with the rms, for various relative weights. How sensitive are the two measures of scatter to outliers? Repeat the exercise, with a width derived from order statistics.

3.7 **Change of variable.** Suppose that ϕ is uniformly distributed between zero and 2π. Find the distribution of $\sin\phi$. How could you find the distribution of a sum of sines of independent random angles?

3.8 **Order statistics.** We record a burst of N neutrinos from a supernova, and the probability of recording a neutrino at time t

is, in suitable units, $\exp(t - t_0)$ where t_0 is the time of emission. The maximum-likelihood estimate of t_0 is just T_1, the time of arrival of the first neutrino. Use order statistics (Section 3.4) to show that the average value of T_1 is just $t_0 + \frac{1}{N}$. Is this MLE biased, but consistent (i.e. the correct answer as $N \to \infty$)?

4
Correlation and association

Arguing that the trial judge had failed to explain clearly the use of Bayes' theorem, the defence lodged an appeal. But in a bizarre irony, the Appeal Court last month upheld the appeal and ordered a retrial – on the grounds that the original judge had spent **too much** *time explaining the scientific assessment of evidence. In their ruling, the Appeal judges said: 'To introduce Bayes' theorem, or any similar method, into a criminal trial plunges the jury into inappropriate and unnecessary realms of theory and complexity'.*

(Robert Matthews, New Scientist 1996)

When we make a set of measurements, it is instinct to try to correlate the observations with other results. One or more motives may be involved in this instinct: for instance we might wish (1) to check that other observers' measurements are reasonable, (2) to check that our measurements are reasonable, (3) to test a hypothesis, perhaps one for which the observations were explicitly made, or (4) in the absence of any hypothesis, any knowledge, or anything better to do with the data, to find if they are correlated with other results in the hope of discovering some new and universal truth.

4.1 The fishing trip

Take the last point first. Suppose that we have plotted something against something, on a fishing expedition of this type. There are grave dangers on this expedition, and we must ask ourselves the following questions.

(1) Does the eye see much correlation? If not, calculation of a formal correlation statistic is probably a waste of time.

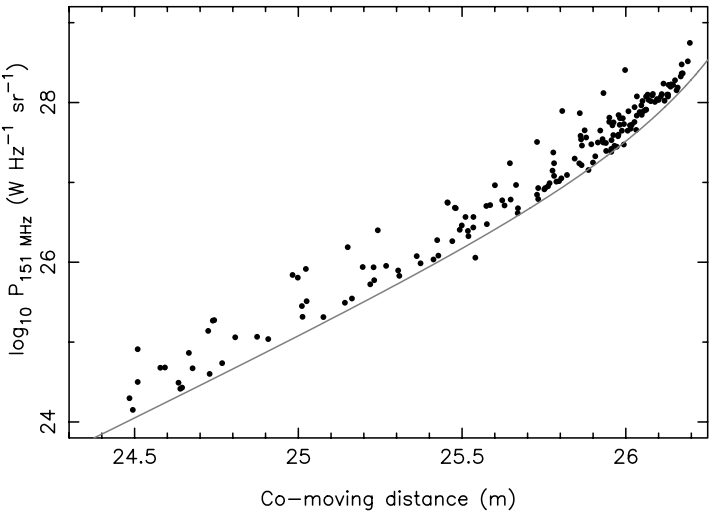

Fig. 4.1. Radio luminosities of 3CR radio sources versus distance modulus. The curved line represents the survey limit, the limit imposed by forming a catalogue from a flux-limited sample (Section 7.2).

(2) Could the apparent correlation be due to selection effects? Consider for instance the beautiful correlation in Fig. 4.1, in which Sandage (1972) plotted radio luminosities of sources in the 3CR catalogue as a function of distance modulus. At first sight, it proves luminosity evolution for radio sources. Are the more distant objects (at earlier epochs) clearly not the more powerful? In fact, as Sandage recognized, it proves nothing of the kind. The sample is flux- (or apparent intensity) limited; the solid line shows the flux-density limit of the 3CR catalogue. The lower right-hand region can never be populated; such objects are too faint to show above the limit of the 3CR catalogue. But what about the upper left? Provided that the luminosity function (the true space density in objects per megaparsec^3) slopes downward with increasing luminosity, the objects are bound to crowd towards the line. This is about all that can be gleaned immediately from the diagram – the space density of powerful radio sources is less than the space density of their weaker brethren.

Astronomers produce many plots of this type, and will describe purported correlations in terms such as 'The lower right-hand region of the diagram is unpopulated because of the detection limit, but there is no reason why objects in the upper left-hand region should have escaped

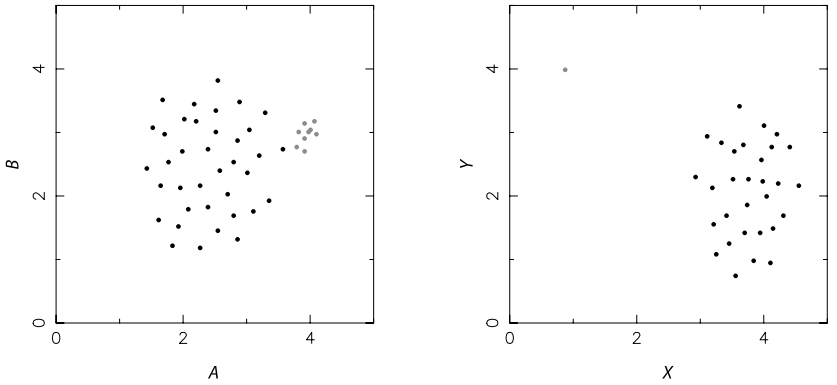

Fig. 4.2. Dodgy correlations: in each case formal calculation will indicate that a correlation exists to a high degree of significance.

detection'. True, but nor can they escape probability; the upper left of Sandage's diagram is not filled with QSOs and radio galaxies because we need to sample large spheres about us to have a hope of encountering a powerful radio source. Small spheres, corresponding to small redshifts and distance moduli, will yield only low-luminosity radio sources because their space density is so much the higher. The lesson applies to any proposed correlation for variables with steep probability density functions dependent upon one of the variables plotted.

(3) If we are happy about (2), we can try formal calculation of the significance of the correlation as described in Section 4.2. Further, if there is a correlation, does the regression line (Section 6.2) make sense?

(4) If we are still happy, we must return to the plot to ask if the formal result is realistic. A rule of thumb: if 10 per cent of the points are grouped by themselves so that covering them with the thumb destroys the correlation to the eye, then we should doubt it, no matter what significance level we have found. Beware in particular of plots which look like those of Fig. 4.2, plots which strongly suggest selection effects, data errors, or some other form of statistical conspiracy.

(5) If we are *still* confident, we must remember that a correlation does not prove a causal connection. The essential point is that correlation may simply indicate a dependence of both variables on a third variable. Cigarette manufacturers said so for years; but finding the physical attribute which caused heart/lung disease *and* the desire to smoke proved difficult. But there are many famous instances, e.g. the correlation

between quality of children's handwriting and their height, and between the size of feet in China and the price of fish in Billingsgate Market. For the former the hidden variable is age (Are tall children cleverer? No, but older), while for the latter it is time.

There are in fact ways of searching for intrinsic correlation between variables when they are known to depend mutually upon a third variable. The problem, however, when on the fishing trip, is how to know about a third variable, how to identify it when we might suspect that it is lurking. We consider it further in Sections 4.3 and 4.5.

Finally we must not get too discouraged by all the foregoing. Consider Fig. 4.3, a ragged correlation if ever there was one, although there are no nasty groupings of the type rejected by the rule of thumb. It is in fact one of the earliest 'Hubble diagrams' – the discovery of the recession of the nebulae, and the expanding universe (Hubble 1936).

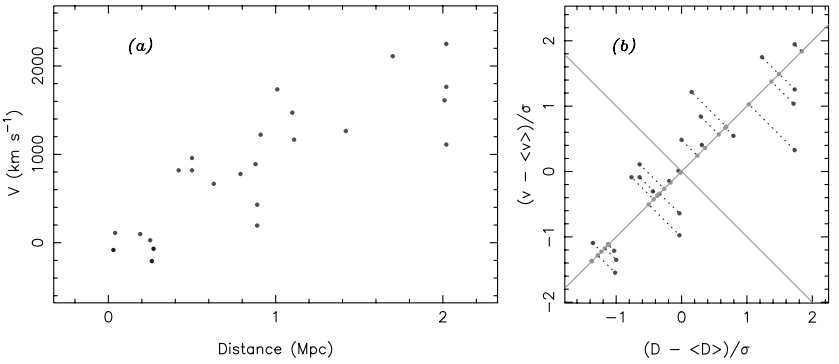

Fig. 4.3. (a) An early Hubble diagram (Hubble 1936); recession velocities of a sample of 24 galaxies versus distance measure. (b) The same plot but with data normalized by standard deviation; the lines represent principal components, as described in Section 4.5.

4.2 Testing for correlation

In dealing with correlations we encounter in detail many important aspects of the use of probability and statistics. The foregoing problem appears simple: we have a set of N measurements (X_i, Y_i) and we ask (formally) if they are related to each other.

To make progress we have to make 'related' more precise. The best-developed way of doing this – although not necessarily relevant – is to model our data as a bivariate or joint Gaussian of correlation

coefficient ρ:

$$\text{prob}(x, y \mid \sigma_x, \sigma_y, \rho) = \frac{1}{2\pi\sigma_x\sigma_y\sqrt{1-\rho^2}} \times \exp\left\{\frac{-1}{2(1-\rho^2)}\left[\frac{(x-\mu_x)^2}{\sigma_x^2} + \frac{(y-\mu_y)^2}{\sigma_y^2} - \frac{2\rho xy}{\sigma_x\sigma_y}\right]\right\}. \tag{4.1}$$

This model is so well developed that 'correlation' and '$\rho \neq 0$' are nearly synonymous; if $\rho \to 0$ there is little correlation, while if $\rho \to 1$ the correlation is perfect; see Fig. 4.4.

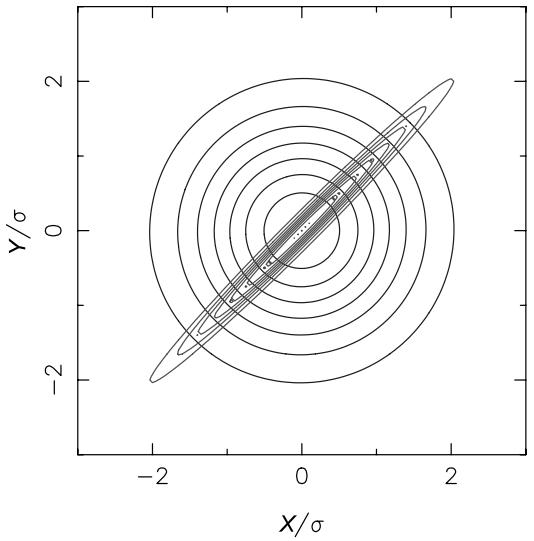

Fig. 4.4. Linear contours of the bivariate Gaussian probability distribution; the near-circular contours represent $\rho = 0.01$, a bivariate distribution with little connection between x and y, while the highly elliptical contours represent $\rho = 0.99$, indicative of a strong correlation between x and y. Negative values of ρ reverse the tilt, and indicate what is loosely referred to as anticorrelation.

The parameter ρ is the correlation coefficient, and in the above formulation, it is given by

$$\rho = \frac{\text{cov}[x, y]}{\sigma_x\sigma_y} \tag{4.2}$$

where cov is the covariance (Section 3.3.1) of x and y, and σ_x^2 and σ_y^2

are the variances. The correlation coefficient can be estimated by

$$r = \frac{\sum_{i=1}^{N}(X_i - \overline{X})(Y_i - \overline{Y})}{\sqrt{\sum_{i=1}^{N}(X_i - \overline{X})^2 \sum_{i=1}^{N}(Y_i - \overline{Y})^2}}. \tag{4.3}$$

r is known as the Pearson product-moment correlation coefficient (Fisher 1944).

The contours of Fig. 4.4 will have dropped by 1/e from the maximum at the origin when

$$\frac{1}{1-\rho^2}\left(\frac{x^2}{\sigma_x^2} + \frac{y^2}{\sigma_y^2} - \frac{2\rho xy}{\sigma_x \sigma_y}\right) = 1, \tag{4.4}$$

or in matrix notation, when

$$\begin{pmatrix} x & y \end{pmatrix} \frac{1}{1-\rho^2} \begin{pmatrix} \frac{1}{\sigma_x^2} & -\frac{\rho}{\sigma_x \sigma_y} \\ -\frac{\rho}{\sigma_x \sigma_y} & \frac{1}{\sigma_y^2} \end{pmatrix} \begin{pmatrix} x \\ y \end{pmatrix} = 1. \tag{4.5}$$

The inverse of the central matrix is known as the covariance matrix or error matrix

$$C = \begin{pmatrix} \sigma_x^2 & \mathrm{cov}[x,y] \\ \mathrm{cov}[x,y] & \sigma_y^2 \end{pmatrix}. \tag{4.6}$$

The off-diagonal elements of the covariance matrix can be estimated by

$$\frac{1}{N-1}\overline{(X_i - \overline{X_i})(X_j - \overline{X_j})}.$$

The matrix is particularly valuable in calculating propagation of errors, but there are numerous applications, for example in principal component analysis (Section 4.5) and in maximum-likelihood modelling (Section 6.1).

The multivariate Gaussian is one example of a class of multivariate distribution functions that depend only on the data vector $\vec{x}$ via a so-called quadratic form

$$\vec{x}^T C\ \vec{x}.$$

The multivariate Gaussian is the most familiar of these.

To return to the point at issue: what we really want to know is whether or not $\rho = 0$; it is this condition for which we are testing. Using the bivariate Gaussian is a very specific model; a Gaussian is assumed, it allows only two variances, and assumes that both x and y are random variables. Thus σ_x and σ_y include both the errors in the data, and their

intrinsic scatter – all presumed Gaussian. The model does not apply, for example, to data where the x-values are well defined and there are 'errors' only in y, perhaps different at different x. In such cases we would use model fitting, perhaps of a straight line (Sections 6.1 and 6.2). This is a different problem. These effects mean that we have to approach the correlation coefficient with caution, as the way we set up our experiment may result in graphs like those of Figs. 4.1 or 4.2.

As always, there are two quite different ways of proceeding from this point, Bayesian and non-Bayesian.

4.2.1 Bayesian correlation testing

The Bayesian approach is to use Bayes' theorem to extract the probability distribution for ρ from the likelihood of the data and suitable priors. Since we want to know about ρ independently of any inference about the means and variances, we have to integrate these 'nuisance variables' out of the full posterior probability prob$(\rho, \sigma_x, \sigma_y, \mu_x, \mu_y \mid \text{data})$. For the bivariate Gaussian model, the result is given by Jeffreys (1961) as

$$\text{prob}(\rho \mid \text{ data}) \propto \frac{(1-\rho^2)^{(N-1)/2}}{(1-\rho r)^{N-3/2}} \left(1 + \frac{1}{n-1/2}\frac{1+r\rho}{8} + \ldots\right). \quad (4.7)$$

The Bayesian test for correlation is thus simple: compute r from the (X_i, Y_i), and calculate prob(ρ) for the range of ρ of interest.

EXAMPLE We generated 50 samples from a bivariate t distribution with three degrees of freedom. The true correlation coefficient was 0.5. The large tails of the distribution produce outliers, not accounted for by the assumed Gaussian used in interpreting the r statistic. Figure 4.5 shows what equation (4.7) gives: the distribution of ρ peaks at around 0.2. If now we remove the samples outside 4σ, the distribution peaks at around 0.5 and is appreciably narrower. The method is thus fairly robust, although obviously affected by being used with the 'wrong' distribution.

Given this probability distribution for ρ, we can answer questions like 'what is the probability that $\rho > 0.5$?' or (perhaps more usefully) 'what is the probability that ρ from dataset A is bigger than ρ from dataset B?' (see Section 2.5). As is often the case, the utility of the Bayesian

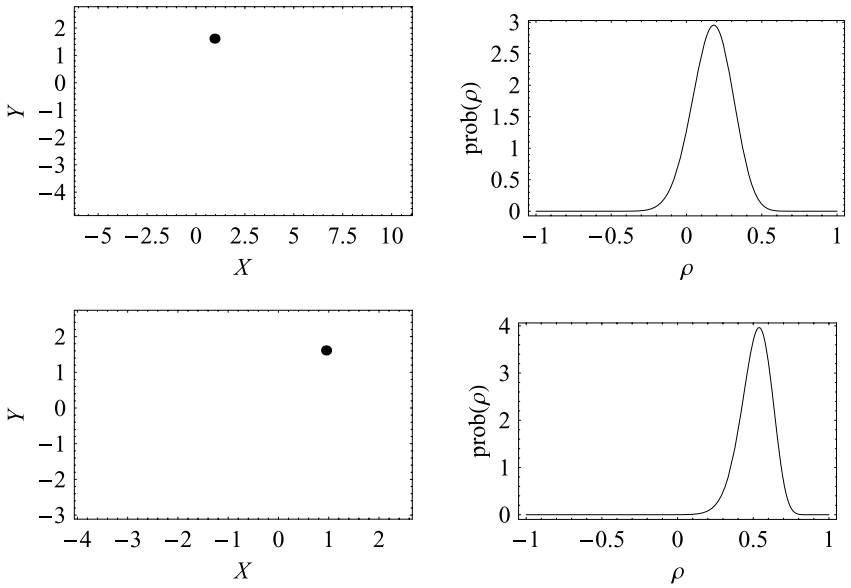

Fig. 4.5. Fifty X_i, Y_i chosen at random from a bivariate Gaussian with $\rho = 0.5$, with some outliers added. The Jeffreys probability distribution of the correlation coefficient ρ is shown, peaking at around 0.2 for the upper panel. The data have been restricted to $\pm 4\sigma$ in the lower panel; the distribution now peaks at 0.44.

approach is not that prior information is accurately incorporated, but rather that we get an answer to the question we really want to ask.

Jeffreys used a uniform prior for ρ – not obviously justifiable, and certainly not correct if ρ is close to 1 or -1, as he points out. But in these cases a statistical test is a waste of time anyway.

EXAMPLE An interesting use of Jeffreys's distribution is to calculate the probability that ρ is positive, as a function of sample size (Fig. 4.6.) This tells us how much data we need to be confident of detecting correlations.

4.2.2 The classical approach to correlation testing

The alternative approach to the correlation problem starts by regarding ρ as a fixed quantity, not a variable about which probabilistic statements

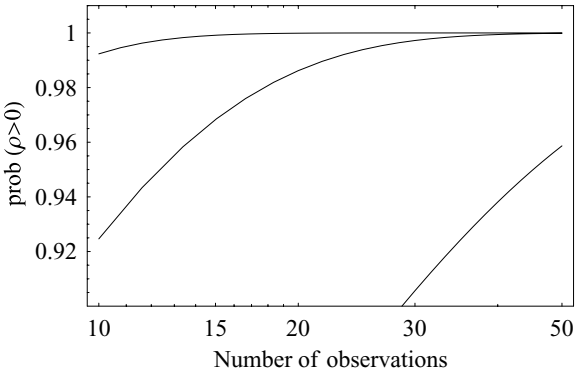

Fig. 4.6. The probability of ρ being positive, as a function of sample size, for r-values of 0.25 (lowest curve), 0.5 and 0.75 (uppermost curve).

might be made. This approach therefore arrives at the probability of the data, given ρ (and of course the background hypothesis that a bivariate Gaussian is adequate). The result (Fisher 1944) is

$$\text{prob}(r \mid \rho, H) \propto \frac{(1-\rho^2)^{(N-1)/2}(1-r^2)^{(N-4)/2}}{(1-\rho r)^{N-3/2}} \times \left(1 + \frac{1}{N-1/2}\frac{1+r\rho}{8} + \cdots\right). \tag{4.8}$$

What can we do with this answer? The standard approach is to pick the easy 'null hypothesis' $\rho = 0$, compute r, and then compute the probability, under the null hypothesis, of r being this big or bigger. If this probability is very small, we may feel that the null hypothesis is rather unlikely.

The standard parametric test is to attempt to reject the hypothesis that $\rho = 0$ and we do this by computing r. The standard deviation in r is

$$\sigma_r = \frac{(1-r^2)}{\sqrt{N-1}}. \tag{4.9}$$

Note that $-1 < r < 1$; $r = 0$ for no correlation. To test the significance of a non-zero value for r, compute

$$t = \frac{r\sqrt{N-2}}{\sqrt{1-r^2}} \tag{4.10}$$

which obeys the probability distribution of the 'Student's' t statistic[1]

[1] After its discoverer W. S. Gosset (1876–1937), who developed the test while working on quality control sampling for Guinness. For reasons of industrial secrecy,

with $N - 2$ degrees of freedom. (The transformation simply allows us to use tables of t.) We are hypothesis testing now, and the methodology is described more systematically in Section 4.1. Consult Table A2.3, the table of critical values for t; if t exceeds that corresponding to a critical value of the probability (two-tailed test), then the hypothesis that the variables are unrelated can be rejected at the specified level of significance. This level of significance (say 1 per cent, or 5 per cent) is the maximum probability which we are willing to risk in deciding to reject the null hypothesis (no correlation) when it is in fact true.

This approach has probably not answered the question – we embark on this sort of investigation when it is apparent that the data contain correlations; we merely want some justification by knowing 'how much'. Also, the inclusion in the testing procedure of values of r that have not been observed poses the usual difficulties.

The test is widely used, and is formally powerful. But as one statistics book says 'There are data to which this kind of correlation method cannot be applied.' This is a gross understatement. The data must be on continuous scales, obviously. The relation between them must be linear. (How would we know this? In many cases in astronomy we change the scales at will (log–log, log–linear, etc.) to give a roughly linear appearance to our plots.) The data must be drawn from Normally distributed populations. (How would we know this? Certainly if we have changed our data axes to log form, there must be doubt.) They must be free from restrictions in variability or groupings. There are parametric tests that help: the F test for non-linearity and the correlation ratio test which gets around non-linearity. However, to circumvent the problems it is far better to go to a non-parametric test. These permit additional tests on data which are not numerically defined (binned data, or ranked data), so that in some instances they may be the only alternative.

4.2.3 Correlation testing: classical, non-parametric

The best-known non-parametric test consists of computing the Spearman rank correlation coefficient (Conover 1999; Siegel & Castellan 1988):

$$r_{\mathrm{s}} = 1 - 6\frac{\sum^{N}(X_i - Y_i)^2}{N^3 - N} \tag{4.11}$$

Gosset was required to publish under a pseudonym; he chose 'Student', which he used for years in correspondence with his (former) professor at Oxford, Karl Pearson.

where there are N data pairs, and the N values of each of the two variables are ranked so that (X_i, Y_i) represents the ranks of the variables for the ith pair, $1 < X_i < N$, $1 < Y_i < N$.

The range is $0 < r_s < 1$; a high value indicates significant correlation. To find how significant, refer the computed r_s to Table A2.5, a table of critical values of r_s applicable for $4 \leq N \leq 30$. If r_s exceeds an appropriate critical value, the hypothesis that the variables are unrelated is rejected at that level of significance. If N exceeds 30, compute

$$t_r = r_s \sqrt{\frac{N-2}{1-r_s^2}}, \tag{4.12}$$

a statistic whose distribution for large N asymptotically approaches that of the t statistic with $N-2$ degrees of freedom. The significance of t_r may be found from Table A2.3, and this represents the associated probability under the hypothesis that the variables are unrelated.

How does use of r_s compare with use of r, the most powerful parametric test for correlation? Very well: the efficiency is 91 per cent. This means that if we apply r_s to a population for which we have a data pair (x_i, y_i) for each object and both variables are Normally distributed, we will need on average 100 (x_i, y_i) for r_s to reveal that correlation at the same level of significance which r attains for 91 (x_i, y_i) pairs. The moral is that if in doubt, little is lost by going for the non-parametric test.

The Kendall rank correlation coefficient does the same thing as r_s, and with the same efficiency (Siegel & Castellan 1988).

EXAMPLE A 'correlation' at the notorious 2σ level is shown in Fig. 4.7. Here, $r_s = 0.28$, $N = 55$, and the hypothesis that the variables are unrelated is rejected at the 5 per cent level of significance. Here we have no idea of the underlying distributions; nor are we clear about the nature of the axes. The assumption of a bivariate Gaussian distribution would be rash in the extreme, especially in view of a uniformly filled Universe producing a V/V_{max} statistic uniformly distributed between 0 and 1 (Schmidt 1968). The V_{max} method is discussed in Section 7.3.

There is yet another way, the permutation test. In the case of correlation analysis, we have data $(X_1, Y_1), (X_2, Y_2), \ldots$ and we wish to test the null hypothesis that x and y are uncorrelated. In this regard if we

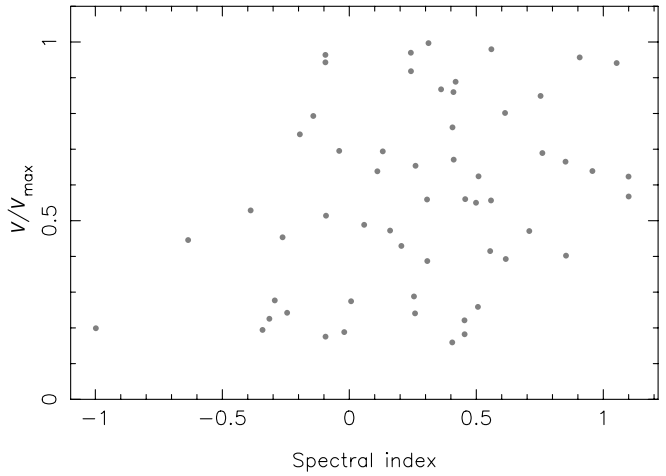

Fig. 4.7. $V/V_{\max}$ as a function of high-frequency spectral index for a sample of radio quasars selected from the Parkes 2.7-GHz survey.

have some home-made test statistic η, we can calculate its distribution, on the assumption of the null hypothesis, by simply calculating its value for many permutations of the x's amongst the y's. For any reasonable dataset there will be far more possible permutations than we can reasonably explore, but choosing a random set will give an adequate estimate of the distribution of the test statistic.

If it turns out that the observed value of η is very improbable, under the null hypothesis, we may be interested in estimating the distribution for non-zero correlation. This is a route to useful Bayesian analysis, of the kind we described for the correlation coefficient ρ. Here Monte Carlo simulation (Section 6.5) will come into its own, allowing us to explore a wide range of parameter space, so building up the posterior distribution prob(parameters/η).

These methods can be used to derive distributions of statistics such as Spearman's or Kendall's correlation coefficients in cases when a correlation is apparently present.

4.2.4 Correlation testing: Bayesian versus non-Bayesian tests

Let us be clear: the non-parametric tests circumvent some of the issues involved in the non-Bayesian approach, but they have no bearing on the

fundamental issue – what was the real question? However, the Bayesian approach, strong in answering the real question, forces reliance on a model.

There is rather little difference, in practice, between the Fisher test and results from Jeffreys's distribution. We can show this with some random Gaussian data with a correlation of zero. In the standard way, we can use the r distribution to find the probability of r being as large, or larger, than we observe, on the hypothesis that $\rho = 0$. If this probability is small, the test is hinting at the possibility that the correlation is actually positive. Therefore we compare with the probability, from the Jeffreys distribution, that ρ is positive. If the probability from Fisher's r distribution is small we expect the probability from ρ to be large; and in fact we can see, either from simulations or from the algebraic form of the distributions, that the sum of these two probabilities is close to 1. In other words, interpreting the standard Fisher test (illegally!) to be telling us the chance that ρ is positive, actually works very well.

4.3 Partial correlation

The 'lurking third variable' can be dealt with (provided that its influence is recognized in the first place) by *partial correlation*, in which the 'partial' correlation between two variables is considered by nullifying the effects of the third (or fourth, or more) variable upon the variables being considered. Partial correlation is a science in itself; it is covered in both parametric and non-parametric forms by Stuart & Ord (1994), Macklin (1982), and Siegel & Castellan (1988).

In the parametric form, consider a sample of N objects for which parameters x_1, x_2, and x_3 have been measured. The *first-order partial correlation* coefficient between variables x_1 and x_2 is

$$r_{12.3} = \frac{r_{12} - r_{13}r_{23}}{\sqrt{(1 - r_{13}^2)(1 - r_{23}^2)}} \tag{4.13}$$

where the r are the product-moment coefficients defined in Section 4.2.2. If there are four variables, then the *second-order partial correlation coefficient* is

$$r_{12.34} = \frac{r_{12.3} - r_{14.3}r_{24.3}}{\sqrt{(1 - r_{14.3}^2)(1 - r_{24.3}^2)}} \tag{4.14}$$

where the correlation is being examined between x_1 and x_2 with x_3

and x_4 held constant. Examination of the correlation between the other variables requires manipulation of the subscripts in the foregoing.

And so forth for higher-order partial correlations between more than four variables, with the standard error of the partial correlation coefficients being given by

$$\sigma_{r_{12.34\ldots m}} = \frac{1 - r^2_{12.34\ldots m}}{\sqrt{N - m}}$$

where m is the number of variables involved. The significance then comes from the 'Student's' t test as above.

EXAMPLE Consider data from a sample of lads aged 12–19. The correlation between height and weight will be high because the older boys are taller on average. But with age held constant, the correlation would still be significantly positive because at all ages, taller boys tend to be heavier. In such a sample of 10, the correlation between height and weight (r_{12}) is calculated as 0.78; between height and age (r_{13}), 0.52, and between weight and age, $r_{23} = 0.54$. The first-order partial coefficient of correlation (Equation 4.13) is thus $r_{12,3} = 0.69$; $\sigma_{r_{12.3}} = 0.198$; and the correlation is significant at the level of 0.2 per cent.

Consider further a measure of strength for each lad. The correlation between strength and height (r_{41}) is 0.58; between strength and weight (r_{42}) 0.72. Will lads of the same weight show a dependence of strength upon height? The answer is given by $r_{41.2} = 0.042$; the correlation between strength and height essentially vanishes and we would conclude that height as such has no bearing on strength; only by virtue of its correlation with weight does it show any correlation at all.

As for second-order partials, is there a correlation between strength and age if height and weight are held constant? The raw correlation between age and strength was 0.29; the second-order partial also yields 0.29. It seemingly makes little difference if height and weight are allowed to vary; the relation between age and strength is the same.

4.4 But what next?

If we have demonstrated a correlation, it is logical to ask what the correlation is, i.e. what is the law which relates the variables. It is

common practice to dash off and fit a regression[2] line, usually applying the method of least squares (Section 6.2). It is essential to note that this is model fitting now; the distinction between data modelling (Chapter 6) and hypothesis testing (here; and Chapter 5) is important.

Before doing so, there are several considerations, most of which are addressed in more detail in Section 6.2. Are there better quantities to minimize than the squares of deviations? What errors result on the regression-line parameters? Why should the relation be linear? And – most crucial of all – what are we trying to find out? If we have found a correlation between x and y, which variable is dependent; do we want to know x on y or y on x? The coefficients are generally completely different.

As an argument against blind application of correlation testing and line fitting, consider the famous Anscombe (1973) quartet, shown in Fig. 4.8. Anscombe's point is the essential role of graphs in good statistical analysis. However, the examples illustrate other matters: the rule of thumb (Section 4.1), and the distinction between independence of data points and correlation. In more than one of Anscombe's datasets the points are clearly related. They are far from independent, while not showing a particularly strong (formal) correlation. The upper right example in Figure 4.8 is a case in which a linear fit is of indifferent quality, while the choice of the 'right' relation between X and Y would result in a perfect fit. The quartet further emphasizes how dependent our analyses are on the assumption of Gaussianity: the covariance matrix, which intuitively we might expect to reflect some of the structure in the individual plots, is identical for each.

Note that X independent of Y means $\text{prob}(X, Y) = \text{prob}(X)\text{prob}(Y)$, or $\text{prob}(X \mid Y) = \text{prob}(X)$; while X correlated with Y means $\text{prob}(X, Y) \neq \text{prob}(X)\ \text{prob}(Y)$ in a particular way, giving $r \neq 0$. It is perfectly possible to have $\text{prob}(X, Y) \neq \text{prob}(X)\text{prob}(Y)$ and $r = 0$, the standard example being points distributed so as to form the Union Jack.

If we simply wish to map the dependence of variables on each other with minimal judgemental input, it strongly suggested, here and in

[2] Galton (1889) introduced the term *regression*; it is from his examination of the inheritance of stature. He found that the sons of fathers who deviate x inches from the mean height of all fathers themselves deviate from the mean height of all sons by less than x inches. There is what Galton termed a 'regression to mediocrity'. The mathematicians who took up his challenge to analyse the correlation propagated his mediocre term, and we're stuck with it.

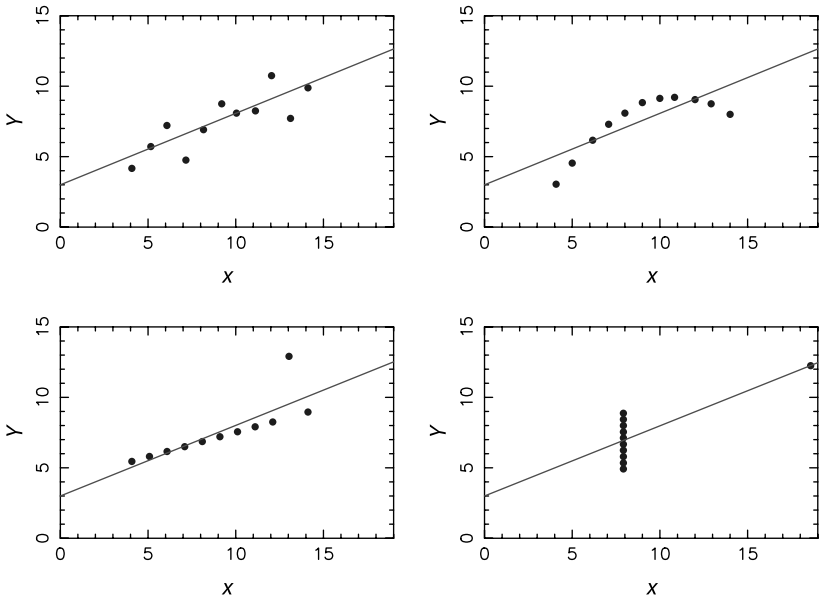

Fig. 4.8. Anscombe's quartet: four fictitious sets of 11 (X_i, Y_i), each with the same $(\overline{X}, \overline{Y})$, identical coefficients of regression, regression lines, residuals in Y and estimated standard errors in slopes.

Section 6.2, that principal component analysis is the appropriate technique.

4.5 Principal component analysis

Principal component analysis (PCA) is the ultimate correlation searcher when many variables are present. Given a sample of N objects with n parameters measured for each of them, how do we find what is correlated with what? What variables produce primary correlations, and what produce secondary, via the lurking third (or indeed $n-2$) variables?

PCA is one of a family of algorithms (known as multivariate statistics; see e.g. Manly (1994), Kendall (1980), Joliffe (2002)) designed for this situation. Its task is the following: given a sample of N objects with n measured variables x_n for each, find a new set of ξ_n variables that are orthogonal (independent), each one a linear combination of the original variables:

$$\xi_i = \sum_{j=1}^{n} a_{ij} x_j \tag{4.15}$$

with values of a_{ij} such that the **smallest number** of new variables accounts for as much of the variance as possible. The ξ_i are the **principal components**. If most of the variance involves just a few of the n new variables, we have found a simplified description of the data. Finding which of the variables correlate (and how) may lead to that successful fishing expedition – we may have caught new physical insight.

PCA may be described algebraically, through covariance matrices (Section 4.2), or geometrically. Taking the latter approach, consider the N objects represented by a large cloud in n-dimensional space. If two of the n parameters are correlated, the cloud is elongated along some direction in this space. PCA identifies these extension directions and uses them as a sequential set of axes, sequential in the sense that the most extended direction is identified first by minimizing the sums of squares of deviations. This direction forms the first principal component (or **eigenvector 1**), accounting for the largest single linear variation amongst the object properties. Then the $(n-1)$-dimensional hyperplane orthogonal to the first principal component is considered and searched for the direction representing the greatest variance in $(n-1)$-space; and so forth, defining a total of n orthogonal directions.

EXAMPLE As an elementary PCA example via geometry, let us return to the early Hubble diagram of Fig. 4.3, 24 galaxies with two measured variables, velocity of recession v and distance d. It is standard practice to normalize by subtracting the means from each variable and to divide by the standard deviation, i.e. to plot $v_i' = (v_i - < v >)/\sigma_v$ versus $d_i' = (d_i - \quad)/\sigma_d$, as shown in Fig. 4.3(b). Then we find the first principal component by simply rotating the axis through the origin to align with maximum elongation, the direction of apparent correlation, and we do this with least squares (Section 6.2) – maximizing the variance along PC1 is equivalent to minimizing the sums of the squares of the distances of the points from this line through the origin. The distance of a point from the direction PC1 (shown dotted in Fig. 4.3b) represents the value (score) of PC1 for that point. PC1 is clearly a linear combination of the two original variables; in fact it is $v' = d'$. Because the new coordinate system was found by simple rotation, distances from the origin are unchanged; the total variance of v' and d' is unchanged and is 2.0. The variance of PC1, the normalized distances squared from PC2, is 1.837. The remaining variance of the sample must be accounted for by

Table 4.1. Principal components from Fig. 4.3

	PC1	PC2
Eigenvalue	1.837	0.163
Proportion	0.918	0.082
Cumulative	0.918	1.000
Variable	PC1	PC2
d (Mpc)	1.0	1.0
v (km s^{-1})	1.0	−1.0

the projection of data points onto the axis PC1, perpendicular to PC2; the length of these projections are the object's values or scores of the second principal component, and this is verified as 0.163, with the sum of these variances 2.0 as expected. Table 4.1 sets out the results in the standard way of PCA.

Now consider the matrix approach. In the process of PCA the usual methodology is to construct the error matrix (Section 4.2), e.g. for the two-variable case of the example, $a(1,1) = \sum d'^2, a(1,2) = a(2,1) = \sum v'd', a(2,2) = \sum v'^2$. We then seek a principal axis transformation that makes the cross-terms vanish; we seek an axis transformation to rotate the ellipses of Fig. 4.4 so that the axes of the ellipses coincide with the principal axes of the coordinate system. This of course is simply done in matrix notation. We determine the eigenvalues of the error matrix and form its eigenvectors (readily shown for the example to be $v' = d'$ and $v' = -d'$ as seen in Fig. 4.3b). These eigenvectors then form the transpose matrix T, for variable transformation and axis rotation. The axis rotation diagonalizes the matrix, i.e. in the new axis system, the cross-terms are zero; we have rotated the axes until there is no x, y covariance.

Note that for the purpose our set of data has been reduced from 48 numbers for the 24 galaxies to four numbers, a 2×2 matrix. How did this happen? PCA assumes that the covariance (or error) matrices describe the data; this is the case if the data are drawn from a multivariate Gaussian (Section 4.2, Fig. 4.4), or in general when a simple quadratic form, using the covariance matrix, can describe the distribution of the data. It is far from generally true that the clouds of

points in most n-variate hyperspaces will be so simply distributed – see the following example. The distribution need not be symmetrical, for example.

In multivariate datasets, the disparate units are taken care of by normalizing as in the above example: subtracting mean values and dividing by variances. This is not a prescription, however. For example, the variance for any particular variable might be dominated by a monstrous outlier which there are good grounds to reject. The choice of weights does therefore depend on familiarity with the data and preferences – there is plenty of room for subjectivity. It should also be noted that PCA is a linear analysis and tests need to be performed on the linearity of the principal components. For example, plotting the scores of PC1 versus PC2 should show a roughly Gaussian distribution consistent with $\rho = 0$. It may be apparent how to reject outliers or to transform coordinates to reduce the problem to a linear analysis. In large datasets such processes can reveal unusual objects.

EXAMPLE Some PCA problems have a larger number of variables than input observables, $p > n$, resulting in singular matrices requiring modifications to standard techniques to solve the eigenvector equations (Wilkinson 1978; Mittaz, Penston & Snijders 1990). This situation occurs in spectral PCA for which the p variables are fluxes in p wavelength or frequency bins (Francis et al. 1992; Wills et al. 1997). The technique is ideal for dealing with a huge sample and was therefore adopted in the 2dF survey which aims to measure 250 000 galaxy spectra to provide a detailed picture of the galaxy distribution out to a redshift of 0.25. The PCA approach to 2dF galaxy classification is discussed in detail by Folkes et al. (1999). Figure 4.9, drawn from this paper, shows examples of 2dF spectra prepared for PCA, the mean spectrum, and the first three principal components. These three components represent the eigenvectors of the covariance matrix of these prepared spectra. In this example, the first PC accounts for 49.6 per cent of the variance; the first three components account for 65.8 per cent of the variance. Much of the remainder is due to noise.

The key aspect Folkes et al. (1999) wished to address was how the luminosity function depends on galaxy type. The objects in the PC1–PC2 plane form a single cluster (Fig. 4.9, blue emission-line objects to the left, red objects with absorption lines to the right, and strong

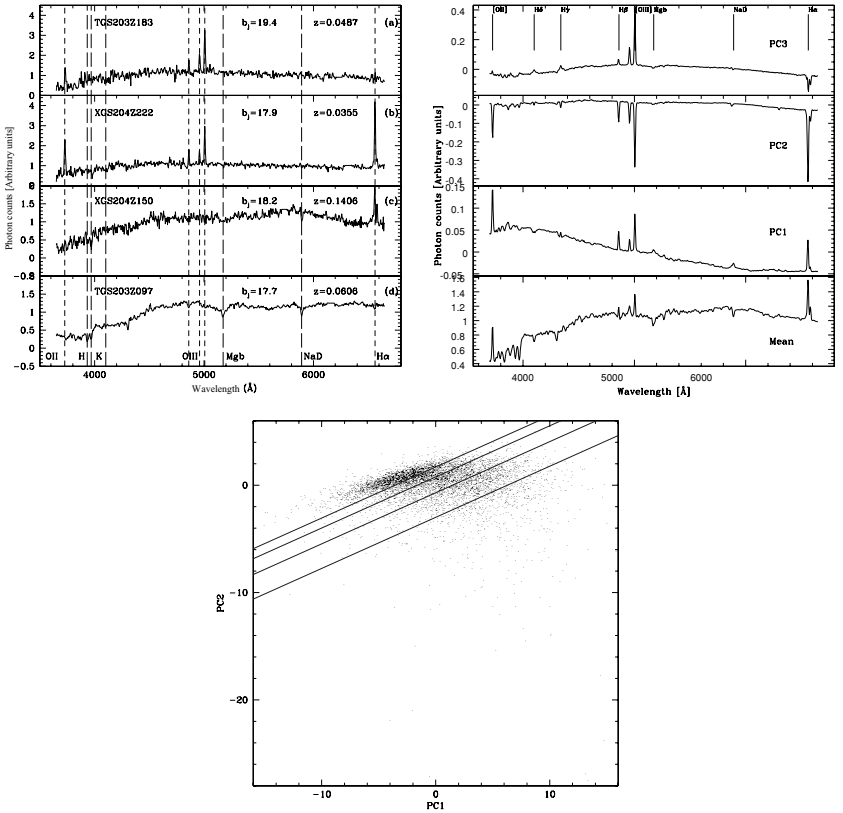

Fig. 4.9. Top left: examples of 2dF spectra prepared for PCA. Instrumental and atmospheric features have been removed, with the spectra transformed to the rest frame, resampled to 4Å bins and normalized to unit mean flux. Top right: the mean spectrum and first three principal components; the sign of the PCs is arbitrary. Below: distribution of 2dF galaxy spectra in the PC1–PC2 plane. Slanted lines divide the plane into the five spectral classes adopted by Folkes *et al.*

emission-line objects straggling downward). Five spectral classes were then adopted, shown by the slanted lines in this figure. Confirmation that these spectral classes correspond to morphological classification came from placing the 55 Kennicut (1992) standard galaxies into this plot; the five classes are roughly E/SO, Sa, Sb, Scd and Irr. The way ahead to use the PCA classes to work out luminosity functions for each is clear, and the punch line is that significantly different Schecter functions emerged for each class.

Note how asymmetrical the distribution looks. This need not invalidate the analysis – here primarily one of classification – but the effectiveness must in general be reduced. Asymmetrical shapes in the PC planes must result in unquantifiable errors in the classification.

In addition to spectral classification and analysis, spectral time variability is amenable to PCA (Mittaz, Penston & Snijders 1990; Turler & Courvoisier 1998).

Of course we would like to know if the PCs are 'real' and so some indication of the distribution of each one would be useful. This can be computed by a bootstrap (Section 6.6) on the original dataset. This will show how stable the eigenvectors and eigenvalues actually are, in particular whether the largest eigenvector is reliably detected.

Exercises

In the exercises denoted by (D), datasets are provided on the book's website; or create your own.

4.1 **Correlation testing (D).** Consider the Hubble plot of Fig. 4.3. What is (a) the most likely value for ρ via the Jeffreys test, (b) the significance of the correlation via the standard Fisher test and (c) the significance via the Spearman rank test? Estimate distributions for these statistics with a bootstrap (Section 6.6), and compare the results with the standard tests.

4.2 **Permutation tests (D).** (a) Take a small set of uncorrelated pairs (X, Y), preferably non-Gaussian. By permutation methods on the computer, derive distributions of Fisher r, Spearman's and Kendall's statistics. (b) Try the same numerical experiment with correlated data, using the bootstrap and the jackknife to estimate distributions (Sections 6.6). Correlated non-Gaussian data are provided for the multivariate t distribution, which is Cauchy-like for one degree of freedom and becomes more Gaussian for larger degrees of freedom. How robust are the conclusions against outliers?

4.3 **Principal component analysis (D).** Carry through a PCA on the data of the quasar sample given in Francis & Wills (1999). Compute errors with a bootstrap analysis or jackknife (Section 6.6).

4.4 **Lurking third variables.** Consider the following correlations, and speculate on how a third variable might be involved. (a) During the Second World War, J.W. Tukey discovered a strong positive correlation between accuracy of high-altitude bombing and the presence of enemy fighter planes. (b) There is a well-known correlation between stock market indices and the sunspot cycle. (c) The apparent angular size of radio sources shows a strong inverse correlation with radio luminosity.

5
Hypothesis testing

How do our data look?
I've carried out a Kolmogorov–Smirnov test ...
Ah. **That** *bad.*
(interchange between Peter Scheuer and his then student, CRJ)

It is often the case that we need to do sample comparison: we have someone else's data to compare with ours; or someone else's model to compare with our data; or even our data to compare with our model. We need to make the comparison and to decide something. We are doing hypothesis testing – are our data consistent with a model, with somebody else's data? In searching for correlations as we were in Chapter 4, we were hypothesis testing; in the model fitting of Chapter 6 we are involved in data modelling and parameter estimation.

Classical methods of hypothesis testing may be either parametric or non-parametric, distribution-free as it is sometimes called. Bayesian methods necessarily involve a known distribution. We have described the concepts of Bayesian versus frequentist and parametric versus non-parametric in the introductory Chapters 1 and 2. Table 5.1 summarizes these apparent dichotomies and indicates appropriate usage.

That non-parametric Bayesian tests do not exist appears self-evident, as the key Bayesian feature is the probability of a particular model in the face of the data. However, it is not quite this clear-cut, and there has been consideration of non-parametric methods in a Bayesian context (Gull & Fielden 1986). If we understand the data so that we can model its collection process, then the Bayesian route beckons (see Chapter 2 and its examples).

Table 5.1. Usage of Bayes/frequentist/parametric/non-parametric testing

	Parametric	Non-parametric
Bayesian testing	Model known. Data gathering and uncertainty understood.	Such tests do not exist.
Classical testing	Model known. Underlying distribution of data known. Large enough numbers. Data on ordinal or interval scales.	Small numbers. Unknown model. Unknown underlying distributions or errors. Data on nominal or categorical scales.

And yet there are situations when classical methods are essential:

- If we are comparing data with a model and we have very few of these data; or if we have poorly defined distributions or outliers then we do not have an adequate model for our data. We need non-parametric methods.
- Classical methods are widely used. We therefore need to understand results quoted to us in these terms.

The classical tests involve us in 'rejecting the null hypothesis', i.e. in rejecting rather than accepting a hypothesis at some level of significance. The hypothesis we reject may not be one in which we have the slightest interest. This is a process of elimination. A classical test works with probability distributions of a statistic while the Bayesian method deals with probability distributions of a hypothesis.

5.1 Methodology of classical hypothesis testing

Classical hypothesis testing follows these steps.

(1) Set up two possible and exclusive hypotheses, each with an associated terminal action:

H_0, the null hypothesis or hypothesis of no effect, usually formulated to be rejected, and

H_1, an alternative, or research hypothesis.

(2) Specify a priori the *significance level* α; choose a test which (a) approximates the conditions and (b) finds what is needed; obtain the *sampling distribution* and the *region of rejection*, whose area is a fraction α of the total area in the sampling distribution.
(3) Run the test; reject H_0 if the test yields a value of the statistic whose probability of occurrence under H_0 is $\leq \alpha$.
(4) Carry out the terminal action.

It is vital to emphasize (2). The significance level has to be chosen before the value of the test statistic is glimpsed; otherwise some arbitrary convolution of the data plus the psychology of the investigator is being tested. This is not a game; you must be prepared to carry out the terminal action on the stated terms. There is no such thing as an inconclusive hypothesis test!

There are two types of error involved in the process, traditionally referred to (surprisingly enough) as Types I and II. A *Type I error* occurs when H_0 is in fact true, and the probability of a Type I error is the probability of rejecting H_0 when it is in fact true, i.e. α. The *Type II error* occurs when H_0 is false, and the probability of a Type II error is the probability β of the failure to reject a false H_0; β is not related to α in any direct or obvious way. The *power* of a test is the probability of rejecting a false H_0, or $1 - \beta$.

The *sampling distribution* is the probability distribution of the test statistic, i.e. the frequency distribution of area unity including all values of the test statistic under H_0. The probability of the occurrence of any value of the test statistic in the *region of rejection* is less than α, by definition; but where the region of rejection lies within the sampling distribution depends on H_1. If H_1 indicates *direction*, then there is a single region of rejection and the test is *one-tailed*; if no direction is indicated, the region of rejection is comprised of the two ends of the distribution and we are dealing with a *two-tailed* test. This is the only use we make of H_1; the testing procedure can only convince us to accept H_1 if it is the sole alternative to H_0. The procedure of elimination serves to reject H_0, not prove H_1. Beware – it is human nature to think that your H_1 is the only possible alternative to H_0.

Both *parametric* and *non-parametric* (classical) tests follow this procedure; both use a test statistic with a known sampling distribution. The non-parametric aspect arises because the test statistic does not itself depend upon properties of the population(s) from which the data were

drawn. There are persuasive arguments for following non-parametric testing in using classical methods, as outlined at the head of Section 1.4. But first we consider the parametric route in some detail in order to establish methodology.

5.2 Parametric tests: means and variances, t and F tests

A very common question arises when we have two sets of data (or one set of data and a model) and we ask if they differ in location or spread. The best-known parametric tests for such comparisons concern samples drawn from Normally distributed parent populations; these tests are of course the 'Student's' t test (comparison of means) and the F test (comparison of variances), and are discussed in most books on statistics, e.g. Martin (1971), Stuart & Ord (1994). The t and F statistics have been introduced in Section 3.4.

To contrast the classical and Bayesian methods for hypothesis testing, we look at the simple case of comparison of means. We deal with a Gaussian distribution, because its analytical tractability has resulted in many tests being developed for Gaussian data; and then, of course, there is the central limit theorem.

Let us suppose we have n data X_i drawn from a Gaussian of mean μ_x, and m other data Y_i, drawn from a Gaussian of identical variance but a different mean μ_y. Call the common variance σ^2.

The Bayesian method is to calculate the joint posterior distribution

$$\text{prob}(\mu_x, \mu_y, \sigma) \propto \frac{1}{\sigma^{n+m+1}} \exp\left[-\frac{\sum_i (x_i - \mu_x)^2}{2\sigma^2}\right] \exp\left[-\frac{\sum_i (y_i - \mu_y)^2}{2\sigma^2}\right] \tag{5.1}$$

in which we have used the Jeffreys prior (Exercise 2.6 of chapter 2) for the variance. Integrating over the 'nuisance' parameter σ, we would get the joint probability $\text{prob}(\mu_x, \mu_y)$ and could use it to derive, for example, the probability that μ_x is bigger than μ_y.

From this we can calculate the probability distribution of $(\mu_x - \mu_y)$ (see e.g. Lee 1997, Chapter 5). The result depends on the data via a quantity

$$t' = \frac{(\mu_x - \mu_y) - (\overline{X} - \overline{Y})}{s\sqrt{m^{-1} + n^{-1}}} \tag{5.2}$$

where

$$s^2 = \frac{nS_x + mS_y}{\nu}$$

with the usual mean squares $S_x = \sum(X_i - \overline{X})^2/n$, similarly for S_y, and $\nu = n + m - 2$.

The distribution for t' is

$$\text{prob}(t') = \frac{\Gamma\left[\frac{\nu+1}{2}\right]}{\sqrt{\pi\nu}\Gamma\left[\frac{\nu}{2}\right]}\left(1 + \frac{t'^2}{\nu}\right)^{-(\nu+1)/2}. \tag{5.3}$$

We regard the data as fixed and $(\mu_x - \mu_y)$ as the variable, simply computing the probability of any particular difference in the means. We might alternatively work out the range of differences which are, say, 90 per cent probable, or we might carry the distribution of $(\mu_x - \mu_y)$ on into a later probabilistic calculation.

If we instead follow the classical line of reasoning, we do not treat the μ's as random variables. Instead we guess that the difference in the averages $\overline{X} - \overline{Y}$ will be the statistic we need; and we calculate its distribution on the null hypothesis that $\mu_x = \mu_y$. We find that

$$t = \frac{\overline{X} - \overline{Y}}{s\sqrt{m^{-1} + n^{-1}}} \tag{5.4}$$

follows a t distribution with $n + m - 2$ degrees of freedom. This is the classical Student's t. Critical values are given in Table A2.3.

This gives the basis of a classical hypothesis test, the t test for means. Assuming that $(\mu_x - \mu_y) = 0$ (the null hypothesis), we calculate t. If it (or some greater value) is very unlikely, we think that the null hypothesis is ruled out.

The t statistic is heavy with history and reflects an era when analytical calculations were essential. The penalty is the total reliance on the Gaussian. However, with cheap computing power we may expect to be able to follow the basic Bayesian approach outlined above for any distribution.

By analogous calculations, we can arrive at the F test for variances. Again, Gaussian distributions are assumed. The null hypothesis is $\sigma_x = \sigma_y$, the data are X_i $(i = 1, \ldots, n)$ and Y_i $(i = 1, \ldots, m)$ and the test statistic is

$$\mathcal{F} = \frac{\sum_i (X_i - \overline{X})/(n-1)}{\sum_i (Y_i - \overline{Y})/(m-1)}. \tag{5.5}$$

This follows an F distribution with $n-1$ and $m-1$ degrees of freedom (Table A2.4) and the testing procedure is the same as for Student's t.

Clearly this statistic will be particularly sensitive to the Gaussian assumption.

EXAMPLE Suppose we have two small sets of data, from Gaussian distributions of equal variance: −1.22, −1.17, 0.93, −0.58, −1.14 (mean −0.64), and 1.03, −1.59, −0.41, 0.71, 2.10 (mean 0.37), with a pooled standard deviation of 1.2. The standard t statistic is 1.12. If we do a two-tailed test (so being agnostic about whether one mean is larger than another), we find a 30 per cent chance that these data would arise if the means were the same. The one-tailed test (testing whether one mean is larger) gives 16 per cent. From a Bayesian point of view, we can calculate the distribution of $(\mu_x - \mu_y)$ for the same data. In Fig. 5.1 we can see clearly that one mean is smaller; the odds on this being so are about 10 to 1, as can be calculated by integrating the posterior distribution of the difference of means.

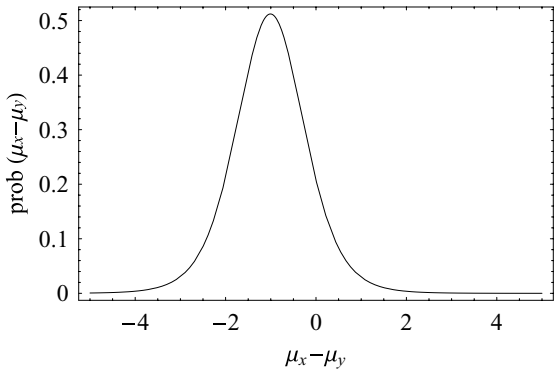

Fig. 5.1. The distribution of the difference of means for the example data.

5.2.1 The Behrens–Fisher test

Relaxing the assumption of equal variances may be important. It is indeed possible to derive the distribution of the difference in means without the assumption of equal variances in the two samples; the resulting distribution is called the Behrens–Fisher distribution. It is of great interest in statistics because it is a rare example of a Bayesian analysis having no classical analogue; there is no classical test for the case of possibly unequal variances. Lee (1997) discusses this in some detail.

The analytical form of the Behrens–Fisher distribution is complicated and involves a numerical integration anyway, so we may as well resort to a computer right away to calculate it from Bayes' theorem. We suppose that our data are drawn from Gaussians with means μ and standard deviations σ. The joint posterior distribution (using the Jeffreys prior on the σ) is

$$\begin{aligned}\mathrm{prob}(\mu_x, \mu_y, \sigma_x, \sigma_y) \propto \frac{1}{\sigma_x^{n+1}} \exp\left[-\frac{\sum_i (x_i - \mu_x)^2}{2\sigma_x^2}\right] \\ \times \frac{1}{\sigma_y^{n+1}} \exp\left[-\frac{\sum_i (y_i - \mu_y)^2}{2\sigma^2}\right]. \qquad (5.6)\end{aligned}$$

We have a multidimensional integration to do in order to get rid of the two nuisance parameters (σ_x and σ_y) and to ensure that the resulting joint distribution $\mathrm{prob}(\mu_x, \mu_y)$ is properly normalized. This is now not much of a problem, although until recently these integrations (for anything other than Gaussians) were a formidable obstacle to Bayesian methods. The analytical derivation of the Behrens–Fisher distribution eliminates all the numerical integrations bar one.

Given the joint distribution of μ_x and μ_y, we would like the distribution of $\mu_y - \mu_x$. By changing variables we can easily see that

$$\mathrm{prob}(u = \mu_y - \mu_x) = \int_\infty^\infty \mathrm{prob}(v, v + u)\, \mathrm{d}v.$$

(Another integration!)

EXAMPLE Consider the same example data as before, relaxing the assumption that the variances are equal. So although we cannot tell (classically) that the variances differ, we will obtain somewhat different results by not assuming that they are the same. We see from Fig. 5.2 that the distributions of $\mu_y - \mu_x$ are very similar in either case, although as we might expect the distribution is a little wider if we do not assume that the variances are equal. The wings are broader and so tests are a little weaker (but may be more honest).

This general sort of Bayesian test can be followed for any distribution – as long as we know what it is, and can do the integrations.

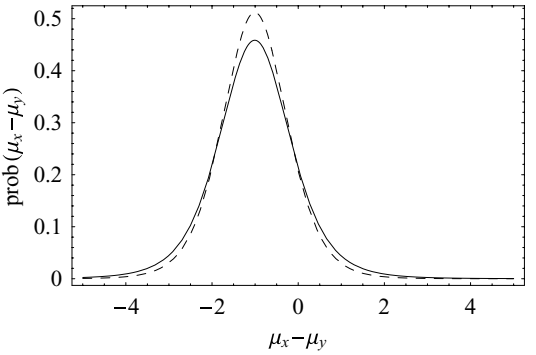

Fig. 5.2. Distribution of the difference of means assuming equal variances (dashed) and without this assumption (solid).

5.2.2 Non-Gaussian parametric testing

In astronomy we frequently have little or no information about the distributions from which our data are drawn, yet we need to test whether they are the same or not. Since there is only one way in which two unknown distributions can be the same, but a multitude in which they may differ, it is not surprising that we currently have to work with classical hypothesis tests – ones which assume the distributions are the same.

If we have some information about the distributions, we can use Bayesian methods. The trick here is to use a multiparameter generalization of a familiar distribution, where we carry the extra parameters to allow distortions in the shape. Eventually we can marginalize out these extra nuisance parameters, integrating over our prior assumptions about their magnitude.

The most common example of this sort of generalization is the Gram–Charlier series:

$$\exp\left(-\frac{x^2}{2\sigma^2}\right)\left(1+\sum_i a_i H_i(x)\right) \tag{5.7}$$

in which the H's are the Hermite polynomials. The coefficients a_i are the free parameters we need. (Because the Hermite polynomials are orthogonal with respect to Gaussian weights, these coefficients are also related to the moments of the distribution we are trying to create.) The effect of these extra terms is to broaden and skew a Gaussian, and so for some data a few-term Gram–Charlier series may give quite a useful basis for a parametric analysis. Priors on the coefficients have to be set

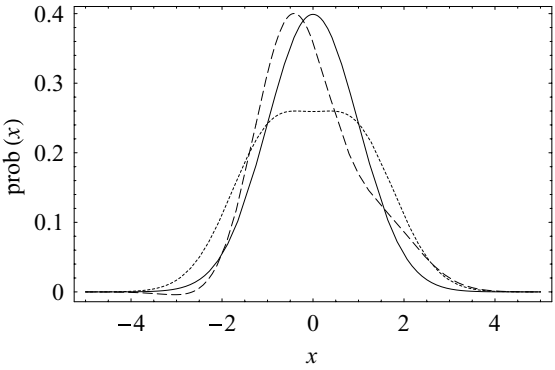

Fig. 5.3. Various distributions resulting from using just two terms in a Gram–Charlier distribution; the solid curve is a pure Gaussian.

by judgment. The even Hermite polynomials have the effect of changing scale, and so should follow the same Jeffreys prior as the standard deviation. The odd polynomials will change both scale and location and here setting the prior is less obvious.

There are two other variants on the Gram–Charlier series. For a distribution allied to the exponential $\exp(-x/a)$, a Laguerre series will function in the same way as a Gram–Charlier series, except the distorting functions are the Laguerre polynomials. The Gamma series is based on the distribution $x^{\alpha}(1-x)^{\beta}$, defined on the interval from 0 to 1; the distorting functions are the even less familiar Jacobi polynomials. However, computer algebra packages such as MATHEMATICA give comprehensive support for special functions and make the application of these series rather straightforward (Reinking 2002).

This approach clarifies the workings of non-parametric tests. Suppose we fix on a two-term Gram–Charlier expansion as a realistic representation of our data; the versatility is demonstrated in Fig. 5.3. For dataset 1, we then get the posterior $\text{prob}(\mu^{(1)}, \sigma^{(1)}, a_1^{(1)}, a_2^{(1)})$, and similarly for dataset 2. If we ask the apparently innocuous question 'are these data drawn from different distributions?' we see that there are many possibilities (in fact, 2^4) of the form, for instance, $\mu^{(1)} > \mu^{(2)}$ and $\sigma^{(1)} < \sigma^{(2)}$ and $a_1^{(1)} > a_1^{(2)}$ and $a_2^{(1)} < a_2^{(2)}$. Working through these possibilities could be quite tedious. A different question might be 'are these distributions at different locations, regardless of their widths?', in which case we could marginalize out the σ's and a_2's (Section 2.2); the location, in a Gram–Charlier expansion, is a simple combination of μ and a_1.

5.2.3 Which model is better?

This does suggest that comparison of models in the sense 'are these data drawn from the same distribution?' might be a more tractable question. Notice that we are not asking if $\mu^{(1)} = \mu^{(2)}$, etc., as the probability of this event is zero.

A useful way of answering this involves something called the Bayes factor or weight of evidence. Suppose we try to describe all of the data X_i, Y_i with just one distribution G. This distribution may have parameters so let us denote this hypothesis by (G, θ). Alternatively (and by hypothesis exhaustively) we may use (G_x, θ_x) for the data X_i and (G_y, θ_y) for the data Y_i. This hypothesis is $(G_x, \theta_x, G_y, \theta_y)$. Note we need prior probabilities for our two options, G or $G_x G_y$.

Bayes' theorem then tells us that

$$\begin{aligned}&\text{prob}(G, \theta \mid X, Y)\\ &= \frac{\text{prob}(X, Y \mid G, \theta)\text{prob}(G, \theta)}{\left(\int \text{prob}(G, \theta \mid X, Y)\ \mathrm{d}\theta + \int \text{prob}(G_x, \theta_x \mid X)\ \mathrm{d}\theta_x \int \text{prob}(G_y, \theta_y \mid Y)\ \mathrm{d}\theta_y\right)}\end{aligned} \tag{5.8}$$

in which the second term of the denominator arises because our alternative to (G, θ) is that the data are described as the product of two distinct distributions. The odds on the distinct distributions are (see Section 2.5)

$$\frac{\int \text{prob}(G_x, \theta_x \mid X)\ \mathrm{d}\theta_x \int \text{prob}(G_y, \theta_y \mid Y)\ \mathrm{d}\theta_y}{\int \text{prob}(G, \theta \mid X, Y)\ \mathrm{d}\theta}, \tag{5.9}$$

and this ratio is closely related to the Bayes factor (see Lee 1997 for more details). To work out these odds we integrate the likelihood functions, weighted by the priors, over the range of parameters of the distributions.

EXAMPLE Suppose we have the following two datasets: $X_i = -0.16$, 0.12, 0.44, 0.60, 0.70, 0.87, 0.88, 1.44, 1.74, 2.79 and $Y_i = 0.89$, 0.99, 1.29, 1.73, 1.96, 2.35, 2.51, 2.79, 3.17, 3.76. The means differ by about one standard deviation. We consider two a-priori equally likely hypotheses. One is that all 20 data are drawn from the same Gaussian. The other is that they are drawn from different Gaussians. In the first case, the likelihood function is

$$\frac{1}{(\sqrt{2\pi}\sigma)^{20}} \exp\left[-\frac{\sum_i (X_i - \mu)^2 + \sum (Y_i - \mu)^2}{2\sigma^2}\right]$$

and we take the prior on σ to be $\frac{1}{\sigma}$. We also assume a uniform prior for the μ's. In the second case, the likelihood is

$$\frac{1}{(\sqrt{2\pi}\sigma_x)^{10}} \exp\left[-\frac{\sum_i (X_i - \mu_x)^2}{2\sigma_x^2}\right] \frac{1}{(\sqrt{2\pi}\sigma_y)^{10}} \exp\left[-\frac{\sum_i (Y_i - \mu_y)^2}{2\sigma_y^2}\right]$$

and the prior is $\frac{1}{\sigma_x \sigma_y}$. Integrating over the range of the μ's and σ's, the odds on the data being drawn from different Gaussians are about 40 to 1 – a good bet. In the exercises we suggest following classical t and F tests on these data, and contrasting to the Bayes factor approach.

5.3 Non-parametric tests: single samples

We now leave Bayesian methods and return to classical territory for the remainder of this chapter.

'Non-parametric tests' implies that 'no distribution is assumed'. But let us not kid ourselves: something must be assumed, to make any progress. What is it? Various tests exploit different things, but a common method is to use counting probabilities. Take as an example the chi-square test (Section 5.3.1). The number of items in bin i is N_i, and we expect E_i. For smallish numbers, Poisson statistics tell us that the variance is also E_i. So $(N_i - E_i)^2/E_i$ should be roughly a squared Gaussian variable, of unit variance. As another example, the runs test (Section 5.3.3) is just using the assumption that each successive observation is equally likely to be 'up' or 'down', so a Binomial distribution applies. The assumptions underlying non-parametric tests are weaker, and so more general, than for parametric tests.

It is worth emphasizing again why we are going to advocate the non-parametric tests.

- These make fewer assumptions about the data. If indeed the underlying distribution is unknown, there is no alternative.
- If the sample size is small, probably we must use a non-parametric test.
- The non-parametric tests can cope with data in non-numerical form, e.g. ranks, classifications. There may be no parametric equivalent.
- Non-parametric tests can treat samples of observations from several different populations.

What are the counter-arguments? The main one concerns binning – binning is bad; it loses information and therefore loses efficiency. The power of non-parametric tests may be somewhat less, but typically no more than 10 per cent less than their parametric equivalents.

5.3.1 Chi-square test

Pearson's (1900) paper in which chi-square was introduced is a foundation stone of modern statistical analysis[1]; a comprehensive and readable review (plus bibliography) is given by Cochran (1952).

Consider observational data which can be binned, and a model/hypothesis which predicts the population of each bin. The chi-square statistic describes the goodness-of-fit of the data to the model. If the observed numbers in each of k bins are O_i, and the expected values from the model are E_i, then this statistic is

$$\chi^2 = \sum_{i=1}^{k} \frac{(O_i - E_i)^2}{E_i}. \tag{5.10}$$

The null hypothesis H_0 is that the number of objects falling in each category is E_i; the chi-square procedure tests whether the O_i are sufficiently close to E_i to be likely to have occurred under H_0. The sampling distribution under H_0 of the statistic χ^2 follows the chi-square distribution (Fig. 5.4) with $\nu = (k-1)$ degrees of freedom. One degree of freedom is lost because of the constraint that $\Sigma_i O_i = \Sigma_i E_i$. The chi-square distribution is given by

$$f(x) = \frac{2^{-\nu/2}}{\Gamma[\nu/2]} x^{\nu/2-1} \mathrm{e}^{-x/2} \tag{5.11}$$

(for $x \geq 0$), the distribution function of the random variable $Y^2 = Z_1^2 + Z_2^2 + \ldots + Z_\nu^2$ where the Z_i are independent random variables of the standard Normal distribution. Table A2.6 presents critical values; if χ^2 exceeds these values, H_0 is rejected at that level of significance.

[1] Pearson's paper is entitled *On the criterion that a given system of deviations from the probable in the case of a correlated system of variables is such that it can be reasonably supposed to have arisen from random sampling.* It is wonderful polemic and gives several examples of the previous abuse of statistics, covering the frequency of buttercup petals to the incompetence of Astronomers Royal. ('Perhaps the greatest defaulter in this respect is the late Sir George Biddell Airy.') He demonstrates, for extra measure, that a run of bad luck at his roulette wheel, Monte Carlo, in July 1892 had one chance in 10^{29} of arising by chance; he avoids libel by phrasing his conclusion '... it will be more than ever evident how little chance had to do with the results ...'

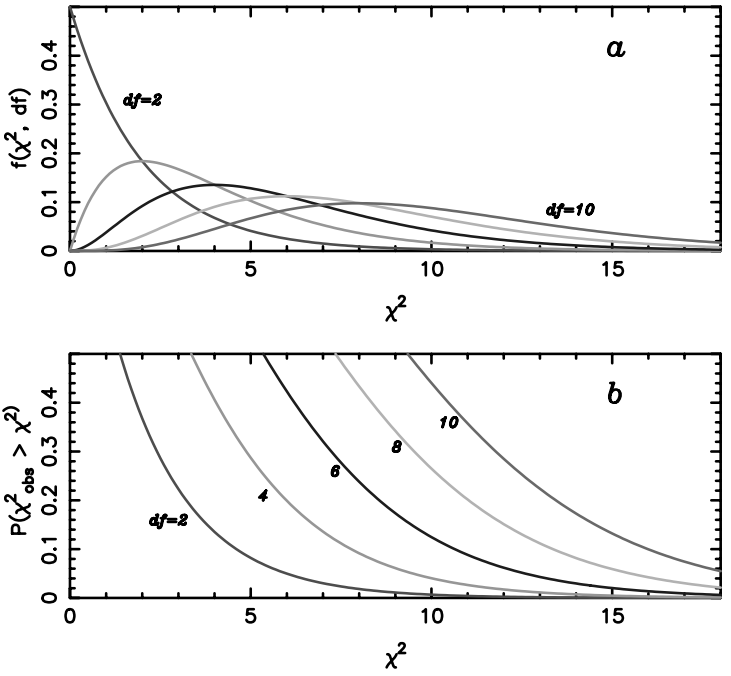

Fig. 5.4. The chi-square distribution: (a) $f(\chi^2, \mathrm{df})$, the probability density function of χ^2 for *df* degrees of freedom; (b) the distribution function $\int_{\chi^2}^{\infty} f(\chi^2, \mathrm{df})\, \mathrm{d}\,\chi^2$ of Table A2.6, consulted to determine if χ^2 is 'large enough' to reject H_0.

The premise of the chi-square test then is that the deviations from E_i are due to statistical fluctuations from limited numbers of observations per bin, i.e. 'noise' or Poisson statistics, and the chi-square distribution simply gives the probability that the chance deviations from E_i are as large as the observations O_i imply. As we shall see, we need enough data per bin to ensure that each term in the chi-square summation is approximately Gaussian.

There is good news and bad news about the chi-square test. First the good: it is a test of which most scientists have heard, with which many are comfortable, and from which some are even prepared to accept the results. Moreover because χ^2 is additive, the results of different datasets which may fall in different bins, bin sizes, or which may apply to different aspects of the same model, may be tested all at once. The contribution to χ^2 of each bin may be examined and regions of exceptionally good or

bad fit delineated. In addition, χ^2 is easily computed, and its significance readily estimated as follows. The mean of the chi-square distribution equals the number of degrees of freedom, while the variance equals twice the number of degrees of freedom; see the plots of the function in Fig. 5.4. So as another rule of thumb, if χ^2 should come out (for more than four bins) as $\sim$ (number of bins -1) then accept H_0. But if χ^2 exceeds twice (number of bins $-$ 1), probably H_0 will be rejected. Finally minimizing χ^2 is an exceptionally common method of model fitting (see Section 6.4); and an example of the chi-square test (and model fitting) is shown as Fig. 6.6.

Now the bad news: the data must be binned to apply the test, and the bin populations must reach a certain size because it is obvious that instability results as $E_i \to 0$. As another rule of thumb then: > 80 per cent of the bins must have $E_i > 5$. Bins may have to be combined to ensure this, an operation which is perfectly permissible for the test. However, the binning of data in general, and certainly the binning of bins, results in loss of efficiency and information, resolution in particular.

Thus the advantages of the chi-square test are its general acceptance, the ease of computation, the ease of guessing significance, and the fact that model testing is for free. The disadvantages are the loss of power and information via binning, and the lack of applicability to small samples, in particular the serious instability at < 5 counts per bin. Moreover, the chi-square test cannot tell direction, i.e. it is a ' two-tailed' test; it can only tell whether the differences between sample and prediction exceed those which can be reasonably expected on the basis of statistical fluctuations due to the finite sample size. There must be something better, and indeed there is:

5.3.2 Kolmogorov–Smirnov one-sample test

The test is extremely simple to carry out:

(i) Calculate $S_e(x)$, the predicted cumulative (integral) frequency distribution under H_0.

(ii) Consider the sample of N observations, and compute $S_o(x)$, the observed cumulative distribution, the sum of all observations to each x divided by the sum of all N observations.

(iii) Find

$$D = \max|S_e(x) - S_o(x)| \tag{5.12}$$

(iv) Consult the known sampling distribution for D under H_0, as given in Table A2.7, to determine the fate of H_0. If D exceeds a critical value at the appropriate N, then H_0 is rejected at that level of significance.

Thus, as for the chi-square test, the sampling distribution indicates whether a divergence of the observed magnitude is 'reasonable' if the difference between observations and prediction is due solely to statistical fluctuations.

The Kolmogorov–Smirnov test has some enormous advantages over the chi-square test. Firstly it treats the individual observations separately, and no information is lost because of grouping. Secondly, it works for small samples; for very small samples it is the only alternative. For intermediate sample sizes it is more powerful. Finally, note that as described here, the Kolmogorov–Smirnov test is non-directional or two-tailed, as is the chi-square test. However, a method of finding probabilities for the one-tailed test does exist (Birnbaum & Tingey 1951; Goodman 1954), giving the Kolmogorov–Smirnov test yet another advantage over the chi-square test.

Then why not always use it? There are perhaps two valid reasons, in addition to the invalid one (that it is not so well known). Firstly the distributions must be continuous functions of the variable to apply the Kolmogorov–Smirnov test. The chi-square test is applicable to data which can be simply binned, grouped, categorized – there is no need for measurement on a numerical scale. Secondly, in model fitting and parameter estimation, the chi-square test is readily adapted (Section 6.4) by simply reducing the number of degrees of freedom according to the number of parameters adopted in the model. The Kolmogorov–Smirnov test cannot be adapted in this way, since the distribution of D is not known when parameters of the population are estimated from the sample.

5.3.3 One-sample runs test of randomness

This delightfully simple test is contingent upon forming a binary (1–0) statistic from the sample data, e.g. heads-tails, or the sign of the residuals about the mean, or a best-fit line. It is to test H_0 that the sample is random; that successive observations are independent. Are there too many or too few runs?

Determine m, the number of heads or 1's; n, the number of tails or 0's, $N = n + m$; and r, the number of runs.

Look up the level of significance from the tabled probabilities (Table A2.8) for a one- or two-tailed test, depending on H_1, which can specify (as the research hypothesis) how the non-randomness might occur. In general we are concerned simply with the one-tail test, asking whether or not the number of runs is too few, the issue being independence or otherwise of data in a sequence. Situations giving rise to too many runs are infrequent; but if indeed there are significantly too many runs it does say something serious about the data structure – probably in the sense that we do not understand it.

In fact for m 'heads' and n 'tails' with N data, the expectation value of the number of runs is

$$\mu_r = \frac{2mn}{m+n+1} \tag{5.13}$$

and in the large N approximation this is asymptotically Gaussian with

$$\sigma_{\mathrm{r}} = \sqrt{\frac{2nm(2nm-N)}{N^2(N-1)}}. \tag{5.14}$$

For large samples, then, it is possible to use the Normal distribution in the standard way by forming

$$z = \frac{r - \mu_r}{\sigma_{\mathrm{r}}}$$

and consulting Table A2.1, the integral Gaussian or erf function. This is the procedure when the numbers exceed 20 and run off the end of Table A2.8.

EXAMPLE Figure 5.5 shows the optical spectrum of quasar 3C207. The baseline has been estimated by the method of minimum Fourier components (Section 8.4.2). Does it fit properly? Is there low-level signal present in broad emission lines? Carefully selected regions of the spectrum are examined with the runs test.

The runs test is applied by using one-bit digitization – is the datum above or below the fitted baseline? The lower-wavelength region has enhanced continuum, a quasar 'blue bump', where the likelihood of line emission is significantly reduced. The runs test yields concordance, 36 positive deflections, 29 negative, 31 runs against an expectation of

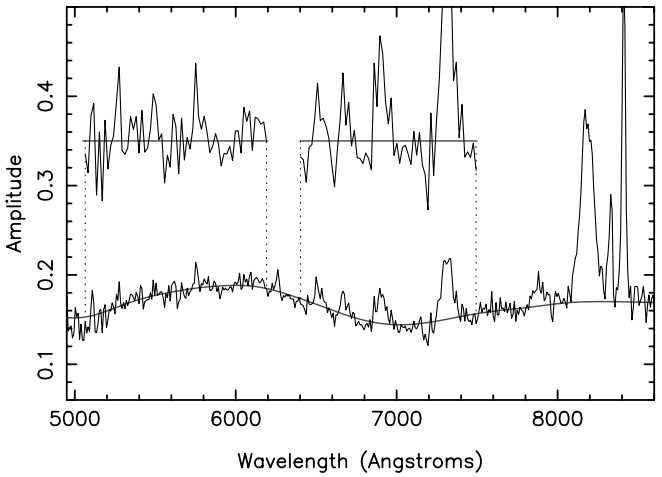

Fig. 5.5. A spectrum of the quasar 3C207, taken with the 4.2-m William Herschel Telescope. The solid curve is a baseline fitted by a Fourier minimum-component technique. The regions considered for the runs test are shown in the separated sections, each with the baseline subtracted and magnified by a factor of 3.

32.1 runs, $z = -0.28$. The second region lies in the range of the hydrogen Balmer-line series, and several members are clearly present in emission. The result, a foregone conclusion here, is rejection of randomness by the runs test at about 4σ: 31 positives, 32 negatives, 16 runs against an expectation of 31.5, $z = -3.94$. The broad emission lines yield the contiguous regions that decrease the number of runs to a highly significant degree.

The test is at its most potent in looking for independence between adjacent sample members, e.g. in checking sequential data of `scan` or `spectrum` type as in the above example. It is frequently used for checking sequences of residuals, scatter of data about a model line, and in this guise it can give a straightforward answer as to whether a model is a good representation of the data.

5.4 Non-parametric tests: two independent samples

Now suppose we have two samples; we want to know whether they could have been drawn from the same population, or from different

populations, and if the latter, whether they differ in some predicted direction. Again assume we know nothing about probability distributions, so that we need non-parametric tests. There are several.

5.4.1 Fisher exact test

The test is for two independent small samples for which discrete binary data are available, e.g. scores from the two samples fall in two mutually exclusive bins yielding a 2×2 contingency table as shown in Table 5.2.

Table 5.2. 2×2 contingency table

Sample =	1	2
Category = 1	A	C
= 2	B	D

H_0: the assignment of 'scores' is random.

Compute the following statistic:

$$p = \frac{(A+B)!(C+D)!(A+C)!(B+D)!}{N!A!B!C!D!}. \tag{5.15}$$

This is the probability that the total of N scores could be as they are when the two samples are in fact identical. But in fact the test asks: What is the probability of occurrence of the observed outcome or one more extreme under H_0? Hence by the laws of probability (see e.g. Stuart & Ord 1994), $p_{\text{tot}} = p_1 + p_2 + \cdots$; computation can be tedious. Nevertheless this is the best test for small samples; and if $N < 20$, it is probably the only test to use.

5.4.2 Chi-square two-sample (or k-sample) test

Again the much-loved chi-square test is applicable. All the previous shortcomings apply, but for data which are not on a numerical scale, there may be no alternative. To begin, each sample is binned in the same r bins (a $k \times r$ contingency table) – see Table 5.3.

H_0 is that the k samples are from the same population.

Then compute

$$\chi^2 = \sum_{i=1}^{r} \sum_{j=1}^{k} \frac{(O_{ij} - E_{ij})^2}{E_{ij}}. \tag{5.16}$$

Table 5.3. Multi-sample contingency table

Sample: j =	*1*	*2*	*3*
Category: i = *1*	O_{11}	O_{12}	O_{13}
2	O_{21}	O_{22}	O_{23}
3	O_{31}	O_{32}	O_{33}
4	O_{41}	O_{42}	O_{43}
5	O_{51}	O_{52}	O_{53}
.	...	...	...

The E_{ij} are the expectation values, computed from

$$E_{ij} = \frac{\sum_{j=1}^{k} O_{ij} . \sum_{i=1}^{r} O_{ij}}{\sum_{i=1}^{r} \sum_{j=1}^{k} O_{ij}}. \tag{5.17}$$

Under H_0 this is distributed as χ^2, with $(r-1)(k-1)$ degrees of freedom.

Note that there is a modification of this test for the case of the 2×2 contingency table (Table 5.2) with a total of N objects. In this case,

$$\chi^2 = \frac{N(\mid AD - BC \mid -N/2)^2}{(A+B)(C+D)(A+C)(B+D)} \tag{5.18}$$

has just one degree of freedom.

The usual chi-square caveat applies – beware of the lethal count of 5, below which the cell populations should not fall in any number. If they do, combine adjacent cells, simulate the distribution of the test statistic under the null hypothesis or abandon the test. And if there are only 2×2 cells, the total (N) must exceed 30; if not, use the Fisher exact probability test.

There is one further distinctive feature about the chi-square test (and the 2×2 contingency-table test); it may be used to test a directional alternative to H_0, i.e. H_1 can be that the two groups differ in some predicted sense. If the alternative to H_0 is directional, then use Table A2.6 in the normal way and halve the probabilities at the heads of the columns, since the test is now one-tailed. For degrees of freedom > 1, the chi-square test is insensitive to order, and another test thus may be preferable.

5.4.3 Wilcoxon–Mann–Whitney U test

This test is usually preferable to χ^2, mostly because it avoids binning. There are two samples, A (m members) and B (n members); H_0 is that A and B are from the same distribution or have the same parent population, while H_1 may be one of three possibilities:

(i) that A is stochastically larger than B;
(ii) that B is stochastically larger than A;
(iii) that A and B differ in some other way, perhaps in scatter or skewness.

The first two hypotheses are directional, resulting in one-tailed tests; the third is not and correspondingly results in a two-tailed test. To proceed, first decide on H_1 and of course the significance level α. Then

(i) Rank in ascending order the combined sample A + B, preserving the A or B identity of each member.
(ii) (Depending on the choice of H_1) Sum the number of A-rankings to get $U_{\rm A}$, or vice versa, the B-rankings to get $U_{\rm B}$. Tied observations are assigned the average of the tied ranks. Note that if $N = m+n$,

$$U_{\rm A} + U_{\rm B} = \frac{N(N+1)}{2},$$

so that only one summation is necessary to determine both – but a decision on H_1 should have been made a priori.
(iii) The sampling distribution of U is known (of course, or there would not be a test). Table A2.9, columns labelled $c_{\rm u}$ (upper-tail probabilities), presents the exact probability associated with the occurrence (under H_0) of values of U greater than that observed. The table also presents exact probabilities associated with values of U less than those observed; entries correspond to the columns labelled $c_{\rm l}$ (lower-tail probabilities). The table is arranged for $m \leq n$, which presents no restriction in that group labels may be interchanged. What does present a restriction is that the table presents values only for $m \leq 4$ and $n \leq 10$. For samples up to $m = 10$ and $n = 12$, see Siegel & Castellan (1988). For still larger samples, the sampling distribution for $U_{\rm A}$ tends to Normal with mean $\mu_{\rm A} = m(N+1)/2$ and variance $\sigma^2_{\rm A} = mn(N+1)/12$. Significance can be assessed from the Normal distribution, Table A2.1,

by calculating

$$z = \frac{U_{\rm A} \pm 0.5 - \mu_{\rm A}}{\sigma_{\rm A}}$$

where $+0.5$ corresponds to considering probabilities of $U \leq$ that observed (lower tail), and -0.5 for $U \geq$ that observed (upper tail). If the two-tailed ('the samples are distinguishable') test is required, simply double the probabilities as determined from either Table A2.9 (small samples) or the Normal distribution approximation (large samples).

EXAMPLE An application of the test is shown in Fig. 5.6, which presents magnitude distributions for flat and steep (radio) spectrum quasars from a complete sample of quasars in the Parkes 2.7-GHz survey (Masson & Wall 1977). H_1 is that the flat-spectrum quasars extend to significantly lower (brighter) magnitudes than do the steep-spectrum quasars, a claim made earlier by several observers. The eye agrees with H_1, and so does the result from the U test, in which we found $U = 719, t = 2.69$, rejecting H_0 in favour of H_1 at the 0.004 level of significance.

In addition to this versatility, the test has a further advantage of being applicable to small samples. In fact it is one of the most powerful non-parametric tests; the efficiency in comparison with the 'Student's' t test is ≥ 95 per cent for even moderate-sized samples. It is therefore an obvious alternative to the chi-square test, particularly for small samples where the chi-square test is illegal, and when directional testing is desired. An alternative is the

5.4.4 Kolmogorov–Smirnov two-sample test

The formulation parallels the Kolmogorov–Smirnov one-sample test; it considers the maximum deviation between the cumulative distributions of two samples with m and n members. H_0 is (again) that the two samples are from the same population, and H_1 can be that they differ (two-tailed test), or that they differ in a specific direction (one-tailed test).

To implement the test, refer to the procedure for the one-sample test (Section 5.3.2); merely exchange the cumulative distributions $S_{\rm e}$ and $S_{\rm o}$

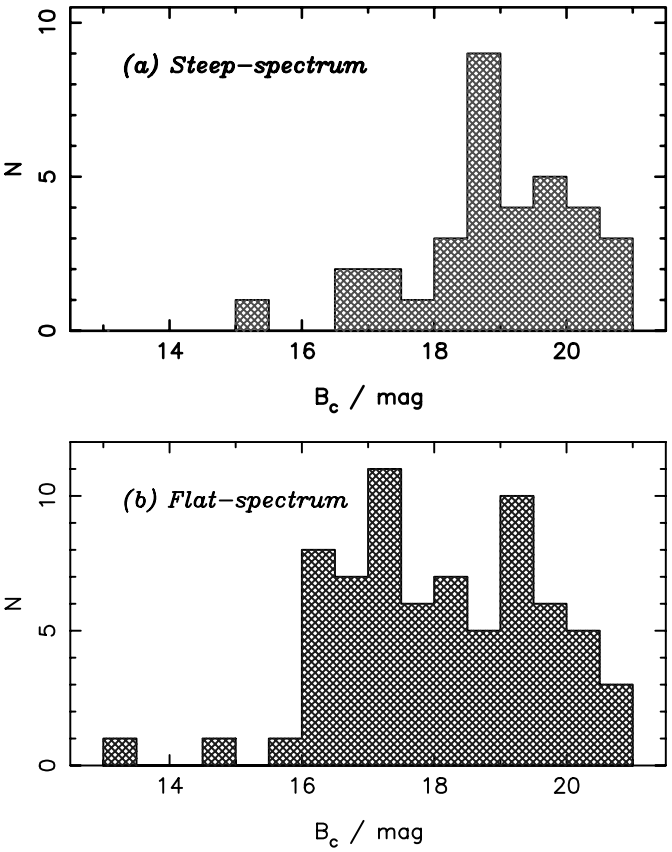

Fig. 5.6. Magnitude histograms for a complete sample of quasars from the Parkes 2.7-GHz survey, distinguished by radio spectrum. H_0, that the magnitude distributions are identical, is rejected using the Mann–Whitney–Wilcoxon U test at the 0.004 level of significance.

for S_m and S_n corresponding to the two samples. Critical values of D are given in Tables A2.10 and A2.11. Table A2.10 gives the values for small samples, one-tailed test, while Table A2.11 is for the two-tailed test. For large samples, two-tailed test, use Table A2.12. For large samples, one-tailed test, compute

$$\chi^2 = 4D^2 \frac{mn}{m+n}, \tag{5.19}$$

which has a sampling distribution approximated by chi-square with two degrees of freedom. Then consult Table A2.6 to see if the observed D

results in a value of χ^2 large enough to reject H_0 in favour of H_1 at the desired level of significance.

The test is extremely powerful with an efficiency (compared to the t test) of > 95 per cent for small samples, decreasing somewhat for larger samples. The efficiency always exceeds that of the chi-square test, and slightly exceeds that of the U test for very small samples. For larger samples, the converse is true, and the U test is to be preferred.

Note that the Kolmogorov–Smirnov test can also be used to compare *two-dimensional* distributions (Peacock 1983).

EXAMPLES Two examples, drawn from an investigation of flattening and radio emission among elliptical galaxies (Disney, Sparks & Wall 1984), are shown in Fig. 5.7. The upper diagrams compare the axial ratio b/a (minor to major axis) for (a) 102 bright ellipticals for which no radio emission was detected and (b) 30 ellipticals for which emission was detected. The Kolmogorov–Smirnov test rejects H_0, that the two distributions are from the same parent population, at the 1 per cent level of significance. The lower pair, to do with ascertaining whether seeing is affecting measurement of axial ratio (the radio ellipticals are on average more distant), shows some difference by eye, but no significant difference when the Kolmogorov–Smirnov test is carried out.

These and tests on additional subsamples were used to show that there is a strong correlation between radio activity and flattening, in the sense that radio ellipticals are both inherently and apparently rounder than the average elliptical.

5.5 Summary, one- and two-sample non-parametric tests

Tables 5.4, 5.5 and 5.6, adapted from Siegel & Castellan (1988), attempt a summary, demonstrating an apparent wide world of non-parametric tests available for sample comparison. But is this really so? In deciding which test(s), the following points should be noted; the decision may be made for you.

(i) The two-sample and k-sample cases each contain columns of tests for related samples, i.e. matched-pair samples, or samples of paired replicates. This is common experimental practice in biological and

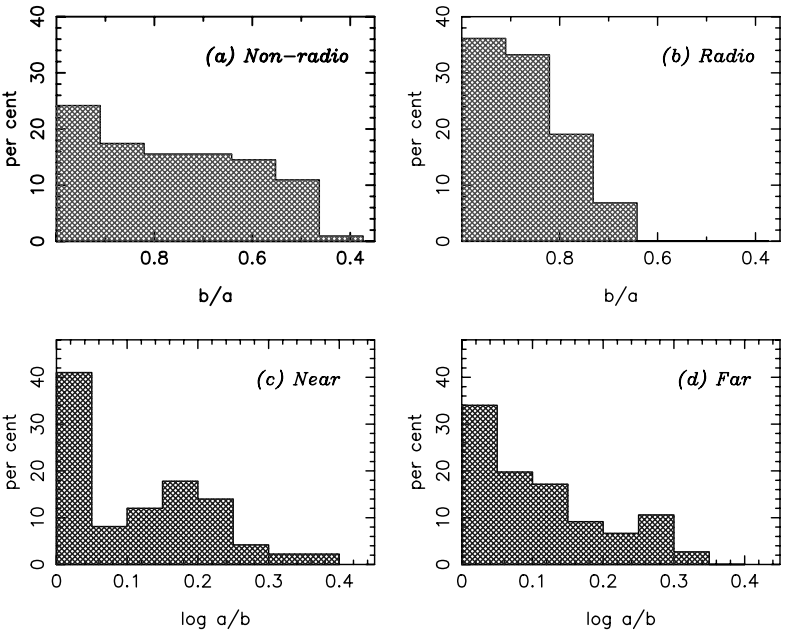

Fig. 5.7. Kolmogorov–Smirnov tests on subsamples of ellipticals from the Disney–Wall (1977) sample of bright ellipticals. Upper panels – distribution functions in b/a, minor to major axis, for (a) the 102 undetected and (b) the 30 radio-detected ellipticals in the sample. The Kolmogorov–Smirnov two-sample test rejects H_0, that the subsamples are drawn from the same population, at a significance level of < 1 per cent. Lower panels – distribution functions in $\log a/b$ for (c) the 51 ellipticals closer than 30 Mpc, (d) 76 bright ellipticals in the sample more distant than this. The Kolmogorov–Smirnov test indicates no significant difference between these latter subsamples.

behavioural sciences, where the concept of the control sample is highly developed. It is not so common in astronomy for obvious reasons, but has been exploited on occasion. The powerful tests available to treat such experiments are listed in Table 5.4, and are described by Siegel & Castellan.

(ii) Table 5.4 runs downward in order of increasing sophistication of measurement level, from `Nominal` (in which the test objects are simply dumped into classes or bins) through `Ordinal` (by which objects are ranked or ordered) to `Interval` (for which objects are placed on a scale, not necessarily numerical, in which distance along the scale matters). None of the tests requires measurement on a `Ratio` scale, the strongest scale of measurement in which to

Table 5.4. Non-parametric tests for comparison of samples

Level of measurement	One-sample case	Two–sample case		k–sample case	
		Related	Independent	Related	Independent
Nominal or categorical	Binomial test *Chi-square test	McNemar change test	*Fisher exact test for 2×2 tables *Chi-square test for $r \times 2$ tables	Cochran Q test	*Chi-square test for $r \times k$ tables
Ordinal or ordered	*Kolmogorov–Smirnov one-sample test *One-sample runs test Change-point test	Sign test Wilcoxon signed-ranks test	Median test *U (Wilcoxon–Mann–Whitney) test Robust rank-order test *Kolmogorov–Smirnov two-sample test Siegel–Tukey test for scale differences	Friedman two-way analysis of variance by ranks Page test for ordered alternatives	Extension of median test Kruskal–Wallis one-way analysis of variance Jonckheere test for ordered alternatives
Interval		Permutation test for paired replicates	Permutation test for two independent samples Moses rank-like test for scale differences		

*Described in this chapter; Siegel & Castellan (1988) discuss the other tests.

the properties of the interval scale a true zero point is added. (Degrees Celsius for temperature measurement represents an interval scale, and Kelvins a ratio scale.) An important feature of test selection lies in the level of measurement required by the test; the table is cumulative downward in the sense that at any level of measurement, all test above this level are applicable.

(iii) The efficiency of a particular test depends very much on the individual application. Is the search for goodness-of-fit and general difference, i.e. is this sample from a given population? Are these

Table 5.5. Single-sample non-parametric tests

Test	Applicability†	$N < 10$?	Comment
Binomial test	Goodness-of-fit (N)	Yes	Appropriate for two-category (dichotomous) data; do *not* dichotomize continuous data.
*Chi-square test	Goodness-of-fit (N)	No	For testing categorized, pre-binned, or classified data; choose categories with expected frequencies 6–10.
*Kolmogorov–Smirnov one-sample test	Goodness-of-fit (O)	Yes	The most powerful test for data from a continuous distribution; may always be more efficient than the chi-square test.
*One-sample runs test	Randomness of event sequences (O)	Yes	Does not estimate differences between groups.
Change-point test	Change in the distribution of an event sequence (O)	Yes	Robust with regard to changes in distributional form; efficient.

*Described in this chapter; Siegel & Castellan (1988) discuss the other tests.
† *Goodness-of-fit* indicates general testing for any type of difference, i.e. H_0 is that the distribution is drawn from the specified population. The level of measurement required is indicated by N – Nominal, O – Ordinal, or I – Interval.

samples from the same population? Or is it a particular property of the distribution which is of interest, such as the location, e.g. central tendency, mean or median; or the dispersion, e.g. extremes, variance, rms. For instance in the two-sample case, the chi-square and the Kolmogorov–Smirnov (two-tailed) tests are both sensitive to any type of difference in the two distributions, location, dispersion, skewness, while the U test is reasonably sensitive to most properties, but is particularly powerful for location discrimination. To aid the process of choice, Tables 5.5 (single samples) and 5.6 (two samples) summarize the attributes of the one- and two-sample tests.

Table 5.6. Two-sample non-parametric tests

Test	Applicability†	$N < 10$?	Comment
*Fisher exact test for 2×2 tables	Difference (N)	Yes	The most powerful test for dichotomous data.
*Chi-square test for $r \times 2$ tables	Difference (N)	No	Best for pre-binned, classified, or categorized data.
Median test	Location (O)	Yes	Best for small numbers; efficiency *decreases* with N.
*U (Wilcoxon–Mann–Whitney) test	Location (O)	Yes	One of the most efficient non-parametric tests.
Robust rank-order test	Location (O)	Yes	Efficiency similar to U test.
*Kolmogorov–Smirnov two-sample test	Two-tailed: Difference One-tailed: Location (O)	Yes	The most powerful test for data from a continuous distribution.
Siegel–Tukey test for scale differences	Dispersion (O)	Yes	The medians must be the same (or known) for both distributions. Low efficiency.
Permutation test	Location (I)	Yes	Very high efficiency.
Moses rank-like test for scale differences	Dispersion (I)	(No)	Does not require identical medians; valid for small samples, but increases with sample size.

*Described in this chapter; Siegel & Castellan (1988) discuss the other tests.
† *Difference* signifies sensitivity to any form of difference between the two distributions, i.e. H_0 is that the two distributions are drawn from the same population; *Location* indicates sensitivity to the position of the distributions, e.g. means or medians; and *Dispersion* indicates sensitivity to the spread of the distributions, i.e. variance, rms, extremes. The level of measurement required is indicated by N – Nominal, O – Ordinal, or I – Interval.

The choice of test may thus come down to Hobson's. However, if it does not, and two (or more) alternatives remain, beware of this plot of the Devil. It might be possible to 'test the tests' in searching for support of a point of view. If such a procedure is followed, quantification of the amount by which significance is reduced must be considered: for a chosen significance level p in a total of N tests, the chance that one test will (randomly) come up significant is $Np(1-p)^{N-1} \simeq Np$ for small p. The application of efficient statistical procedure has power; but the application of common sense has more.

Exercises

In the exercises denoted by (D), datasets are provided on the book's website; or create your own.

5.1 **Kolmogorov–Smirnov (D).** Use the data provided, two datasets, one with a total of m = 290 observations, the other with 385 measurements. The former is of flux densities measured at random positions in the sky; the latter of flux densities at the positions of a specified set of galaxies. Using the Kolmogorov–Smirnov two-sample test, examine the hypothesis that there is excess flux density at the non-random positions.

5.2 **Wilcoxon–Mann–Whitney (D).** Repeat the test with the Wilcoxon–Mann–Whitney statistic. Is the significance level different? How would you combine the results from these two tests, plus the chi-squared test in the text?

5.3 t **test and outliers (D).** Create two datasets, one drawn from a Gaussian of unit variance, the other drawn from a variable combination of two Gaussians, the dominant one of unit variance and the other three times wider. All Gaussians are of zero mean. Perform a t test on sets of 10 observations and investigate what happens as contamination from the wide Gaussian is increased. Compare the effect on the posterior distribution of the difference of the means. Now shift the narrow Gaussian by half a unit, and repeat the experiment. What effect do the outliers have on our ability to refute the null hypothesis? How does the Bayesian approach compare?

5.4 **F test (D).** Create some random data, as in the first part of Exercise 3. Investigate the sensitivity of the standard F test to a small level of contamination by outliers.

5.5 **Non-parametric alternatives (D).** Repeat the analysis of the last two exercises, using a non-parametric test; the Wilcoxon–Mann–Whitney test for the location test, and the Kolmogorov–Smirnov test for the variance test. How do the results compare with the parametric tests? Can you detect genuine differences in variance, apart from the outliers?

5.6 **Several datasets, one test.** Suppose you have N independent datasets, and with a certain test you obtain a significance level of p_i for each one. A useful overall significance is given by the W statistic (Peacock 1985) which is

$$W = \prod_{i=1}^{N} p_i.$$

Find the distribution of $\log W$ and describe how it could be used. Note this contrasts to the case discussed in the text, where we might perform several different tests on the `same` dataset. (Each p_i will be uniformly distributed between zero and one, under the null hypothesis. The distribution of $\log W$ is the sum of these uniformly distributed numbers, and tends to a Gaussian of mean N and variance N.)

5.7 **Gram–Charlier (D).** Take some data drawn from a Gaussian and investigate the posterior likelihood if just one term (the quadratic) is used in a Gram-Charlier expansion as an assumption for the 'true' distribution. Take the location as known. Find the distribution of the variance, marginalizing out the Gram–Charlier parameter. Also, find the odds on including the parameter in the model. What does this tell you about assuming a Gaussian distribution when the amounts of data are limited?

5.8 **Odds versus classical tests.** Use the small dataset from the example in Section 5.2.3. Perform a classical analysis, using t and F tests. Compare and contrast to the odds calculated in the text. Does the Behrens–Fisher distribution give a better answer than either or both? See Jaynes's comments on confidence intervals (Jaynes 1983).

6

Data modelling; parameter estimation

But what are the errors on your errors?
(Graham Hine at a Mark Birkinshaw colloquium, Cambridge 1979)

Many pages of statistics textbooks are devoted to methods of estimating parameters, and calculating confidence intervals for them. For example, if our N data Z_i follow a Gaussian distribution

$$\text{prob}(z) = \frac{1}{\sqrt{2\pi}\sigma} \exp\left[-\left(\frac{z-\mu}{2\sigma^2} \right)^2 \right],$$

then the statistic

$$m = \frac{1}{N} \sum_i Z_i$$

is a good estimator for μ and has a known distribution (a Gaussian again) which can be used for calculating confidence limits. Or, from the Bayesian point of view, we can calculate a probability distribution for μ, given the data.

Any data-modelling procedure is just a more elaborate version of this, assuming we know the relevant probability distributions. Suppose our data Z_i were measured at various values of some independent variable X_i, and we believed that they were 'really' scattered, with Gaussian errors, around the underlying functional relationship

$$\mu = \mu(x, \alpha_1, \alpha_2, \ldots),$$

in which $\alpha_1, \alpha_2, \ldots$ are unknown parameters (slopes, intercepts, ...) of

the relationship. We then have

$$\text{prob}(z \mid \alpha_1, \alpha_2 \ldots) = \frac{1}{\sqrt{2\pi}\sigma} \exp\left[-\frac{(z - \mu(x, \alpha_1, \alpha_2, \ldots))^2}{2\sigma^2}\right]$$

and, by Bayes' theorem, we have the posterior probability distribution for the parameters

$$\text{prob}(\alpha_1, \alpha_2, \ldots \mid Z_i, \mu) \propto \Pi_i \frac{1}{\sqrt{2\pi}\sigma}$$
$$\times \exp\left[-\frac{(Z_i - \mu(x, \alpha_1, \alpha_2, \ldots))^2}{2\sigma^2}\right] \text{prob}(\alpha_1, \alpha_2, \ldots) \qquad (6.1)$$

including as usual our prior information. We have included μ as one of the 'givens' to emphasize that everything depends on it being the correct model.

This, at least formally, completes our task; we have a probability distribution for the parameters of our model, given the data.

This is a very general approach. In the limiting case of uninformative or diffuse priors, it is very closely related to the method of maximum likelihood; if the distribution of the residuals from the model is indeed Gaussian, it is closely related to the method of least squares. Moreover, it can be used in a clear way to update models as new data arrive; the posterior from one stage of the experiments becomes the prior for the next.

We can also deal nicely with unwanted parameters ('nuisance' parameters). Typically we will end up with a probability distribution for various parameters, some of interest (say, cosmological parameters) and some not (say, instrumental calibrations). We can marginalize out the unwanted parameters by an integration, leaving us with the distribution of the variable of interest that takes account of the range of plausible values of the unwanted variables. Later examples will develop these ideas.

Modelling can be a very expensive part of any investigation. Analytic approximations were developed in past years for very good reasons. Modelling processes always involve finding an extreme value, a maximum or minimum, of some merit function. Without help from an analytic solution, this means evaluating the function, and perhaps its derivatives, many times. The model itself may be the result of a complex and time-consuming computation, so evaluating it over a range of parameters is even worse.

Another difficulty that arises in the Bayesian approach is numerical integration. Interesting problems have many parameters; marginalizing

these out, or calculating evidences for discriminating between models, involves multidimensional integrals. These are often very time-consuming, and laborious to check. Any analytical help we can get is especially welcome in doing integrations. We will see the relevance of this in the next section, where powerful theorems may allow great simplifications.

Perhaps the most important thing to remember about models is blindingly obvious; they may be wrong. The most insidious case of this is a mistake in the assumed distribution of residuals about the model. Inevitably, the parameters deduced from the model will be wrong. Worse, the inferred errors on these parameters will be wrong too, often giving a quite false sense of security. It is important to have a range of models available, and always to check optimized models against the data, inspecting the residuals for strange outliers or clusters of positive or negative residuals. The runs test (Section 5.3.3) is helpful in this respect.

6.1 The maximum-likelihood method

Maximum likelihood (ML) has a long history: it was derived by Bernoulli in 1776 and Gauss around 1821, and worked out in detail by Fisher in 1912.

We have met the likelihood function several times already; together with the prior probabilities, it makes up the posterior probability from Bayes' theorem. Suppose our data are described by the probability density function $f(X;\alpha)$, where x is a variable, and α is a parameter (maybe many parameters) characterizing the known form of f. We want to estimate α. If $X_1, X_2, \ldots, X_N$ are data, presumed independent and all drawn from f, then the likelihood function is

$$\begin{aligned}\mathcal{L}(X_1, X_2, \ldots, X_N) &= f(X_1, X_2, \ldots, X_N \mid \alpha) \\ &= f(X_1 \mid \alpha) f(X_2 \mid \alpha) \ldots f(X_N \mid \alpha) \\ &= \prod^{N} f(X_i \mid \alpha). \end{aligned} \tag{6.2}$$

From the classical point of view this is the probability, given α, of obtaining the data. From the Bayesian point of view it is proportional to the probability of α, given the data and assuming that the priors are 'diffuse'. Practically speaking, this means that they change little over the peaked region of the likelihood function. Finding the constant of proportionality involves the troublesome integrals we referred to before.

If the priors are not diffuse, this means they are having as strong an effect on our conclusions as the data. This is not an unlikely situation, but it does rule out the handy analytical approximations we will describe later.

From either point of view, more intelligibly from the Bayesian, the peak value of $\mathcal{L}$ seems likely to be a useful choice of the 'best' estimate of α. This does rather depend on what we want to do next with our estimate, however.

Formally, the maximum-likelihood estimator (MLE) of α is $\hat{\alpha} =$ (that value of α which maximizes $\mathcal{L}(\alpha)$ for all variations of α). Often we can find this from

$$\frac{\partial}{\partial \alpha} \ln \mathcal{L}(\alpha)\bigg|_{\alpha=\hat{\alpha}} = 0 \tag{6.3}$$

but sometimes we cannot – an example of this will be given later.

Maximizing the logarithm is often convenient, both algebraically and numerically. The MLE is a statistic – it depends only on the data, and not on any parameters.

EXAMPLE Consider our old friend the regression line, for which we have values of Y_i measured at given values of the independent variable X_i. Our model is

$$y(a, b) = ax + b$$

and assuming that the Y_i have a Gaussian scatter, each term in the likelihood product is

$$\mathcal{L}_i(y|(a, b)) = \exp\left[-\frac{(Y_i - (aX_i + b))^2}{2\sigma^2}\right]$$

i.e. the residuals are $(Y_i -$ model), and our model has the free parameters (a, b). Maximising the log of the likelihood products then yields

$$\frac{\partial \Sigma}{\partial a} = -2\Sigma(Y_i - a - bX_i) = 0$$

$$\frac{\partial \Sigma}{\partial b} = -2\Sigma X_i(Y_i - a - bX_i) = 0$$

from which two equations in two unknowns we get the well-known

$$a = \frac{\Sigma Y_i(X_i - \overline{X})}{\Sigma(X_i - \overline{X}^2)}$$

$$b = \overline{Y} - a\overline{X}.$$

With this simple maximum-likelihood example, we have accidentally derived the standard OLS, the ordinary least squares estimate of y on the independent variable x. But note how this happened: we were given the fact that the Y_i were Normally distributed with their scatter described by a single deviation σ; and of course we were given the fact that a straight-line model was correct. It need not be this way: we could have started knowing that each Y_i had an associated σ_i, or even that the distribution in y about the line was not Gaussian, perhaps say uniform, or dependent on $|Y_i - \text{model}|$ rather than $(Y_i - \text{model})^2$. The formulation is identical, although the algebra may not work out as neatly as it does for an OLS regression line. But this of course is another advantage of maximum likelihood – the likelihood function can be computed and the maximum found without recourse to algebra.

EXAMPLE Jauncey (1967) showed that maximum likelihood was an excellent way of estimating the slope of the number–flux-density relation, the dependence of source surface density on intensity, for extragalactic radio sources. The source count is assumed to be of the power-law form

$$N(> S) = kS^{-\gamma}$$

where N is the number of sources on a particular patch of sky with flux densities greater than S, k is a constant, and $-\gamma$ is the exponent, or slope in the log N – log S plane, which we wish to estimate; see Fig. 6.1.

The probability distribution for S (the chance of getting a source with a flux density near S) is then

$$\text{prob}(S) = \gamma k S^{-(\gamma+1)}$$

and k is determined by the normalization to unity

$$\int_{S_0}^{\infty} \text{prob}(S)\,\mathrm{d}S = 1.$$

(We have taken the maximum possible flux density to be infinity, with small error for steep counts.) k is then γ/S_0^{γ} and the log-likelihood is, dropping constants,

$$\ln \mathcal{L}(\gamma) = M \ln \gamma - \gamma \sum_i \ln \frac{S_i}{S_0}$$

where we have observed M sources with flux densities S brighter than

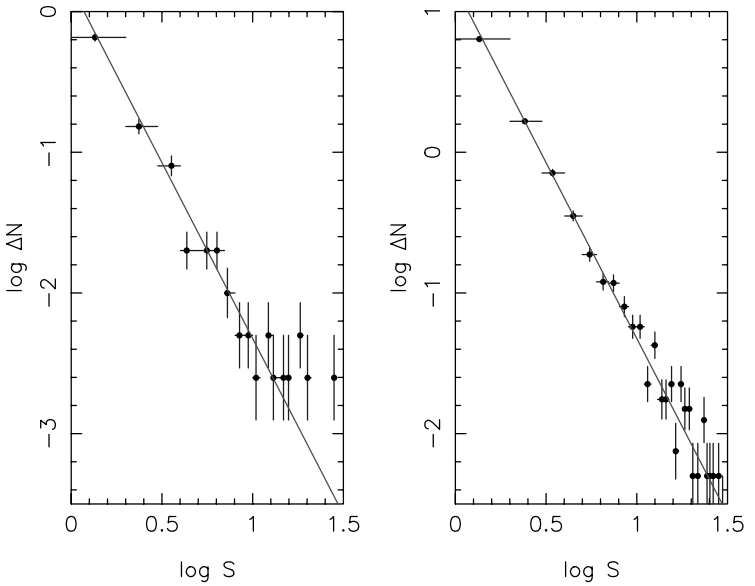

Fig. 6.1. A maximum-likelihood application. The figures show differential source counts generated via Monte Carlo sampling with an initial uniform deviate (see Section 6.5) obeying the source-count law $N(>S) = kS^{-1.5}$. The straight line in each shows the anticipated count with slope -2.5: left, $k = 1.0$, 400 trials; right, $k = 10.0$, 4000 trials. The ML results for the slopes are -2.52 ± 0.09 and -2.49 ± 0.03, the range being given by the points at which the log likelihood function has dropped from its maximum by a factor of 2. The anticipated errors in the two exponents, given by $|\text{slope}|/\sqrt{\text{trials}}$ (see the next-but-one example), are 0.075 and 0.024.

S_0. Differentiating this with respect to γ to find the maximum then gives the equation for $\hat{\gamma}$, the MLE of γ:

$$\hat{\gamma} = \frac{M}{\sum_i \ln \frac{S_i}{S_0}}$$

a nicely intuitive result. This application of ML makes optimum use of the data in that the sources are not grouped and the loss of power which always results from binning is avoided.

The MLE cannot always be obtained by differentiation, as the following example shows.

EXAMPLE A supernova produces an intense burst of neutrinos. The intensity of this burst decays exponentially after the core collapse of the precursor star. A handful of neutrinos (say N in number) were detected from supernova 1987, with arrival times (in order) T_1, T_2, ... The probability of a neutrino arriving at time t is

$$\text{prob}(t) = \exp[-(t - t_0)]$$

for $t > t_0$ and zero otherwise. Times are measured in units of the half-life and t_0 is the parameter we want, the start of the burst.

The log-likelihood is just

$$\ln \mathcal{L}(t_0) = Nt_0 - \sum_i T_i$$

and this doesn't appear to have a maximum. However, clearly $t_0 < T_1$ and so the likelihood is maximized, within the allowable range of t_0, at $\hat{t}_0 = T_1$.

After the MLE estimate has been obtained, it is essential to perform a final check: does the MLE model fit the data reasonably? If it does not then the data are erroneous when the model is known to be right; or, the adopted or assumed model is wrong; or (most commonly) there has been a blunder of some kind. There are many ways of carrying out such a check; two of these, the chi-square test and the Kolmogorov–Smirnov test, were described in Sections 5.3.1 and 5.3.2, respectively.

If the deviations between the best-fit model and the data (the residuals) are Gaussian, the log-likelihood function becomes a sum of squares of residuals and we have the famous method of least squares. More on this later.

Now for those theorems. The strongest reason for picking the MLE of a parameter is that it has desirable properties – it has minimum variance compared to any other estimate, and it is asymptotically Normally distributed around the true value. An MLE is not always unbiased, however.

If we estimate a vector $\hat{\vec{\alpha}}$ by the maximum-likelihood method, then the components of the estimated vector are asymptotically distributed around the true value like a multivariate Gaussian (Section 4.2). 'Asymptotically' means when we have lots of data, strictly speaking infinite

amounts. The covariance matrix that describes this Gaussian can be derived from the second derivatives of the likelihood with respect to the parameters. This involves a famous matrix called the Hessian, which is

$$H = \begin{bmatrix} \frac{\partial^2 \ln \mathcal{L}}{\partial \alpha_1^2} & \frac{\partial^2 \ln \mathcal{L}}{\partial \alpha_1 \partial \alpha_2} & \frac{\partial^2 \ln \mathcal{L}}{\partial \alpha_1 \partial \alpha_3} & \cdots \\ \frac{\partial \ln \mathcal{L}}{\partial \alpha_2 \partial \alpha_1} & \frac{\partial^2 \ln \mathcal{L}}{\partial \alpha_2^2} & \frac{\partial^2 \ln \mathcal{L}}{\partial \alpha_2 \partial \alpha_3} & \cdots \\ \frac{\partial^2 \ln \mathcal{L}}{\partial \alpha_3 \alpha_1} & \frac{\partial^2 \ln \mathcal{L}}{\partial \alpha_3 \partial \alpha_2} & \frac{\partial^2 \ln \mathcal{L}}{\partial \alpha_3^2} & \cdots \\ \vdots & \vdots & \vdots & \end{bmatrix}. \tag{6.4}$$

This matrix of course depends on the data. Taking its expectation value (the 'average' value of each component of the matrix, $E[H]$ for short, Section 3.1), we have a simple expression for the covariance matrix of the multivariate Gaussian distribution of the maximum-likelihood estimators of the parameters:

$$C = (E[H])^{-1}, \tag{6.5}$$

the $(\ldots)^{-1}$ signifying the inverse matrix.

The probability distribution of our N MLEs $\hat{\vec{\alpha}}$ is then

$$\text{prob}(\hat{\alpha_1}, \hat{\alpha_2}, \ldots) = \frac{1}{\sqrt{(2\pi)^N \mid C \mid}} \exp\left[-\frac{1}{2}(\hat{\vec{\alpha}} - \alpha) \cdot C^{-1} \cdot (\hat{\vec{\alpha}} - \alpha)^{\mathrm{T}}\right] \tag{6.6}$$

so that, as stated, the MLE $(\hat{\vec{\alpha}})$ is distributed around the true value $\vec{\alpha}$ with a spread described by the covariance C. $\mid C \mid$ is the determinant of C.

Taking the expectation value is obviously important, as otherwise the matrix would be different for each set of data. Sometimes we can carry out the expectation, or averaging, operation analytically in terms of $\vec{\alpha}$, the parameters of the original model. Sometimes the matrix does not involve the data at all. Most commonly, we just have to take the single matrix, given by our one set of data, as the best estimate we can make of the average value.

Why should the maximum-likelihood estimators obey this theorem? Take a simple case, a Gaussian of true mean μ and variance σ^2. If we

have N data X_i, the log likelihood is (dropping constants)

$$\log \mathcal{L} = \frac{-1}{2\sigma^2} \sum_i (X_i - \mu)^2 - N \log \sigma$$

and

$$\frac{-\partial^2 \log \mathcal{L}}{\partial \mu^2} = \frac{N}{\sigma^2}.$$

This is the Hessian 'matrix' for our simple problem. Taking its expectation and then inverse, not too hard in this case, gives us the variance on the estimate of the mean as σ^2/N, the anticipated result.

This example provides some justification for the theorem. In the exercises we set the somewhat more complicated case of estimating μ and σ together. This gives a matrix problem rather than a scalar one, and some real expectations have to be performed.

EXAMPLE In the source-count example, we have just one parameter. The variance on $\hat{\gamma}$ is then

$$\frac{-1}{E\left[\frac{\partial^2 \mathcal{L}(\gamma)}{\partial \gamma^2}\right]}$$

which is γ^2/M, the expectation is easy in this case. However, we see that the error is given in terms of the thing we want to know, namely γ. As long as the errors are small we can approximate them by $\hat{\gamma}^2/M$.

6.2 The method of least squares: regression analysis

Least squares is a famous old method of dealing with noisy data; it was invented, for astronomical use, by Gauss and Laplace at the beginning of the nineteenth century. There is a huge literature, e.g. Williams (1959); Linnik (1961); Montgomery & Peck (1992). The justification for the method follows immediately from the method of maximum likelihood; if the distribution of the residuals is Gaussian, then the log likelihood is a sum of squares of the form

$$\log \mathcal{L} = \text{constant} - \sum_{i=1}^{N} \xi_i (X_i - \mu(\alpha_1, \alpha_2, \ldots))^2 \tag{6.7}$$

where the ξ are the weights, obviously inversely proportional to the variance on the measurements. Usually the weights are assumed equal for all the data, and least squares is just that; we seek the model parameters which minimize

$$\log \mathcal{L} = \text{constant} - \frac{1}{2\sigma^2} \sum_{i=1}^{N} (X_i - \mu(\alpha_1, \alpha_2, \ldots))^2.$$

These will just be the maximum-likelihood estimators, and everything we have said before about them carries over. In particular, they are asymptotically distributed like a multivariate Gaussian. If we do not know the error level (the σ) we do not need to use it, but we will not be able to infer errors on the MLE; we will get a model fit, but we will never know how good or bad the model is.

The matrix of second derivatives defining the covariance matrix of the estimates, the Hessian matrix (Section 6.1), takes on a particular significance in the method of least squares because it is often used by the numerical algorithms which find the minimum. There are many powerful variations on these algorithms – see Numerical Recipes (Press et al. 1992) for details. Typically the value of the Hessian matrix, at the minimum, pops out as a by-product of the minimization. We can use this directly to work out the covariance matrix, as long as our model is linear in the parameters; in this case, the expectation operation is straightforward and the matrix does not depend on any of the parameters. We saw before why this is a problem (in the source-count example) – we want to find the parameters, and using the estimates in the covariance matrix is not an ideal procedure.

The notion of a linear model is worth clarifying. Suppose our data X_i are measured as a function of some independent variable Z_i. Then a linear model – linear in the parameters – might be $\alpha z^2 + \beta \exp(-z)$, whereas $\alpha \exp(-\beta z)$ is not a linear model. Of course a model may be approximately linear near the MLE. However, how close must it be? This illustrates again the general feature of the asymptotic Normality of the MLE – we can use the approximation, but we can't tell how good it is. Usually things will start to go wrong first in the wings of the inferred distributions (we have seen this in a previous example) and so high degrees of significance usually cannot be trusted unless they have been calculated exactly, or simulated by Monte Carlo methods.

EXAMPLE In the notation we used before, suppose our model is

$$\mu(\alpha, \beta) = \alpha z + \beta z^2,$$

a simple polynomial. The covariance matrix can be calculated from H, the matrix of derivatives of the log likelihood; it is just

$$C = \frac{1}{\sigma^2} \begin{bmatrix} \sum_i Z_i^2 & 0 \\ 0 & \sum_i Z_i^4 \end{bmatrix}$$

so the variance on β, for example, is $\sigma^2 / \sum_i Z_i^4$. Evidently where we make the measurements (the Z_i) will affect the variance. The effects are obvious enough in this simple case, but in more complicated cases it may be worth examining the experimental design, via the covariance matrix, to minimize the expected errors.

Quite often we will not be confident that we are dealing with Gaussian residuals, and usually this is because of outliers – residuals which are extremely unlikely on the Gaussian hypothesis. One convenient distribution which has 'fat' tails, and is a useful contrast to a Gaussian, is the simple exponential

$$\text{prob}(x) = \frac{1}{2a} \exp\left[-\frac{\mid x - \mu \mid}{a} \right].$$

If the residuals are distributed in this way, then it is easy to see that maximum likelihood leads to the minimization of the sum of the absolute values of the residuals. A t distribution may also be a helpful model. Working out a MLE in this way will give some indication of whether outliers are driving the answer. The only problem may be that relatively slow numerical routines have to be used; least squares minimization routines are highly developed by comparison.

Let us return for the last time to our simple regression line, the least squares fit of the model $y = ax + b$ through N pairs of (X_i, Y_i) by minimizing the squares of the residuals. This yields the well-known expressions for slope and intercept (differing slightly from those in the first example of Section 6.1, but readily shown to be equivalent):

$$a = \frac{N \sum^N X_i Y_i - \sum^N X_i \sum^N Y_i}{N \sum^N X_i^2 - \left(\sum^N X_i \right)^2} \tag{6.8}$$

and

$$b = \left(\sum^{N} Y_i - a \sum^{N} X_i \right) / N. \tag{6.9}$$

In the absence of knowledge of the how and why of a relation between the X_i and the Y_i (Section 4.4), any two-parameter curve may be fitted to the data pairs just with simple coordinate transformations; for example

(i) an exponential, $y = b \exp a$ requires Y_i to be changed to $\ln Y_i$ in the above expressions,
(ii) a power-law, $y = bx^a$; change Y_i to $\ln Y_i$ and X_i to $\ln X_i$;
(iii) a parabola, $y = b + ax^2$; change X_i to $\sqrt{X_i}$.

Note that the residuals cannot be Gaussian for all of these transformations (and may not be Gaussian for any): of course it is always possible to minimize the squares of the residuals, but it may well not be possible to retain the formal justification for doing so. The tests of Chapter 4 can be revealing as to which (if any) model fits, particularly the runs test.

This simple formulation of the least squares fit for y on x represents the tip of an iceberg – there is an enormous variety of least squares linear regression procedures. Amongst the issues involved in choosing a procedure:

- Are the data to be treated weighted or unweighted?
- (And the related question) Do all the data have the same properties, e.g. in the simple case of y on x, is one σ_y^2 applicable to all y? Or does σ_y^2 depend on y? In the uniform σ case, the data are described as homoskedastic, and in the opposite case, heteroskedastic.
- Is the right fit the standard ordinary least squares solution y on x (OLS(Y/X)) or x on y (OLS(X/Y)? Or something different, as discussed below?
- If we know we have heteroskedasticity, with the uncertainty different but known in each y_i and perhaps also in each x_i, how do we use this information to estimate the uncertainty in the fit?
- Are the data truncated or censored; do we wish to include upper limits in our fit? This is perfectly possible; see Section 7.5.

The thorough papers of Feigelson and collaborators (Isobe et al. 1990; Babu & Feigelson 1992; Feigelson & Babu 1992b) consider these issues, describe the complexities, indicate how to find errors with bootstrap

and jackknife resampling (Section 6.6), and identify appropriate software routines. In the astronomical context, Feigelson & Babu (1992b) emphasize that much of the proliferation of linear regression methods in the cosmic distance-scale literature is due to *lack of precision in defining the scientific question*. The question defines the statistical model. The serious fitter must consult the Feigelson references. In the interim and as an indication of why you must, consider the following example.

EXAMPLE Return to our bivariate Gaussian of Section 4.2 and Fig. 4.4, and now consider random variates (x_i, y_i) selected (a) in accord with $\rho = 0.05$ (little correlation) and $\rho = 0.95$ (strongly correlated). The ellipses of the contours are shown in Fig. 6.2. For the case of little correlation, the two OLS lines are stunningly different, almost orthogonal; for the relatively strong correlation, the lines are very similar.

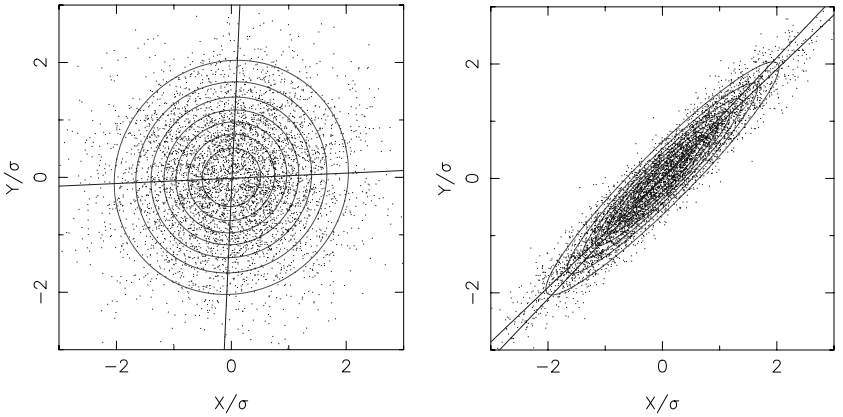

Fig. 6.2. Linear contours of the bivariate Gaussian probability distribution. Left: $\rho = 0.05$, a bivariate distribution with weak connection between x and y; right: $\rho = 0.95$, indicative of a strong connection between x and y. In each case 5000 (x, y) pairs have been plotted, selected at random from the appropriate distribution as described in Section 6.5. Two lines are shown as fits for each distribution, the OLS(X/Y) and the OLS(Y/X).

The point is that we know the answer here for the relation: it is a line of slope unity, 45°. With little (yet formally significant) correlation, the OLS lines mislead us dramatically. Of course the so-called bisector

line (the average of the two OLSs) would get it right, as would the orthogonal regression line which minimizes the perpendicular distances. But for the former, if the points were not Gaussian in distribution, would you trust it? A few outliers (mistakes?) would soon wreck it. The latter is principal component analysis (Section 4.5) precisely. It has already been emphasized that when the dependences of variables on each other are not understood, PCA is the way to go. It gives the right answer in this example; it tells us what the relation between y and x is, without us assuming which variable is in control. It is the right answer if we want to describe a relation between x and y.

So far, we have followed classical lines in our discussion of likelihood. The method is attractive and very useful; the main limitation is the difficulty in calculating the parameters of the asymptotic distribution of the MLE. And, of course, without an exact solution it is difficult to be sure how useful this asymptotic distribution is anyway.

6.3 Bayesian likelihood analysis

Bayes' theorem says, for model parameters (a vector, in general) $\vec{\alpha}$ and data X_i,

$$\text{prob}(\vec{\alpha} \mid X_i) \propto \mathcal{L}(\vec{\alpha} \mid X_i)\text{prob}(\vec{\alpha}) \tag{6.10}$$

so the likelihood function is important here too. However, given the posterior probability of $\vec{\alpha}$, we may choose to emphasize properties other than the most probable $\vec{\alpha}$ – we may only be interested in the probability that it exceeds a certain value, for example.

Two great strengths of the Bayesian approach are the ability to deal with nuisance parameters via marginalization, and the use of the evidence or Bayes factor to choose between models. Another useful product of the Bayesian approach is the asymptotic distribution of the likelihood function itself. $\mathcal{L}(\vec{\alpha})$ is asymptotically a multivariate Gaussian distributed around the MLE $\hat{\vec{\alpha}}$, with covariance matrix given by the inverse of

$$-\begin{bmatrix} \frac{\partial^2 \ln \mathcal{L}}{\partial \alpha_1^2} & \frac{\partial^2 \ln \mathcal{L}}{\partial \alpha_1 \partial \alpha_2} & \frac{\partial^2 \ln \mathcal{L}}{\partial \alpha_1 \partial \alpha_3} & \cdots \\ \frac{\partial \ln \mathcal{L}}{\partial \alpha_2 \partial \alpha_1} & \frac{\partial^2 \ln \mathcal{L}}{\partial \alpha_2^2} & \frac{\partial^2 \ln \mathcal{L}}{\partial \alpha_2 \partial \alpha_3} & \cdots \\ \frac{\partial^2 \ln \mathcal{L}}{\partial \alpha_3 \alpha_1} & \frac{\partial^2 \ln \mathcal{L}}{\partial \alpha_3 \partial \alpha_2} & \frac{\partial^2 \ln \mathcal{L}}{\partial \alpha_3^2} & \cdots \\ \vdots & \vdots & \vdots & \end{bmatrix}. \tag{6.11}$$

evaluated at the peak, namely the MLE of $\vec{\alpha}$.

We will illustrate this approach by developing a simple two-parameter example, fitting a power law to some radio flux-density data. This example will appear in various guises in this chapter, but each time we will assume Gaussian statistics and uniform, or diffuse priors. These assumptions do not simplify the calculations, which were all done numerically in any case; they do simplify the presentation. Use the error distribution and prior that fits your problem.

EXAMPLE Let us suppose we have flux density measurements at 0.4, 1.4, 2.7, 5 and 10 GHz. The corresponding data are 1.855, 0.640, 0.444, 0.22 and 0.102 flux units – see Fig. 6.3.

Let us label the frequencies as f_i and the data as S_i. These follow a power law of slope -1, but have a 10 per cent Gaussian noise added. The noise level is denoted ϵ, and the model for the flux density as a function of frequency is $kf^{-\gamma}$. Assuming we know the noise level and distribution, each term in the likelihood product is of the form

$$\frac{1}{\sqrt{2\pi}\epsilon k f_i^{-\gamma}} \exp\left[\frac{-\left(S_i - k f_i^{-\gamma}\right)^2}{2\left(\epsilon k f_i^{-\gamma}\right)^2}\right].$$

The likelihood is therefore a function of k and γ. A contour map of the log likelihood is in Fig. 6.4. We can calculate the Gaussian approximation to the likelihood, also shown in Fig. 6.4. At this point, there are at least two possibilities for further analysis. We may wish to know which pairs of (k, γ) are, say, 90 per cent probable. This in general involves a very awkward integration of the posterior probabilities. The multivariate Gaussian approximation to the likelihood is much easier to use; it is automatically normalized and there are analytic forms for its integral over any number of its arguments (see, for example, Jaynes 2003). As

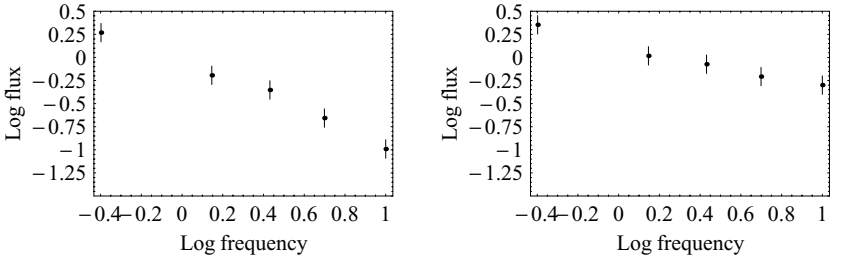

Fig. 6.3. The two experimental spectra we will examine; the right-hand one contains an offset error as well as random noise.

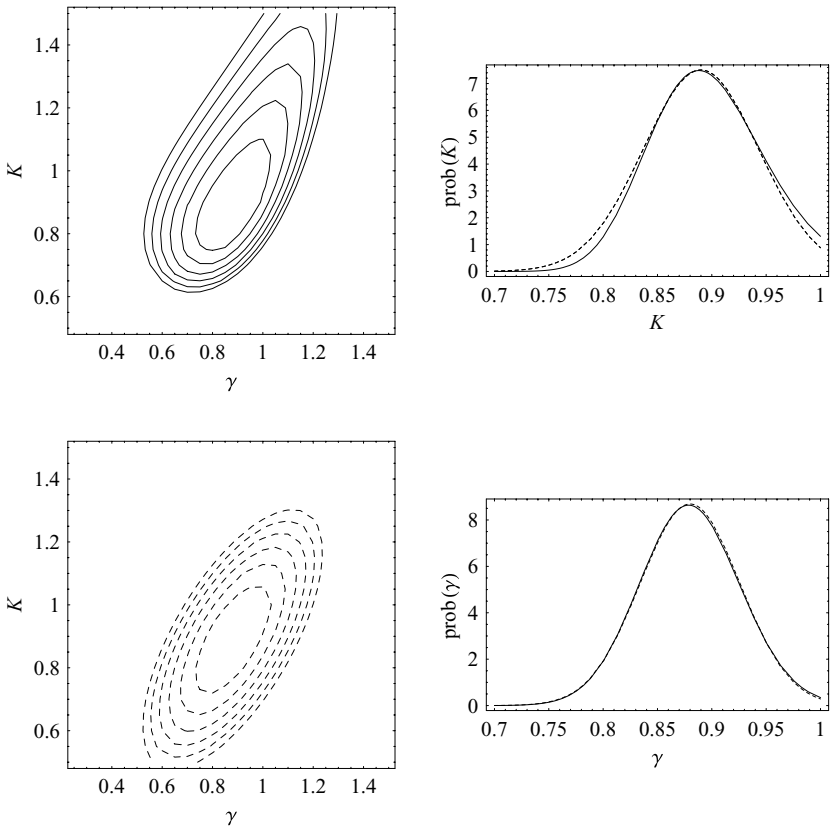

Fig. 6.4. Top left, a contour plot of the log likelihood function; bottom left, the Gaussian approximation; right panels, the marginal distributions of k and γ, comparing the Gaussian approximation to the full likelihood.

can be seen in the figure, the areas defined by a particular probability requirement are simple ellipses.

Another possibility is to ask for the probability of, say, k regardless of γ. So we have a posterior probability $\text{prob}(k, \gamma \mid S_i)$ and we form

$$\text{prob}(k \mid S_i) = \int \text{prob}(k, \gamma \mid S_i)\, d\gamma.$$

The probability distributions for k and γ are also shown in Fig. 6.4, along with the distributions deduced from the Gaussian approximation. As we can see the agreement is quite good.

Marginalization (Section 2.2) can be a very useful technique. Often we are not interested in all the parameters we need to estimate to make a model. If we were investigating radio spectra, for instance, we would want to marginalize out k in our example. We may also have to estimate instrumental parameters as part of our modelling process, but at the end we marginalize them out in order to get answers which do not depend on these parameters. Of course, the marginalization process will always broaden the distribution of the parameters we do want, because it is absorbing the uncertainty in the parameters we don't want – the nuisance parameters.

EXAMPLE In our radio spectrum example (Fig. 6.3) we will add (somewhat artificially) an offset of 0.4 flux units to each measurement. This has the effect of flattening the spectrum quite markedly. We will calculate two possibilities. Model A is the simple one we assumed before, with no offsets built in. Model B uses a model for the flux densities of the form $\beta + kf^{-\gamma}$. Each likelihood term is then

$$\frac{1}{\sqrt{2\pi}\epsilon k f_i^{-\gamma}} \exp\left[\frac{-\left(S_i - \left(\beta + k f_i^{-\gamma}\right)\right)^2}{2(\epsilon k f_i^{-\gamma})^2}\right].$$

We also suppose that we have some suspicion of the existence of this offset, so we place a prior on β of mean 0.4, standard deviation ϵ. Model B therefore returns a posterior distribution for k, γ and β. We are not actually interested in β (although an instrumental scientist might be) so we marginalize it out. The likelihoods from the two models are shown in Fig. 6.5, and it is clear that the more complex model does a better job of recovering the true parameters. The procedure works because there is information in the data about both the instrumental and the source parameters, given the model of the spectrum. If our model for the spectrum had a 'break' in it, we would not be able to recover much information about β, if any. If our fluxes had a pure scale error, we would not have been able to recover this either.

In the real world, of course, we do not have the truth available to guide us as to our choice of model A or model B. As remarked before, we ought to check the 'fit' of the two models. In one dimension there are

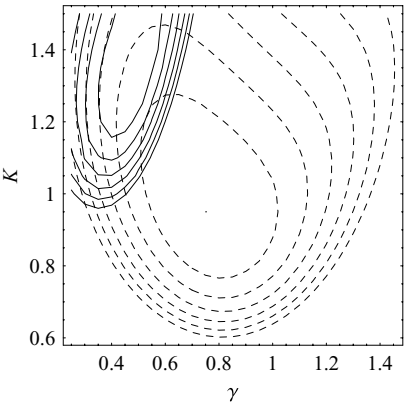

Fig. 6.5. The log likelihoods for the two models; the black contours are for model A and the dashed contours are for model B.

various ways to do this, as discussed in Chapter 4. In many dimensions things are harder. At the risk of repetition, let's look again at the use of evidence (the Bayes factor).

Suppose we are choosing between model A and model B and we believe they are the only possibilities. The prior probability of A is, say, p_{A} and of B is p_{B}. The posterior probability of the parameters α, given data X_i, is

$$\begin{aligned}&\mathrm{prob}(\alpha \mid X_i, \mathrm{A}, \mathrm{B})\\ &\quad = \frac{p_{\mathrm{A}}\mathcal{L}(X_i \mid \alpha, \mathrm{A})\mathrm{prob}(\alpha \mid \mathrm{A}) + p_{\mathrm{B}}\mathcal{L}(X_i \mid \alpha, \mathrm{B})\mathrm{prob}(\alpha \mid \mathrm{B})}{\mathrm{prob}(X_i)}\end{aligned} \tag{6.12}$$

where we are emphasizing which model enters the various likelihoods. $\mathrm{prob}(X_i)$ is the normalizing factor which ensures that the posterior distribution is properly normalized; its calculation usually involves a multidimensional integral. $\mathrm{prob}(\alpha \mid \mathrm{A})$ is the prior on α in model A, and similarly for B.

The posterior odds on model A, compared to model B, are then simply

$$\frac{\int_\alpha p_{\mathrm{A}}\mathcal{L}(X_i \mid \alpha, \mathrm{A})\mathrm{prob}(\alpha \mid \mathrm{A})}{\int_\alpha p_{\mathrm{B}}\mathcal{L}(X_i \mid \alpha, \mathrm{B})\mathrm{prob}(\alpha \mid \mathrm{B})} \tag{6.13}$$

in which we have to integrate over the range of parameters appropriate to each model. This is worth the effort because we get a straightforward answer to the question: which of A or B would it be better to bet on?

EXAMPLE In the previous two examples we have worked out the likelihood functions, which we abbreviate $\mathcal{L}(X_i \mid k, \gamma, \mathrm{A})$ for model A and similarly for model B. In model B we also have a prior on the offset β, which is

$$\mathrm{prob}(\beta \mid \mathrm{B}) = \frac{1}{\sqrt{2\pi}\,\epsilon} \exp\left[\frac{-(\beta - 0.4)^2}{2(\epsilon)^2}\right].$$

We then form the ratio of the integrals

$$p_{\mathrm{A}} \int \mathrm{d}k \int \mathrm{d}\gamma \mathcal{L}(X_i \mid k, \gamma, \mathrm{A})$$

and

$$p_{\mathrm{B}} \int \mathrm{d}k \int \mathrm{d}\gamma \int \mathrm{d}\beta \mathcal{L}(X_i \mid k, \gamma, \mathrm{B}) \mathrm{prob}(\beta \mid \mathrm{B}).$$

Let's take $p_{\mathrm{A}} = p_{\mathrm{B}}$, an agnostic prior state; note we have implicitly assumed uniform priors on k and γ. Cranking through the integrations numerically, we get:

odds on B compared to A: about 8 to 1.

Another way of looking at this is that we would have had to have been prepared to offer prior odds of 8:1 against the existence of the offset, for the posterior odds to have been even.

6.4 The minimum chi-square method

Yet of course there are occasions when Bayesian methods fail us – perhaps we have been given the data in binned form, or indeed somebody else has used classical modelling methods which we wish to examine. A dominant classical modelling process is minimum chi-square, a simple extension of the chi-square goodness-of-fit test described in Section 4.2. It will be seen that it is closely related to least squares and weighted least squares methods, and in fact the minimum chi-square statistic has asymptotic properties similar to ML.

Consider observational data which can be (or are already) binned, and a model and hypothesis which predicts the population of each bin. The chi-square statistic describes the goodness-of-fit of the data to the model. If the observed numbers in each of k bins are O_i, and the expected

values from the model are E_i, then this statistic is

$$\chi^2 = \sum_{i=1}^{k} \frac{(O_i - E_i)^2}{E_i}. \tag{6.14}$$

(The parallel with weighted least squares is evident: the statistic is the squares of the residuals weighted by what is effectively the variance if the procedure is governed by Poisson statistics.) The minimum chi-square method of model fitting consists of minimizing the chi-squared statistic by varying the parameters of the model. The premise on which this technique is based is simply that the model is assumed to be qualitatively correct, and is adjusted to minimize (via χ^2) the differences between the E_i and O_i which are deemed to be due solely to statistical fluctuations. In practice, the parameter search is easy enough as long as the number of parameters is less than four; if there are four or more, then sophisticated search procedures may be necessary. The appropriate number of degrees of freedom to associate with χ^2 for k bins and N parameters is $\nu = k-1-N$. The essential issue, having found appropriate parameters, is to estimate confidence limits (Section 3.1) for them. The answer is as given by Avni 1976; the region of confidence (significance level α) is defined by

$$\chi^2_\alpha = \chi^2_{\min} + \Delta(\nu, \alpha)$$

where Δ is from Table 6.1. (It is interesting to note that (a) Δ depends only on the number of parameters involved, and not on the goodness of fit ($\chi^2_{\min}$) actually achieved, and (b) there is an alternative answer given by Cline & Lesser (1970) which must be in error: the result obtained by Avni has been tested with Monte Carlo experiments by Avni himself and by M. Birkinshaw (personal communication).)

Table 6.1. Chi-square differences (Δ) above minimum

Significance α	Number of parameters		
	1	2	3
0.68	1.00	2.30	3.50
0.90	2.71	4.61	6.25
0.99	6.63	9.21	11.30

EXAMPLE The model to describe an observed distribution (Fig. 6.6, left) requires two parameters, γ and k. Contours of χ^2 resulting from the parameter search are shown in Fig. 6.6 (right). When the Avni prescription is applied, it gives $\chi^2_{0.68} = \chi^2_{\rm min} + 2.30$, for the value corresponding to 1σ (significance level = 0.68); the contour $\chi^2_{0.68} = 6.2$ defines a region of confidence in the (γ, k) plane corresponding to the 1σ level of significance. (Because the range of interest for γ was limited from other considerations to $1.9 < \gamma < 2.4$, the parameter search was not extended to define this contour fully.)

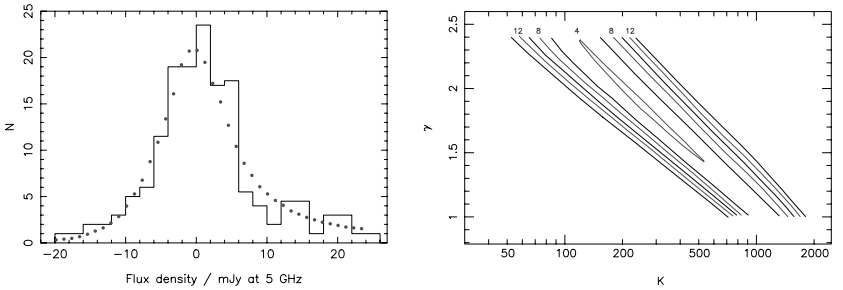

Fig. 6.6. An example of model fitting via minimum χ^2. The object of the experiment was to estimate the surface-density count [$N(S)$ relation; see Section 6.1, Fig. 6.1] of faint extragalactic sources at 5 GHz, assuming a power-law $N(>S) = KS^{-(\gamma-1)}$, γ and K to be determined from the distribution of background deflections, the so-called *P(D) method*, Section 7.6. The histogram of measured deflections is shown left, together with the curve representing the optimum model from minimizing χ^2. Contours of χ^2 in the $\gamma - K$ plane are shown right, with χ^2 indicated for every second contour.

There are three good features of the minimum chi-square method, and two bad and ugly ones. The good:

(i) Because χ^2 is additive, the results of different datasets that may fall in different bins, bin sizes, or that may apply to different aspects of the same model, may be tested all at once.

(ii) The contribution to χ^2 of each bin may be examined and regions of exceptionally good or bad fit delineated.

(iii) One of the finest features of the method is that you get model testing for free. Table A2.6 indicates probabilities of χ^2 for given degrees of freedom. It is to be hoped that the model comes out

with a value of order 0.50; indeed the peak of the χ^2 distribution is $\sim$ (number of degrees of freedom) when $\nu \geq 4$ (Fig. 5.4). In the example above, there are seven bins, two parameters, and the appropriate number of degrees of freedom is therefore 4. The value of $\chi^2_{\min}$ is about 4, just as one would have hoped, and the optimum model is thus a satisfactory fit.

The bad and downright ugly:

(i) Low bin-populations in the chi-square sums will cause severe instability. As a rule of thumb, 80 per cent of the bins must have $E_i > 5$. As for the chi-square test, it does not work for small numbers.

(ii) Finally it is important to repeat the mantra: data binning is bad. In general, it loses information and efficiency. What is worse is the bias it can cause. Just consider a skewed distribution with rather few data defining it – the consequent need for wide bins may 'erase' the skewness entirely.

6.5 Monte Carlo modelling

6.5.1 Monte Carlo generators

By now one truth will have dawned – there are many occasions in hypothesis testing and model fitting when it is essential to have simple recourse to a set of numbers distributed perhaps how we guess the data might be. We may wish to test a test to see if it works as advertised; we might need to test efficiency of tests; we might wish to determine how many iterations we require; or we might even want to test that our code is working. We need random numbers, either uniformly distributed, or drawn randomly from a parent population of known frequency distribution.

It is vital not to compromise the tests with bad random data. Numerical Recipes (Press et al. 1992) presents a number of methods, from single expressions to powerful routines. A key issue is cycle length; how long is it before the pseudo-random cycle is repeated? (Or, how many random numbers do you need?) In these respects it is very necessary to understand the characteristics of the generator. Moreover it is essential to follow the prescribed implementation precisely. It may be tempting to try some 'extra randomizing', for example by combining routines or by modifying seeds. Be very scared of any such process.

Finally it is easy to forget that the routines generate pseudo-random numbers. Run them again from the same starting point and you'll get the same set of numbers. With these points in mind for the random-number generator for uniform deviates over the range $0-1$, consider the following four aspects of random-number generation.

1. How do we draw a set of random numbers following a given frequency distribution? Suppose we have a way of producing random numbers that are uniformly distributed, in say the variable α; and we have a functional form for our frequency distribution $\mathrm{d}n/\mathrm{d}x = f(x)$. We need a transformation $x = x(\alpha)$ to distort the uniformity of α to follow $f(x)$. But we know that

$$\frac{\mathrm{d}n}{\mathrm{d}x} = \frac{\mathrm{d}n}{\mathrm{d}\alpha}\frac{\mathrm{d}\alpha}{\mathrm{d}x} = \frac{\mathrm{d}\alpha}{\mathrm{d}x} \tag{6.15}$$

and as $\mathrm{d}n/\mathrm{d}\alpha$ is uniform, thus

$$\alpha(x) = \int^{x} f(x)\,\mathrm{d}x, \tag{6.16}$$

from whence the required transformation $x = x(\alpha)$.

EXAMPLE Thus the example in Section 6.1: the source-count random distribution is $f(x)\,\mathrm{d}x = -1.5x^{-2.5}\,\mathrm{d}x$, a 'Euclidean' differential source count. Here $\mathrm{d}\alpha = -1.5x^{-2.5}\,\mathrm{d}x$, $\alpha = x^{-1.5}$, and the transformation is $x = f^{-1}(\alpha) = \alpha^{1/1.5}$.

---

2. The very same procedure works if we do not have a functional form for $f(x)\,\mathrm{d}x$. If this is a histogram, we need simply to calculate the integral version, and perform the reverse function operation as above.

EXAMPLE Fig. 6.7 shows an example of choosing uniformly distributed random numbers and transforming them to follow the frequency distribution prescribed by a given histogram.

---

3. How do we draw numbers obeying a Gaussian distribution? The prescription above is all very well, and works when integration of the function can be done; it can't in many cases, the Gaussian being an

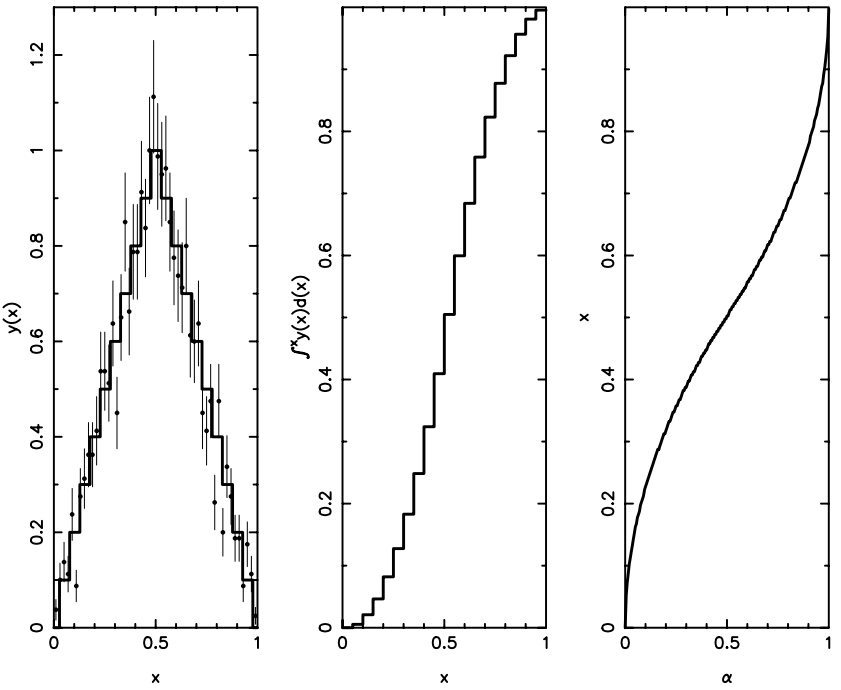

Fig. 6.7. An example of generating a Monte Carlo distribution following a known histogram. Left: the step-ladder histogram, with points from 2000 trials, produced by (a) integrating the function (middle) and (b) transforming the axes to produce f^{-1} of the integrated distribution (right). The points with $\sqrt{N}$ error bars in the left diagram are from drawing 2000 uniformly distributed random numbers and transforming them according to the right diagram.

obvious one. Of course we could evaluate the integral for example by Monte Carlo methods as described below, but computationally this is ridiculous should we want a large number of deviates. There is thus another method, the rejection method, of generating random numbers to a prescription starting with uniform deviates. The method is computationally expensive relative to the integral transform method; but for something like a Gaussian, not prohibitively so; and it can be coded in just a few lines. Details are described in Lyons (1986) and Press et al. (1992).

4. How do we generate numbers obeying a bivariate (or even multivariate) Gaussian, with given σ_i and ρ_i? This is crucial for testing many tests or model-fitting routines (or for generating Fig. 6.2); and thanks

to our discussion of error matrices in Section 4.2 and PCA in Section 4.5, quite simple to formulate:

- Set up the covariance matrix. (For the bivariate case, the error matrix is $e_{1,1} = \sigma_x^2$, $e_{2,1} = e_{1,2} = \mathrm{cov}[x, y] = \rho\sigma_x\sigma_y$, $e_{2,2} = \sigma_y^2$, as we have seen.)
- Find the eigenvalues and eigenvectors of the covariance matrix.
- Combine the eigenvectors, the column vectors, into the transformation matrix T, the matrix that diagonalizes the covariance matrix.
- Then draw (x', y') Gaussian pairs, uncorrelated, with variances equal to the two eigenvalues. Compute the (x, y) pairs according to

$$\begin{pmatrix} x \\ y \end{pmatrix} = [T] \begin{pmatrix} x' \\ y' \end{pmatrix}. \tag{6.17}$$

The points in Fig. 6.2 were obtained in this manner.

6.5.2 Monte Carlo integration

One very important use of Monte Carlo is integration. This is a technical subject, well covered in Evans & Swartz (1995) and Chib & Greenberg (1995). A more technical reference is O'Ruanaidh & Fitzgerald (1996). Many-dimensional numerical integration is a big problem for Bayesian methods and so we will introduce some terminology and ideas here very briefly.

Suppose we have a probability distribution $f(x)$ defined for $a \leq x \leq b$. If we draw N random numbers X, uniformly distributed between a and b, then we have

$$\int_a^b f(x)\,\mathrm{d}x \simeq \frac{1}{N}\sum_i f(X_i). \tag{6.18}$$

This is Monte Carlo integration.

If the X_i are drawn from the distribution f itself, then obviously they will sample the regions where f is large and the integration will be more accurate. This technique is called importance sampling.

So, in a Bayesian context, we would like to be able to generate random numbers from a probability distribution f/C where C is an unknown normalizing factor. Further, f will in general be a multivariate distribution (if it wasn't, we could use deterministic numerical integration).

The workhorse method for obtaining random numbers in this situation is the Metropolis algorithm or its cousin, the Metropolis–Hastings

algorithm. This is a very simple method, which copies the way in which physical systems, in thermal equilibrium, will populate their distribution function. It produces a string of related random numbers called a Markov chain. The enormous advantage of the method is that it works when we do not know the normalization. Indeed, we nearly always want to find the normalization.

The simplest implementation of the Metropolis algorithm is one-dimensional. What if we want random numbers from a multivariate $f(\alpha_1, \alpha_2, \gamma, \ldots)$? This is a much more likely application in a Bayesian context.

Here we use the Gibbs sampler. This is actually one version of a multi-dimensional Metropolis algorithm (Chib & Greenberg 1995). We guess a starting vector $(\alpha_0, \beta_0, \gamma_0, \ldots)$ and then draw α_1 from $f(\alpha_0, \beta_0, \gamma_0, \ldots)$. Next we draw β_1 from $(\alpha_1, \beta_0, \gamma_0, \ldots)$ and then γ_1 from $(\alpha_1, \beta_1, \gamma_0, \ldots)$; and so on. After we have cycled through all the variables once, we have our first multivariate sample.

Obviously the first sample will be strongly influenced by the initial guess, and a number of iterations are necessary before burn-in is complete and the procedure is in a stationary state. The same applies to the Metropolis algorithm, which starts from a 'seed' value. The combination of the Metropolis algorithm and the Gibbs sampler equips us to perform the multidimensional integrations we often need in Bayesian problems.

You should be aware that there is considerable technical debate around the question of how long burn-in will last in particular cases. If you want to use Monte Carlo Markov chain integration, check the references and make sure you have tested your random numbers in all the standard ways.

6.6 Bootstrap and jackknife

In some data-modelling procedures, confidence intervals for the parameters fall out of the procedure. But are these realistic? And what about the procedures where they do not? Computer power can provide the answer, with the bootstrap method invented by Efron (1979); see also Diaconis & Efron (1983) and Davison & Hinkley (1997). It apparently gives something for nothing, and Efron so named it from the image of lifting oneself up by one's own bootstraps.

The method is so blatant (described, for example, in Numerical Recipes as 'quick-and-dirty Monte Carlo') that it took some time to gain

respectability, but the foundations are now secure (see, e.g. LePage & Billiard 1993; Efron & Tibshirani 1993). Suppose the sample consists of N data points, each consisting of one or more numbers (e.g. single measurements, or x, y pairs), and we wish to ascertain the error on a parameter estimated from these data points (e.g. mean, or slope of a best-fit). We calculate the parameter using a modelling process such as one of those described above. We then 'bootstrap' to find its uncertainty, as follows:

(i) Label each data point;
(ii) Draw at random a sample of N with replacement (simply done by computer with a random-number generator);
(iii) Recalculate the parameter.
(iv) Repeat this process as many times as possible.

That's it. Provided that the data points are independent (in distribution and in order), the distribution of these recalculated parameters maps the uncertainty in the estimate from the original sample.

EXAMPLE Bhavsar (1990) described how ideally suited the bootstrap is to estimating uncertainty in measuring the slope of the angular two-point correlation function for galaxies. This function $w(\theta)$ (Section 9.4) measures the excess surface density over that expected from a uniform independent and random distribution at angular scales θ. The data points are the (x, y) pairs of galaxy coordinates on the sky, and the difficulty in estimating the accuracy of this slope is even more notorious than that of estimating the slope of the counts of radio sources. The reason is similar: $\sqrt{N}$ error bars are readily assigned, but they are not independent; and unlike the case of source counts for which a differential version is possible, there is no ready way of assessing the significance of the correlated errors in a correlation function. Figure 6.8 shows an example of such a two-point correlation function estimate, part of a search for clustering in the distribution of radio sources on the sky (Wall, Rixon & Benn 1993).

The bootstrap is ideal for computing errors in a PCA analysis. It is a good way of telling you if any of the principal components has been detected above the sampling error.

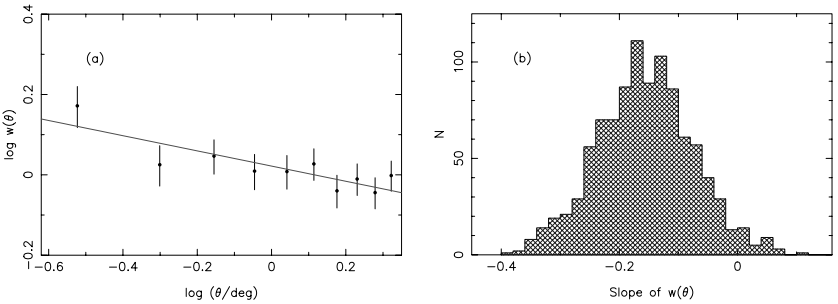

Fig. 6.8. A bootstrap application. (a) The two-point correlation function for 2812 radio sources with extended radio structure, from the White–Becker catalogue of the NRAO 1.4-GHz survey of the northern sky. A least-squares fit gives a slope of -0.19. (b) The distribution of slopes obtained in bootstrap-testing the sample with 1000 trials. The mean slope is -0.157, while the rms scatter is ± 0.082; the slope is less than zero (i.e. signal is present) for 96.8 per cent of the trials.

The bootstrap takes us back to the quotation starting this chapter. If errors are not well known, it is still possible to ascertain errors on a model. Moreover the errors may be known well; but as in the above example, their significance in terms of defining a model may not be understood. In either case it is possible to bootstrap one's way to safety.

The jackknife is a rather similar technique to the bootstrap, but much older, first described by Tukey (one of the inventors of the FFT) in 1958.

The algorithm is again quite simple. Suppose we are interested in some function $f(X_1, X_2, \ldots)$ which depends on the N observations X_i. Usually this will be because f is a useful estimator of a parameter α. Thus we have

$$\hat{\alpha} = f(X_1, X_2, \ldots).$$

The jth partial estimate is obtained by deleting the jth element of the dataset:

$$\hat{\alpha}_j = f(X_1, X_2, \ldots, X_{j-1}, X_{j+1}, \ldots, X_N),$$

giving N partial estimates. The next step (and the crucial one) is to define the pseudo-values

$$\hat{\alpha}_j^* = N\hat{\alpha} - (N-1)\hat{\alpha}_j,$$

and finally the jackknifed estimate of α is the simple average of the

pseudo-values

$$\hat{\alpha}^* = \frac{1}{N}\sum_{i=1}^{N}\hat{\alpha}_j^*. \tag{6.19}$$

The great merit of the jackknife is that it removes bias. Often the bias will depend inversely on the sample size (a simple example of this is the maximum-likelihood estimate for the variance of a normal distribution) and the jackknifed estimate will not contain this bias. In general, we can construct an mth-order jackknifed estimate by removing m observations at a time, and this will eliminate bias that depends on $1/N^m$.

For estimators which are asymptotically Normal (e.g. maximum-likelihood estimators) it is useful to calculate the sample variance on the pseudo-values, which is

$$(\sigma^*)^2 = \frac{1}{N(N-1)}\sum_j(\hat{\alpha}_j^* - \hat{\alpha}^*)^2. \tag{6.20}$$

This can be used to give a confidence interval on $\alpha - \alpha^*$ which is distributed according to $\sigma^* t$ with t having $N-1$ degrees of freedom. This works to the extent that Normality has been obtained. In practice it is easier to use a bootstrap for confidence intervals, because the assumption of Normality is not needed. If the jackknife intervals can be checked with a bootstrap, they are of course much less computationally intensive to calculate.

6.7 Models of models, and the combination of datasets

Having the correct model is essential, as otherwise both deduced parameters, and errors on them, will be wrong. Frequently, however, we are in a circular type of reasoning where we guess the model and then try to assess if the deduced parameters are reasonable. A useful way of expanding the set of models, as an insurance policy against having the wrong one, is to use hierarchical models. These in turn make use of the even more impressively named hyperparameters. It turns out that, in addition to helping with modelling, these notions are useful in the familiar problem of combining sets of data which have different levels of error.

The idea of the hierarchical model can be illustrated by our earlier example, where we needed to include some kind of offset in the model for each of our flux measurements. Each term in the likelihood function

took the form

$$\frac{1}{\sqrt{2\pi}\epsilon k f_i^{-\gamma}} \exp\left[\frac{-\left(S_i - \left(\beta + k f_i^{-\gamma}\right)\right)^2}{2\left(\epsilon k f_i^{-\gamma}\right)^2}\right].$$

We are assuming that the offset error β is the same for each measurement. Before, we supposed that the distribution of β was normal, with a known mean and standard deviation – quite a strong assumption. Suppose we knew only the standard deviation, but the mean μ was unknown. The likelihood is then

$$\exp\left[\frac{-(\beta-\mu)^2}{2\sigma_\beta^2}\right] \prod_i \frac{1}{\sqrt{2\pi}\epsilon k f_i^{-\gamma}} \exp\left[\frac{-\left(S_i - \left(\beta + k f_i^{-\gamma}\right)\right)^2}{2\left(\epsilon k f_i^{-\gamma}\right)^2}\right]$$

where μ is now a hyperparameter, described (appropriately enough) by a hyperprior. So, for hierarchical models, Bayes' theorem takes the form

$$\text{prob}(\alpha, \theta \mid X_i) \propto \mathcal{L}(X_i \mid \alpha)\text{prob}(\alpha \mid \theta)\text{prob}(\theta) \tag{6.21}$$

where as usual X_i are the data and θ is the hyperparameter (and may of course be a vector). If we integrate out θ, we get a posterior distribution for the parameter α which includes the effect of a range of models.

EXAMPLE In our radio spectrum example, we make a simple hierarchical model as described above. Take the standard deviation $\sigma_\beta = \epsilon$ and the prior $\text{prob}(\mu) = \text{constant}$. We compute the likelihood surface by marginalizing over both μ and β; these integrations are not too bad because we have Gaussians, and because we integrate from $-\infty$ to ∞. (More realistic integrations, over finite ranges, get very messy.) In Fig. 6.9 we see the likelihood surface for K and γ, compared to the previous 'strong' model for which we knew μ. There is a tendency, not unexpected, for flatter power laws to be acceptable if we do not know much about μ.

In a more elaborate form of a hierarchical model, we can connect each datum to a separate model, with the models being joined by an overarching structural relationship. In symbols, Bayes then reads

$$\text{prob}(\alpha_i, \theta \mid X_i) \propto \mathcal{L}(X_i \mid \alpha_i)\text{prob}(\alpha_i \mid \theta)\text{prob}(\theta). \tag{6.22}$$

In a common type of model we may have observations X_i drawn from Gaussians of mean μ_i, with a structural relationship that tells us that the

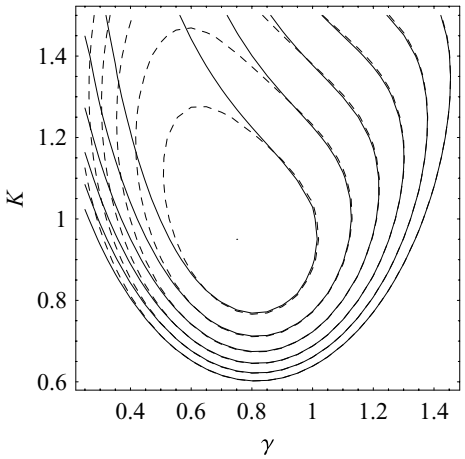

Fig. 6.9. The log likelihoods for the two models; the black contours are for the hierarchical model and the dashed contours are for known μ.

μ_i are in turn drawn from a Gaussian of mean, say, θ. This is a weaker model than the first sort we considered, because we have allowed many more parameters, linked only by a stochastic relationship. In the case of Gaussians there is quite an industry devoted to this type of model; see Lee (1997) for details.

EXAMPLE Back to our power-law spectrum. If we allow a separate offset β_i at each frequency, then each term in the likelihood product takes the form

$$\exp\left[\frac{-(\beta_i-\mu)^2}{2\sigma_\beta^2}\right]\frac{1}{\sqrt{2\pi}\epsilon\, k f_i^{-\gamma}}\exp\left[\frac{-\left(S_i-\left(\beta_i+k f_i^{-\gamma}\right)\right)^2}{2\left(\epsilon\, k f_i^{-\gamma}\right)^2}\right]$$

and we take again the usual (very weak) prior prob(μ) = constant. Marginalizing out each β_i by an integration is then exactly the same task for each i, and having done this we can compare the likelihood contours with the very first model of these data (no offsets allowed). The likelihood contours of Fig. 6.10 are very instructive. The hierarchical model, by allowing a range of models, has moved the solution away from the well-defined (but wrong) parameters of the no-offset model. The hierarchical likelihood in fact peaks quite close to the true values of (k, γ) but the error bounds on these parameters are much wider.

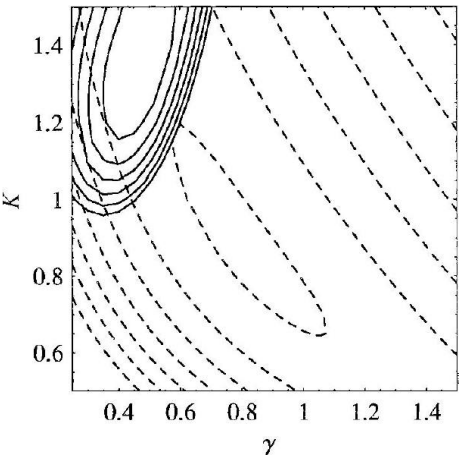

Fig. 6.10. The log likelihoods for the two models; the black contours are for the simplest model, with no provision for offsets; the dashed contours are for the weak hierarchical model, allowing separate offsets at each frequency.

This is a general message; allowing uncertainty in our models may make the answers apparently less precise, but it is an insurance against well-defined but wrong answers from modelling.

Broadening the range of models is a useful technique in combining data. To see this, let us revise the idea of weights.

The optimum weight for an observation of standard deviation σ is just $1/\sigma^2$ (see the exercises). This weight turns up naturally in modelling using minimum-χ^2.

Suppose we have data X_i, of standard deviation σ_x, and some other data Y_i of standard deviation σ_y. Then, to fit to some model function $\mu(\alpha_1, \alpha_2, \ldots)$ we minimize

$$\chi^2 = \sum_{i=1}^{N} \frac{(X_i - \mu)^2}{\sigma_x^2} + \sum_{i=1}^{M} \frac{(Y_i - \mu)^2}{\sigma_y^2}$$

and it is obvious how the different datasets are weighted.

Quite often the quoted error levels on data are wrong; it is no small task to make accurate error estimates. One simple way of dealing with this is simply to tinker with the σs in the χ^2 so that the minimum value comes out to be about $N + M$. This can be a useful technique but of course it is rather arbitrary how we allocate the tinkering between σ_x and σ_y.

Let us broaden our model by allocating weights ξ_x and ξ_y to these datasets. This is a hierarchical model, and the weights are hyperparameters (Hobson, Bridle & Lahav 2002). On the assumption of Gaussian residuals, the likelihood function is then

$$\begin{aligned}\mathcal{L}(X_i, Y_i \mid \alpha, \beta, \ldots, \xi_x, \xi_y) \propto & \frac{1}{\xi_x^{N/2}\sigma_x^N \xi_y^{M/2}\sigma_y^M} \\ & \times \exp\left[-\sum_{i=1}^{N} \xi_x \frac{(X_i-\mu)^2}{2\sigma_x^2}\right] \\ & \times \exp\left[-\sum_{i=1}^{M} \xi_y \frac{(Y_i-\mu)^2}{2\sigma_y^2}\right]. \end{aligned} \tag{6.23}$$

Bayes' theorem will now tell us the posterior probability distribution for the parameters of our model μ, plus the weights. It would be nice to marginalize out the weights, as in this context they are nuisance parameters.

The tidy aspect of this approach is that it is one of the rare cases in which we have a convincing (uncontroversial?) prior to hand. Hobson, Bridle & Lahav (2002) show that, on the assumption that the mean value of the weight is unity (perhaps an idealistic assumption), we have simply

$$\text{prob}(\xi) = \exp(-\xi). \tag{6.24}$$

This is derived by the method of maximum entropy, as described in, for example, Jaynes (2003). Carrying out the integration over the ξ's is easy, and we find the posterior probability for our problem to be

$$\begin{aligned}\text{prob}(\alpha_1, \alpha_2, \ldots \mid X_i, Y_i) \propto & \frac{1}{\sigma_x^N}\frac{1}{\sigma_y^M} \\ & \times \frac{1}{\left(2 + \sum_{i=1}^{N} \frac{(X_i-\mu)^2}{2\sigma_x^2}\right)^{N/2+1}} \\ & \times \frac{1}{\left(2 + \sum_{i=1}^{M} \frac{(Y_i-\mu)^2}{2\sigma_y^2}\right)^{M/2+1}} \\ & \times \text{prob}(\alpha_1, \alpha_2, \ldots). \end{aligned} \tag{6.25}$$

EXAMPLE Here (Fig. 6.11) are two noisy spectra of a single line. Both are alleged to have the same noise level, $\sigma = 5$, but one is slightly worse and is not centred at zero, unlike the better one. For simplicity, let us assume that we know the line to be Gaussian and only its position is unknown. Combining the data, taking the quoted errors at face value, we get a log likelihood for the line centre which peaks some way away from zero. If our prior on the line centre is diffuse, the posterior probability is proportional to the likelihood. Including the data weights as hyperparameters, we get a simple answer after marginalization, shown in Fig. 6.12; the posterior probability for the line centre shows two clear peaks, the larger at zero (the good data) and the lesser at 2 units (the poorer data).

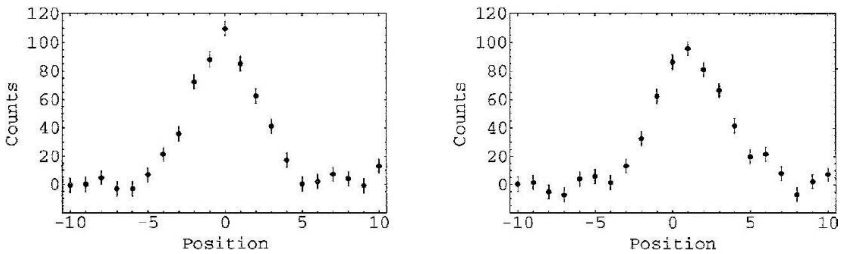

Fig. 6.11. The two synthetic spectra which are our input data.

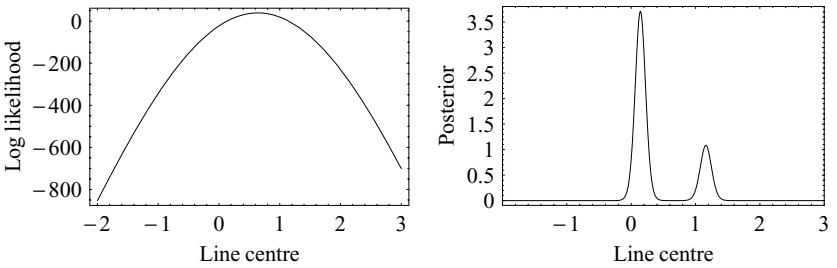

Fig. 6.12. The log likelihood function for the combined, unweighted data (left) and the posterior distribution for the line centre, after marginalizing out the weights (right).

Since the weights are an amplification of our model, we may want to know if they ought to be included; this can be calculated in the usual

way by computing the odds in favour of or against the more complex model. To do this we need to keep track of all the constants we have elided so far. Here is the full set of equations, for a multivariate Gaussian model for the data.

Let us index each (homogeneous) set of N_i data by i, and call the covariance matrix C_i, the data vector $\vec{X}_i$ and the model vector $\vec{\mu}_i$. μ_i depends on the parameters of interest. Abbreviating

$$\chi_i^2 = (\overline{X_i} - \vec{\mu}_i)^{\mathrm{T}} C_i^{-1} (\vec{X}_i - \vec{\mu}_i)$$

the multivariate Gaussian model for the ith dataset is, as usual,

$$\mathrm{prob}(\vec{X}_i \mid \vec{\mu}_i, \text{no weights}) = \frac{1}{(2\pi)^{N_i/2} \mid C_i \mid^{1/2}} \exp(-\tfrac{1}{2}\chi_i^2)\, \mathrm{prob}(\vec{\mu_i}).$$

Introducing a weight simply means multiplying the covariance matrix by a factor ξ_i. The multivariate model for the ith dataset, after marginalizing over the weight parameter with respect to the exponential prior, is just

$$\mathrm{prob}(\vec{X}_i \mid \vec{\mu}_i,\ \text{weights}) = \frac{2\Gamma\left(\frac{N_i}{2}+1\right)}{\pi^{N_i/2} \mid C_i \mid^{1/2}} \left(\frac{1}{2+\chi_i^2}\right)^{N_i/2+1} \mathrm{prob}(\vec{\mu}_i). \tag{6.26}$$

Each of these distributions depends on the parameters of the model. The odds in favour of weighting the data entail integrating over the parameters (let us abbreviate this by $\int_\alpha$), taking account of any priors $\mathrm{prob}(\alpha)$, and then forming the ratio

$$\frac{\int_\alpha \mathrm{prob}(\alpha)\mathrm{prob}(\vec{X}_i \mid \vec{\mu}_i,\ \text{weights})}{\int_\alpha \mathrm{prob}(\alpha)\mathrm{prob}(\vec{X}_i \mid \vec{\mu}_i, \text{no weights})}\,. \tag{6.27}$$

Exercises

6.1 **Covariance matrix.** Consider N data X_i, drawn from a Gaussian of mean μ and standard deviation σ. Use maximum likelihood to find estimators of both μ and σ, and find the covariance matrix of these estimates.

6.2 **Weighting data.** Show that the optimum weight for an observation of standard deviation σ is just $1/\sigma^2$. This weight turns up naturally in modelling using minimum-χ^2.

6.3 **MLE and power laws.** In the example in Section 6.1 we fit a power law truncated at the faint end, and assume we know where to cut it off. What happens if you try to infer the faint-end cutoff by ML as well? Formulate this problem at least.

6.4 **Univariate random numbers.** Work out the inverses of the integral functions required to generate (a) $f(x) = 2x^3$, (b) a power law, representative of luminosity functions, $f(x) = x^{-\gamma}$. Use these results to produce random experiments following these probabilities by drawing 1000 random samples uniformly distributed between 0 and 1; verify by comparison with the given functions.

6.5 **Multivariate random numbers.** (a) Give the justification for why the prescription (Section 6.5) for generating (x, y) pairs following a bivariate Gaussian of given variances and correlation coefficient is correct. (b) Using a Gaussian Monte Carlo generator, find 1000 (x, y) pairs following a given prescription, i.e. σ_x^2, σ_y^2 and ρ. Plot these on contours of the bivariate probability distribution, as in Fig. 6.2, to check roughly that the prescription works. (c) Find the error matrix for the (x, y) pairs to verify that the prescription works.

6.6 **Monte Carlo integration.** The Gaussian or Normal distribution function

$$\frac{1}{\sigma\sqrt{2\pi}} \exp\left(-\frac{x^2}{2\sigma^2}\right)$$

does not have an analytic integral form. Use Monte Carlo integration to find erf, the so-called error function of Table A2.1. Show that (a) approximately 68 per cent of its area lies between $\pm\sigma$, and (b) that the total area under the curve is unity.

6.7 **Maximum likelihood estimates.** Find an estimator of μ when the distribution is (a)

$$\text{prob}(x) = \exp(-|x - \mu|)$$

and (b) the Poisson

$$\text{prob}(n) = \mu^n \frac{\mathrm{e}^{-\mu}}{n!}.$$

6.8 **Least squares linear fits.** Derive the 'minimum distance' OLS for errors in both x and y, assuming Gaussian errors.

6.9 **Marginalization.** Using the data supplied, use maximum likelihood to find the distribution of the parameters of a fitted Gaussian plus a baseline. Test to see how the estimates are affected by marginalizing out the baseline parameters.

6.10 **The jackknife.** Using the MLE for a power-law index (Section 6.1), work out and compare the confidence intervals with the analytic result from that section using the jackknife and bootstrap tests. Check how the results depend on sample size.

7

Detection and surveys

> Watson, you are coming along wonderfully. You have really done very well indeed. It is true that you have missed everything of importance, but you have hit upon the method...
>
> (*Sherlock Holmes in 'A Case of Identity', Sir Arthur Conan Doyle)*

'Detection' is one of the commonest words in the practising astronomers' vocabulary. It is the preliminary to much else that happens in astronomy, whether it means locating a spectral line, a faint star or a gamma-ray burst. Indeed of its wide range of meanings, here we take the location, and confident measurement, of some sort of feature in a fixed region of an image or spectrum.

When a detection is obvious to even the most sceptical referee, statistical questions usually do not arise in the first instance. The parameters that result from such a detection have a signal-to-noise ratio so high that the detection finds its way into the literature as fact. However, elusive objects or features at the limit of detectability tend to become the focus of interest in any branch of astronomy. Then, the notion of detection (and non-detection) requires careful examination and definition.

Non-detections are especially important because they define how representative any catalogue of objects may be. This set of non-detections can represent vital information in deducing the properties of a population of objects; if something is never detected, that too is a fact, and can be exploited statistically. Every observation potentially contains information. If we are resurveying a catalogue at some new wavelength, each observation constrains the energy from the object to some level. Likewise, surveying unmapped regions of sky yields information even when there are apparently no detections. In both cases population properties

can be extracted, even though individual objects remain obscured in the fog of low signal-to-noise ratio.

This chapter will examine detection, first in the context of the use to which we will put detected objects; it moves on to consider the usefulness of non-detections in deducing properties of populations; and finally it examines notions of detection which say little about individual objects, but which focus instead on population-level properties. In many experiments, we wish to define wide distributions of widely spread parameters: the initial mass function, luminosity function, and so on. We may approach these from the point of view of 'detections' and 'non-detections' (the catalogue point of view) or we may attempt to extract the distributions directly from the data, without the notion of detection ever intruding.

7.1 Detection

Detection is a model-fitting process. When we say 'We've got a detection' we generally mean 'We have found what we were looking for'. This is obvious enough at reasonable signal-to-noise. In examining a digital image, for example, detection of stars (point-like objects) is achieved by comparing model point-spread functions to the data. In the case of extended objects, a wider range of models is required to capture the possibilities.

In all cases, a clear statistical model is required. The noise level (or expected residuals from the model) may be expected in many cases to follow Poisson ($\sqrt{N}$) statistics, or, for large N, Gaussian statistics. The statistics depend on more than the physical and instrumental model. How were the data selected for fitting in the first place? We will see for example that picking out the brightest spot in a spectrum (Section 8.6.1) means that we have a special set of data. The peak pixel, in this case, will follow the distribution appropriate to the maximum value of a set of, say, Gaussian variables. Adjacent pixels will follow an altogether less well-defined distribution; Monte Carlo simulation may be the only way forward.

Indeed much evaluation of detection is done with simulation. 'Model sources' are strewn on the image or spectrum, and the reduction software is given the job of telling us what fraction is detected. These essential large-scale techniques are very necessary for handling the detail of how the observation was made. Evaluating detection level in radio-astronomy

synthesis images is an example. The noise level at any point depends at least on gains of all antennas, noise of each receiver, sidelobes from whatever sources happen to be in the field of view, map size, weighting and tapering parameters, the ionosphere, cloud, and so on. Modelling all this is not just impossible from a computational point of view – vital input data simply are not known. Although complex and varied issues are involved, the basic notions and algorithms of detection remain just as relevant as in apparently simpler cases.

The basic problem from a statistical point of view is the problem of modelling, as discussed in the last chapter. A full Bayesian approach is desirable but computationally intensive and certainly not practical in a surveying application. An entry point to the Bayesian literature on this subject is Hobson & McLachlan (2003).

We may need a simpler method, and a classical approach is useful. Firstly, we have to ask: what do we really want from the survey we are planning? Are we more concerned with detecting as much as possible (*completeness*) or are we more worried about false detections (*reliability*)? Moreover, we need to know what we want to do with the 'detections' once we have them. Perhaps we should publish, in a catalogue, the complete set of posterior probabilities, at each location, of the observed parameters? Or just the covariance matrix, as an approximation? Or perhaps the marginalized signal-to-noise ratio, integrating away all nuisance parameters? Scientific judgement must be used to answer these questions. The more information we catalogue, the better; and in the Internet age, this is so inexpensive as to be almost mandatory.

From the classical point of view, if we are trying to measure a parameter α then the likelihood sums up what we have achieved: $\mathcal{L} = \mathrm{prob}(\mathrm{data} \mid \alpha)$.

To be specific, suppose that α is a flux density and we wish to set a flux limit for a survey. We are only going to catalogue detections when our data exceed this limit s_{lim}. (Other quantities of astrophysical interest may need a somewhat different formulation, but the essential points remain the same.) Two properties of the survey are useful to know.

(i) The false-alarm rate is the chance that pure noise will produce data above the flux limit:

$$\mathcal{F}(\mathrm{data}, s_{\mathrm{lim}}) = \mathrm{prob}(\mathrm{data} > s_{\mathrm{lim}} \mid \alpha = 0). \qquad (7.1)$$

The *reliability* is $1 - \mathcal{F}$, i.e. $\mathcal{F} = 5/100$ gives 95 per cent reliability. That may sound good, but note that it is the infamous 2σ result.

(ii) The completeness is the chance that a measurement of a real source will be above the flux limit:

$$\mathcal{C}(\text{data}, s_{\lim}, S) = \text{prob}(\text{data} > s_{\lim} \mid \alpha = s). \qquad (7.2)$$

These notions go back as least as far as Dixon & Kraus (1968); an interesting recent treatment is by Saha (1995).

We would like to set the flux limit to maximize the completeness, and minimize the false-alarm rate. But higher completeness (or even complete completeness, $s_{\lim} = 0$!) comes at the price of an increasing number of false detections. Moreover this definition of completeness only takes account of statistical effects. There may be other reasons for missing objects, poor recognition algorithms in particular.

EXAMPLE Suppose our measurement is of a flux density s and the noise on the measurement is Gaussian, of unit standard deviation. The source we are observing has a 'true' flux density of s_0, measured in units of the standard deviation. We then have

$$\text{prob}(s \mid s_0) = \frac{1}{\sqrt{2\pi}} \exp\left[-\frac{(s - s_0)^2}{2}\right]$$

for the probability density of the data, given the source; and

$$\text{prob}(s \mid s_0 = 0) = \frac{1}{\sqrt{2\pi}} \exp\left(-\frac{-s^2}{2}\right)$$

for the probability density of the data when there is no source. Integrating these functions from 0 to $s_{\lim}$ (Table A2.1) makes it easy to plot up the completeness against the false-alarm rate, taking the flux limit as a parameter (Fig. 7.1). High completeness does indeed go hand in hand with a high false-alarm rate. However it is apparent that there are quite satisfactory combinations for flux limits and source intensities of just a few standard deviations. In real life no one would believe this, mainly because of outliers not described by the Gaussians assumed. Exercise 7.4 asks for a repeat of this calculation using an exponential noise distribution.

The conditional probabilities we have encountered suggest taking a Bayesian approach. We have

$$\text{prob}(\text{data} \mid \text{a source is present, brightness } s)$$

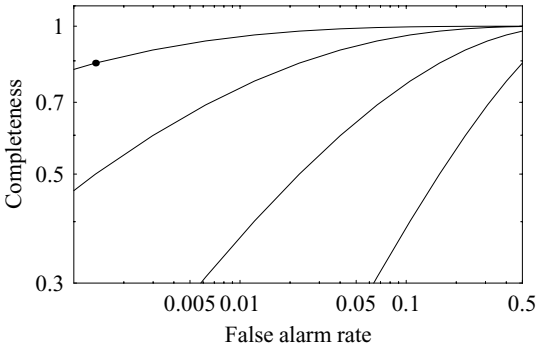

Fig. 7.1. Completeness versus false-alarm rate, plotted for source flux densities in terms of $\sigma_{\rm noise}$ ranging from 1 unit (right) to 4 units (left). The flux limits are indicated by the dots, starting at zero on the right and increasing by one unit at a time. For example, a 4σ source and a 2σ flux limit give a false-alarm rate of 2 per cent and a completeness of 99 per cent with the Gaussian noise model.

and

$$\text{prob(data} \mid \text{no source is present).}$$

Take the prior probability that a source, intensity s, is present in the measured area to be $\epsilon\, N(s)$, where $N(s)$ is a normalized distribution. This is the probability that a single source will have a flux density s. The prior probability of no source is $(1-\epsilon)\delta(s)$; δ is a Dirac delta function. Then the posterior probability density

$$\text{prob(a source is present, brightness } s \mid \text{ data)}$$

is given by

$$\frac{\epsilon \text{prob(data} \mid s) N(s)}{\epsilon \int \text{prob(data} \mid s) N(s)\, \mathrm{d}s + (1-\epsilon) \int \text{prob(data} \mid s = 0)}.$$

Integrating this expression over s gives the probability that a source is present, for given data.

EXAMPLE Pursuing the previous example, take the noise distribution to be Gaussian and take the prior $N(s)$ to be a simple uniform distribution from zero to some large flux density – a very uninformative prior! The value of ϵ reflects our initial confidence that a source is present at all, and so in many cases will be small. Figure 7.2 shows that the posterior distribution of flux density s peaks at the value of the data, as expected;

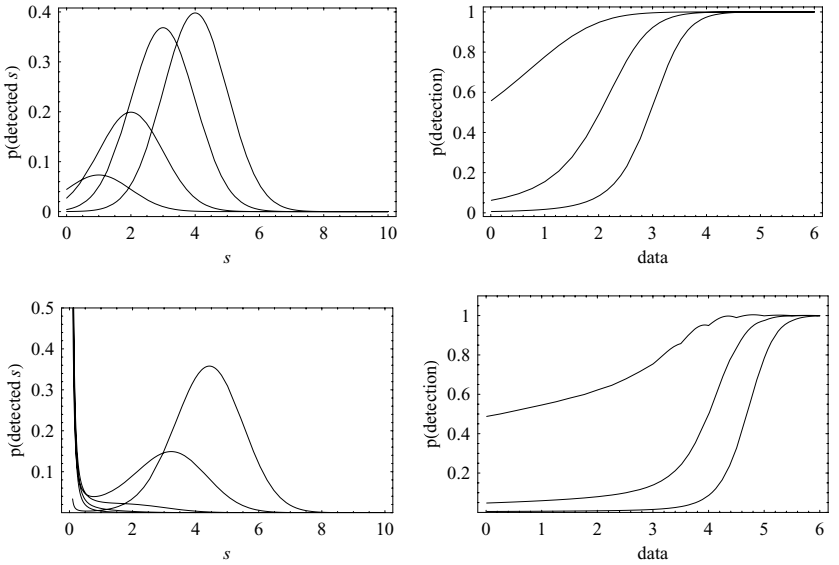

Fig. 7.2. The top left panel shows the probability of a detected source of flux density s; the curves correspond to measurements of 1–4 units (as before, a unit is one noise standard deviation). A prior $\epsilon = 0.05$ was used. On the top right these curves are integrated to give the probability of detection at any positive flux density, as a function of the data values; the curves are for $\epsilon = 0.5, 0.05$ and 0.005. The bottom panels show the results of the calculation for the power-law prior, truncated at 0.1 unit.

the role of ϵ is to suppress our confidence of a detection in low signal-to-noise cases. Again we see that for Gaussian noise, 4σ data points mean detection with high probability. Real life is more complicated.

Using a power-law prior $N(s) \propto s^{-5/2}$ gives results rather similar to the example of Fig. 2.2, which ignored the possibility that no source might be present. The rarity of bright sources in this prior now means that we need a rather better signal-to-noise to achieve the same confidence that we have a detection.

A Bayesian treatment of detection gives a direct result; from the figures in the previous example, we may read off a suitable flux limit that will give the desired probability of detection. This is affected by the prior on the flux densities, but often we will have a robust idea of what this should be from previous survey parameters such as source counts.

In many cases, however, the notion of detection of individual objects is poorly defined. Images or spectral lines crowd together, even overlap as we reach fainter and fainter. Within the region we measure, several different objects may contribute to the total flux. Even if only one object is present, if the source count $N(s)$ is steep it will be more likely that the flux we measure results from a faint source plus a large upward noise excursion, rather than vice versa. In these cases we can expect only to measure population properties – parameters of the flux-density distribution $N(s)$. If these parameters are denoted by α then a probabilistic model for the observations, when the average number of sources per measurement area is less than 1, is

$$\text{prob}(\alpha \mid \text{data}) \propto \sum_s \text{prob}(\text{data} \mid s)\text{prob}(s \mid N, \alpha)\text{prob}(\alpha).$$

(This is an example of a hierarchical model, discussed in Section 6.7. The quantities α are really hyperparameters.)

The summation in this equation will often denote a convolution between $N(s)$ and the error distribution; given a prior on the parameters of s we can obtain a better estimate of the distribution of the flux densities of sources.

If there are many sources per measurement area (and this will often be the case for faint sources) then we are in the 'confusion-limited' regime. Now we need to draw a distinction between $N(s)$, the distribution of flux densities when only one source contributes, and a more complicated distribution which takes account of the possibility that several sources may add up to give s. This complicated situation is considered in Section 7.6; the details for the simpler case are left to Exercise 7.2, and they are very similar to the previous examples.

In summary, detection is a modelling process; it depends on what we are looking for, and how the answer is expressed depends on what we want to do with it next. The simple idea of a detection, making a measurement of something that is really there, only applies when signal-to-noise is high and individual objects can be isolated from the general distribution of properties. At low signal-to-noise, measurements can constrain population properties, with the notion of 'detection' disappearing.

7.2 Catalogues and selection effects

Typically, a body of astronomical detections is published in a catalogue. On the basis of some clear criterion, objects will either be listed in the

catalogue, or not. If they are not, usually we know nothing more about them; they are simply 'below the survey limit'.

Most astronomical measurements are affected by the distance to the object. In Euclidean space, a proper motion, for a fixed velocity of the star, becomes a smaller angle inversely as the distance to that star. Apparent intensity drops off as the square of the distance. Other effects may be more subtle; the ellipticity of a galaxy becomes harder to detect, depending on distance, the blurring effect of seeing, and the detailed luminosity profile of the galaxy. The common factor in all these examples is that we measure a so-called *apparent* quantity X and infer an *intrinsic* quantity by a relationship $Y = f(X, R)$ where R is the distance to the object in question. The function f may be complicated, for observational reasons and also because it may depend on a distance involving redshift and details of space-time geometry.

We take a simple and definite case (remembering that the principles will apply to the whole range of functions f). We observe a flux density S and infer a luminosity L given by

$$L = SR^2;$$

we are considering a flat-space problem. The smallest value of S we are prepared to believe is $s_{\lim}$; if a measurement is below this limit, the corresponding object does not appear in our catalogue. (As before, we use upper-case letters to denote measured values of the variable written in lower case.)

Our objects (call them 'galaxies') are assumed to be drawn from a *luminosity function* $\rho(l)$, the average number of objects near l per unit volume. Using only our catalogue set of measurements $\{L_1, L_2, \ldots\}$, however, we will not be able to reproduce ρ at all. Instead, we will get the *luminosity distribution* η, where

$$\eta(l) \propto \rho(l)V(l). \tag{7.3}$$

Crucially, $V(l)$ is the volume within which sources of intrinsic brightness l will be near enough to find their way into our catalogue. We get

$$\eta(l) \propto \rho(l) \left(\frac{l}{s_{\lim}} \right)^{3/2}. \tag{7.4}$$

Obviously η will be biased to higher values of luminosity than ρ. This sort of bias occurs in a multitude of cases in astronomy, and is often called *Malmquist bias*.

EXAMPLE The luminosity function of field galaxies is well approximated by the Schechter function

$$\rho(l) \propto \left(\frac{l}{l_*}\right)^{\gamma} \exp\left(-\frac{l}{l_*}\right),$$

in which we take $\gamma = 1$ and $l_* = 10$ for illustration. To obtain the form of the luminosity distribution in a flux-limited survey, we multiply the Schechter function by $l^{3/2}$. The differences between the luminosity function and luminosity distribution are shown in Fig. 7.3.

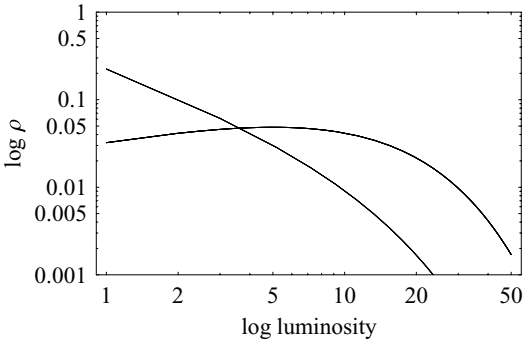

Fig. 7.3. The luminosity function ρ (steep curve) and the (flat-space) luminosity distribution are plotted for the Schechter form of the luminosity function.

Malmquist bias is a serious problem in survey astronomy. The extent of the bias depends on the shape of the luminosity function, which may not be well known. More seriously, the bias will also be present for objects whose properties correlate with something that is biased. For example, the luminosity of giant HII regions is correlated with the luminosity of the host galaxy, so that any attempt to use the HII regions as standard candles will have to consider the bias in luminosity of the hosts.

Malmquist bias arises because intrinsically bright objects can be seen within proportionately much greater volumes than small ones. Because most of the volume of a sphere is at its periphery, it follows that in a flux-limited sample the bright objects will tend to be further away than the faint ones – there is an in-built distance–luminosity correlation.

EXAMPLE We adopt a Schechter function with $\gamma = 1$ and $l_* = 10$ for the purposes of illustration. The probability of a galaxy being at distance R is proportional to R^2, in flat space. The probability of it being of brightness l is proportional to the Schechter function. The probability of a galaxy of luminosity L, located at distance R being in our sample is

$$\text{prob(in sample)} = \begin{cases} 1 & L < s_{\lim} R^2 \\ 0 & \text{otherwise.} \end{cases}$$

The product of these three probability terms is the bivariate distribution $\text{prob}(l, r)$, the probability of a galaxy of brightness l and distance r being in our sample. This distribution is shown in Fig. 7.4; there is a clear correlation between distance and luminosity. (It is this effect that produces diagrams like Fig. 4.1.) A direct check of this is to simulate a large spherical region filled with galaxies whose luminosities are drawn from a Schechter function, and then select a flux-limited sample. (The Schechter function has to be truncated at $l > 0$ as it otherwise cannot be normalized.) Figure 7.5 shows the effect indicated by the contours of Fig. 7.4.

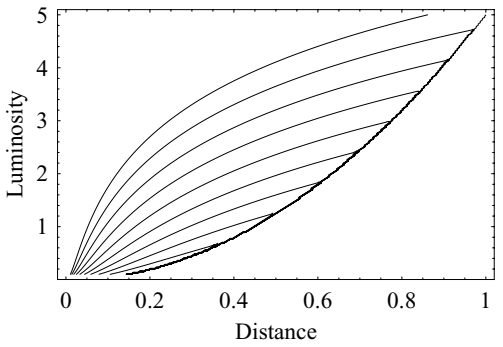

Fig. 7.4. Contour plots of the bivariate $\text{prob}(l, r)$. The contours are at logarithmic intervals; galaxies tend to bunch up against the selection line, leading to a bogus correlation between luminosity and distance.

The luminosity–distance correlation is widespread, insidious and very difficult to unravel. It means that for flux-limited samples, intrinsic properties correlate with distance; thus two unrelated intrinsic properties will

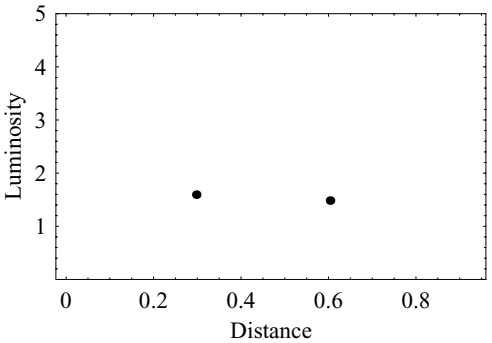

Fig. 7.5. Results of a simulation of a flux-limited survey of galaxies drawn from a Schechter function.

appear to correlate because of their mutual correlation with distance. Plotting intrinsic properties – say, X-ray and radio luminosity – against each other will be very misleading. Much further analysis is necessary to establish the reality of correlations, or (more generally) statistical dependence. Such analyses may require detailed modelling of the detection process. Take the case of measuring the ellipticity of galaxies – distant ones may well look rounder because of the effects of seeing. As more distant galaxies seem to be more luminous as well, we are on course for deducing without evidence that round galaxies are more luminous or vice versa. A detailed model will be necessary to establish the relationship between true ellipticity, measured ellipticity, and the size of the galaxy relative to the seeing disc.

EXAMPLE We take the same simulation as before, but attribute two luminosities to each galaxy, drawn from different Schechter functions. These might be luminosities in different colour bands, for example, and by definition are statistically independent. If we construct a flux-limited survey in which a galaxy enters the final sample only if it falls above the flux limit in both bands, we see in Fig. 7.6 that a bogus but convincing correlation emerges between the two luminosities.

Finally, we should note that an effect that competes with Malmquist bias is caused by observational error. The number of objects as a function of apparent intensity $N(s)$, the number counts or source counts, usually

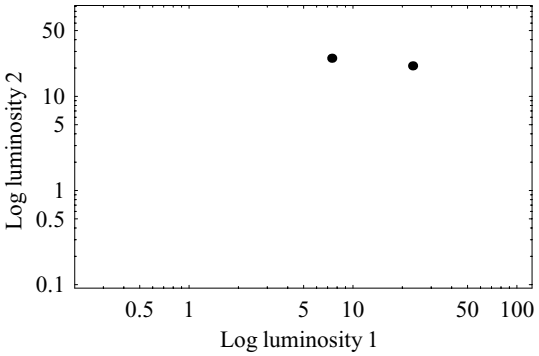

Fig. 7.6. Results of a simulation of a flux-limited survey of galaxies, where each galaxy has two statistically independent luminosities associated with it.

rises steeply to small values of s – there are many more faint objects than bright ones. In compiling a catalogue we in effect draw samples from the number-count distribution, forget those below $s_{\rm lim}$, and convert the retained fluxes to luminosities. The effect of observational error is to convolve the number counts with the noise distribution. Because of the steep rise in the number counts at the faint end the effect is to contaminate the final sample with an excess of faint objects. (An object of observed apparent flux density is much more likely to be a faint source with a positive noise excursion than a bright source with a negative excursion.) This can severely bias the deduced luminosity function towards less luminous objects. This effect does not occur if the observational error is a constant fraction of the flux density, and the source counts are close to a power law.

Many types of astronomical observations suffer from the range of problems due to Malmquist bias, parameter–distance correlation and source-count bias. This discussion has dealt with galaxies and luminosities for illustration; plenty of other examples could have been chosen.

7.3 Luminosity (and other) functions

In this section we assume that we are dealing with a catalogue of objects, of high reliability and well-understood limits. If we are interested in some intrinsic variable l (say a luminosity), then the luminosity function $\rho(l)$ is often important. In principle we could get an approximation to ρ by measuring L_i for all of the objects in some (large) volume. In practice we

need another way, because high luminosities are greatly over-represented in flux-limited surveys, as we have seen.

One of the best methods to estimate $\rho(l)$ is the intuitive $V_{\max}$ method (Rowan-Robinson 1968; Schmidt 1968). The quantities $V_{\max}(L_i)$ are the maximum volumes within which the ith object in the catalogue could lie, and still be in the catalogue. $V_{\max}$ thus depends on the survey limits, the distribution of the objects in space, and the way in which detectability depends on distance. In the simplest case, a uniform distribution in space is assumed. Given the $V_{\max}(L_i)$, an estimate of the luminosity function is

$$\hat{\rho}(B_{j-1} < l \leq B_j) = \sum_{B_{j-1} < L_i \leq B_j} \frac{1}{V_{\max}(L_i)} \tag{7.5}$$

in which its value is computed in bins of luminosity, bounded by the B_j.

The $V_{\max}$ method is hard to beat. It is a maximum-likelihood estimator (Marshall et al. 1983), and so has minimum variance for any estimate based on its statistical model. The errors are uncorrelated from bin to bin and can easily be estimated – the fractional error in each bin is close to $1/\sqrt{N_j}$, where N_j is the number of objects in each bin. More accurate error estimates can be obtained by a bootstrap. Like any method involving bins, the estimate is biased because it can only return the average value over the width of the bin. This bias may be significant in steep regions of the luminosity function.

The main practical issue is simply the determination of $V_{\max}$; as we have seen, choosing the flux limit of a survey affects the number of sources that are missed, the number of bogus ones that are included, and the extent to which faint sources are over-represented. In general these complicated effects are best examined with Monte Carlo simulations, as even a rough idea of the thing we want to know (the luminosity function) suffices to check these biases. In practice the processes of survey evaluation and calculating the luminosity function are iterative.

With V the volume defined by the distance to the source as its radius, the distribution of $V/V_{\max}$ is very useful in estimating the actual limit of a survey. If the correct flux limit has been used in the calculation of $V_{\max}$ for each object, then we would expect $V/V_{\max}$ to be uniformly distributed between zero and one. This can easily be checked by, for example, a Kolmogorov–Smirnov test. In fact this test can be regarded as a model-fitting procedure to estimate the effective flux limit of a survey. For large cosmological distances (say those corresponding to

$z > 0.2$), this technique is upset by cosmological evolution, the derivation of which was a driving force behind development of the technique (Schmidt 1968).

The literature on the $V_{\max}$ method is, justifiably, vast; Willmer (1997) provides a summary of recent work, and an entry point.

EXAMPLE Taking the previous simulation based on the Schechter function, a flux limit of 20 units gives a sample of about 200 objects. The distribution in luminosity (Fig. 7.7) shows a strong peak at about 5 units, related to the characteristic luminosity $l_* = 10$ for the simulation. Faint sources are greatly under-represented, because they are only above the flux limit for small distances. Applying the $V_{\max}$ method and bootstrapping to derive error bars gives Fig. 7.8. Because $V_{\max}$ is so small for the faint sources, the few faint sources in the sample give a large contribution to $\hat{\rho}$, although the errors are correspondingly large. For simplicity the luminosity functions have been normalized, so giving luminosity probability distributions; the two are related by a number density.

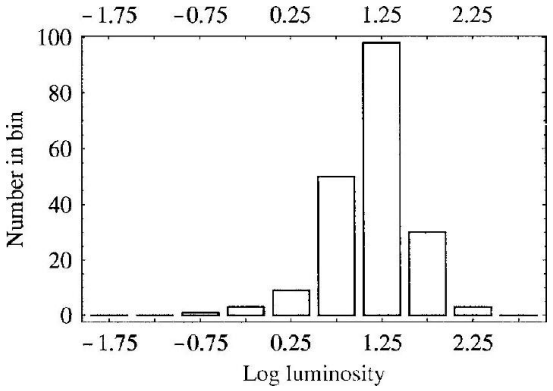

Fig. 7.7. The luminosity distribution for the simulation, in bins 0.5 dex wide, derived from the Schechter function of the previous example with a flux limit of 20 units.

A key assumption of the simple form of the $V_{\max}$ method is that the objects of interest are uniformly distributed in space. If this is not a good

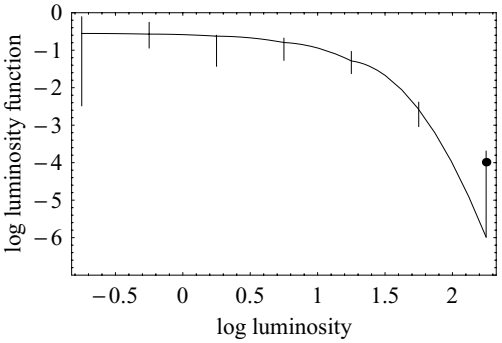

Fig. 7.8. The input luminosity function for the simulation (solid line) and the estimate via $V_{\max}$ (histogram). The error bars are the interquartile range, estimated from a bootstrap.

assumption (and it is not in most cosmological investigations) then there are three ways of making a better estimate.

One simple improvement is to bin the data into narrow ranges of distance, and estimate the luminosity function within each bin. As we can see from Fig. 7.5, at large distances we will know nothing about low luminosities, a consequence of the agnosticism of this approach. The approach is further limited by the decreasing numbers of objects as the number of distance bins is increased.

We can further consider spatial dependence by making somewhat stronger assumptions. Our data is the set of pairs (R_i, L_i) and our task is to compute the bivariate distribution $\xi(r, l)$. Obviously we are not going to be able to do this without some constraints on the form of ξ. The usual assumption is that the distribution factorizes, so that

$$\xi(r, l) = \rho(l)\phi(r). \tag{7.6}$$

This just means that the form of the luminosity function does not change with distance, but the normalization can. This method will allow us to extrapolate information from small distances and low luminosities into the bottom right portion of Fig. 7.5.

In this case, the standard estimator of ρ is the C^- method, due originally to Lynden-Bell (1971) and redeveloped by Chołoniewski (1987). This method is not nearly as intuitive as the $V_{\max}$ method, but it is important because it is also a maximum-likelihood estimator. The likelihood function, from which both methods are derived, is given by Marshall et al. (1983).

The C^- estimator is best described by a piece of pseudo-code:

```
Arrange the data (R_i, L_i) in decreasing order of l
set C_i = 0
for each L_j < L_i: add 1 to C_i if this source is within
        V_max(L_i)
otherwise, go to the next L_j until finished.
```

Remarkably, the C-numbers suffice to determine the cumulative luminosity function:

$$\int_0^{L_i} \rho(l)\,\mathrm{d}l \propto \prod_{k \le i} \left(\frac{C_k + 1}{C_k} \right) \tag{7.7}$$

with

$$\frac{C_1 + 1}{C_1} = 1.$$

as the starting point. The constant of proportionality is the inverse of the largest $V_{\max}(L_i)$ in the sample; it can also be obtained by requiring that the estimated distribution $\hat{\rho}$ yields a total number of detections that matches the observed luminosity distribution. If there are ties in the sample, the simplest remedy is to shuffle the data by small amounts (say, a tenth of the observational error) so that the C^- algorithm can be applied straightforwardly.

Obtaining the result as a cumulative distribution is slightly inconvenient, but a conversion to binned form is easy enough. This yields errors that are more independent from bin to bin, and as usual can easily be computed by bootstrap. The distance distribution ϕ (or evolution function) can also be extracted by similar methods, if required; see Chołoniewski (1987) and the cited references.

If parametric forms are known for ρ and ϕ, then a normal modelling method can be used. In fact, the C^- method obtains an analytic solution of the form

$$\xi(l, r) = \sum_i a_i \delta(l - L_i) \sum_j b_j \delta(r - R_j) \tag{7.8}$$

where distances are denoted by r and R, and the a_i and b_j are the parameters of the luminosity distribution and evolution function respectively. The $V_{\max}$ method is obtained from a similar model via maximum likelihood, except that the distribution with distance is assumed to be uniform. Models may be available with far fewer parameters (the

Schechter function only has three, for example) and then a model fit will usually give lower random errors. As usual, however, care is needed to be sure that the model represents reality.

The two approaches we have described are at opposite ends of the spectrum of assumptions: fitting factorizable functions $\xi(r, l)$, or simply counting objects in bins of distance. Intermediate between these two are the 'free-form' methods (Peacock 1985; Dunlop & Peacock 1990), which attempt to fit fairly general functions to the data populating the r-l plane. Examples of these functions are

$$\sum_{i,j} a_i (\log r)^i (\log l)^j,$$

where the cross-terms break the factorizability. However, the use of a relatively small number of terms in the expansion does permit extrapolation into areas of the r-l plane unpopulated by observations.

7.4 Tests on luminosity functions

7.4.1 Error propagation

A luminosity function may be used to derive some other parameter – an estimate of a contribution to background light, for example. Propagating the errors, whether from a binned estimate or a model fit, is straightforward enough, as long as we have a simple analytic relationship between the desired parameter and the model parameters. If not, a simulation may be the easiest solution.

If the luminosity function has been derived by maximum likelihood, then an asymptotic error estimate is available (Section 6.1). Suppose we have a model, with parameters $\vec{\alpha}$, and we are interested in the error bars on some function $e = f(\vec{\alpha})$. The 'unconstrained' maximum likelihood is $\mathcal{L}(\vec{\alpha} = \hat{\vec{\alpha}})$ and the constrained maximum likelihood is $\mathcal{L}(\vec{\alpha} = \hat{\vec{\alpha}}, e = f(\hat{\vec{\alpha}}))$. The classical theory of the likelihood ratio tells us that

$$-2 \log \mathcal{L} \left(\vec{\alpha} = \hat{\vec{\alpha}}, e = f(\hat{\vec{\alpha}}) \right) + 2 \log \mathcal{L} \left(\vec{\alpha} = \hat{\vec{\alpha}} \right) = \Delta \qquad (7.9)$$

is asymptotically distributed as χ^2, with one degree of freedom. The first term may be calculated with numerical routines for constrained maximization, and so an error bar for e can be obtained. For instance, a value of $\Delta = 4$ corresponds to a confidence level of 95 per cent. Avni (1978) discusses the technique in an astronomical context.

7.4.2 Luminosity function comparison

We may however have two estimates for different types of objects, and we may want to know if the luminosity functions are different. Here the range of possible tests is very wide. Considered as probability distributions (so normalized to unity) it is possible to apply many of the tests described in Chapter 5. The chi-square test can be applied directly to the differences between distributions derived in binned form. The methodology of other tests may also be applied. For example the Kolmogorov–Smirnov statistic would be a natural one to use for a cumulant derived by the C^- method. In this case, however, the distribution of the statistic (under the null hypothesis) would have to be derived by a Monte Carlo simulation of the experiment.

Another type of test is based on the likelihood ratio (Jenkins 1989), and is applicable to cases where the luminosity functions have been derived in parametric (or binned) form from a maximum-likelihood analysis. This idea is discussed further below.

7.4.3 Correlation: multivariate luminosity functions

A further sort of test is correlation, leading on to the subject of multivariate luminosity functions. If we generate a sample (say from X-ray observations) we obtain a catalogue which we may then resurvey at, say, radio wavelengths. Retaining the objects which are detected at both wavelengths, we can construct a bivariate luminosity function $\rho(l_{\rm X}, l_{\rm R})$. The most straightforward way of doing this is by a generalization of the $V_{\rm max}$ method. To obtain the $V_{\rm max}$ for each object, compute its $V_{\rm max}$ for each of the variables for a particular object, and take the minimum. The justification is simply that an object will drop out of the catalogue if it is below the detection limit in either band (Schmidt 1968).

Multivariate luminosity functions take much effort to construct. However, they do provide a solution to the problem of bogus luminosity – luminosity correlations, mentioned earlier in this chapter. The main problem is the increase in the number of bins: four times as many for a bivariate function, nine times as many for a trivariate. These bins become sparsely populated with objects.

If we have an estimator of (say) a bivariate luminosity function of X-ray and radio luminosity, three possibilities are available to see if $l_{\rm X}$ and $l_{\rm R}$ are correlated. The easiest is by simple inspection of $\rho(l_{\rm X}, l_{\rm R})$ which may show an obvious 'ridge line'. Another possibility is that some

statistic, say the median $l_{\rm X}$, computed from the luminosity function in narrow slices of $l_{\rm R}$, will correlate with $l_{\rm R}$. Here we could use end-to-end Monte Carlo simulations of a correlation coefficient to establish the significance of any result.

EXAMPLE Phillips *et al.* (1986) reported an emission-line survey of an optical magnitude-limited sample of nearby galaxies. They derived an emission-line luminosity function, binned into one-magnitude ranges of absolute magnitude. Dividing by the optical luminosity function gives an estimate of the fraction of galaxies that are emitting at a given emission-line power. Moreover, integrating these normalized luminosity functions gives an estimate of the fraction of galaxies that have emission-line power anywhere in the range sampled by the survey.

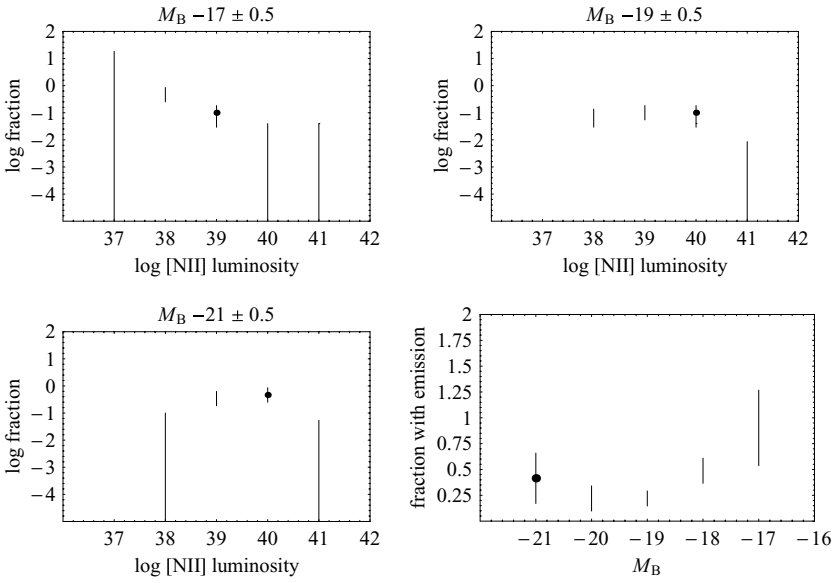

Fig. 7.9. Top left and right, bottom left: estimates of the normalized emission-line luminosity function, derived from the $V_{\rm max}$ method. Bottom right: the integral of the normalized functions, plotted against absolute optical magnitude. The fraction of galaxies producing emission lines appears to fall with increasing optical luminosity.

As seen in Fig. 7.9, the emission-line luminosity function shifts to higher powers at brighter absolute magnitudes. Clearly the Malmquist bias of the original sample would make it impossible to make an unbiased

estimate of the emission-line luminosity function, which is why the data were binned into magnitude ranges.

These data have been corrected, following an erratum to the original paper which illustrates the pitfalls of this type of analysis. For the sample on which the emission-line survey was based, the normalization of the optical luminosity function depends somewhat on distance. But, being a flux-limited sample, the emission-line luminosity correlates with distance too. This means that normalizing the emission-line luminosity function must take into account 'which' optical luminosity function to use, depending on the spread of distances in each magnitude bin.

Finally we need to remember that correlation is just one case of statistical dependence. Variables may be related non-linearly – for example, $\rho(l_{\rm X}, l_{\rm R})$ may be steeper (as a function of $l_{\rm X}$) at larger $l_{\rm R}$, without changing its median. Quite generally, what we want to know is whether

$$\rho(l_{\rm X}, l_{\rm R}) = \rho_{\rm X}(l_{\rm X})\rho_{\rm R}(l_{\rm R})$$

is statistically plausible.

Probably the best tests to use in this case are those based on the likelihood ratio. Suppose we fit both factorizable and unfactorizable models of the luminosity function, using maximum likelihood. Call the maximum likelihood in each case $\mathcal{L}_{\rm f}$ and $\mathcal{L}_{\rm uf}$. The log likelihood ratio

$$\mathcal{R} = \log \frac{\mathcal{L}_{\rm f}}{\mathcal{L}_{\rm uf}} \tag{7.10}$$

will give an indication of which model is better – we have encountered this general idea in a Bayesian context in Chapter 6. If we are fitting many parameters (and more than one poses difficulties), it is easier to use the `maximum` of the likelihood to derive the ratio. Evidently the ratio will depend on how many free parameters we have in the competing models; classical results tell us that $\mathcal{R}$ is distributed asymptotically as chi-square, with a number of degrees of freedom that depends on the number of free parameters in each model. As usual, a pragmatic conclusion is not to reach for the tables of chi-square, but rather to regard $\mathcal{R}$ as a potentially useful test statistic, and derive its distribution by Monte Carlo for the problem to hand. This approach is described by Schmitt (1985) in the context of survival analysis, but is applicable whenever a likelihood approach is used.

7.5 Survival analysis; censored data

When we produce a primary sample of objects in astronomy, we do so by making a series of measurements and picking out the ones we regard as detections. The results often find their way into catalogues, of which venerable examples are the New General Catalogue or the 3CR Catalogue. Objects which are not in the catalogue – usually because they are below the flux limit – are simply unknown. Since in general we do not know if there is anything there at all, quoting an upper limit for every position or wavelength surveyed is not a useful thing to do.

However, frequently an established primary sample is then resurveyed in some other way; we may investigate the Hα luminosity of galaxies in the NGC, for instance. In this case, it is very useful to quote upper limits for the undetected galaxies, because we know that such limits refer to real objects. Sometimes a resurvey may yield lower limits as well. If we were to measure X-ray and radio flux densities for the NGC galaxies we would probably obtain both upper limits and lower limits for the radio to X-ray spectral index.

The branch of statistics that deals with limits is called *survival analysis*. The term arises in medical statistics, where at the conclusion of a study some of the subjects may have survived and some died. For presumably unrelated reasons, measurements which are only limits are called 'censored'. The methods of survival analysis were introduced into astronomy by Avni *et al.* (1980), Feigelson & Nelson (1985), Schmitt (1985), and Isobe, Feigelson & Nelson (1986). Other astronomers had independently discovered aspects of the technique, but these papers offer the best introductions. A useful text is Kalbfleish & Prentice (2002).

Survival analysis offers (i) estimation of intrinsic distributions (such as luminosity functions), (ii) modelling and parameter estimation, (iii) hypothesis testing and (iv) tests for correlation and statistical independence, for cases in which some of the available measurements are limits. The key assumption is that the censoring is random; this means that the chance of only an upper limit being available for some property is independent of the true value of that property. This assumption is often met for flux-limited samples. For an object of true luminosity L and distance R, the condition for censoring is that

$$\frac{L}{R^2} < S_{\rm lim}$$

the flux limit for the survey. If R is a random variable, independent

of L, and $S_{\rm lim}$ is fixed, then the chance of censoring is independent of L. Evidently a careful examination of the way in which a sample was selected is necessary to determine that survival analysis is applicable.

7.5.1 The normalized luminosity function

To be definite, suppose we select a sample of objects at wavelength A and then resurvey the sample at wavelength B. For some objects, we will achieve a detection and so have a measurement of luminosity L_B; for others, we will only have an upper limit $L_B^{\rm U}$. The methods of survival analysis use the detections, and upper limits, to reconstruct the distribution of L_B. This will be proportional to the luminosity function ρ_B. However, it is vital to remember that the censoring has to be random. Also, the luminosities L_A will have Malmquist bias; if L_A and L_B are correlated, then of course the estimate of the distribution of L_B will also be biased. In general it is safest to calculate the estimate in narrow bins of L_A. Indeed this is one way of checking for a relationship between L_A and L_B in the sample, as we shall see.

Two equivalent algorithms are available for computing the normalized luminosity function. If we are happy to bin the data (both the detections, and the upper limits) into intervals of L_B, the estimated probability per bin $\hat{p}_k$ can be derived by a recursive relation due to Avni et al. (1980):

$$\hat{p}_k = \frac{n_k}{M - \sum_{j=1}^{k} \left(\dfrac{u_j}{1 - \sum_{i=1}^{j-1} \hat{p}_i} \right)}. \tag{7.11}$$

This intimidating formula in fact results from a straightforward maximum-likelihood argument. (Avni et al. give an expression for the likelihood function; it can be useful in various tests.) In the formula n_k is the number of detected objects in bin k; u_k is the number of upper (or lower) limits allocated to bin k; and M is the total number of observations (detections plus limits). To use the formula with upper limits, number the bins from large to small values of the observed quantity; conversely for lower limits. In either case, undetected objects must be counted in higher-numbered bins than the bin where their limit is allocated. Calculation begins with bin 1, for which the solution is

$$\hat{p}_1 = \frac{n_1}{M - u_1}.$$

Allocating limits to bins takes a little care. For narrow bins the scheme

used should not matter, but for wider bins a little experimentation may be instructive; the problem here is bias, as is usual with wide bins. This method will produce a normalized distribution as long as the highest-numbered bin contains detections, not limits. This makes sense; in the case of upper limits, the highest-numbered bin is the faintest, and if there are limits in the faintest bin we have no way of using them.

EXAMPLE Here are some data from Avni *et al.* (1980), giving the distribution of the X-ray to optical luminosity spectral index for quasars. In this case the u_k are lower limits corresponding to no detections in the X-ray band and the k are the indices of equation (7.11).

k	n_k	u_k	$\hat{p}_k$	$\hat{\mathcal{K}}_k$
1	2	0	0.057	0.057
2	1	1	0.029	0.086
3	4	1	0.122	0.204
4	4	0	0.122	0.326
5	3	1	0.096	0.418
6	6	0	0.191	0.612
7	3	3	0.128	0.709
8	1	1	0.051	0.758
9	2	0	0.102	0.879
10	1	1	0.102	0.939

We see from Fig. 7.10 that inclusion of the upper limits does give a little more information. Since the method should extract the distribution that was subject to the censoring, the reconstructed distribution will be proportional to the luminosity function – in this case, the number of quasars per unit volume with each spectral index. As Avni *et al.* discuss in detail, much depends on the selection of the sample in the first place. Here an optically selected sample was subsequently surveyed at X-ray wavelengths, and only at X-rays were upper limits available; the original selection will therefore have biased the sample to optically luminous quasars.

Distances were available for all the objects in this sample, so that in fact a $V_{\max}$ method could have been used to reconstruct the luminosity function (or more accurately, the distribution function of spectral index). The retention of upper limits in the analysis means that *no distances were necessary* to reconstruct the distribution. (The spectral index itself does not require a distance, unless K-corrections are considered.)

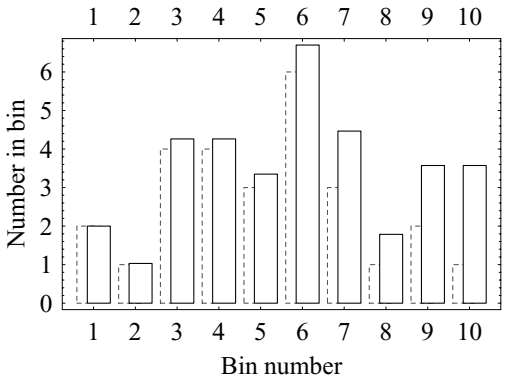

Fig. 7.10. Distribution of spectral indices (optical to X-ray) for a sample of optically selected quasars, showing the observed distribution (dashed boxes) and the estimated true distribution (solid boxes) after including the lower limits.

An alternative estimate of the cumulative distribution is provided by the Kaplan–Meier estimator. The Kaplan–Meier estimator is better known in the wider statistical world, and it is a maximum-likelihood estimator just like the Avni estimator. It has the advantage of not relying on any binning scheme. However, being cumulative, errors are highly correlated from one point on the estimate to the next.

$$\hat{\mathcal{K}}(L_k) = 1 - \prod_{i=1}^{k-1} (1 - d_i/n_i)^{\delta_i} \tag{7.12}$$

is the Kaplan–Meier estimator of the cumulative probability distribution, at the kth observation. As with the Avni estimator, this formula will work for either upper or lower limits.

For lower limits, arrange the data in increasing order. Then d_i is the number of observations of L_i, and n_i is the number of observations equal to or larger than L_i. By 'observation' we here mean either detections or non-detections. δ_i is 1 for a detection and zero for an upper limit. For upper limits, arrange the data in decreasing order. Then d_i is the number of observations of L_i and n_i is the number of observations equal to or smaller than L_i. In both analyses, ties in the detections can be removed by shuffling the data by amounts small compared to observational error.

EXAMPLE Using the data from the previous example, we can calculate the Kaplan–Meier estimator for the spectral indices. The results are in

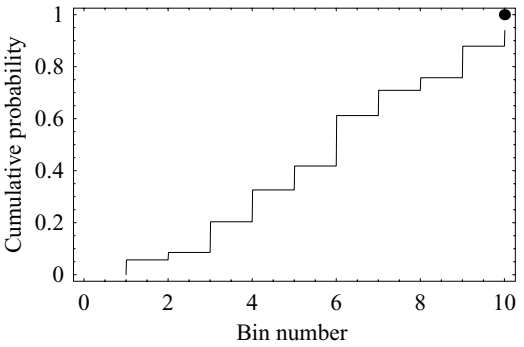

Fig. 7.11. The Kaplan–Meier estimator (solid line), compared to the cumulant derived from the Avni estimator (dots).

the '$\hat{\mathcal{K}}_k$' column in the data table of the previous example. If we form a cumulant from the Avni estimator, we find that the two results are very similar (Fig. 7.11), as expected since both are maximum-likelihood estimators. The treatment of the upper limit in the last bin follows a slightly different convention in the two methods.

Since these estimators are derived from a likelihood function, we might expect that there would be a formula for the variance on the estimate. This is indeed the case; it is called Greenwood's formula, and we refer you to Feigelson & Nelson (1985) for details. But being an asymptotic formula, it is not terribly useful in practice. Fortunately, we can estimate errors in other ways – either by a direct Monte Carlo simulation, or by a bootstrap on the sample we have. Bootstrapping censored data is not well investigated (Feigelson & Nelson 1985) but we have found it to be satisfactory. In their review paper on the bootstrap, Efron & Tibshirani (1986) work through an example of bootstrapping censored data.

EXAMPLE Returning to our simulated field-galaxy sample selected at one wavelength, we find on 'resurveying' at another wavelength that we have 67 detections and 317 upper limits. The simulation allocated luminosities from independent Schechter functions at both wavelengths. Binning the data gives the histogram shown in Fig. 7.12; note that upper limits are counted in one bin lower down than would be the case for equivalent detections. Applying the Avni estimator, we find a luminosity

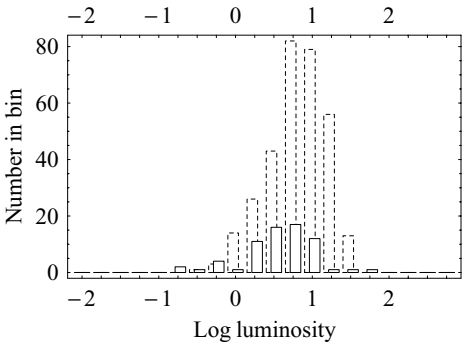

Fig. 7.12. The luminosity distribution, and upper limits, for the field-galaxy simulation; there are 67 detections and 317 upper limits. The bins (dashed) for the upper limits are slightly displaced for clarity.

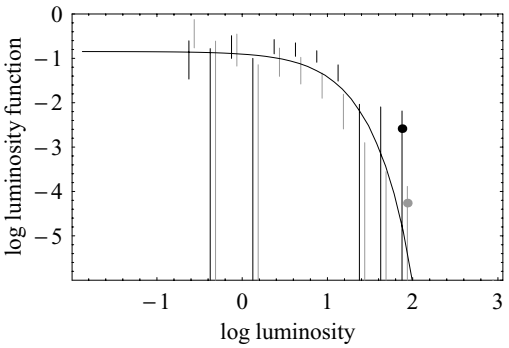

Fig. 7.13. The luminosity probability distribution (black dots), and theoretical distribution (solid line), together with bootstrapped error estimates (the interquartile range is shown). The lighter dots are a $V_{\max}$ estimate, displaced slightly in luminosity for clarity.

probability distribution (Fig. 7.13) that agrees well with the input theoretical distribution. The error bars are derived from a bootstrap, and the errors are reasonably uncorrelated from one bin to the next. The luminosity function itself is estimated by finding the constant of proportionality (galaxies per unit volume) which gives the correct total number of observed galaxies. This means matching the estimated luminosity probability distribution to the luminosity distribution η. (Do not confuse the luminosity probability distribution with a luminosity distribution; the terminology is unhelpful, but is, unfortunately, established.)

Figure 7.13 also demonstrates that $V_{\max}$ and survival analysis results are in close agreement. This is what we should expect; both are maximum-likelihood estimators, based on rather similar models, and the maximum-likelihood estimator for a given model is unique. The advantage of survival analysis is not that it gives better estimates of luminosity functions, but rather that it will help in correlation analysis, or the reconstruction of distributions without using distances (such as the spectral index distribution of Fig. 7.10 and 7.11).

7.5.2 Modelling and parameter estimation

Once we have obtained a luminosity probability distribution ($\hat{\rho}(L_B)$ in our example) we may well want to estimate some other quantity from it, or decide if it differs from some other distribution. The same remarks apply as in the case of an ordinary luminosity function, except that we must never forget the Malmquist bias of the primary sample.

One useful technique, given enough data, is to divide the data into bins of L_A and compute a distribution of L_B for each bin; call these $\hat{\rho}(L_B \mid L_A)$. With luck (and enough data) we may be able to estimate a location parameter, say a median, at each slice of L_A. This sort of analysis may well answer the question of whether L_A and L_B are correlated. Error analysis, as usual, can be via bootstrap or direct Monte Carlo. We may also need to compare estimates, say $\hat{\rho}_1(L_B)$ and $\hat{\rho}_2(L_B)$. Perhaps sample 1 consists of one morphological type, and sample 2 of another. Again, we have to be extremely careful of Malmquist bias; the samples may have different distributions of L_A, and any difference in the luminosity distributions of L_B may just reflect this, plus L_A–L_B correlation.

EXAMPLE Sadler, Jenkins & Kotanyi (1989) faced a representative problem in this area. They had radio and Hα measurements of a sample that was originally selected at optical wavelengths. Many of the radio- and Hα measurements were upper limits, and moreover there was good reason to think that both of these variables were intrinsically correlated with optical luminosity.

Sadler *et al.* divided the data into narrow bins of optical absolute magnitude, and then computed distributions of radio luminosity and Hα luminosity, using survival analysis.

As can be seen in Fig. 7.14, the 30th percentile of these distributions correlates well with absolute magnitude in each case. However, it

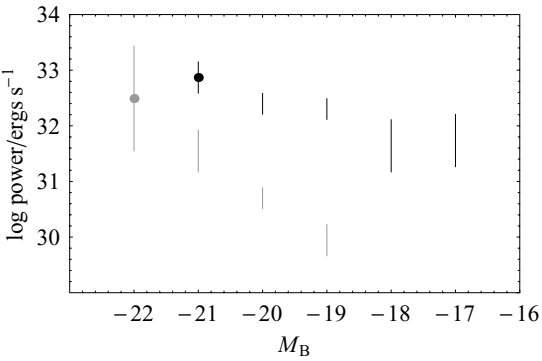

Fig. 7.14. The sample of Sadler, Jenkins & Kotanyi (1989): the 30th-percentile radio power (light symbols) and emission-line power (dark symbols), as a function of absolute magnitude.

is clearly not easy to establish whether radio and Hα luminosity are correlated, given this mutual correlation. Sadler *et al.* used Schmitt's factorizability test to show that radio and Hα emission did not correlate.

Error estimates on parameters derived from distributions can be calculated analytically, by likelihood ratios, or by simulation, as discussed for luminosity functions (Section 7.4.1).

7.5.3 Hypothesis testing

If we wish to test two distributions of observations against each other, using detections as well as limits, we have a number of choices. In all cases, however, we have to be aware of how our samples were selected in the first place, in case this forces differences to exist. In general we will expect a problem whenever the variable of interest is correlated with the variable used to define the sample. The Malmquist bias of the defining variable will then be manifest in the other variable. If the bias is not the same for the two samples (and it depends on observational method) then a bogus difference will be detected. Feigelson & Nelson (1985) give a useful introduction to the test statistics available. Distributions for these are known under the null hypothesis, in the asymptotic limit; it is probably best for derive small-number distributions by Monte Carlo or bootstrap simulations.

Some ideas for the test statistic are familiar from the Wilcoxon–Mann–Whitney test (Section 5.4.3). Suppose our two samples are drawn from

the same probability distribution. If we combine the two samples we want to test and order them in size, intuitively we expect the observations from the two samples to be randomly intermingled. If the 'rank' (position in the sorted list) of observations from one of the samples were to be, say, systematically low, we would suspect a difference. Evidently a similar procedure could be used for data containing limits, as we would expect limits to be randomly intermingled in just the same way. Constructing a test statistic depends on the penalty we assign for non-random intermingling, and how we distribute this penalty between detections and limits. Feigelson & Nelson (1985) described two variations on this idea, the Gehan and log-rank tests. A major concern in using these tests must be the distribution of the limits, as these are affected both by observational technique and by intrinsic differences between the samples. As always, the result of the test will be to give the probability that the differences between the distributions of the data is due to chance. Asymptotic distributions are known for the statistics, but simulation will be more reliable for small samples.

The Gehan test is probably the simplest to use. We describe the procedure for the case of no ties, which can always be arranged for experimental data; the test is somewhat simpler in this case.

Suppose we have two samples of data, labelled A and B, including both detections and limits. Combine the samples.

Arrange the detections in order; ascending order for data with lower limits, descending order for data with upper limits. Number the observations; this gives each datum a rank. Call the ith rank for data from sample A $r_{i\mathrm{A}}$.

For the ith detection from sample A, calculate $n_{i\mathrm{A}}$, the number of observations of A which are to the right. By 'right' we mean data that are greater than or equal to the ith observation (in the case of lower limits) or less than or equal to the ith observation (in the case of upper limits). Thus this part of the calculation uses the limits.

The number of limits from sample A between detection i and detection $i+1$ is $m_{i\mathrm{A}}$.

The Gehan statistic is then

$$\Gamma = \sum_{\text{detections in A}} (n_{i\mathrm{A}} - r_{i\mathrm{A}}) - r_{i\mathrm{A}} m_{i\mathrm{A}}. \tag{7.13}$$

This is asymptotically distributed as a Gaussian of mean zero and

variance

$$\sigma^2 = \sum_{\text{detections}} n_{i\mathrm{A}} n_{i\mathrm{B}} \tag{7.14}$$

in which the assumption of 'no ties' has simplified the formula given in Feigelson & Nelson.

EXAMPLE We simulated two samples of objects, one drawn from the field-galaxy Schechter function with a characteristic luminosity $L_* = 10$, and the other with $L_* = 30$. In one sample there were 23 detections and 149 limits; in the other, 45 detections and 167 limits. The estimated luminosity functions are in Fig. 7.15, and show an appreciable difference. The Gehan test gives $\Gamma/\sigma = 3.3$, significant at the 0.1 per cent level (if the asymptotic approximation holds for these small numbers, this far out in the wings).

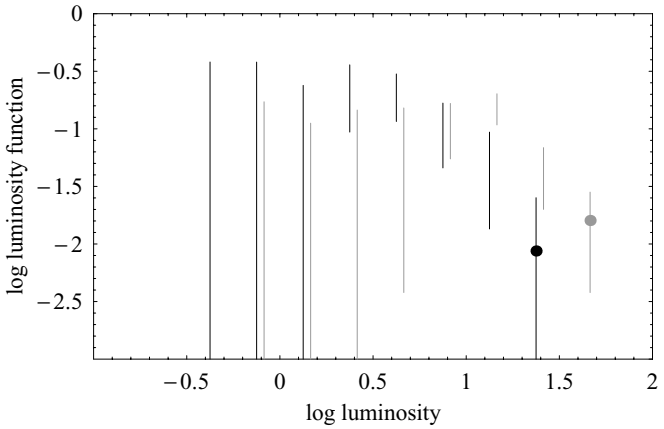

Fig. 7.15. Luminosity functions for two simulated samples drawn from field-galaxy Schechter functions (see text), estimated by the Avni method with bootstrap errors. The error bars are the interquartile ranges.

Other possibilities (Feigelson & Nelson 1985) include a species of Kolmogorov–Smirnov test on the estimated cumulative distributions. The theoretical (and notational, and naming) situation is very complicated; different tests are sensitive to different things, and the best advice is to try each on Monte Carlo simulations of the problem to hand.

One quite simple test (Jenkins 1989) is based on the likelihood function for the Avni estimator. This test compares the likelihood of two possibilities. In one, the pooled data from both samples are used to estimate a single distribution. In the other, the separate sets of data are used to derive two distributions. The test takes into account the larger number of parameters that are available when dealing with the data separately, and has the same theoretical basis as the methods described for estimating confidence limits on parameters of luminosity functions (Avni 1978). In detail, if we have Avni estimates $\hat{p}_k^{\mathrm{A}}$ and $\hat{p}_k^{\mathrm{B}}$ for two samples A and B, plus an estimate $\hat{p}_k$ for the pooled sample, we can then compare the log likelihoods with the statistic

$$\begin{aligned} -2\log\Lambda = &-2\left(\sum_{j=1}^{k} n_j \log\hat{p}_j + \sum_{j=1}^{k} u_j \log\sum_{i=j}^{k}\hat{p}_i\right) \\ &+2\left(\sum_{j=1}^{k} n_j^{\mathrm{A}} \log\hat{p}_j^{\mathrm{A}} + \sum_{j=1}^{k} u_j^{\mathrm{A}} \log\sum_{i=j}^{k}\hat{p}_i^{\mathrm{A}}\right) \\ &+2\left(\sum_{j=1}^{k} n_j^{\mathrm{B}} \log\hat{p}_j^{\mathrm{B}} + \sum_{j=1}^{k} u_j^{\mathrm{B}} \log\sum_{i=j}^{k}\hat{p}_i^{\mathrm{B}}\right) \end{aligned} \tag{7.15}$$

in the same notation as before. The test works only if the separate and pooled data are binned into the same k cells, each with at least one detection; in this case the distribution of $-2\log\Lambda$ is asymptotically χ^2 with $k-1$ degrees of freedom. Experimentally, it is found that it can be quite a long way from χ^2 with typical amounts of data, and it is best to simulate the distribution. The test is simple to use if the Avni estimators have already been computed; the main nuisance is the need to ensure that the rightmost, or highest-numbered bin, does not contain only a limit. This can be achieved by making this bin arbitrarily large, but it is best to alter the binning scheme in the same way for all the distribution function estimates that are used in the test.

7.5.4 Testing for correlation or statistical independence

Testing for correlation or statistical independence is an area in which survival analysis has something very useful to offer. This is because it

deals automatically with the pernicious luminosity–distance correlation that appears in flux-limited samples. Recall that to test for correlation using survival analysis, we need a primary sample, followed by observations of two further parameters. As noted, the Malmquist bias of the primary sample may well affect any conclusions based on resurveying the sample. If we can safely focus on correlations of the two new parameters only, thus assuming that mutual correlations with the primary selection parameter do not matter, then we may use various survival-analysis regression techniques. Because these incorporate limits, they deal automatically with mutual correlations with distance – the bane of any correlation analysis of intrinsic parameters. It remains crucial that the two sets of data are censored in the same way and the distribution of the limits amongst the data can affect the results of tests.

Isobe, Feigelson & Nelson (1986) gave a detailed review, essential reading for application of these types of test. Broadly, we may test for correlation or we may fit regression lines. Isobe *et al.* carried out tests with simulations of flux-limited samples and found several methods which do avoid the trap of the correlation with distance.

Of these methods, the generalized Kendall rank correlation test is fairly simple to use. We start with $n+m$ observations of pairs (X_i, Y_i). In n of these, both variables are detected and the pair is completely known; in the remaining m, either or both of the variables may be censored. Each variable is then ranked. We give a procedure for data with upper limits, but an obvious alternative will work for lower limits. In pseudo-code:

```
create a square matrix a of size n + m × n + m
initialize it to zero
for each X_i
if X_j > X_i and X_j is detected, set a_ij = 1
if X_j < X_i and X_i is detected, set a_ij = −1
```

Repeat this procedure to create a matrix b for the y-variable. This method is assigning a very simple rank, depending on whether a variable is *definitely* known to be bigger than, or less than, the one with which it is being compared.

The Kendall statistic is just

$$\kappa = \sum_{i=1}^{n+m} \sum_{j=1}^{n+m} a_{ij} b_{ij} \tag{7.16}$$

and is asymptotically Gaussian, of variance

$$\sigma^2 = \frac{4}{(n+m)(n+m-1)(n+m-2)} \times \left(\sum_{i=1}^{n+m} \sum_{j=1}^{n+m} \sum_{k=1}^{n+m} a_{ij} a_{jk} - \sum_{i=1}^{n+m} \sum_{j=1}^{n+m} a_{ij}^2 \right) \times \left(\sum_{i=1}^{n+m} \sum_{j=1}^{n+m} \sum_{k=1}^{n+m} b_{ij} b_{jk} - \sum_{i=1}^{n+m} \sum_{j=1}^{n+m} b_{ij}^2 \right) + \frac{2}{(n+m)(n+m-1)} \sum_{i=1}^{n+m} \sum_{j=1}^{n+m} b_{ij}^2 \sum_{i=1}^{n+m} \sum_{j=1}^{n+m} a_{ij}^2. \quad (7.17)$$

For an extension of this test to partial correlation, see Akritas & Siebert (1996).

EXAMPLE In our usual simulated galaxy sample, we select at one wavelength and then observe at two more. Each of the assigned luminosities is drawn from a Schechter function, and is independent of the others. Retaining the upper limits only, we obtain the convincing 'correlation' between data at the two new wavelengths shown in Fig. 7.16. (There are 87 detections of both variables, out of a primary sample of 349.) However, the Kendall rank correlation calculation yields $\kappa/\sigma = 0.56$, showing that the use of upper limits has automatically retrieved the

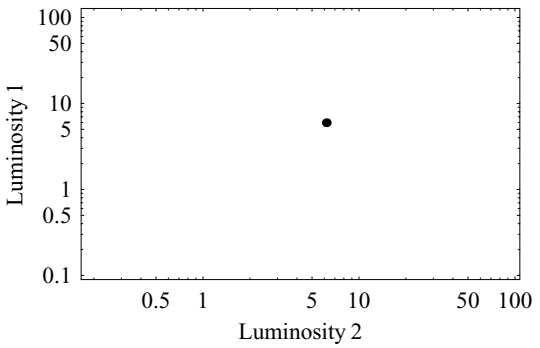

Fig. 7.16. The apparent correlation between two new luminosities in the doubly resurveyed sample.

true non-correlation. A correlation was never detected in repeated runs of the simulation. The distribution of κ, for sample sizes of around 30, was quite markedly non-Gaussian. For samples of typical astronomical size (= small), it would be worth estimating the distribution of the test statistic by Monte Carlo.

Quite often in astronomy, intrinsic parameters are so widely scattered that it is unrealistic to look for a correlation of X with Y, in the sense of trying to identify some linear relationship plus scatter. It may make more sense to ask if the variables are statistically independent, a more agnostic question. This amounts to asking if the probability distribution $\rho(x, y)$ can be factorized into $\rho_x(x)\rho_y(y)$. Schmitt (1985) developed a useful test for this based on the Avni estimator; it is rather fiddly to use, and there is a detailed discussion of the practical issues by Sadler, Jenkins & Kotanyi (1989).

7.6 The confusion limit

In many cases of astronomical interest, we find that faint objects are much more numerous than bright ones. Faint objects therefore crowd together; ultimately they start to be unresolved from each other and our signal becomes a mixture of objects of various intensities, blended together by the point-spread function of our instrument. Examples include radio sources, spectral lines in the Lyman-α forest, and faint galaxies observed in the optical.

The notion of the confusion limit was first developed during a memorable controversy amongst radio astronomers and cosmologists in the 1950s, the source-count – Big Bang – Steady State controversy – see Scheuer (1991) for a historical perspective. The root of the problem was instrumental, wildly different source counts being obtained at Sydney (Mills Cross; essentially filled aperture) and Cambridge (interferometer). In an enviable paper written at the heart of the storm, Scheuer (1957) analysed the statistics of the source counts and showed that the Cambridge results were seriously affected by confusion. Because of the wide beam of the interferometer, many radio sources were contributing to each peak in the record; these had erroneously been interpreted as discrete sources.

EXAMPLE To show the pronounced effect of confusion, in Fig. 7.17 we show a simulation of a one-dimensional scan of sources obeying a Euclidean source count $N(f) \propto f^{-5/2}$. The beam is a simple Gaussian and there is, on average, one source per beam. (The source count has to be truncated at the faint end to avoid infinities, of course.) Even in this relatively benign case we see that the apparent source count is altered. A simple count of the peaks in the record gives a maximum-likelihood slope for the source count of -1.8 with standard deviation 0.3 (Section 6.1), very different from the true value. In the case of an interferometer, the presence of sidelobes biases the faint counts to much steeper than true values; the apparent cosmological evolution this implies was the subject of the original controversy.

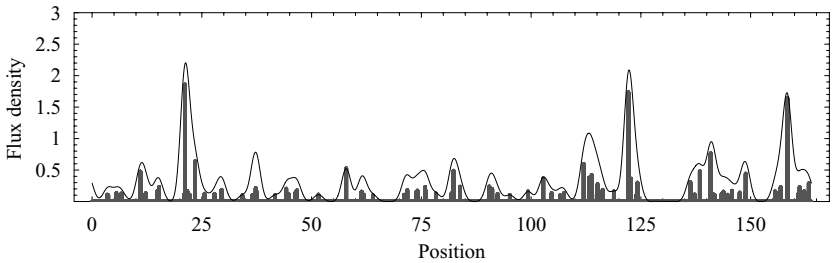

Fig. 7.17. A confusion simulation at a level of one source per beam area. The input sources are shown as vertical lines, with the solid line representing the response when observed (convolved) with a Gaussian beam.

The technique developed by Scheuer is known to astronomers as '$p(D)$', or 'probability of Deflection'. The word 'deflection' refers to the deflections of the needle of a chart recorder and is now hallowed by long usage. However the $p(D)$ technique has been used in radio (Wall & Cooke 1975), X-ray (Scheuer 1974), infrared (Jenkins & Reid 1991) and Lyman-α (Webb et al. 1992) data analysis. The method derives the probability distribution of measurements in terms of the underlying source count, which may be recovered by a model-fitting process. Its benefit is that information is obtained from sources which are much too faint to be 'detected' as individuals.

Full details of $p(D)$ are given in the papers of Scheuer (1957), Scheuer (1974) and Condon (1974). However, the steps in the derivation of the distribution are interesting and we outline them here.

Consider a one-dimensional case, for simplicity. A source of brightness f is observed with a beam, or point-spread function, denoted $\Omega(x)$. Here x is the distance (in angle, wavelength or whatever) from where our instrument is pointed. We measure an intensity

$$s(x) = f\Omega(x).$$

If the sources have a source count $N(f)$, so that the number of sources of intensity near f per beam is

$$\int N(f)\Omega(x)\,\mathrm{d}x$$

then the observed source count, for just one source in the beam at a time, is the result of a calculation involving conditional probability. From this we obtain $p_1(s)$, the probability of an intensity s resulting from just one source somewhere in the beam. Of course, a given deflection D could arise from many sources adding together in the beam. Therefore we need not just p_1 but p_2, p_3, ... If the sources are randomly distributed we expect their numbers to follow a Poisson distribution and then

$$p(D) = \sum_{k=1}^{\infty} p_k(s)\frac{\mu^k}{k!}\,\mathrm{e}^{-\mu}$$

in which μ is the mean number of sources per beam.

To do this summation we need $p_k(s)$; this is the probability distribution of an intensity s which is the sum of k intensities drawn from the distribution p_1. In Section 3.3.3 we showed that the probability of a sum was given by the autocorrelation of the distribution of the terms of the sum, assuming them to be identically distributed. This means that there is a simple relationship between the Fourier transforms:

$$P_k(\omega) = P_1(\omega)^k.$$

Here upper case denotes a Fourier transform and ω is the Fourier variable.

Putting all this together, we get Scheuer's result for the Fourier transform of the $p(D)$ distribution

$$P(\omega) = \exp(R(\omega) - R(0)) \tag{7.18}$$

in which

$$r(s) = \int N\left(\frac{s}{\Omega(x)}\right)\frac{\mathrm{d}x}{\Omega(x)} \tag{7.19}$$

contains the source count N. R is the Fourier transform of r.

Analytic solutions are available for $\tilde{r}(\omega)$ when $N(f)$ is a power law (Condon 1974), but the inverse transform to get $p(D)$ has to be done numerically. In real life we often need to take account of differential measurement techniques in which measurements from two positions are subtracted to avoid baseline errors (Wall & Cooke 1975; Wall *et al.* 1982). In addition the ideal $p(D)$ is always convolved with a noise distribution. All of this needs to be included in the modelling process which recovers the parameters of $N(f)$. The derivation of source counts from $p(D)$ is another technique in which population characteristics are derived from observations of discrete objects or features without forming an object list or catalogue.

EXAMPLE Wall & Cooke (1975) applied the $p(D)$ technique for filled-aperture telescopes to extend the 2.7-GHz radio source counts to much fainter levels than could be achieved by identifying individual sources; their results are shown in Fig. 7.18. A more sophisticated version of the technique was subsequently used at 5 GHz (Wall *et al.* 1982), and data from this experiment are shown in the minimum-χ^2 model-fitting example of Fig. 6.6. The technique continues to be used to extend source counts (for example, Windhorst *et al.* 1993), and the counts from deeper survey observations carried through subsequently have invariably shown agreement with the $p(D)$ estimates.

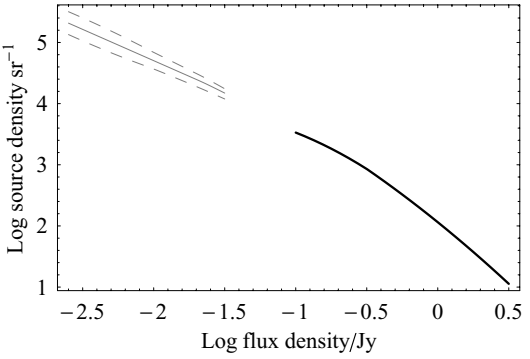

Fig. 7.18. The 2.7-GHz counts from Wall & Cooke (1975): the darker line is derived from ordinary source counts with error bars not much wider than the line, while the $p(D)$ results are shown in grey, the dashed lines representing one standard deviation of the fitted parameters.

Exercises

In the exercises denoted by (D), datasets are provided on the book's website; or create your own.

7.1 **Source counts and luminosity function.** Derive the relationship between the number count and the luminosity function for a general luminosity function; show that the result takes a simple form for a power-law luminosity function.

7.2 **Noise and source-count slope.** Generate data from a power-law source count and add noise; by a maximum-likelihood fit, investigate the effect of the noise level on the inferred source-count slope. Use the results from Exercise 1 to show the effect of the noise on the luminosity function.

7.3 **Survey completeness and noise.** Make a 1D Gaussian signal plus noise plus baseline, fit a profile, and verify completeness versus signal-to-noise ratio. Do the same for an empty field.

7.4 **Reliability and completeness.** Calculate the relationship between reliability and completeness for an exponential noise distribution. This shows the effect of wide wings on the noise distribution. Compare with the result for a Gaussian.

7.5 $V_{\max}$ **method (D).** Simulate a flux-limited sample of galaxies by populating a large volume of space with galaxies drawn from a Schechter distribution. (The cumulative form of the Schechter distribution is rather complicated so you may prefer to use a power law.) Apply the $V_{\max}$ method and see if you can recover the input distribution. Check the simple $\sqrt{N}$ error bars against repeated runs of the simulation.

7.6 **Error estimates (D).** Adapt the simulation of Exercise 5 to produce bootstrap error estimates. Compare these with $\sqrt{N}$ and Monte Carlo estimates, especially for the case of few objects per bin.

7.7 **Luminosity–distance 'correlation' (D).** Adapt the simulation of Exercise 5 to the case for which each galaxy has two independent luminosities assigned to it (at different wavelengths, say). Check that these luminosities show a bogus correlation unless upper limits are included in the analysis. Adapt the simulation to produce intrinsically correlated luminosities and show that the Kendall test can detect these correlations.

7.8 **Parameter error estimates.** Use the X-ray and radio data from Avni *et al.*, as given in the example in the text, to work out the mean spectral index in their survey. Using their likelihood function as a starting point, work out error bounds on the mean, using a likelihood ratio. You will need to use a Lagrange multiplier in the maximization of the likelihood.

7.9 **Source counts from confusion (D).** In a confusion-limited survey where there are potentially several sources per beam, the apparent source count can be very different from the true one. On the assumption that sources can lie anywhere in the beam and are not clustered, derive the result for the source count

$$r(s) = \int N\left(\frac{s}{\Omega(x)}\right)\frac{\mathrm{d}x}{\Omega(x)}$$

as given in Section 7.6.

8

Sequential data – 1D statistics

> The stock market is an excellent economic forecaster. It has predicted six of the last three recessions.
>
> *(Paul Samuelson)*

In contrast to previous chapters, we now consider data transformation, how to transform data in order to produce better statistics, either to extract signal or to enhance signal.

There are many observations consisting of sequential data, such as intensity as a function of position as a radio telescope is scanned across the sky or as signal varies across a row on a CCD detector, single-slit spectra, time-measurements of intensity (or any other property). What sort of issues might concern us?

(i) baseline detection and/or assessment, so that signal on this baseline can be analysed;
(ii) signal detection, identification for example of a spectral line or source in sequential data for which the noise may be comparable in magnitude to the signal;
(iii) filtering to improve signal-to-noise ratio;
(iv) quantifying the noise;
(v) period-finding; searching the data for periodicities;
(vi) trend-finding; can we predict the future behaviour of subsequent data?
(vii) correlation of time series to find correlated signal between antenna pairs or to find spectral lines;
(viii) modelling; many astronomical systems give us our data convolved with some more-or-less known instrumental function, and we need to take this into account to get back to the true data.

The distinctive aspect of these types of analysis is that the feature of interest only emerges after a transformation. Take filtering as a simple example; after smoothing, we are able easily to see the feature of interest in a previously noisy spectrum. But what now? Further modelling is suggested after examining the cleaned-up data, and ideally this will be done following the Bayesian methods of Chapter 6. In this case, the smoothing may only be used in the exploratory stage of the analysis.

Alternatively, the transformation may be an integral part of the final analysis. If we were looking for periodicity in a dataset, the Fourier transform would be an obvious first step, following by model fitting to the peaks so revealed. In this case, the statistical properties of the transform are very important to the modelling step.

In this chapter we discuss by means of examples the statistical and computational techniques employed. We refer to sequential data as 'scans' – they are in many cases, but the sampling may be in the frequency/wavelength domain (spectra), in the time domain (time series), or in the spatial domain (true scans).

The computational aspects alone would justify a large textbook, and we will only give the briefest of outlines; correspondingly, statistical detail here is thinner than in other chapters. Instead, we concentrate on general advice on the statistical issues involved. An excellent detailed guide at a graduate level is Bendat & Piersol (1971).

8.1 Data transformations, the Karhunen–Loeve transform, and others

We are concerned here with expansions in orthogonal functions, a method most familiar from the Fourier series. Moving from one presentation of the data to another may have advantages; noise may be isolated, or features of importance emphasized. Such transformations have a close affinity with principal component analysis; the main features can be extracted from a baffling jumble of data. However, what we extract depends entirely on the basis set we use. How to use data transformations is a craft, with experience playing a large part as guide.

We start with a scan $f(t)$; t is some kind of sequential or ordered index, time, space, or wavelength perhaps. Invariably f is sampled at discrete intervals, and so our data are a finite set $\{f(t_1), f(t_2), \ldots\}$. From a statistical point of view, this set will be described by some sort of

multivariate distribution function; to make much progress, we hope it will be Gaussian, in which case the covariance matrix of the f's will be a sufficient description.

We start out by ignoring the (vital) differences between finite-length scans, sampled at discrete intervals, and introduce the ideas with an idealized case. In certain (mathematical) circumstances, a long scan $f(t)$ may be represented by

$$f(t) = \int_{-\infty}^{\infty} F(\omega)\mathcal{B}(t,\omega)\,\mathrm{d}\omega \tag{8.1}$$

in which the basis functions are $\mathcal{B}$ and the expansion coefficients are F. For finite lengths of data, we have instead

$$f(t) = \sum_i F_{\omega_i}\mathcal{B}(t,\omega_i), \tag{8.2}$$

in which the variable ω changes from continuous to discrete. To be useful, we need transformations which can be reversed; in these cases we get equations of the form

$$F_{\omega_j} = \sum_i f_{t_i}\mathcal{B}'(t_i,\omega) \tag{8.3}$$

with sampling at discrete values of t, and with some simple relationship between $\mathcal{B}$ and $\mathcal{B}'$. If $\mathcal{B}$ is the exponential function, we have the familiar Fourier transforms and series.

Before we specialize to the Fourier case, we should use this notation to indicate a way of constructing transformations other than the dominant Fourier transforms. If our scan f is a random variable, then the coefficients F are random too, and will have different values for each of the (discrete) values of ω, labelled ω_1, ω_2, ...

The covariance matrix of the coefficients

$$C_{\mathrm{F}} = \begin{bmatrix} E[F_{\omega_1}F_{\omega_1}] & E[F_{\omega_1}F_{\omega_2}] & \cdots \\ E[F_{\omega_2}F_{\omega_1}] & E[F_{\omega_2}F_{\omega_2}] & \cdots \\ \vdots & \vdots & \ddots \end{bmatrix} \tag{8.4}$$

tells us everything we need to know about F, provided that the statistics are Gaussian; the components of F are then described by a multivariate Gaussian. It turns out that a basis set which gives a diagonal C is very efficient at capturing the variance in the data, and then the data variation is compressed as much as possible into the smallest number of coefficients F_ω. Clearly this has advantages for reducing the volume

of the data, and may also be useful in isolating noise in some of the coefficients. Requiring that C_{F} be diagonal leads quite directly to the Karhunen–Loeve equation (Papoulis & Unnikrishna Pillai 2002) which, for our discrete case, is an eigenvalue problem:

$$R\vec{\mathcal{B}} = \lambda\vec{\mathcal{B}}. \tag{8.5}$$

The matrix R is closely related to the autocorrelation function which we will encounter soon, and is

$$R_{ij} = E[\, f_n f_{n+(i-j)}\,]. \tag{8.6}$$

(In this equation, we are assuming for simplicity that f has been reduced to zero mean value; we are also assuming that f is stationary, which means that R_{ij} does not depend on the index n.) R is evidently just the covariance matrix of the original data components $f(t_i)$.

If we have a reasonable model for the statistics of our data, we can construct R and solve the Karhunen–Loeve equations. Now the reason for introducing this approach: the eigenvectors $\vec{\mathcal{B}}$ will be discretized basis functions, the $\mathcal{B}_\omega$ introduced earlier. Depending on the structure of the data, they may indeed be the familiar sines and cosines of Fourier analysis; but other, quite ordinary looking assumptions, will yield different basis functions. Fourier analysis is therefore not unique, and if we are interested in data compression we may well want to construct tailor-made functions that do a better job.

Apart from the systematic Karhunen–Loeve method, we may try basis functions from the abundant menagerie of mathematical physics. The many special functions arising in the solution of standard partial differential equations generally have suitable orthogonality conditions, and in some problems may happen to provide just the behaviour needed. An example is the set of Chebyshev polynomials, which when used as a finite series to approximate a function will minimize the maximum error. See Andrews (1985) for further information on special functions.

Wavelets represent another possible source of suitable basis functions. We introduce these briefly later in this chapter; at this stage we need only note that this is yet another way of transforming data, which may work well for the particular problem to hand.

By now it will be apparent that choosing a basis set, and using it, is a modelling problem. The more we know about our data, the better the choice we will make, although we may also need specific mathematical properties that go with certain choices. There is therefore the possibility

of a thoroughgoing Bayesian approach; we assert equation (8.2), and with knowledge of the statistics of f, deduce the posterior multivariate distribution of the components F. This, as always, is The Answer; we may propagate uncertainties in a rigorous way through to the final results we infer from the transformation (equation 8.2). The limitations, again, are the usual ones: the computational burden, which may be prohibitive, and the lack of useful prior information. If it is possible to be Bayesian, then a conceptually simpler analysis is possible than classical approaches we now describe.

8.2 Fourier analysis

The Fourier transform however, remains king amongst the data transforms, and there are numerous reasons for this. Perhaps the most weighty is a simple practical one – the existence of the fast Fourier transform (FFT), perhaps the most-used algorithm on the planet. We will encounter the FFT later in this chapter.

Many if not most physical processes at both macro- and micro-levels involve oscillation and frequency: orbits of galaxies, stars or planets, atomic transitions at particular frequencies, spatial frequencies on the sky as measured by correlated output from pairs of telescopes. It is natural to examine the frequencies composing data streams; the amplitudes of these frequencies may be the answer (as in the case of detection of a spectral line), or they may be adjusted to find the answer (as in digital filtering).

In astronomy as in many physical sciences there is frequent need to measure signal from a data series. In measuring a specific attribute of this signal, such as redshift, the power of Fourier analysis has long been recognized (e.g. Sargent et al. 1977; Tonry & Davis 1979). Solutions to many questions posed of the data lie in taking the one-dimensional scan to pieces in a Fourier analysis.

Fourier theory (e.g. Bracewell 1999, and note the simple treatment in the monograph by James 1995) indicates that any continuous function may be represented as the sum of sines and cosines, i.e.

$$f(t) = \int_{-\infty}^{+\infty} F(\omega)\ \mathrm{e}^{-\mathrm{i}\omega t}\mathrm{d}t \tag{8.7}$$

where the function F representing the phased amplitudes of the sinusoidal components of f is known as the Fourier transform (FT).

Fourier transforms have a number of enormously important mathematical properties, and these carry over (with some caveats, described in Bracewell 1999 and Bendat & Piersol 1971) to the real life of finite-length, discrete transforms, the province of the FFT.

- The FT of a sine wave is a delta function in the frequency domain. This is why we use the FT, or its relatives, to look for periodicities in data.
- The FT of $f \otimes g$, the cross-correlation or convolution of functions f and g, is $F \times G$. Many instruments produce data which result from a convolution with a stable instrumental function: for example linewidths in spectra are convolutions of intrinsic line shapes with velocity dispersion functions.
- The transform of $f(t+\tau)$ is just the transform of f, times a simple exponential $\mathrm{e}^{-\mathrm{i}\omega\tau}$. Use of this shift theorem has measured many redshifts.
- The Wiener–Khinchine theorem states that the power spectrum $|F(\omega)|^2$ and the autocorrelation function $\int f(\tau)f(t+\tau)\,\mathrm{d}\tau$ are Fourier pairs. The autocorrelation function, as noted earlier, is very closely related to the covariance matrix and hence is a fundamental statistical quantity. Its relationship to the power spectrum is the basis of every digital spectrometer.
- Closely related is Parseval's theorem; this relates the variance of f, and the variance in the mean of f, to the power spectrum. We give the details later; this theorem is very useful in cases where we have correlated noise, especially the prevalent and pernicious '$1/f$' noise.
- The FT of a Gaussian is another Gaussian. Given the prevalence of Gaussians in every walk of astronomical and statistical life, this is a very convenient result.

Most astronomy deals with uniformly sampled functions, spectra at wavelength intervals, the output of a receiver/bolometer sampled at fixed time intervals for example. In contrast, time-varying phenomena such as observations of variable stars or quasars require techniques for dealing with irregular sampling and gappy data.

The discrete Fourier transform (DFT) has a number of special features. If the function is sampled N times at uniform intervals Δt in the spatial (observed) frame, the total length in the t-direction is $L = \Delta t \times (N-1)$, and the result is the continuous function multiplied by the 'comb' function, producing a function $f'(t)$ which (with the interval in spatial

frequency as $\Delta\nu = 2\pi/\Delta t$) may be represented (e.g. Gaskill 1978) either as a sum of sines and cosines

$$f'(t) = A_n \Sigma \sin(n\Delta\nu) + B_n \Sigma \cos(n\Delta\nu)\,; \tag{8.8}$$

or as a cosine series

$$f'(t) = A'_n \Sigma \cos(n\Delta\nu + \Phi'_n) \tag{8.9}$$

where the amplitudes A'_n and phases ϕ'_n are given by

$$A'_n = \sqrt{A^2{}_n + B^2{}_n}, \quad \phi'_n = \arctan\left(\frac{A_n}{B_n}\right). \tag{8.10}$$

In the latter formulation, obtaining the DFT produces – by virtue of the 2π cyclic nature of sine and cosine – a 'Fourier-transform plane' for $f'(t)$ which shows the amplitudes mirror-imaged about zero frequency, with a sampling in spatial frequency at intervals of $2\pi/[\Delta t(N-1)]$ and a repetition of the pattern at intervals of $2\pi/\Delta t$.

There are five criteria for successful discrete sampling.

(1) The Nyquist criterion or Nyquist limit guarantees that there is no information at spatial frequencies above $\pi/\Delta t$. (Consider the silly case of a signal which is a spatial sine wave of wavelength $2\Delta t$: sampling at intervals of Δt finds points of identical amplitude and thus does not carry information on amplitude or phase of this spatial frequency.) Thus the sampling interval Δt sets the highest spatial frequency $2\pi/\Delta t$ which can be present; if higher frequencies are present in the data, this sampling rate loses them.

(2) At the same time, the sampling theorem (Wittaker 1915; Shannon 1949) indicates that any bandwidth-limited function can be specified exactly by regularly sampled values provided that the sample interval does not exceed a critical length (which corresponds approximately to half the FWHM resolution), i.e. for an instrumental half-width B, $f'(t) \rightarrow f(t)$ if $\Delta t \leq B/2$. In practice any physical system is indeed band-pass limited (although noise added by the subsequent detector is not necessarily so), and therefore with adequate sampling interval, the signal may be fully recovered.

(3) To avoid any ambiguity – aliasing – in the reconstruction of the scan from its DFT, the sampling interval must be small enough for the amplitude coefficients of components at frequencies as high as $\pi/\Delta t$ to be effectively zero. If $A'_n \geq 0$ for components

of frequency this high, the positive high-frequency tail of the repeating $A'(\nu)$ tangles up with the negative tail of the symmetric function repeating about $\nu = 2\pi/\Delta t$ to produce an indeterminate transform.

(4) The sampling span or scan length must be long enough. The lowest frequencies which harmonic analysis can delineate are at $2\pi/(N\Delta t)$. Such low-frequency spatial components may be real as in the case of a stellar spectrum, or may be instrumental in origin as for sky scans with a single-beam radio telescope. In either case, to have any chance of distinguishing the signal from these low-frequency features, the scan length must exceed the width of single resolved features by a factor preferably ≥ 10. This issue of the 'contaminant' low frequencies is considered below.

(5) The integration time per sample must be long enough so that the signal is not lost in the noise.

In practice most data satisfy these properties. By design, sampling is frequent enough to maintain resolution, to obtain spatial frequencies beyond those present in signal, and to avoid aliasing. By design we take spectra or scans over ranges substantially greater than the width of the features. But despite experiment design, the Universe may not oblige with enough photons to satisfy (5), while our instruments or sky + object circumstance may require some analysis to eliminate (4).

8.2.1 The fast Fourier transform

The FFT, discovered by Cooley & Tukey (1965), is a clever algorithm which does the transform of N points in a time proportional to $N \log N$, rather than the N^2 timing of a brute-force implementation. It has a number of quirks, amongst which are its typical arrangement of its output data, and its normalization – see, for example, Bendat & Piersol (1971), Bracewell (1999), or Press et al. (1992) for details. Although its discovery defined a generation of signal processing, the algorithm was apparently known to Gauss – even before Fourier had discovered his series (Bracewell 1986).

8.3 Statistical properties of Fourier transforms

For data assessment or model fitting in the Fourier domain, we need to know the probability distribution of the Fourier components and their

derived properties. There are detailed discussions of these matters in Bendat & Piersol (1971).

For the comparatively simple case where the 'data' f are pure Gaussian noise, of known covariance C_f, there are analytical results for the Fourier components, as well as for the power spectrum and the auto- and cross-correlation functions. We will focus on the practical case of the uniformly spaced DFT, as implemented by a standard fast transform. As usual, we assume that f is of zero mean; also that we have just one set of data. Our best estimate $\hat{F}$ is just provided by equation (8.2), applied to the single set of data we have.

The real and imaginary components of each component $\hat{F}_{\omega_i}$ are then independent Gaussian random variables, and each component is uncorrelated with the others; so the covariance matrix C_{F} is diagonal. However this is a very specific result, and depends on doing the discrete transform on data sampled at uniform intervals, returning exactly as many components as there are measured data points. Non-uniform sampling, or embedding the data in zeros to sample the transform more finely, will result in correlations between the components.

A useful result is the following, a version of Parseval's theorem: an estimate of the variance σ^2 in our data $f(t_1), f(t_2), \ldots$ is just the integral of the estimated power spectrum. For a DFT estimate,

$$\hat{\sigma}^2 = \sum_i |\hat{F}_{\omega_i}|^2. \tag{8.11}$$

A related and equally useful result is the variance in the estimated mean of f:

$$\mathrm{Var}[\hat{\mu}] = |\hat{F}_0|^2. \tag{8.12}$$

For both relations, one of several possible scaling factors has to be divided out of the answer depending on the FFT implementation. Invariably we do not know the value of the power spectrum at zero (it will have been artificially set to zero to avoid ringing problems with DFTs) but we can extrapolate from values of ω where it is known. This is a very useful check in cases where we have correlated noise in the data, and the simple $1/\sqrt{N}$ rule for the error in a mean will not apply. We discuss this point later in the context of $1/f$ noise.

The components of the estimated power spectrum $|\hat{F}_{\omega_i}|^2$, in the simple case, will be distributed like

$$\chi^2 |F_{\omega_i}|^2$$

with two degrees of freedom in χ^2.

This leads to a surprising and important result: since this distribution does not depend on the number of observations $f(t_1), f(t_2), \ldots$ it follows that the DFT method of estimating the power spectrum is inconsistent; the signal-to-noise on the components is unity and does not improve, no matter how much data we have. The reason is simple; longer scans give finer sampling of the transform, degrading the signal-to-noise at the same rate as the greater quantity of data tries to improve things for us. To improve the signal-to-noise we have to average components together, effectively smoothing the power spectrum. This leads to bias errors, for example where sharp peaks in the spectrum will be reduced in amplitude by smoothing. We might try to split the data up into shorter sections, and average the estimated spectra from the short sections, but then the same bias problem will resurface because of the reduced spectral resolution that we will get from shorter scans. In fact the only satisfactory solution is to take more data, and average power spectra at full resolution.

We also notice from this analysis that the distribution function, for the power spectrum components, depends on the 'true' spectrum $|F_{\omega_i}|^2$, usually what we are seeking.

The same problem surfaces in the case of the autocorrelation or cross-correlation functions; before we can do the error analysis, we need the answer we are looking for, because the true value of these functions enters into the distribution function of the estimates. Worse, the discrete values of the correlations, such as we might obtain via a DFT, are highly correlated amongst themselves. This means that the error level in a correlation function is difficult to represent and we certainly cannot use simple techniques like χ^2 to assign confidence levels to fitted parameters. A typical example of a parameter derived from a correlation function might be the relative velocity between two objects, as determined from the peak in the cross-correlation of their spectra. Simulation is really the only practical way to derive the probability distribution of the measured position of the peak.

Why do we have these perverse difficulties in estimating power spectra? The Wiener–Khinchine theorem tells us that if we know the power spectrum, we know the autocorrelation function, and that means we know the covariance matrix which defines our data f. In other words, estimating a power spectrum is closely allied to estimating a probability distribution function; and here it is familiar that we have a trade-off between signal-to-noise and bias. Regarding the distribution as a

histogram, we can have either large bins (good signal-to-noise but bias) or narrow bins (the opposite).

A common use of power spectra is the estimation of some instrumental response function. If we have input test data $f(t)$ and output data g, in many cases

$$g(t) = f(t) \otimes h(t) \tag{8.13}$$

meaning that the instrument introduces a convolution with some response function h. In the Fourier domain we then have

$$G(\omega) = F(\omega)H(\omega). \tag{8.14}$$

A prominent example of this technique in astronomy is the 'Fourier quotient', a method which measures velocity dispersion and redshift simultaneously in galaxy spectra (Sargent et al. 1977). Here the input g is a suitable template stellar spectrum, and the output f is the target galaxy spectrum; a model function, containing a velocity dispersion parameter and an overall redshift, is then fitted to G/F. While successful, it turns out that high signal-to-noise is required in the template spectrum, essentially because of the appearance of its transform in the numerator of the expression for the response function:

$$\hat{H}(\omega) = \frac{\hat{G}(\omega)}{\hat{F}(\omega)}. \tag{8.15}$$

At values of ω where $F(\omega) \simeq 0$, very wide noise excursions occur in $\hat{H}$. The method has to be used with some care. The quotient may have a non-Gaussian distribution so that goodness-of-fit tests with χ^2 could be very misleading.

To estimate the error distribution of $\hat{H}$ we need the coherence function

$$\gamma^2(\omega) = \frac{|F(\omega)G(\omega)^*|^2}{|F(\omega)|^2\,|G(\omega)^*|^2} \tag{8.16}$$

and we will usually have to insert estimates of all the transforms. Evidently, if there is no noise in the system, we will have $H = G/F$ and $\gamma = 1$. The estimate of H follows an F distribution

$$|\hat{H}(\omega) - H(\omega)|^2 \leq \frac{2}{n-2}\mathcal{F}_{2,n-2}(1-\hat{\gamma}^2(\omega))\frac{|\hat{G}(\omega)|^2}{|\hat{F}(\omega)|^2} \tag{8.17}$$

in which $\mathcal{F}_{2,n-2}$ is an F distributed random variable with 2 and $n-2$ degrees of freedom. n is twice the number of separate spectral components

that are averaged to yield a single estimate; a single component has two degrees of freedom, because of its independent real and imaginary parts. We can see that this is an approximate result for a confidence interval on $\hat{H}$, as the right-hand side contains estimates (and may even contain guesses).

The occurrence of the term $n-2$ is of importance. It is telling us that we must smooth the power spectrum before we can use it, since the F distribution is not defined if one of its degrees of freedom is zero. We can also see that errors will be very large at frequencies where the spectrum of the template approaches zero.

The discussion so far has only considered the data $f(t_1), f(t_2), \ldots$ to be random; we have not yet added in the effects of systematic signal. In many astronomical problems, matters are a great deal more complicated. The input distribution functions are unlikely to be Gaussian. The central limit theorem will quickly give a Gaussian core to a distribution in many cases, but the wings can dominate the results of statistical testing and will converge slowly to Gaussian form (Newman, Haynes & Terzian 1992). Most astronomical data are not random; there is a signal, which does not average to zero. Paper-and-pencil statistical analysis is very involved. An example is in Jenkins (1987).

In many cases, the only method for obtaining reliable errors on derived parameters is a detailed Monte Carlo simulation, which can build in all the messy aspects of a real observation. The analytical results we have sketched do, however, provide valuable guidance; they tell us that power spectra will have problems of consistency and bias, that correlation functions will contain highly correlated errors, and that we will probably have to sacrifice detail in estimates of response functions. These are pointers to the behaviour of Fourier analysis in real cases and indicate that we do need a reasonable idea of basic statistical properties – the power spectrum or correlation function – to make much progress in understanding our data when it is in the form of scans.

8.4 Filtering

Filtering is an area in which analysis by Fourier or other techniques can play a significant role. Before we begin filtering data, however, as usual we need to ask what we want to achieve.

Filtering always has two related aims: to reduce noise, and to compress data. Suppose for concreteness we have a noisy spectrum, containing an emission line. Using a suitable filter (even a running mean will help)

will usually reduce noise and make the line more prominent. What does this achieve? If we want to measure some parameter of the line, say the height, filtering the data may make it possible to make a measurement 'off the screen' with a cursor. This kind of real-time, fast data assessment is a very common application of filtering; it also provides attractive data for publication. However any more detailed analysis will involve fitting a model, perhaps a Gaussian, to the line. The usefulness of filtering is less obvious here. A fitting procedure requires starting estimates (line location, width, baseline level) to converge to the correct answer; the filtered data will provide these. Also, fitting algorithms will be stabilized, and prevented from converging to wrong answers, if they operate on less noisy data. Unfortunately, since filtering alters the statistical properties of data, the analysis of the fitting procedure will probably be more complicated. However it is worth remembering that any instrument will filter data to some extent and this effect may have to be modelled anyway.

8.4.1 Low-pass filters

Fourier filtering to improve the signal-to-noise ratio can be highly effective. The reason is simple: if noise is shot noise or photon noise, it is 'white', and its spectrum extends flat to the limit given by the sampling theorem. Provided that the signal is not governed by high-frequency components, tapering off the amplitudes of high frequencies is a winning strategy. (Recall that the FT of a Gaussian is another Gaussian, so that if instrumental response or line shape is anything like Gaussian, there should be little high-frequency information.)

It is simple to manipulate the transform of the data to cut out the higher frequencies. An example is shown in Fig. 8.1. Whatever we do by chopping out or reducing the amplitudes at high frequencies is bound to decrease the noise, but it must decrease some signal as well, particularly if signal is on small scales in the spatial domain. Chopping is generally a poor idea, however; square filters produce ringing in the signal, so that a tapering to high frequencies is desirable. There are many techniques for assessing how to taper. In fact it is readily shown both by minimizing the variances and by conditional probabilities that an estimate of the optimum filter is given by

$$F(f) = \frac{|S(f)|^2}{|S(f)|^2 + |N(f)|^2} \tag{8.18}$$

where S is the signal spectrum and N the noise spectrum.

This is Wiener filtering. It requires us to assess or model the FT of both noise and signal. This is difficult of course if signal and noise have similar power spectra, but then, no filter can cope under these circumstances.

EXAMPLE The example of Fig. 8.1 shows a Gaussian sitting on a flat baseline, with Gaussian random noise added, as in a photon-starved observation. It is possible to guess at models in the Fourier plane for the

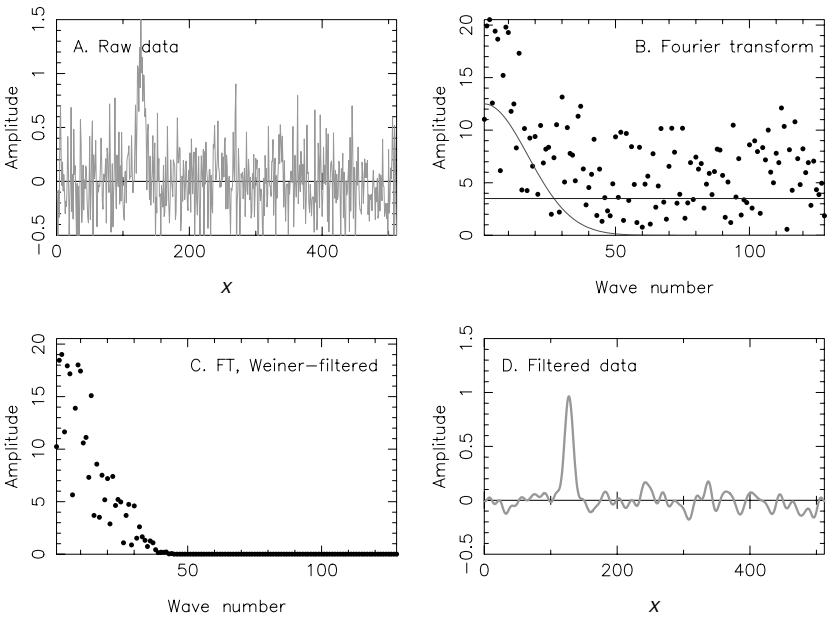

Fig. 8.1. A Wiener filter in action. The raw data of A is a Gaussian sitting on a flat baseline, with random Gaussian noise added. The DFT in B shows the signal and noise components, modelled by the Gaussian and horizontal curves, respectively. The Wiener filter, applied in the frequency domain, produces the DFT of C, and the reverse transform produces the greatly improved signal/noise of D.

noise and signal components. Here we knew how to model this; we knew the FT of both signal and noise, and as a result, drawing in the separate components in the Fourier plane, making our Wiener filter according to equation (8.18) is straightforward, as the diagram shows; and the result indicates its efficacy. However we generally do know properties of the signal, from, e.g. instrumental response, so that the signal FT

model can usually be constructed. Even without this the robustness of the procedure is impressive. Take away the eye-guiding lines from panel B of Fig. 8.1 and approximate signal (with a triangle say) and noise with a straight line at some level, and discover that very similar results to Panel D are obtainable with minimum a priori knowledge.

There are many types of numerical filters available, most of them having been developed for real-time applications. Such filters are causal, that is, they only use 'past' data. One of the most famous causal filters is the Kalman filter. Most astronomical applications are not so restricted and the main problem is probably the range of choice. Lyons (1997) is a good source of ideas for filtering.

The Savitsky–Golay filters are worth a separate mention; these operate by fitting low-order polynomials to a sliding window on the data. Unlike the filters which operate via the Fourier domain, a Savitsky–Golay filter need not inevitably broaden features in order to reduce noise. On the other hand, their effect on data and signal-to-noise is not as simply visualized. Press et al. (1992) show a nice set of examples of Savitsky–Golay filters in action, together with code for an algorithm.

8.4.2 High-pass filters

A more difficult issue is presented in removing unwanted low-frequency components from observations. This is usually known as fitting baselines in the trade, and it is carried out to assess the continuum in spectra, for example. There is a long tradition of doing this by eye; but least squares fits of polynomials, heavy smoothing and spline fitting are common ways of proceeding. The difficulty is inevitably the signal. Those parts of the scan with signal must be removed from consideration in order to place the continuum; and with irregular and a-priori unknown spacing of the signal, development of a formal technique becomes prejudicial or perhaps impossible. Moreover, smoothing techniques and polynomial fits make initial assumptions which the data may not justify. For some types of signal such as emission or absorption lines with extreme breadth of wings, the behaviour of the continuum in the regions masked by signal is critical in measurement of that signal.

There are formal tools to apply. For example Bayesian spectral analysis (e.g. Sivia & Carlile 1992) is appropriate when some specific prior

knowledge such as linewidth is available. However the analysis must be repeated for each different prior-knowledge set and for each different question posed of the data. The situation frequently arising in spectral analysis is one in which the prior knowledge is the somewhat unquantifiable recognition of which parts of the spectrum are signal-free, while very general parameter sets (e.g. line shape, linewidth, line flux, equivalent width, centroid position) may be required from the measurements.

Unlike low-pass filtering in which separation of signal and noise in the Fourier plane is relatively straightforward, the problem here is the tangle between the two. Gaussians helped us in the former because their transforms drain away so fast at high frequencies. But at low frequencies? This is where Gaussians have most of their harmonic signal. We have to be cleverer than just staring at the transform.

A simple technique, *minimum-component filtering*, based on DFT and harmonic analysis is described by Wall (1997). The key to success is forming a baseline array by patching across regions in which signal is clearly present. The sequence to follow is this:

(i) *patching*: forming a 'baseline array' from the original data series by patching across regions of the scan where signal is evident;
(ii) *end matching*: subtracting from this baseline array a first approximation to the patched scan, obtained with a linear fit, a very low-order polynomial or a heavy-smoothing estimate;
(iii) *Fourier transforming* the resultant baseline array;
(iv) *removal of the high frequencies* by applying a heavy-tapered multiplicative filter in the Fourier plane to taper off the higher-frequency Fourier amplitudes;
(v) *reverse transforming* using these minimum remaining components; and
(vi) *gradient restoration*, by adding back in the first approximation (step (ii)) to the baseline.

We are concerned with datasets of the type represented by the optical spectra in Fig. 8.2. The appearance is dominated by substantial emission or absorption lines covering more than 30 per cent of the length of the spectrum; moreover in the second case, the continuum slope is severe.

In addition to its objectivity and its ease of application, a further advantage of the technique is that an analysis of the error introduced by the baseline assessment can be carried out (Wall 1997), an aspect

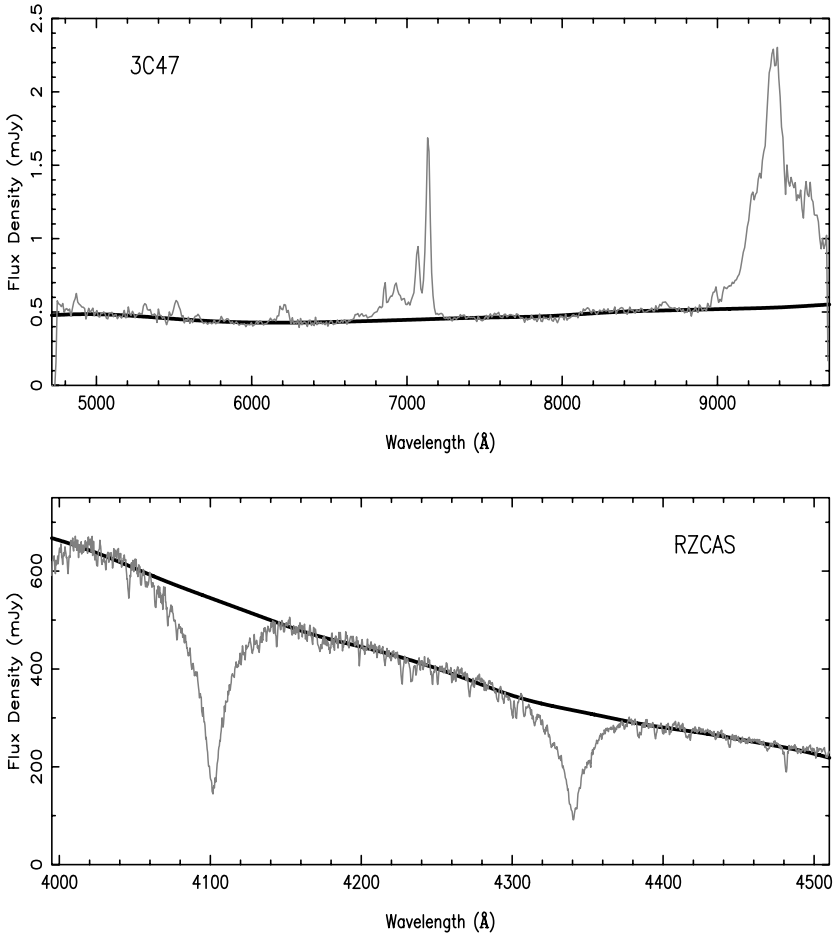

Fig. 8.2. Top a spectrum of 3C47 obtained by Laing *et al.* (1994) with the Faint Object Spectrograph of the William Herschel Telescope, La Palma. The redshift is 0.345; broad lines of the hydrogen Balmer series can be seen, together with narrow lines of [OIII]. Bottom: a spectrum of the a star RZ Cas (Maxted *et al.* 1994). The continuum obtained with the minimum-component technique is shown as the black line superposed on the original data.

seriously lacking in virtually all baseline assessment (and therefore line-intensity estimation) in the literature. The following points emerge:

- Except for very narrow signal, the baseline difference, i.e. the error in continuum assessment due to minimum-component fitting, will not dominate errors.

- The patch width is critical. For noisy situations in which the signal is relatively weak, it is imperative to choose a patch width as narrow as possible. Gaussians cut off quickly and for the weaker signals, patch and flux measurement should be confined to $\pm 3\sigma_s$, as determined from an accurate an estimate of σ_s (the instrumental standard deviation). For strong signals, the patch should be significantly broader.
- For even the weakest apparent signals it is crucial to patch over the region in which signal measurement is carried out. This may seem self-evident, but when signal is weak it is tempting to fit a minimum-component continuum with minimal patching because the fit looks satisfactory. This is not so; the error introduced in the flux measurement may far exceed the noise uncertainty.

The analysis indicates how rapidly errors in equivalent widths can escalate with continua which are curved, i.e. which have low-frequency components present, even when the procedures for continuum assessment and signal measurement are well defined. When yet broader wings are involved, the errors produced will be substantially greater. The analysis goes some way to explaining why estimates of line fluxes in the literature can differ by a factor of two, even with reasonable signal-to-noise.

It should be noted that 'removal' of continuum is high-pass filtering, removal of the lowest frequencies. In conjunction with low-pass filtering, a band-pass filter has been generated, one which cuts off towards low frequencies and towards high frequencies.

8.4.3 An integrated approach

We see that analysis of a scan will often involve some kind of baseline-fitting procedure, plus a localized fitting procedure to derive, say, linewidths and positions. The baseline parameters are only required as a step on the way to some final answer and so are classical nuisance parameters.

From a Bayesian point of view, we may be able to formulate the whole problem as a standard model-fitting procedure. From this we will derive joint posterior distributions for line parameters (the interesting ones) $\vec{\lambda}$ and for baseline parameters $\vec{\beta}$. Since the baseline parameters are not required, we can marginalize them out with an integration over $\vec{\beta}$ and its prior. This gives us the distribution of the interesting parameters, with the effects of the uncertainty in the baseline included.

It may be difficult to formulate the baseline problem in such a conceptually clear way; as we have seen, a good deal of judgment may be involved. However in principle each of the human decisions involves a set of parameters. We should be able to formulate a Bayesian estimation procedure for these, and this will have benefits in making the procedure more objective, and reproducible.

Quite often, baselines will be the result of $1/f$ noise (Section 8.8). This results in the sort of large, aimless wanderings that are quite difficult to fit with harmonics. The usual remedy is to fit polynomials to the lowest frequencies. Another possibility, if the baseline statistics (power spectrum or correlation function) are reasonably well known, is to construct the associated Karhunen–Loeve functions. By definition, using these to approximate the baseline will do the best possible job with the smallest number of coefficients.

8.5 Correlating

8.5.1 Redshifts by correlation

We have seen how the shift theorem can be used, in the Fourier quotient method, to measure a redshift. Redshifts are a common and important example of an offset between two scans. As we have seen, there are some disadvantages to the quotient method. Direct cross-correlation between a template and target spectrum will generally yield a peak in the cross-correlation function; a modelling procedure can give redshifts and velocity dispersions (Sargent et al. 1977; Tonry & Davis 1979). This is a successful and widely used technique. The best method for error analysis in this case is direct simulation, because of the highly correlated nature of the errors in a correlation function.

8.5.2 The coherence function

We have met the coherence function briefly before; it is estimated by

$$\hat{\gamma}^2(\omega) = \frac{|\hat{F}(\omega)\hat{G}(\omega)^*|^2}{|\hat{F}(\omega)|^2\,|\hat{G}(\omega)^*|^2}. \tag{8.19}$$

The estimation is done in the usual way for power spectra: either by smoothing the power spectrum, or by averaging several power spectra derived from separate scans. The coherence function is just the correlation coefficient between f and g in frequency space.

The coherence is extremely useful in cases where we have an input f and an output g and we want to find out more about the 'black box' that changes f into g. If the box has a purely linear effect (like many simple physical systems) then $f = g \otimes h$ for some h, and $\gamma = 1$. More usually, of course, we have noise ϵ, not present in the input, so that $g = f \otimes h + \epsilon$. Now, depending on the frequency content of the noise and the input, we will have structure to γ, which will generally be less than 1. Other interesting reasons for $\gamma < 1$ will be that the causal relationship between f and g is non-linear, or that there are extra causal factors in play. These will not be present in the input we know about, and, depending on their frequency content, will lower the coherence.

EXAMPLE Here is a simple example with some simulated data. We have a relationship for our synthetic data

$$g(t) = f \otimes h + \epsilon(t) + b(t)$$

in which f is white Gaussian noise, h is a Gaussian filter, ϵ is noise added at the output side of the box, and b is an unrelated low-frequency effect (obtained in this case by vigorous recursive filtering of Gaussian white noise). In Fig. 8.3 we see the input data, the output (somewhat filtered, apparently) and the extraneous low-frequency effect. Finally the coherence function between f and g shows a loss of coherence at low frequencies (because of the extraneous effect, which is not present in the input) and the loss at high frequencies (due to noise, which is likewise not present in the input). At intermediate frequencies there is a region relatively unaffected by noise, in which our box must be a linear system, where only the input f affects the output.

This means that we can model our box as a simple convolution of input data with an instrumental function and we also suspect that there must be an extra causal effect at low frequencies. This yields the region of the spectrum which carries the uncontaminated part of the signal that we can model simply.

8.5.3 The correlator

At radio frequencies, frequency resolution is achieved with a correlator. The principle is simple, but illustrates some useful statistical points.

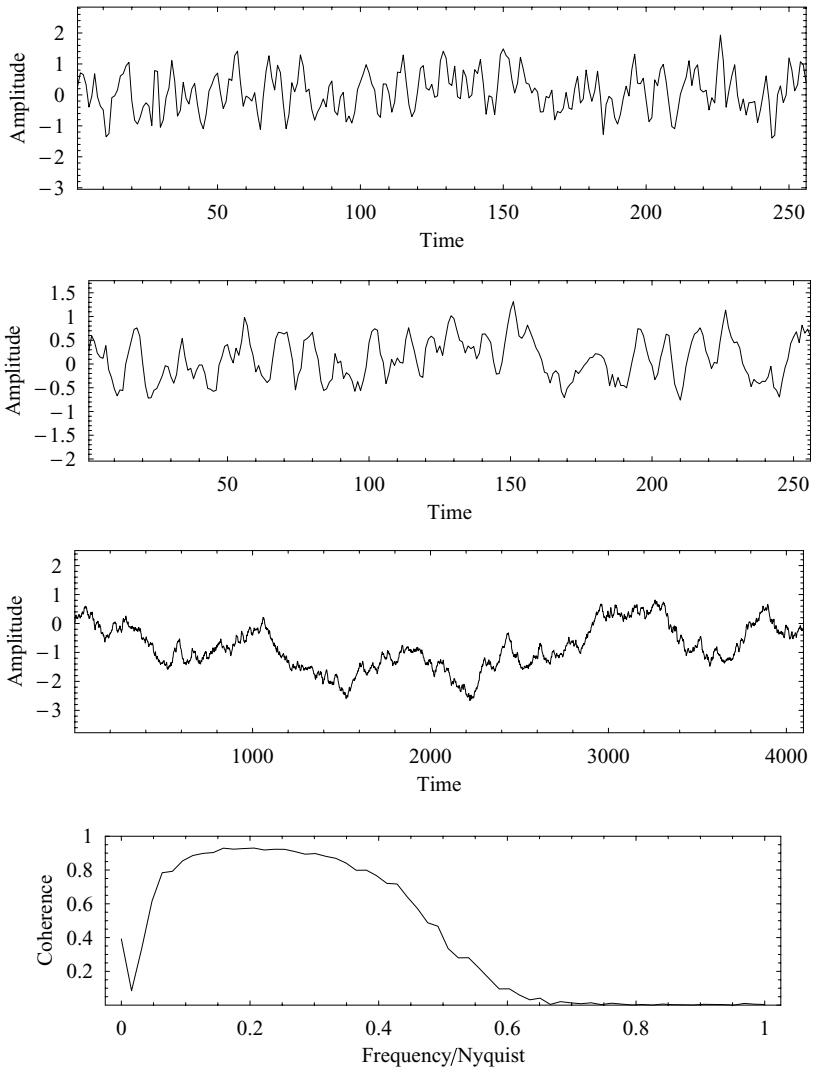

Fig. 8.3. From top to bottom; the input to the system f; the input, convolved, with a small amount of noise added $f \otimes h + \epsilon(t)$, the extraneous effect $b(t)$, and at bottom, the coherence between f and g.

We start with an incoming stream of sampled data from a receiver, our usual $f_{t_1}, f_{t_2}, \ldots$. A correlator will take (relatively) short chunks of these data and form the autocorrelation function (a fast operation in hardware). The separate estimates of the correlation function are

averaged, and finally Fourier transformed to obtain (via the Wiener–Khinchine theorem) the power spectrum of the data.

Why does this work? Physically, our stream of data will consist of a multitude of wave packets, each corresponding to emission from a single atom or molecule. Thus the time series of, say, electric field amplitudes will be

$$f(t) = \sum_i w(t + \phi_i) \tag{8.20}$$

where ϕ_i are the random phases of each wave packet w. The Fourier transform is

$$F(\omega) = W(\omega) \sum_i \exp(\mathrm{i}\omega\phi_i) \tag{8.21}$$

and the average power spectrum will be

$$|W(\omega)|^2 E\left[\left|\sum_i \exp(\mathrm{i}\omega\phi_i)\right|^2\right]. \tag{8.22}$$

The exponential term, being an average of positive quantities, will converge to some positive value as more and more chunks of data are averaged, even although the phases are random. By contrast, the average Fourier transform will contain the term

$$E\left[\sum_i \exp(\mathrm{i}\omega\phi_i)\right]$$

which will converge to zero.

EXAMPLE A simulation of this procedure is shown in Fig. 8.4.

A further key feature of the digital correlator is the quantization – astonishingly little sensitivity is lost by digitizing at the one-bit level, simply recording whether f is positive or negative. This speeds up data rates and reduces numbers of operations; for a given processing speed far higher resolution is possible, dependent on the number of channels in the shift-and-add register of the correlator, rather than the sampling speed of the data (as long as this is high enough to exceed the Nyquist criterion).

Given the correlation coefficient ρ between the data values f_{t_i} and f_{t_j}, we know that the joint distribution function is a bivariate Gaussian. It is then a fairly simple marginalization calculation (see Chapter 8 of

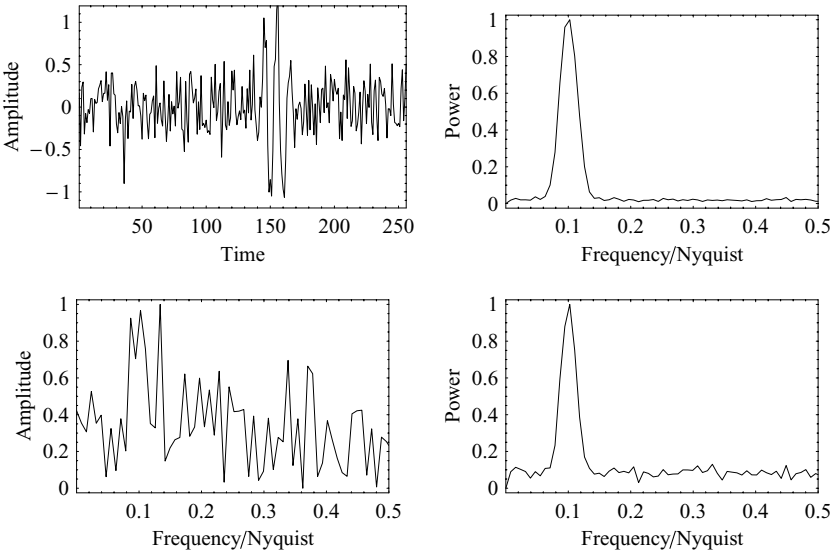

Fig. 8.4. Top left: part of the input data stream for the correlator, consisting of 64 wave packets, randomly located, with on average one per 128 units of time. Top right: the average power spectrum from forming the autocorrelation function over 128 time units. Bottom left: the average Fourier transform of one-bit quantized data, again from 128-long chunks. Bottom right: the power spectrum derived from the quantized data with the same averaging.

Thompson, Moran & Swenson, Jr. 2001) to compute the probabilities of quantized values like

$$\text{prob}(f_{t_i} > 0 \,\text{and}\, f_{t_j} > 0)$$

and so on; from this, the quantized correlation coefficient ρ_{q} can be calculated. The result is beautifully simple:

$$\rho_{\text{q}} = \frac{2}{\pi} \sin^{-1} \rho \tag{8.23}$$

and is called the van Vleck equation. It has the distinction of having been a classified result during World War II.

8.6 Unevenly sampled data

8.6.1 The periodogram

There are numerous astronomical applications in which scan data are unevenly sampled. The classical case is the search for periodicities in

light curves of objects of variable luminosity. Much as we might like to sample the light output evenly, daytime, bad weather, or telescope time-assignment committees may intervene. The problem has thus received extensive treatment and most modern analysis is based on the Lomb–Scargle method (Lomb 1976; Scargle 1982). A concise description of the Lomb normalized periodogram is given by Press et al. (1992). The key feature is that the method weights the data on a 'per point' basis rather than on a 'per time interval' basis as does the FFT; an even better feature is that the null hypothesis can be tested rigorously. Scargle (1982) showed that in testing for a peak at frequency ω, the height of the peak at this point, $Y(\omega)$, has an exponential probability distribution with unit mean; the probability that $Y(\omega)$ lies between $Y(>O)$ and $Y + \mathrm{d}Y$ is $\exp(-Y)\mathrm{d}Y$. If n independent frequencies are considered, then the probability that none gives a value $> Y$ is $(1 - \mathrm{e}^{-Y})^n$. Thus

$$P(>Y) = 1 - (1 - \mathrm{e}^{-Y})^n \tag{8.24}$$

represents the significance level of any peak $Y(\omega)$. But this raises the embarrassing question of what is n – how many independent frequencies have we looked at? In the limit of interest, when significance levels are $\ll 1$, $P(>Y) = n\mathrm{e}^{-Y}$, scaling linearly with the estimate of n, so that n need not be estimated precisely. Monte Carlo experiments (Horne & Baliunas 1986) show that if N is the number of scattered but approximately evenly spaced data points which oversample the range up to the Nyquist frequency, then $n \sim N$, and there is little difference for n between random spacing and equal spacing. When a larger frequency range is sampled, n increases proportionally.

These points raise two further questions. Firstly, how can we sample frequencies beyond the Nyquist? Recall that the Nyquist frequency refers to equally spaced data with sampling interval Δt; it is $2\pi/\Delta t$. With randomly spaced data evenly distributed through the sampling series, an equivalent (but non-physical) Nyquist frequency can be obtained from the mean time interval. However, the fundamental limitation of equally spaced data is avoided by unequally spaced data. It is possible to sample well above the equivalent Nyquist frequency without significant aliasing; see the example of Fig. 8.5. A similar situation arises with 2D and 3D statistics of space distribution, as discussed in Chapter 9; clustering on scales much smaller than the mean separation between objects can be sampled if the objects are randomly sampled.

EXAMPLE Operation of the Lomb–Scargle periodogram, with continuous and gappy data, is implemented in the Numerical Recipes routines of Press et al. (1992). An example is shown in Fig. 8.5.

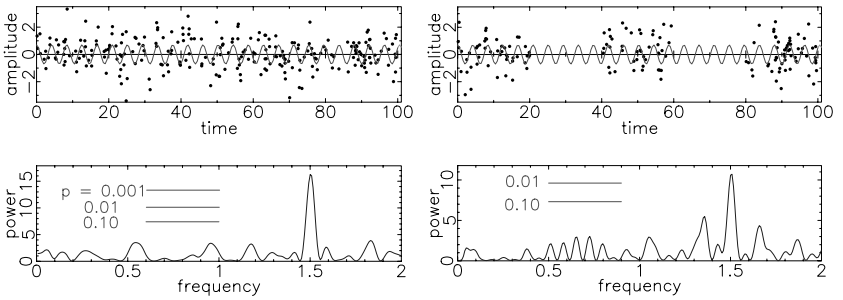

Fig. 8.5. The Lomb–Scargle periodogram method. Left: randomly spaced data generated by a sine wave of amplitude 0.7 and period 1.5 with noise of unit variance superposed. Right: data taken at the same mean interval but with serious gaps to approximate night-to-night sampling of optical astronomy.

For the continuous data, even with the sine wave shown as a guide, the eye cannot pick out the periodicity. The Lomb periodogram has no doubts whatsoever. For the gappy data, note the reduced significance of the peak in the periodogram, as well as the serious aliasing resulting from windowing the data as shown.

Secondly, what about the more usual situation for astronomers with data seriously clumped, e.g. into night-time observations? Monte Carlo to the rescue again: generate synthetic datasets by holding fixed the number of data points and their sampled locations, generate synthetic sets of Gaussian noise using these, find the largest values of $Y(\omega)$, and find the best fit of the distribution in equation (7.7) to determine n. The example of Fig. 8.5 shows what happens with gappy data – aliasing becomes serious. With data of even poorer quality than that shown in Fig. 8.5 (no problem for astronomers), choosing the right peak amongst these is the issue; and here, folding techniques come into play. In the simplest instance, observing a similar data stream some time later will enable a choice to be made; only one of the frequencies will have the right phase to give anything like a reasonable fit.

8.6.2 Times of arrival

A rather different kind of evenly sampled dataset arises in pulsar timing or gamma-ray astronomy. Here we sometimes have rather small numbers of events, times of arrival of pulses or photons. Do these times betray a period?

If we have a period P in mind, we can test as follows. Call the times of arrival $t_1, t_2, \ldots$. Assign a phase to each time by the algorithm

$$\phi_i = 2\pi \,(\text{remainder of } t_i \text{ divided by } P) \tag{8.25}$$

and form the statistic

$$R^2 = \left(\sum_{i=1}^{n} \cos\phi_i\right)^2 + \left(\sum_{i=1}^{n} \sin\phi_i\right)^2 \tag{8.26}$$

and for $n > 10$, $2R^2/n$ is distributed as χ^2 (Table A2.6) with two degrees of freedom.

This is a classical test (the Rayleigh test). If R is large, it is unlikely that the phases are random. This will happen if we have guessed the correct period, so we would then infer (illegally, of course) that the period is indeed P.

We may also wish to determine P, which we would do simply by searching for a value of P that maximizes R. Having determined a parameter from the data, we will lose one degree of freedom from χ^2 in the significance test.

Details of this, and more elaborate tests, are in De Jager, Swanepoel & Raubenheimer (1989).

8.7 Wavelets

One disadvantage of Fourier analysis, and its relatives, is a loss of information about where in a scan things may be happening. Take the spectrum of Fig. 8.1 as an example; the noise level might well be different in the spectral line, but a Fourier filter applies the same degree of smoothing everywhere. This feature is a result of the basis functions, the sines and cosines, being infinite in extent. In fact their infinite extent is the cause of many of the difficulties associated with transforms of finite-length data streams.

In many cases we would like a transform which picks out details of frequency content while preserving information about where in the scan

those particular frequencies are prominent. There are approximate ways of doing this with Fourier transforms, by taking transforms in short windows which slide along the data, but this has obvious disadvantages. `Wavelets` offer a better way.

A wavelet is a short function which, being convolved with the data, gives some frequency (or scale) information at a particular location in the scan. By placing the wavelets at different places in the scan ('translating') and changing their widths ('scaling') it is possible to obtain a frequency decomposition which preserves some location information. Figure 8.6 shows some examples of wavelets in current use; it is worth noting that there are particular mathematical restrictions on what kind of function can be a wavelet. As can be seen from the figure, different wavelets are likely to be sensitive to different things; the asymmetrical wavelet, for example, will be sensitive to local gradients, while the Mexican hat will be good at picking out oscillations.

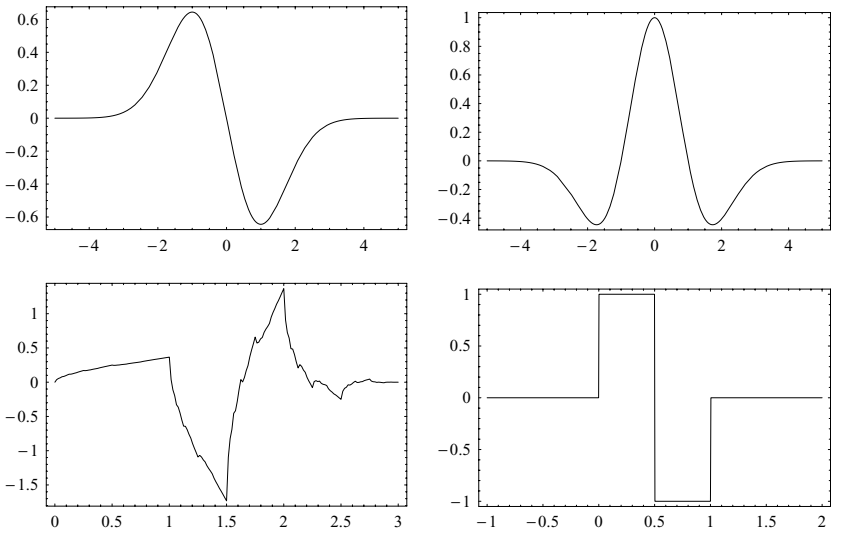

Fig. 8.6. Four possible wavelets; a wavelet decomposition will be in terms of scaled and translated versions of each of these. Top left, asymmetrical; top right, Mexican hat; bottom left, Daubechies (this wavelet is actually a fractal); bottom right, Haar.

Wavelet analysis is a huge and growing area; useful references include Strang (1994), Koornwinder (1993), Bruce, Donoho & Gao (1996) and Daubechies (1992). An implementation of a discrete wavelet transform

is given in Press et al. (1992), along with the usual wise advice. An excellent recent text is Walker (1999).

Much of the attraction of wavelets is that they can give very effective filtering and data compression. A well-known triumph for wavelets was the decision by the FBI to use a wavelet-based technique for the digitization and compression of their fingerprint database. From an astronomical point of view, we often deal with scans where important properties change from place to place; there are noisy regions in a spectrum, for instance, or times when a light curve seems to show quasi-periodicity. Wavelets offer new possibilities in data assessment, and a whole new armoury of filtering techniques, especially those where the filtering may be different in different parts of a scan.

EXAMPLE In Fig. 8.7 we compare wavelet filtering to the Wiener filtering of the example spectrum in Fig. 8.1. We chose to filter with Haar wavelets; others were not as satisfactory. The greyscale plot shows the strength of the various wavelets, as a function of position in the spectrum. The finer-scale wavelets are at the top of the plot. From this plot, dropping the three finest scales of wavelet coefficients is suggested as a suitable simple filter. The result is quite pleasing as noise is markedly reduced without much loss of resolution in the spectral line.

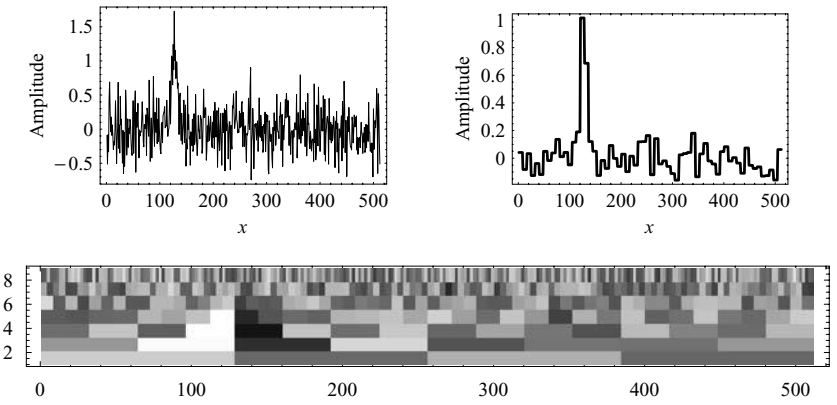

Fig. 8.7. Top left, the original spectrum of Fig. 8.1; top right, the filtered spectrum; bottom, the wavelet coefficients as a function of location and scale.

8.8 Detection difficulties: $1/f$ noise

The bane of the experimenter's life is so-called $1/f$ noise; see the excellent review by Press (1978). It is a major reason why filtering theory, which looks so good in contrived examples (Fig. 8.1) fails to live up to promise; why 2σ results are not results; and why increased integration time fails to produce the expected improvements in signal-to-noise ratio, the simple $1/\sqrt{N}$ improvements we naively expect from averaging N samples.

$1/f$ noise is so called because it has a power spectrum which is inversely proportional to the Fourier variable – frequency, if we are dealing with a time series. Hence the name. It is sometimes called flicker noise, and is a particular case of 'pink' noise of various kinds, in which low frequencies dominate. An even more extreme example is Brownian or random-walk noise. As the name suggests, this arises when successive values of the noise are obtained by adding a random number to the previous value. Random walk noise arises when we integrate a scan; for example, we may integrate a time series of accelerations to deduce the velocity time series.

EXAMPLE Figure 8.8 shows two simulations of low-frequency noise obtained by starting with white noise, multiplying the Fourier transforms by $1/\sqrt{f}$ or $1/f$, and taking the inverse transform of the result.

Despite much theoretical work (it crops up in everything from Beethoven symphonies to traffic flow), it is not known why $1/f$ noise is so common. However, its presence (or the presence of one of its near relatives) is usually the reason why averaging large amounts of data does not produce the improvement expected.

$1/f$ noise has the remarkable property of having infinite variance: the longer you watch it, the larger its excursions become. We can immediately see that this behaviour follows from the fact that the variance on a scan is the integral of its power spectrum. For sampled data of finite length, the variance will depend on the integral of the power spectrum between the Nyquist frequency and the first frequency above zero – this will be $1/L$ if L is the scan length. Thus the variance of sampled $1/f$

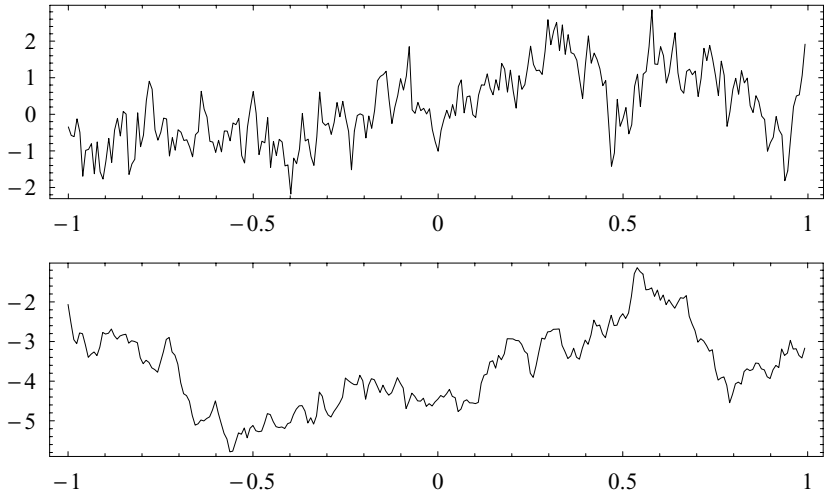

Fig. 8.8. Above: flicker ($1/f$) noise of unit variance. The data are implicitly band-limited by the finite sampling rate. Below: a random walk of unit variance.

noise will be proportional to

$$\int_{1/L}^{f_{\mathrm{nyq}}} \frac{1}{f}\,\mathrm{d}f = \log(Lf_{\mathrm{nyq}}) \tag{8.27}$$

and so will grow logarithmically with scan length. Qualitatively, we see from the simulations in the example that the noise is highly correlated from one sample to the next – we expect that averaging will not work well. In fact it does not work at all for a noise spectrum of $1/f$ or steeper.

Recall from an earlier result (Section 8.3) that the variance on a mean $\hat{\mu}$, derived from a scan f of length L, is

$$\mathrm{var}[\hat{\mu}] = |F(0)|^2/L. \tag{8.28}$$

For white noise, which is uncorrelated for adjacent or successive samples of f, we have $|F(0)|^2 = \sigma^2$, the variance on the scan, and the expected $1/\sqrt{L}$ behaviour follows. If, however, we have $1/f$ noise dominating the power spectrum at low frequencies, the best idea we have of the power spectrum at zero is its value at a frequency $1/L$. Now we see that the variance on the mean is independent of L!

Usually we will have white noise dominating the power spectrum for frequencies greater than some value ω_0, in other words for scans shorter than $1/\omega_0$. As the scans lengthen, however, we will start to uncover the

$1/f$ noise below ω_0. Therefore a general model for the variance on the mean level of a scan of length L will be

$$\mathrm{var}[\hat{\mu}] \simeq \frac{a}{L} + b \tag{8.29}$$

where a and b are parameters which describe the noise levels in white noise and $1/f$ noise. Note the analogy to the discussions of low-pass and high-pass filtering (Section 8.4): dealing with the slowly varying component may be considered as a baseline issue. Of course we must hope that our signal comes at higher frequencies, or it (and our experiment) is lost.

Because the variance diverges for $1/f$ noise, another measure of variation – the Allan variance – is useful. For our scan f it is defined by

$$\sigma_{\mathrm{A}}^2 = \frac{1}{2} E[\,(f_{t_i} - f_{t_{i-1}})^2\,] \tag{8.30}$$

and the differencing of successive samples will help to remove the enormous variance which is carried in long-term drifts. Generalizations can be made by changing the distance between the two samples involved; this is the scale of the Allan variance. There is a fascinating connection between the Allan variance and wavelets: the Allan variance is directly related to the variance in the Haar wavelet coefficient, at the same scale.

Exercises

In the exercises denoted by (D), datasets are provided on the book's website; or create your own.

8.1 **Fourier transform and FFT.** Use a direct numerical integration to do a numerical Fourier transform of an oscillatory function, say a sine wave or a Bessel function. Compare the timings with an off-the-shelf FFT routine, checking how many oscillations you can fit in your region of integration before the FFT accelerates away from the direct method.

8.2 **Wiener filtering and $1/f$ noise (D).** Make some synthetic data along the lines of the example in Fig. 8.1, and make it work with a Wiener filter for uncorrelated Gaussian noise. Now generate some $1/f$ noise. Add this in to the input spectrum, and perform the filtering again, without taking account of the extra low-frequency noise in the form of the Wiener filter. Does the

$1/f$ noise affect (a) the line profile parameters, (b) the baseline parameters?

8.3 **Periodogram (D).** Consider the Lomb–Scargle periodogram method as formulated by Press et al. (1992); use the Numerical Recipes routines to test the following issues.

(a) If we can sample at much above the pseudo-Nyquist rate, how much? Where does this run out? Why in practice can we not realize the sampling at these high frequencies provided by scattered time measurement?

(b) The lines of probability in Fig. 8.5 are roughly correct for the random uniform coverage of the left set of data. For the data on the right, uniformity has been assumed and the probabilities in the diagram are incorrect. Use the Numerical Recipes routine and the Monte Carlo technique outlined to determine how they should be adjusted.

8.4 **Properties of the power spectrum of periodic data.** From the maximum–minimum statistics analysis of Section 3.4:

(a) Find the probability density function equivalent to equation (7.11) for minimum values.

(b) Show that the most likely value of the maximum in the power spectrum of data N long is $\ln N$.

8.5 **Power spectrum of signal + noise.** For a signal containing a deterministic signal S and Gaussian noise x, show that the noise distribution in each component of the power spectrum is in general a non-trivial combination of χ^2 and Gaussian noise.

8.6 $1/f$ **noise.** Harmonic analysis (sampling, Fourier transforming) of Beethoven's symphonies indicates that their power spectra follow the $1/f$ law to a good approximation. Consider why this should be so. See Press (1978) for a few hints.

8.7 **Filtering and mean values.** Take your favourite implementation of the FFT, and form the power spectrum of a scan consisting entirely of uncorrelated Gaussian noise. Integrate the power spectrum. Is the answer the variance of the input data? If not, why not? Now convolve the data with your favourite (normalized) filter. From the zero frequency of the power spectrum, what is the variance in the mean? Does it change if you change the width of the filter? Explain.

8.8 **Baselines (D).** Fit a Fourier baseline interactively to a spectrum containing a moderately obvious but contaminated line. Now, separately, fit a Gaussian to the line and give your best estimate of the uncertainty in the total flux in the line. Compare this with a complete Bayesian analysis, fitting the same number of harmonics plus Gaussian *ab initio*, and then marginalizing out the baseline parameters.

9

Surface distribution – 2D statistics

An examination of the distribution of the numbers of galaxies recorded on photographic plates shows that it does not conform to the Poisson law and indicates the presence of a factor causing 'contagion'.

(Neyman, Scott & Shane 1953)

The distribution of objects on the celestial sphere, or on an imaged patch of this sphere, has ever been a major preoccupation of astronomers. Avoiding here the science of image processing, the province of thousands of books and papers, we consider some of the common statistical approaches used to quantify sky distributions in order to permit contact with theory. Before we turn to the adopted statistical weaponry of galaxy distribution, we discuss some general statistics applicable to the spherical surface.

9.1 Statistics on a spherical surface

Abstractly, the distribution of objects on the celestial sphere is simply the distribution of directions of a set of unit vectors. In this respect, other three-dimensional spaces may be of interest, like the Poincaré sphere with unit vectors indicating the state of polarization of radiation.

This is a thriving subfield of statistics and there is an excellent handbook (Fisher, Lewis & Embleton 1987). Much of the motivation comes from geophysical topics (orientation of palaeomagnetism, for instance) but many other 'spaces' are of interest. The emphasis is on statistical modelling and a variety of distributions is available. The Fisher distribution, one of the most popular, plays a similar role in spherical statistics to that played by the Gaussian in ordinary statistics.

In astronomy we usually need different distributions, often those resulting from well-defined physical processes. The distribution of galaxies within clusters is an example. These distributions remain poorly understood and so the emphasis is on non-parametric methods. Here spherical statistics do have some useful techniques to offer.

If we have a set of directions, defined by n unit vectors $\{X_i, Y_i, Z_i\}$ in a Cartesian system, we can ask if they could have been drawn from a uniform distribution over a sphere. Rayleigh's test forms the statistic

$$\mathcal{R}^2 = \left(\sum_{i=1}^{n} X_i\right)^2 + \left(\sum_{i=1}^{n} Y_i\right)^2 + \left(\sum_{i=1}^{n} Z_i\right)^2 \tag{9.1}$$

and for $n > 10$, $3\mathcal{R}^2/n$ is distributed as χ^2 (Table A2.6) with three degrees of freedom. For $n < 25$, use the tables of critical values of $\mathcal{R}$ in Table A2.13.

If the directions are not uniformly distributed, a useful estimate of their direction is the spherical median. This statistic (call it $\vec{M}_\mathrm{s} = \{\lambda, \mu, \nu\}$) minimizes the sum of the arc lengths from each datum. The sum

$$\sum \arccos(X_i\lambda + Y_i\mu + Z_i\nu)$$

usually has to be minimized numerically to solve for the parameters λ, μ and ν. There is an asymptotic distribution available for $\vec{M}_\mathrm{s}$, but its calculation is rather complicated. A bootstrap (Section 6.6) will give prob(M_s) directly.

The next question might well be 'is the true median some particular direction?'. Constructing a suitable test statistic in this case requires some spherical trigonometry. We assume that the distribution of directions is rotationally symmetric about the assumed median direction. The angular offset of each datum from the calculated spherical median M_s is an angle Φ_i, the longitude with respect to M_s. Calculating Φ_i is best done by making use of rotation matrices, as described in textbooks on spherical trigonometry, e.g. Murray (1983). An estimate of the scatter in the data is given by the matrix

$$\Sigma = \begin{bmatrix} \sigma_{11} & \sigma_{12} \\ \sigma_{21} & \sigma_{22} \end{bmatrix} \tag{9.2}$$

with

$$\sigma_{11} = 1 + \frac{1}{n}\sum_i \cos 2\Phi_i, \quad \sigma_{22} = 1 - \frac{1}{n}\sum_i \cos 2\Phi_i$$

and

$$\begin{aligned}\sigma_{21} &= \sigma_{12} \\ &= \frac{1}{n}\sum_i \sin 2\Phi_i.\end{aligned}$$

The angular offsets from the hypothesized median are Φ_i^0 and the total offset is described by a vector

$$\vec{V} = \frac{1}{\sqrt{n}}\begin{bmatrix}\sum_{i=1}^n \cos\Phi_i^0 \\ \sum_{i=1}^n \sin\Phi_i^0\end{bmatrix}. \tag{9.3}$$

The test statistic is then given by the matrix product

$$\chi^2 = \vec{V}^T\Sigma^{-1}\vec{V} \tag{9.4}$$

and, as the name suggests, this will be asymptotically distributed ($n > 25$) as χ^2 (with two degrees of freedom). As usual, for astronomically sized samples, a bootstrap is a good way of deriving the distribution and doing the test.

Spherical statistics can also deal with 'undirected lines' or axes. These are familiar in astronomy; the normals to orbital planes are an example. Simple, useful analyses can be made that test against the null hypothesis of a uniform distribution on the sphere, in favour of the bipolar hypothesis of clustering of axis orientation. These tests are a variant of principal component analysis (Section 4.5) and depend on the orientation matrix

$$T = \frac{1}{n}\begin{bmatrix}\sum_i X_i^2 & \sum_i X_iY_i & \sum_i X_iZ_i \\ \sum_i X_iY_i & \sum_i Y_i^2 & \sum_i Y_iZ_i \\ \sum_i X_iZ_i & \sum_i Y_iZ_i & \sum_i Z_i^2\end{bmatrix} \tag{9.5}$$

defined for n unit vectors $\{X_i, Y_i, Z_i\}$. The test for the existence of a principal axis depends simply on the largest eigenvalue E_3; critical values are given in Table A2.14.

This test depends on the principal axis being unspecified. If the principal axis is specified, with direction cosines $\{\lambda, \mu, \nu\}$, then the test statistic is

$$\mathcal{S} = \frac{1}{n}\sum_i (X_i\lambda + Y_i\mu + Z_i\nu)^2. \tag{9.6}$$

For smallish $n < 100$, use Table A2.15 to determine the critical values;

otherwise,

$$\mathcal{S}' = \sqrt{n}(S - 1/3)\sqrt{4/45} \tag{9.7}$$

is approximately normally distributed with zero mean and unit variance.

The direction of the principal axis is given by the eigenvector of the orientation matrix that corresponds to E_3, the largest eigenvalue. This eigenvector has an asymptotic bivariate Gaussian distribution. For small samples $n < 25$ its distribution can be obtained by a bootstrap, and in fact this may be more convenient even for quite large samples.

Tests are also available to check if distributions are rotationally symmetric, and to test for a specific value of the principal axis; see Fisher, Lewis & Embleton (1987) for details.

Various other familiar statistical questions can be asked about samples of directions or axes. If we have r distinct samples, we may ask if they all have the same median direction. To answer this, we compute the medians for the pooled sample and for each of the r samples. The ith datum in the jth sample datum has an offset Φ^0_{ij} from the pooled median and an offset Φ'_{ij} from the jth median. For sample j we define, by analogy with a previously used quantity,

$$\Sigma_j = \begin{bmatrix} \sigma^{(j)}_{11} & \sigma^{(j)}_{12} \\ \sigma^{(j)}_{21} & \sigma^{(j)}_{22} \end{bmatrix} \tag{9.8}$$

with

$$\sigma^{(j)}_{11} = 1 + \frac{1}{n_j}\sum_i \cos 2\Phi'_{ij}, \quad \sigma^{(j)}_{22} = 1 - \frac{1}{n_j}\sum_i \cos 2\Phi'_{ij}$$

and

$$\begin{aligned} \sigma^{(j)}_{21} &= \sigma^{(j)}_{12} \\ &= \frac{1}{n_j}\sum_i \sin 2\Phi'_{ij}. \end{aligned}$$

We also use

$$\vec{U}_j = \frac{1}{\sqrt{n_j}} \begin{bmatrix} \sum_i \cos \Phi^0_{ij} \\ \sum_i \sin \Phi^0_{ij} \end{bmatrix}. \tag{9.9}$$

The test statistic is then given by a sum of matrix products

$$\chi^2 = \sum_{j=1}^{r} \vec{U}_j^T \Sigma_j^{-1} \vec{U}_j \tag{9.10}$$

which, for $n_j > 25$, is distributed as chi-square with $2r - 2$ degrees of freedom. This test is non-parametric but does require large samples, as is the case for other non-parametric comparison tests discussed by Fisher, Lewis & Embleton 1987.

There are some useful methods available for correlation and regression. If we have sets of measurements of directions (or unit vectors) in pairs, of the form $(\vec{X}_i, \vec{X'}_i)$, we may wonder if the directions $\vec{X}_i$ and $\vec{X'}_i$ are correlated. The components of these data are $\{X_i, Y_i, Z_i\}$ and $\{X'_i, Y'_i, Z'_i\}$. To test, we form a matrix generalization of the product-moment coefficient, as follows:

$$S_{xx'} = \begin{vmatrix} \sum_i X_i X'_i & \sum_i Y_i X'_i & \sum_i Z_i X'_i \\ \sum_i X_i Y'_i & \sum_i Y_i Y'_i & \sum_i Z_i Y'_i \\ \sum_i X_i Z'_i & \sum_i Y_i Z'_i & \sum_i Z_i Z'_i \end{vmatrix} \tag{9.11}$$

and S_{xx} and $S_{x'x'}$ are defined analogously. Here we are using the determinant ($|\ldots|$) of the matrices to convert the problem into one involving only scalars. The generalization of the correlation coefficient is

$$\rho = \frac{S_{xx'}}{\sqrt{S_{xx} S_{x'x'}}}. \tag{9.12}$$

To test against the hypothesis of no correlation, the distribution of ρ can be estimated by the permutation method described in Section 4.2. If $\vec{X}_i$ and $\vec{X}'_i$ are uncorrelated, it should not matter which $\vec{X}_i$ goes with which $\vec{X}'_i$. Hence, by working through a large number of random permutations of the data, and sampling many possible pairings, we can estimate the distribution of ρ.

If ρ is appreciably different from zero, we cannot use this procedure. The best we can do is to use a jackknife (Section 6.6) to estimate the standard deviation of ρ. We may then perform a test on the assumption that ρ is Normally distributed. This is a large-sample approximation. For a small sample, we could use a bootstrap.

A similar test can be done for undirected lines, or axes. Here we do not use determinants but the data are combined in similar matrices; for example

$$\Sigma_{xx'} = \begin{bmatrix} \sum_i X_i X'_i & \sum_i Y_i X'_i & \sum_i Z_i X'_i \\ \sum_i X_i Y'_i & \sum_i Y_i Y'_i & \sum_i Z_i Y'_i \\ \sum_i X_i Z'_i & \sum_i Y_i Z'_i & \sum_i Z_i Z'_i \end{bmatrix} \tag{9.13}$$

with Σ_{xx} and $\Sigma_{x'x'}$ similarly defined. A 'correlation coefficient' is then

defined to be

$$\rho = \frac{1}{3}\,\mathrm{Trace}\,(\Sigma_{xx}^{-1}\Sigma_{xx'}\Sigma_{x'x'}^{-1}\Sigma_{xx'}), \tag{9.14}$$

the Trace being the sum of the diagonal elements of the matrix.

To test against the no-correlation hypothesis, we again use a permutation method, or (for large samples, $n > 25$) we compare $3n\rho$ with chi-square with nine degrees of freedom. If a correlation is apparent, we may again use the jackknife or bootstrap to assess significance.

This test leads to a quite general one, where $\vec{X}_i$ is a vector (direction) or axis and $\vec{X'}_i$ is a general object with p components. If $p = 1$, for instance, this might be a problem to do with the correlation of directions with time. We proceed in exactly the same way, noting that $\Sigma_{xx'}$ will be a $3 \times p$ matrix, while Σ_{xx} will be 3×3 and $\Sigma_{x'x'}$ will be $p \times p$. The test statistic is

$$\rho = \frac{1}{q}\,\mathrm{Trace}\,(\Sigma_{xx}^{-1}\Sigma_{xx'}\Sigma_{x'x'}^{-1}\Sigma_{xx'}), \tag{9.15}$$

where q is the smaller of 3 and p. The same remarks apply as before, except that in the large-sample case we compare $qn\rho$ with chi-square for $3p$ degrees of freedom.

As a final example of correlation analysis, suppose we were interested in the coherence or serial association in a time series of directions or axes. So our data might be ordered in time and we want to know if $\vec{X}_i$ is correlated with, say, $\vec{X}_{i-1}$. A test statistic is

$$\mathcal{C} = \sum_{i=2}^{n} X_i X_{i-1} + Y_i Y_{i-1} + Z_i Z_{i-1} \tag{9.16}$$

and its distribution, on the assumption of no correlation, can be estimated by permutations. There is a large-sample approximation but it is rather laborious to calculate.

Finally, note that regression between unit vectors and linear variables, or other unit vectors, can be handled by generalizations of least squares; see Fisher, Lewis & Embleton (1987) for details.

9.2 Sky representation: projection and contouring

We frequently have a sample and we want to draw a sky representation of it. It is essential to use an equal-area projection to preserve density of points; we know from schooldays how unsuitable the Mercator projection

is in this respect. There are many such projections available, and the following three are perhaps the best known in astronomy, given right ascension α and declination δ:

(i) The Aitoff projection:

$$x = 2\phi\frac{\cos\delta\sin(\alpha/2)}{\sin\phi}, \quad y = \phi\frac{\sin\delta}{\sin\phi} \tag{9.17}$$

where $\phi = \cos^{-1}(\cos\delta\cos\frac{\alpha}{2})$.

(ii) The Hammer–Aitoff projection:

$$x = 2\phi\cos\delta\sin\frac{\alpha}{2}, \quad y = \phi\sin\delta, \tag{9.18}$$

where $\phi = \sqrt{2}/\sqrt{1+\cos\delta\cos\frac{\alpha}{2}}$.

(iii) The Sanson–Flamsteed projection:

$$x = \alpha\cos\delta, \quad y = \delta. \tag{9.19}$$

In both the Aitoff and the Hammer–Aitoff projections, with the exception of the equator, the lines of constant declination curl at the extremities; those of the Sanson–Flamsteed projection are straight and horizontal. The latter is also very simple arithmetically but this is offset by the shear and crowded meridians in the polar regions. Take your pick, noting that many more projections are available.

Now suppose we have a set of points $P_1, P_2, \ldots, P_n$ on our projection and we wish to map the density of these points. Computing a weighted average is an appropriate way to do this, and a suitable weighting scheme for a given map point P is

$$W_n(P, P_i) = \frac{C_n}{4\pi n\sinh(C_n)}\exp[C_n\cos(\theta_i)] \tag{9.20}$$

where θ_i is the angular distance between P and the data P_i. The weight thus depends only on the angular distance of points from P. Smoothing is controlled by C_n and varies inversely as C_n; we should choose C_n to increase with n, as the more data we have the less smoothing we need. Contouring from here on is a matter of choosing an appropriate grid or map P, choosing levels or log(levels), and locating a suitable contouring routine, available in most graphics packages.

9.3 The sky distribution of galaxies

The distribution of galaxies on the sky is a mess. There's our ∼20-member Local Group, Andromeda and its gang. There are big clusters

like Coma and Virgo. There are clearly clusters of clusters, filaments of clusters and voids. Moreover different galaxies do this differently; the early types (ellipticals) gregariously dominate rich clusters, with the late types (spirals) ostracized for the most part to life as hermits in socially deprived environments. How to quantify all this? It is imperative to do so if comparison with theory is to be made – essential, as galaxy development, their formation and evolution, is central to modern astrophysics and cosmology. Such quantification has been recognized as vital by the pioneers, from Zwicky through Holmberg, Abell, De Vaucouleurs, Scott and Neyman, and, with most impact on modern times, the detailed work, both analytical and theoretical, by Peebles and co-workers (e.g. Peebles 1980). The current picture – the hierarchical growth of density perturbations in a low-density cold dark matter universe with substantial dark energy density – has fed critically on studies of galaxy distribution on the celestial sphere.

The remainder of this chapter takes a fresh look at 2D statistics quantifying the distribution of objects on the celestial sphere. It considers the commonly used techniques of angular correlation functions, counts in cells, and power-spectrum analysis. In the course of this the relations between the quantities are set out and some limitations of these in describing the distribution are demonstrated. The following notation is used. For brevity, angle brackets indicate ensemble averages, expectation values, denoted elsewhere in the text as $\mathrm{E}[\dots]$, while barred quantities such as $\bar{N}$ indicate averages over the survey areas in question; $\varsigma(\theta, \phi)$ denotes object surface density.

9.4 Two-point angular correlation function $w(\theta)$

The two-point angular correlation function $w(\theta)$ is a simple and intuitive statistic to quantify clustering. Clustering increases the number of close pairs; $w(\theta)$ quantifies this increase as a function of galaxy separation θ. It is the fractional increase relative to a random distribution in the probability δP of finding objects in each of two solid angle elements $\delta\Omega_1$ and $\delta\Omega_2$ separated by angle θ:

$$\delta P = \varsigma^2 \, [\, 1 + w(\theta) \,] \, \delta\Omega_1 \, \delta\Omega_2 \tag{9.21}$$

where ς is the object surface density.

The angular correlation function has many advantages as a clustering statistic. It is easy and quick to measure and its simplicity makes it easy to interpret (so that it can reveal systematic effects in the observational

data). It directly accommodates unusually shaped survey areas with complicated boundaries and internal masked-out regions. Moreover, there is a relatively simple way to relate $w(\theta)$ to spatial clustering via the radial distribution of the objects. Hence $w(\theta)$ is a convenient statistic to provide comparison both between data and theoretical prediction and between different observational datasets.

The angular correlation function $w(\theta)$ is not a complete description of the clustering. Phase information is lost. Two different object density fields can have identical angular correlation functions – see Fig. 9.1. A full field description requires a hierarchy of higher-order correlation functions that are much more difficult to measure and interpret. Moreover $w(\theta)$ is very sensitive to shot noise, and may only be measured accurately at small angles. The error on the measurement of $w(\theta)$ is difficult to compute for small survey areas: edge effects render the simple 'Poisson error' incorrect. Furthermore, $w(\theta)$ suffers from correlated errors between adjacent $\Delta\theta$ bins making assessment of true uncertainty in its determination notoriously difficult (Fig. 6.8). Fitting a parameterized function to it is thus awkward from the point of view of minimization and error determination.

The value of $w(\theta)$ at given θ depends on density fluctuations on `all` angular scales, complicating the interpretation of the angular correlation function. In contrast, the angular power spectrum (Section 9.6) measures fluctuations on a specific angular scale. For example, a single sinusoidal density fluctuation (in one dimension) will have a δ-function angular power spectrum but a broad angular correlation function. Likewise, long-wavelength surface density gradients in the data (due to, for example, calibration problems) will offset the measured $w(\theta)$ on `all` angles (see Section 9.4.3.1).

EXAMPLE Figure 9.1 shows two generated sky distributions, one (upper left) simulating low-contrast galaxy clusters in a regular grid on a random background, the other (upper right) simulating galaxy clusters on a background with large-scale structure in the form of a quadrupole. The first 'sky' consists of a uniform random background of 8500 points, with a further 1500 points in 25 equal clusters of Gaussian width 0.4° placed on a uniform 2° by 2°grid across the area. The second has a background of 10 000 points generated from a power-spectrum representation of the sky with signal in one term only: $\ell = 2$. Another 2000 points

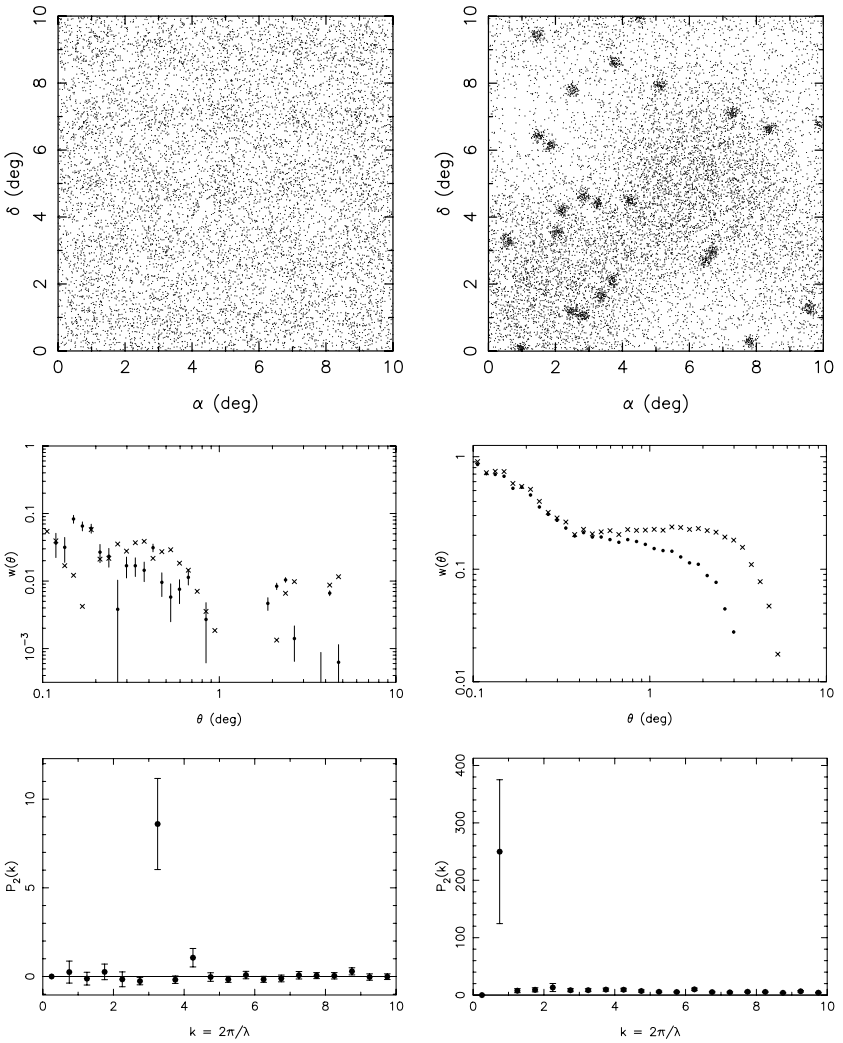

Fig. 9.1. Two sky simulations (see text); left – a uniform 2° grid of 25 low-surface-brightness clusters on a random background, and right – a quadrupole background with 25 randomly placed clusters. Measured $w(\theta)$ and angular power spectra appear below each. The $w(\theta)$ were evaluated with the simple estimator (crosses – equation 9.22) and the Landy–Szalay estimator (dots with error bars – equation 9.25).

were added in 25 equal 'clusters' of Gaussian width 0.1° at random positions. Although the eye struggles to discern any features in the first sky, the two-point correlation function shows a strong signal at small θ describing the clusters themselves, and a resurgent signal at larger separations due to the 2° by 2° grid on which the clusters were placed. Both the quadrupole and the clusters are very evident in the second sky, and the correspondingly stronger $w(\theta)$ again shows two components; the signal at the smallest separations describes the galaxy clusters while the signal on degree scales is due to the dipole. The examples demonstrate the additive property of $w(\theta)$ as well as its ability to 'see' signal on all scales. They also demonstrate how $w(\theta)$ can mask sky information – different scale choices here could easily have resulted in a featureless $w(\theta)$. This is the case for the real sky. We see clusters, superclusters, filaments, and the result of all these scales is the well-known power-law form for $w(\theta)$ out to scales beyond tens of degrees.

The example illustrates the complementary nature of the power-spectrum analysis; it is supremely sensitive to the larger structural features. For the first sky, the angular power spectrum grabs the grid spacing unambiguously, while showing little evidence of signal on the cluster scale. Likewise with the second sky, the quadrupole signal dominates all else, although there is now some significant signal on the cluster scale.

9.4.1 Estimators and errors

In order to estimate $w(\theta)$ from a distribution of n objects, we (a) measure the angular separation θ of all galaxy pairs and (b) bin these separations to form the data-pair count $DD(\theta)$, the number of galaxy separations having lengths θ to $\theta + \mathrm{d}\theta$, and (c) calculate $RR(\theta)$, the corresponding number in each of these bins for a random sky knowing the average surface density of the real sky. (This latter is a simple sum: neglecting edge effects, the expected number of random pairs in the separation bin $\theta \to \theta + \delta\theta$ is $RR(\theta) = \frac{1}{2}\, n\, \varsigma\, 2\pi\theta\, \delta\theta$, where ς is the object surface density.) Hence an estimator for $w(\theta)$ – the fractional enhancement in pairs above random – is

$$w_0(\theta) = \frac{DD(\theta)}{RR(\theta)} - 1, \tag{9.22}$$

and this is $w(\theta)$ in its simplest form.

However, edge effects are important when dealing with a small survey area or with weak clustering. Thus we need to measure the average available bin area around a point ($\approx 2\pi\theta\,\delta\theta$) using Monte Carlo integration, by generating a comparison random distribution of r points over the same survey area. The result of this calculation (Blake 2002) is an improved estimator for $w(\theta)$, the so-called 'natural' estimator:

$$w_1 = \frac{r(r-1)}{n(n-1)}\frac{DD}{RR} - 1. \tag{9.23}$$

This estimator too has its shortcomings, the variance in this case, leading to the development of other estimators for $w(\theta)$ involving the cross-pair separation count between the sets of n data points and r random points. The following have been constructed:

$$w_2 = \frac{2r}{(n-1)}\frac{DD}{DR} - 1 \tag{9.24}$$

$$w_3 = \frac{r(r-1)}{n(n-1)}\frac{DD}{RR} - \frac{(r-1)}{n}\frac{DR}{RR} + 1 \tag{9.25}$$

$$w_4 = \frac{4\,n\,r}{(n-1)(r-1)}\frac{DD \times RR}{(DR)^2} - 1 \tag{9.26}$$

with w_2, w_3 and w_4 known as the Peebles (Davis & Peebles 1983), Landy & Szalay (1993) and Hamilton (1993) estimators.

To reduce statistical fluctuations it is standard practice to use either a small number of very large random sets, or a large number of relatively small random sets, and to average over the random pair counts to obtain $\overline{DR}$ and $\overline{RR}$. Which is better? It is tempting to use a single large random set. But note that the computation time needed to measure the separations between n objects scales as n^2. For a given computation time (an important consideration for large samples), this mitigates against using a few large random datasets and favours the use of a large number of relatively small ones. If the number of random sets is m and the ratio of randoms in each set to the data is $k = r/n$, a reasonable guideline to adopt is $k \sim 1$, $m \gg 1$. With $m \geq 10$, the excess error is ≤ 10 per cent and may be ignored.

The best of the above estimators for $w(\theta)$ is that with the smallest bias and variance in the angular range under investigation.

Excess variance comes about primarily but not exclusively through edge effects, which become more significant with increasing separation (see Exercise 2). Detailed analysis (Landy & Szalay 1993; Hamilton

1993) has quantified the non-Poisson variance and showed that for estimators w_3 and w_4, the non-Poisson terms cancel out and the error in the measurement of $w(\theta)$ is just the Poisson error. Furthermore, estimators w_2 and w_4 show small levels of bias. The Landy–Szalay estimator w_3 is thus the best bet.

It is thus possible to measure $w(\theta)$ with Poisson variance for an individual angular separation bin; but this does not mean that the errors in adjacent separation bins are uncorrelated. They are correlated, simply because a single object appears in many different separation bins through the numerous pairs in which it participates. Edge effects cause further correlation of errors in adjacent separation bins. If there are fewer objects on average near the boundaries, then there are systematically more close pairs in small-angle bins, and the numbers per bin are not independent. These correlations can be significant when assessing the goodness-of-fit of a model x_i to the n data points X_i. The correlations should be incorporated by computing the covariance matrix (Section 4.2 and Press et al. 1992, Chapter 15).

9.4.2 Integral constraint

A point frequently not appreciated about $w(\theta)$ is that positive signal at small angles demands that the function becomes negative at larger separations. The total number of pairs over all bins is fixed at $\frac{1}{2}n(n-1)$; clustering shifts pairs from larger to smaller separations. This gives rise to difficulties, the first being the standard method of fitting the function with a power law. This is secondary to the main problem: if the surveyed area is sufficiently small, $w(\theta)$ appears positive for even the most distant separations sampled. The pair count cannot be enhanced in all separation bins while keeping the total number of pairs constant. The normalization must change, and we can formulate this in terms of an adjustment factor C as follows:

$$< DD(\theta) > = C \times \frac{1}{2} n(n-1)\, \delta G_p \, [\, 1 + w(\theta) \,] \tag{9.27}$$

where δG_p is the equal-area fraction of the surface between θ and $\theta + \delta\theta$. (For a sphere, $\delta G_p = \frac{1}{2}$, satisfying $\int_0^\pi \mathrm{d}G_p = 1$ as it must.) It may be shown (Exercise 3) that if $W = \int w(\theta)\, \mathrm{d}G_p$, then $C = 1/(1+W)$ and for all cases of interest,

$$w(\theta) \approx w(\theta)_{\mathrm{est}} + W, \tag{9.28}$$

i.e. the estimated $w(\theta)$ is in error by a constant offset, which becomes negligible when the survey area becomes large.

9.4.3 Instrumental effects

There are two instrumental effects that have a serious impact on $w(\theta)$: large-scale calibration errors and over-resolution.

9.4.3.1 Calibration errors: surface gradients

Large-scale calibration errors in surveys produce gradients or discontinuities in object surface density. Such calibration problems may result from plate-to-plate calibration errors in a Schmidt-telescope survey or intensity-calibration changes over the area of a radio survey. Changing surface densities will spuriously enhance measured values of $w(\theta)$. This is because the number of close pairs of galaxies in any region depends on the local surface density ($DD \propto \overline{\varsigma^2}$), but the number of pairs expected over the sky by random chance depends on the global average surface density ($RR \propto (\overline{\varsigma})^2$). Systematic fluctuations mean that $\overline{\varsigma^2} > (\overline{\varsigma})^2$, increasing $w(\theta)$ by

$$\Delta w(\theta) = \frac{\overline{\varsigma^2}}{(\overline{\varsigma})^2} - 1 = \overline{\delta^2} \tag{9.29}$$

where $\delta = (\varsigma - \overline{\varsigma})/\overline{\varsigma}$ is the surface over-density. Equation (9.29) applies on angular scales less than those on which the surface density is typically varying; on larger scales the estimate of DD in this model is wrong. As an indication of the strength of this effect, a simple model in which a survey is divided into two equal areas with a surface-density change of 20 per cent produces an offset $\Delta w = 0.01$ (see Exercise 4).

There are three approaches. The obvious one is to return to the survey and to try to minimize surface-density fluctuation with better calibration or analysis. The second is to restrict analysis to a flux, magnitude or sky range in which such effects are minimal. The third is to modulate random comparison sets to have the same surface densities as the data. This is fraught with difficulty; the gradients must be determined from the data, and the data must manifest clustering and structure on scales whose determination is the object of the exercise.

9.4.3.2 Multiple-component objects

If the resolution of the telescope is high enough to break single entities up into one or more components, there is a serious danger that the

smallest-angle measurements of $w(\theta)$ will be contaminated by an excess contribution from apparent close pairs due to parts of the same object. The problem is not particularly serious in the optical regime: galaxy fields could suffer contamination at small angles from double-nucleus objects, while the same could be true of stellar fields if a few optical binaries are present. The problem is acute in the radio regime. Despite attempts to 'collapse' or 'combine' the appropriate components of double and triple sources catalogued in the FIRST survey (Cress *et al.* 1996; Magliocchetti *et al.* 1998), the small-scale region of $w(\theta)$ determinations remained dominated by residual effects of resolved multiple-component sources (Blake & Wall 2002a). The complex morphologies and large physical sizes of radio sources mean that a single radio galaxy can be resolved in a radio survey as two or more closely separated components of radio emission (for example, the two radio lobes of a 'classical double' radio galaxy). The resultant spurious clustering at small separations needs to be quantified before cosmology can result from such analyses.

To do so, consider turning some members of a distribution of n points into multiple-component objects – replacing single points by tight groups of points, with an average of $\overline{c}$ components per group. Take angles θ small enough that the pair count is dominated by pairs within individual groups (rather than between separate groups). If e is the fraction of original points split into multiple components, and $f(\theta)\,\delta\theta$ is the fraction of those component separations in the range $\theta \rightarrow \theta+\delta\theta$, then the number of pair separations in this bin is $nef(\theta)\,\delta\theta$. The number of pairs expected by random chance is $(\overline{c})^2 \times n\varsigma\,\pi\theta\,\delta\theta$ (neglecting edge effects for small θ), where ς is the surface density of the original n points. Hence the angular correlation function at small angles is offset by

$$\Delta w(\theta) = \frac{e\,f(\theta)}{(\overline{c})^2 \varsigma \pi\,\theta}. \tag{9.30}$$

A power-law angular-size distribution, $f(\theta) \propto \theta^{-\beta}$, implies a power-law offset to the angular correlation function $\Delta w(\theta) \propto \theta^{-\beta-1}$. $w(\theta)$ is dramatically sensitive to the double-component excess: $w(\theta)$ measures excess pair count, and the cosmological signal will have values typically below 1 per cent with a relatively flat slope of ~ -0.8. Thus a few per cent of multiple-component objects with a steep $f(\theta)$ will produce a non-cosmological enhancement totally dominant at the small scales. This is what happens in radio surveys, as shown in the following example.

It is only at small separations that the multiple components affect $w(\theta)$. At separations larger than the maximum component separations, DD and RR will be identically increased so that $w(\theta)$ remains unaffected. Multiple-component objects have no effect on the measured angular correlation function on angular separations bigger than the extent of individual sources.

EXAMPLE Figure 9.2 shows the sky distribution of radio sources in the NRAO VLA SKY Survey (NVSS) on an equal-area projection; Fig. 9.3 shows the angular correlation function measured for the survey.

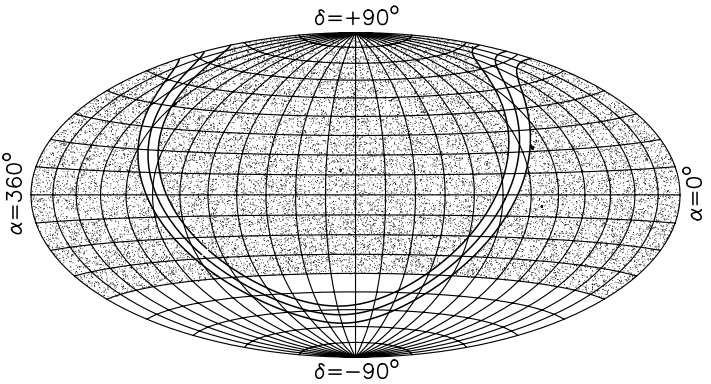

Fig. 9.2. The sources of the NVSS survey; catalogue entries with $S_{1.4\mathrm{GHz}} > 200$ mJy are plotted on an equal-area projection. The Galactic plane and Galactic latitudes $\pm 5^\circ$ are shown and sources within this region are masked from large-scale structure analysis as most are Galactic in origin.

Key to the interpretation of the two power laws is that the amplitude of the small-angle power law decreases with flux-density threshold exactly as predicted (equation 9.30) if this signal is due to multiple source components. The amplitude of the large-angle power law shows no such dependence on threshold, as expected to a first approximation if it is due to true galaxy clustering.

9.5 Counts in cells

A second simple way to quantify clustering is the counts-in-cells (c-in-c) technique. This is the traditional way, in fact the way of the pioneers in clustering investigation (e.g. Shane & Wirtanen 1954). We simply grid

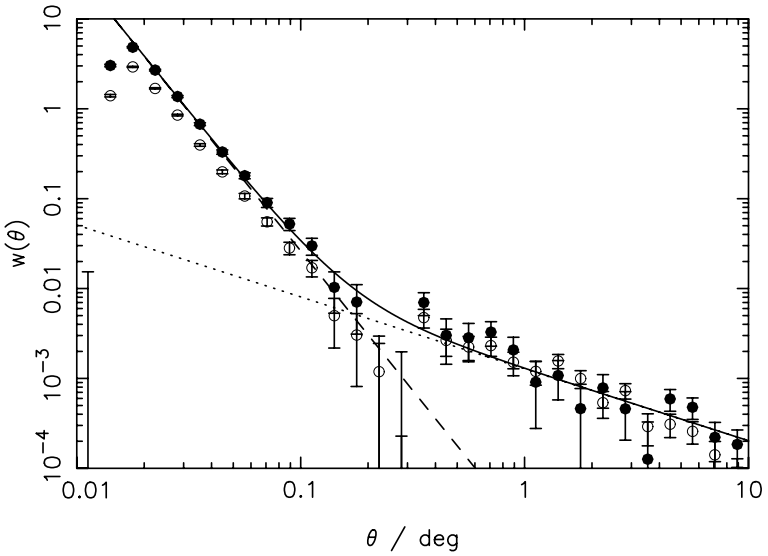

Fig. 9.3. The angular correlation function $w(\theta)$ for the source catalogue of the NVSS survey, at $S_{1.4\mathrm{GHz}} = 20$ mJy (solid circles) and 10 mJy (open circles). The best-fitting sum of two power laws for the 20 mJy data is shown as the solid line, with the two power laws shown individually, dashed due to multiple-component sources, dotted due to galaxy clustering.

the sky into cells of fixed area and shape and count the objects falling in each cell. This yields the probability distribution $P(N)$ of finding N objects in a cell; for no clustering this is a Poisson distribution. The clustering properties are completely characterized by this probability distribution, and thus counts-in-cells results contain more information than the angular correlation function. It is convenient to consider the statistics of the distribution, and in particular the first few moments (Section 3.1) such as the variance $\mu_2 = \overline{(N - \overline{N})^2}$ and the skewness $\mu_3 = \overline{(N - \overline{N})^3}$.

A clustered distribution produces a higher variance than a random distribution because cells may cover clusters or voids, broadening $P(N)$. The clustering pattern can be quantified by measuring the variance μ_2 as a function of cell size. In fact a simple relation exists between μ_2 and the angular correlation function $w(\theta)$ (see below) and thus consistency can be verified. The skewness of counts in cells is a useful statistic physically: skewness in galaxy distributions quantifies non-linear gravitational clustering.

Whereas the angular correlation function bins pair separations into small intervals, a counts-in-cells analysis combines information from a range of angular scales up to the cell size, effectively measuring an average $w(\theta)$. By avoiding the binning of angular separations, counts in cells are less affected by 'shot noise', the main source of uncertainty in $w(\theta)$. Counts in cells is thus a more sensitive probe of long-range correlations than $w(\theta)$. It is, however, harder to make the connection with spatial clustering, and the values of a moment of the counts distribution for different cell sizes will be highly correlated.

9.5.1 Counts-in-cells moments

9.5.1.1 The c-in-c variance and $w(\theta)$

Consider a non-clustered distribution of objects with surface density ς. The expectation value of objects in a cell of area S is $< N >= \varsigma \times S$. The expected probability distribution $P(N)$ is the Poisson distribution with mean $< N >$ and variance $< N >$. We define the following statistic to quantify the increased variance of a clustered distribution:

$$y = \frac{\mu_2 - \overline{N}}{(\overline{N})^2}. \tag{9.31}$$

Hence $< y > = 0$ for no clustering, as $< \mu_2 > = < \overline{N} > = < N >$. For a given $w(\theta)$, the expected value of y (Peebles 1980) is

$$< y >= \frac{\int_{\rm cell} \int_{\rm cell} w(\theta)\, {\rm d}S_1\, {\rm d}S_2}{S^2}. \tag{9.32}$$

Thus $< y >$ may be calculated for an assumed form of the power-law angular correlation function, but survey resolution needs to be built in to this analysis. Suppose in fact that the survey has angular resolution $\theta_{\rm res}$; then the power-law form of $w(\theta)$ can be expressed as

$$w(\theta) = \begin{cases} -1 & \theta < \theta_{\rm res} \\ (\theta/\theta_0)^{-\alpha} & \theta > \theta_{\rm res} \end{cases} \tag{9.33}$$

where θ_0 is an alternative parameterization of the amplitude $A = (\theta_0)^\alpha$ of the angular correlation function. From this a general expression for $< y >$ in terms of survey resolution and $w(\theta)$ power-law parameters may be derived, general in the sense that it is for varying cell shape and size. The derivation (Blake & Wall 2002c) is not simple and requires

numerical integration; it results in an expression of the form

$$< y(L) > = a\, L^{-2} + b\, L^{-\alpha} \tag{9.34}$$

where a and b are constants and L is the cell dimension. The detailed expression for $< y >$ shows that the angular resolution $\theta_{\rm res}$ reduces the variance because the existence of an object in a cell limits the available space in which other objects can appear. This effect varies with cell size because it depends on the scale of the resolution relative to the cell size. Thus a non-clustered distribution viewed with non-zero angular resolution has a variance less than the Poisson value:

$$< y(L) > = -\frac{k}{2} \left(\frac{\theta_{\rm res}}{L} \right)^2 . \tag{9.35}$$

In fact if a survey has high enough angular resolution then the first term of equation (9.34) can be neglected (provided that $\alpha < 2$); then $< y > \propto L^{-\alpha}$.

9.5.1.2 The c-in-c skewness

Skewness is of special importance. Skewness quantifies asymmetry in the non-Poisson clustering, such as a tail in the probability distribution to high cell counts. Assuming Gaussian primordial perturbations and linear growth of clustering, the skewness of counts in cells remains zero (Peebles 1980). Measurement of a non-zero skewness therefore indicates either non-linear gravitational clustering or non-Gaussian initial conditions. As the growth of cosmic structure moves out of the linear regime, the expected skewness increases from zero. Using second-order perturbation theory, Peebles (1980) demonstrated that the density field develops a skewness $<\delta^3>/<\delta^2>^2 = 34/7$ (where δ is the overdensity, or dimensionless density contrast) assuming Gaussian initial perturbations growing purely due to gravity (see also Coles & Frenk 1991). As fluctuations become non-linear, skewness increases because the value of δ grows large in density peaks but approaches the minimum value $\delta = -1$ in under-dense regions.

Recalling that for a Poisson distribution of mean $<N>$ the expectation values for the variance μ_2 and the skewness μ_3 are both equal to $<N>$, the following statistic quantifies the increased skewness due to clustering:

$$z = \frac{\mu_3 - 3\mu_2 + 2\overline{N}}{(\overline{N})^3}. \tag{9.36}$$

Hence $<z>=0$ for no clustering (neglecting a small bias), as $<\mu_2>=<\mu_3>=<\overline{N}>=<N>$. This statistic has the expectation value

$$<z>=\frac{\int_{\rm cell}\int_{\rm cell}\int_{\rm cell} W(\theta_{12},\theta_{13},\theta_{23})\,{\rm d}S_1\,{\rm d}S_2\,{\rm d}S_3}{S^3} \tag{9.37}$$

where $W(\theta_{12},\theta_{13},\theta_{23})$ is the three-point angular correlation function, which quantifies the excess probability (beyond two-point clustering) of finding objects in each of the solid angle elements $\delta\Omega_1$, $\delta\Omega_2$, $\delta\Omega_3$ with mutual separations θ_{12}, θ_{13}, θ_{23}:

$$\delta P=\varsigma^3\,[\,1+w(\theta_{12})+w(\theta_{13})+w(\theta_{23})+W(\theta_{12},\theta_{13},\theta_{23})\,]\,\delta\Omega_1\,\delta\Omega_2\,\delta\Omega_3. \tag{9.38}$$

The statistical error on the estimator of equation (9.36) for a grid of $N_{\rm c}$ cells is

$$\sigma_z=\sqrt{\frac{6}{N_{\rm c}\,(\overline{N})^3}}. \tag{9.39}$$

9.5.2 Measuring counts in cells

The methodology of c-in-c measurement was revolutionized by Szapudi (1998) who showed that it was valid to throw a very large number of randomly placed cells over the sky, heavily over-sampling the survey area. But of course measurement of the variance statistic y remains subject to statistical error due to averaging over a finite number of independent cells $N_{\rm c}$. Calculating the standard error in the case of a non-clustered distribution yields

$$\sigma_y=\sqrt{\frac{2}{N_{\rm c}\,(\overline{N})^2}}. \tag{9.40}$$

The probability distribution of the clustered data does not depart greatly from a Poisson distribution (i.e. $y\ll 1$) so that equation (9.40) is a good approximation to the actual statistical error.

Surveys do not encompass the whole sky: there are boundaries and masked regions. Hence with any form of gridding or random cell placement, some cells are partially filled, the ith cell having a fraction of useful area f_i (say). Populating the survey area with random points is an obvious way to determine f_i for each cell, the number of points falling in each cell used as a measure of cell area. It is then possible to boost the data count in the ith cell by a factor $1/f_i$, unless of course f_i turns out to be so small as to render $1/f_i$ unstable; under this thresholding

circumstance, reject the cell. The design of the Monte Carlo experiment requires some work – it is essential not to add spurious variance by insufficient accuracy in determining cell areas (Blake & Wall 2002c).

When evaluating the moments of the counts-in-cells distribution it is assumed that all cells are populated independently. This is not strictly true given that clustered objects have correlated positions, but the assumption should be a good approximation if the cells are large enough; a minimum cell size $L_{\min}$ must be adopted so that $\overline{N} \geq 1$.

EXAMPLE A counts-in-cells analysis of the distribution of radio sources in the NRAO VLA Sky Survey (see Figure 9.2) was carried out by Blake & Wall (2002c). The results are shown in Figs. 9.4 and 9.5. The figures show how close the distributions are to Poissonian; how well the double power-law interpretation of $w(\theta)$ (Fig. 9.3) predicts the c-in-c variance function $y(L)$; and how good the agreement is for the parameters describing the cosmological portion of $w(\theta)$ as derived from direct measurement and from counts in cells.

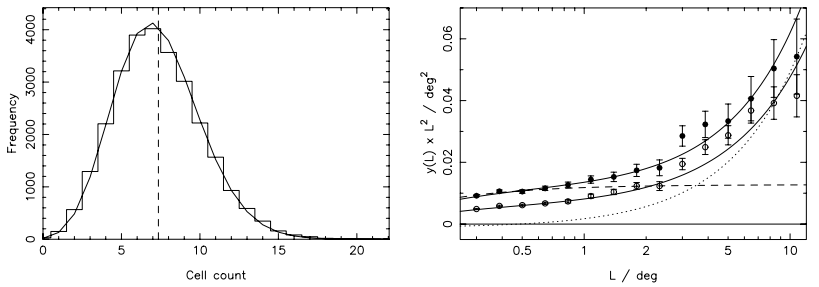

Fig. 9.4. Left: counts of NVSS radio sources with $S_{1.4\mathrm{GHz}} > 20$ mJy in cells of diameter 1°. Vertical dashed line – expected mean count derived from the source surface density; solid curve – the corresponding Poisson distribution. Right: The variance statistic $y(L)$ is plotted for thresholds 20 mJy (solid circles) and 10 mJy (open circles), with predictions of the double power-law $w(\theta)$ models at 20 mJy and 10 mJy (solid lines). The dashed and dotted lines show the separate contributions to $y(L)$ at 20 mJy of the steep (multiple-component) $w(\theta)$ and the shallow (cosmological) $w(\theta)$.

9.5.3 Instrumental effects

The two instrumental effects described for $w(\theta)$ have similar influence on c-in-c moments.

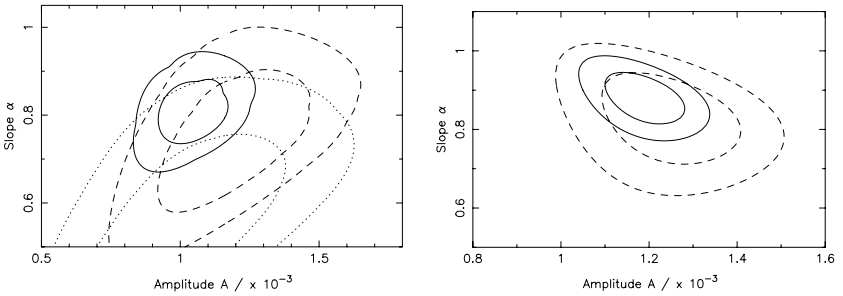

Fig. 9.5. Constraints on the clustering parameters A and α, $w(\theta) = A\theta^{-\alpha}$. Contours of constant χ^2 are shown; these are approximate 1σ and 2σ contours for flux-density thresholds 30 mJy (dotted), 20 mJy (dashed) and 10 mJy (solid). The left diagram is derived from fitting the correlation function (Fig. 9.3) directly; the right diagram from fitting the counts-in-cells variance function shown in the right panel of Fig. 9.4.

9.5.3.1 Calibration errors: surface gradients

Systematic surface density gradients spuriously offset the counts-in-cells variance: a spread in the mean surface density across the cells will inevitably broaden the overall probability distribution $P(N)$, which is constructed from fluctuations about those means. For a cell of area S at local surface density ς, $<N> = \varsigma S$ and $<N^2> = \varsigma S + \varsigma^2 S^2$ for no clustering; averaging over many cells produces $<\overline{N}> = \overline{\varsigma} S$ and $<\overline{N^2}> = \overline{\varsigma} S + \overline{\varsigma^2} S^2$. It follows that the variance statistic y (equation 9.31) is offset by

$$<\Delta y> = \frac{\overline{\varsigma^2}}{(\overline{\varsigma})^2} - 1, \tag{9.41}$$

precisely the same offset as that experienced by $w(\theta)$ in the presence of surface gradients (equation 9.29).

Likewise systematic object surface density gradients offset the skewness by $<\Delta z> = \overline{\delta^3}$ (where δ is the surface over-density).

9.5.3.2 Multiple-component objects

The presence of multiple-component objects increases the counts-in-cells moments – the fraction of objects within a cell split into multiple components varies from cell to cell, which acts to broaden the probability distribution of counts in cells. The simplest model is to suppose that a fraction e of the objects are double (in which case two apparent objects appear as components of the same object close to the centroid position of the object), and a fraction f are triple objects. It can be shown (Blake 2002) that the expected offsets in the variance and skewness statistics

are then

$$<\Delta y> = \frac{1}{\varsigma S}\left(\frac{2e+6f}{1+e+2f}\right) \tag{9.42}$$

$$<\Delta z> = \frac{1}{(\varsigma S)^2}\left(\frac{6f}{1+e+2f}\right) \tag{9.43}$$

where S is the cell area and ς is the surface density of all components.

This result is from a simple model which neglects the range of non-zero separations that components will have. This will only matter if the cell size is not much greater than the maximum component separation. A more sophisticated treatment (Blake 2002) models the separation distribution by the effective (small-angle) form of $w(\theta)$ at small angles, assuming as in the above example that this is dominated by resolved components of objects. The effect on the variance statistic y can then by computed via equation (9.34), with the general expression for $y(L)$ thus modified to

$$<y(L)> = a\,L^{-2} + b\,L^{-\alpha} + c\,L^{-\beta} \tag{9.44}$$

where c is a constant and α and β are respectively the slopes of the shallow (real clustering) and steep (multiple component) $w(\theta)$ power laws. In the appropriate limit this reduces to the simpler treatment initially outlined.

The role of multiple components in skewness measurement is more critical. Equation (9.43) shows that skewness is insensitive to double objects, but very sensitive to triple objects. When triples are present, the skewness offset scales with cell size as $z \propto L^{-4}$. The point is of particular importance in the analysis of radio source catalogues; many radio sources have a triple structure with a compact nuclear component roughly centred between the extended pair of lobes.

9.6 The angular power spectrum

The angular power spectrum, denoted c_ℓ, is the third and final statistic we describe to quantify a surface or sky distribution. This statistic, invoked to look at cluster, galaxy and radio source distributions by Yu & Peebles (1969), Peebles & Hauser (1974), and Webster (1976) respectively, imagines that the object surface density field over the sky is expressed as a sum of angular density fluctuations of different wavelengths.

It is a Fourier analysis (Section 8.2) around the sky. The mathematical tools involved in this process are the spherical harmonic functions, the 2D analogues of sine and cosine, and the quantity c_ℓ expresses the amplitude of the ℓth multipole, which produces fluctuations on angular scales $\theta \sim 180^\circ/\ell$.

In a theoretical sense the c_ℓ spectrum is entirely equivalent to the angular correlation function $w(\theta)$ as a description of the galaxy distribution. The two quantities are connected by the well-known relations (Peebles 1980):

$$c_\ell = 2\pi\, \varsigma_0^2 \int_{-1}^{+1} w(\theta)\, P_\ell(\cos\theta)\, \mathrm{d}(\cos\theta), \tag{9.45}$$

and

$$w(\theta) = \frac{1}{4\pi\, \varsigma_0^2} \sum_{\ell=1}^{\infty} (2\ell+1)\, c_\ell\, P_\ell(\cos\theta), \tag{9.46}$$

with ς_0 the mean object surface density and P_ℓ the Legendre polynomials. However, the angular scales on which the measured signal is highest are very different for each statistic. $w(\theta)$ can only be determined accurately at small angles, beyond which Poisson noise dominates. By contrast, c_ℓ has highest signal at small ℓ, corresponding to large angular scales $\theta \sim 180^\circ/\ell$. The two statistics $w(\theta)$ and c_ℓ are complementary in this sense. However, note that the two statistics quantify very different properties of the galaxy distribution (Section 9.4). The value of c_ℓ quantifies the amplitude of fluctuations on the angular scale corresponding to ℓ. The value of $w(\theta)$ is the average of the product of the galaxy over-density at any point with the over-density at a point at angular separation θ: $w(\theta)$ depends on angular fluctuations on all scales (equation 9.46).

Measurement of the angular power spectrum has practical advantages in comparison with $w(\theta)$. Firstly, it is possible to produce measurements of c_ℓ at different multipoles ℓ that are uncorrelated, whereas the $w(\theta)$ statistic suffers from correlated errors between adjacent separation bins. Secondly, on small scales the evolution of structure is complicated by non-linear effects, and thus it can be advantageous to investigate larger scales where linear theory still applies. Thirdly, there is a natural relation between the c_ℓ spectrum and the spatial power spectrum $P(k)$. This latter quantity provides a very convenient means of describing structure in the Universe because its primordial form is produced by models of

inflation, which prescribe the pattern of initial density fluctuations $\delta\rho/\rho$. Furthermore, in linear theory for the growth of perturbations, fluctuations described by different wavevectors k evolve independently. The angular correlation function $w(\theta)$ is more naturally related to the spatial correlation function $\xi(r)$, the Fourier transform of $P(k)$.

9.6.1 Formalism for c_ℓ

A distribution of objects on the sky can be modelled in two statistical steps. Firstly, a continuous density field $\varsigma(\theta, \phi)$ is specified; this can be described in terms of its spherical harmonic coefficients $a_{\ell,m}$:

$$\varsigma(\theta, \phi) = \sum_{\ell=0}^{\infty} \sum_{m=-\ell}^{+\ell} a_{\ell,m}\, Y_{\ell,m}(\theta, \phi) \tag{9.47}$$

where $Y_{\ell,m}$ are the spherical harmonic functions and θ $(0 \rightarrow \pi)$ and ϕ $(0 \rightarrow 2\pi)$ are spherical polar coordinates. Secondly, discrete galaxy positions are generated in a Poisson process as a realization of this density field (i.e. the probability of finding a galaxy in an element of solid angle $\delta\Omega$ at position θ, ϕ is $\delta P = \varsigma(\theta, \phi)\, \delta\Omega$).

The angular power spectrum c_ℓ prescribes the spherical harmonic coefficients in the first step of this model. It is defined by

$$< |a_{\ell,m}|^2 > = c_\ell \tag{9.48}$$

where the angled brackets imply an averaging over many realizations of the density field. The assumption of isotropy ensures that $< |a_{\ell,m}|^2 >$ is a function of ℓ alone, and not m.

The $Y_{\ell,m}$'s and $a_{\ell,m}$'s of equation (9.47) are in general complex quantities. Because the density field $\varsigma(\theta, \phi)$ is real, $a_{\ell,-m} = a^*_{\ell,m}$. Thus the independent coefficients describing the density field are $a_{\ell,0}$ (which is real) and the real and imaginary parts of $a_{\ell,m}$ for $m \geq 1$. Hence the ℓth harmonic is described by $2\ell + 1$ independent coefficients. The assumption is usually made, motivated by inflationary models, that $\varsigma(\theta, \phi)$ is a Gaussian random field. In this model the real and imaginary parts of $a_{\ell,m}$ are drawn independently from Gaussian distributions such that the normalization satisfies equation (9.48). Thus $< a_{\ell,m} > = 0$ for $\ell > 0$ and $< a^*_{\ell,m}\, a_{\ell',m'} > = 0$ unless $\ell = \ell'$ and $m = m'$.

Consider first a fully surveyed sky. As an initial step we consider the estimation of the harmonic coefficients $a_{\ell,m}$ of the density field. The

orthonormality properties of the $Y_{\ell,m}$'s mean that equation (9.47) may be reversed:

$$a_{\ell,m} = \int \varsigma(\theta,\phi)\, {Y_{\ell,m}}^*(\theta,\phi)\, \mathrm{d}\Omega. \tag{9.49}$$

Equation (9.49) suggests that the $a_{\ell,m}$'s may be estimated by summing over spherical harmonics at the n object positions (θ_i, ϕ_i):

$$A_{\ell,m} = \sum_{i=1}^{n} {Y_{\ell,m}}^*(\theta_i,\phi_i). \tag{9.50}$$

We denote estimators by upper case symbols (e.g. $A_{\ell,m}$) and the underlying 'true' quantities by lower case symbols (e.g. $a_{\ell,m}$). It can now be shown (Blake 2002) that the expectation value of the estimator $|A_{\ell,m}|^2$ is

$$<\overline{|A_{\ell,m}|^2}> = c_\ell + <\varsigma_0> \tag{9.51}$$

and if ς_0 is the average surface density in a given realization, the correct estimator for c_ℓ from our original distribution is

$$C_{\ell,m} = |A_{\ell,m}|^2 - \varsigma_0 \tag{9.52}$$

such that $<\overline{C_{\ell,m}}> = c_\ell$. The discreteness of the distribution causes the correction term '$-\varsigma_0$'. For a given multipole ℓ there are $\ell + 1$ different estimates of c_ℓ, corresponding to $m = 0, 1, \ldots, \ell$. The fact that the density field is real rather than complex implies that $C_{\ell,-m} = C_{\ell,m}$ and thus negative values of m provide no new information. The statistical error on the estimator of equation (9.52) is

$$\sigma(C_{\ell,m}) = \sqrt{<\overline{C^2_{\ell,m}}> - <\overline{C_{\ell,m}}>^2} = (\varsigma_0 + c_\ell) \times \begin{cases} \sqrt{2} & m = 0 \\ 1 & m \neq 0. \end{cases} \tag{9.53}$$

The error for the $m \neq 0$ case is reduced by a factor of $\sqrt{2}$ because there are two independent measurements built in: the real and imaginary parts of $A_{\ell,m}$. Equation (9.53) illustrates that there are two contributions to the statistical error:

- Shot noise (ς_0), because the number of discrete objects is finite and does not perfectly sample the underlying density field. The magnitude of c_ℓ is proportional to ς_0^2 (equation 9.45); hence increasing the number of objects decreases the fractional error.
- Cosmic variance (c_ℓ), because we can only measure a finite number of fluctuations on a given scale around the sky.

By considering $<\overline{C_{\ell,m}\, C_{\ell',m'}}>$ we can show that the estimates of equation 9.52 are statistically independent; and we derive a better estimate of c_ℓ for a given multipole ℓ by averaging over m:

$$C_\ell = \frac{\sum_{m=0}^{\ell} C_{\ell,m}}{\ell+1}. \tag{9.54}$$

From equation (9.53), the resulting error on C_ℓ is

$$\sigma(C_\ell) = (\varsigma_0 + c_\ell)\frac{\sqrt{\ell+2}}{\ell+1}. \tag{9.55}$$

For an incomplete sky, the requisite modification to the derivation is given by Peebles (1973). A summary is as follows. Equation (9.52) becomes

$$C_{\ell,m} = \frac{|A_{\ell,m} - \varsigma_0\, I_{\ell,m}|^2}{J_{\ell,m}} - \varsigma_0 \tag{9.56}$$

where $\varsigma_0 = n/\Delta\Omega$, $\Delta\Omega$ is the survey area and

$$I_{\ell,m} = \int_{\Delta\Omega} {Y_{\ell,m}}^*\, \mathrm{d}\Omega, \quad J_{\ell,m} = \int_{\Delta\Omega} |Y_{\ell,m}|^2\, \mathrm{d}\Omega \tag{9.57}$$

with the integrals being over the survey area. Thus the partial sky is compensated for by replacing $|A_{\ell,m}|^2$ with $|A_{\ell,m} - \varsigma_0 I_{\ell,m}|^2/J_{\ell,m}$: there is a systematic deviation in each harmonic coefficient and the overall normalization changes.

We again estimate the angular power spectrum using $C_\ell = (\sum_{m=0}^{\ell} C_{\ell,m})/(\ell+1)$. The partial sky has some important effects on this estimate. Only for a complete sky does $<\overline{C_\ell}> = c_\ell$: for an incomplete sky there is some 'mixing' of harmonics so that the measured angular power spectrum at multipole ℓ depends on a range of $c_{\ell'}$ around $\ell' = \ell$:

$$<\overline{C_\ell}> = \sum_{\ell'=1}^{\infty} c_{\ell'}\, R_{\ell,\ell'} \tag{9.58}$$

where $\sum_{\ell'} R_{\ell,\ell'} = 1$, and $R_{\ell,\ell'}$ can be determined from the geometry of the survey region (see Hauser & Peebles 1973). In addition, for an incomplete sky the estimates $C_{\ell,m}$ are no longer statistically independent and the error of equation (9.55) is only an approximation. The resulting measurements of c_ℓ at different ℓ are not wholly independent: the covariance matrix is no longer diagonal. Maximum likelihood estimation provides a powerful and general way to take into account the correlations induced by a partial sky area. In fact this alternative method of deriving

the c_ℓ spectrum has been widely used in recent years for quantifying the CMB temperature fluctuations (e.g. Lange *et al.* 2001). These tools can be exploited to analyse the galaxy distribution by pixellating the sky into equal-area cells (see Efstathiou & Moody 2001; Huterer, Knox & Nichol 2001; Tegmark *et al.* 2002).

If the surveyed area $\Delta\Omega$ is reduced for a fixed average object density ς_0 then the signal-to-noise of the measurement decreases, as expected. The statistical error does not change to a first approximation, but the magnitude of the signal (equation 9.56) is reduced because the numerator scales as $(\Delta\Omega)^2$ (as it depends on the square of a sum over $n = \varsigma_0 \Delta\Omega$ objects) and the denominator scales as $\Delta\Omega$. The estimation process takes into account the fact that the surface density ς_0 is not known in advance but is determined from the data ($\varsigma_0 = n/\Delta\Omega$): this is not a source of systematic error in the estimator.

9.6.2 Instrumental effects

Multiple-component objects spuriously increase the measured angular power spectrum. The effect (Blake 2002) is once again to produce an offset, this time in the c_ℓ spectrum:

$$\Delta c_\ell = \frac{\Delta\left(<\overline{|A_{\ell,m}|^2}>\right)}{J_{\ell,m}} = \left(\frac{\overline{c^2}}{\overline{c}} - 1\right) \frac{n <\overline{|Y_{\ell,m}|^2}>}{J_{\ell,m}}. \tag{9.59}$$

where $\bar{c}$ is again the average number of components per object.
But $J_{\ell,m} = <\overline{|Y_{\ell,m}|^2}> \Delta\Omega$ from equation (9.57) and hence this simplifies to:

$$\Delta c_\ell = \left(\frac{\overline{c^2}}{\overline{c}} - 1\right) \varsigma_0. \tag{9.60}$$

If a fraction e of objects is split into doubles then $\overline{c} = 1+e$ and $\overline{c^2} = 1+3e$; thus the quantity in brackets in equation (9.60) is $2e/(1+e)$. The fact that multiple components produce a constant offset in the measured angular power spectrum makes it very easy to correct for their presence. The result of equation (9.60) only breaks down at very large ℓ (> 1000) when the angular scale of the fluctuations probed ($\theta \sim 180^\circ/\ell$) becomes comparable to the overall size of the objects.

The presence of systematic surface gradients also distorts the angular power spectrum but in a non-straightforward way, because the harmonic coefficients need to reproduce these gradients as well as the fluctuations

due to clustering. It is again best to (a) fix the calibration, or (b) stick to thresholds at which the gradients are insignificant.

EXAMPLE A radio survey in particular maps the galaxy distribution out to very large distances $R > 10^3$ Mpc and is hence able to probe $P(k)$ on large scales $k \sim 1/R < 10^{-3}$ Mpc^{-1}, where the shape of the power spectrum is unaltered from its initial form. Determination of the c_ℓ spectrum of radio galaxies therefore has the potential to constrain the primordial pattern of density fluctuations in a manner independent of measurements of fluctuations in the cosmic microwave background (CMB) radiation. Such an analysis (Blake 2002) was carried out for the NVSS (Fig. 9.2).

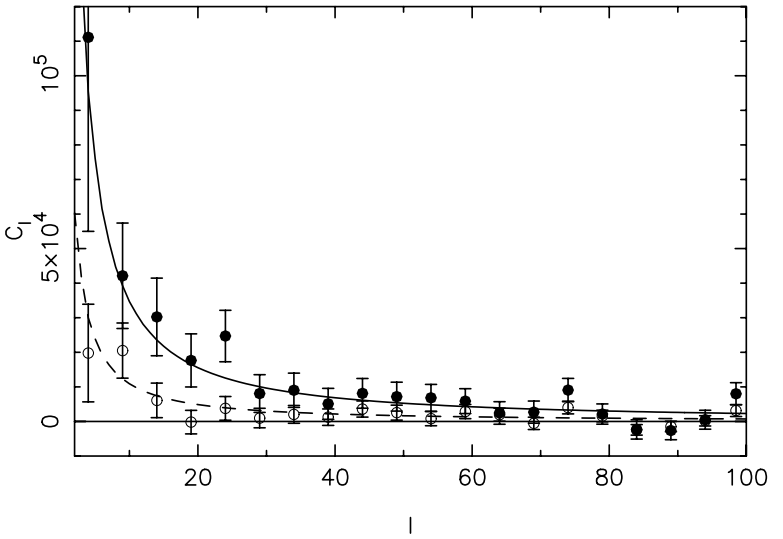

Fig. 9.6. **Measurement of the NVSS c_ℓ spectrum.** Results at flux-density thresholds $S_{1.4\mathrm{GHz}} = 10$ mJy (solid circles) and 20 mJy (open circles) are plotted. The solid and dashed lines show the prediction of equation (9.45) at these thresholds assuming that $w(\theta) = (1 \times 10^{-3})\,\theta^{-0.8}$. The difference in amplitude between the two measurements arises from the factor ς_0^2 in equation (9.45).

The results are shown in Fig. 9.6 together with the predictions resulting from transforming the angular correlation function using equation (9.45), assuming that $w(\theta) = (1 \times 10^{-3})\,\theta^{-0.8}$ (see Fig. 9.5). The predictions turn out to be a good match to the measured c_ℓ

spectrum – with the notable exception of the dipole term $\ell = 1$, 'spuriously' high due to the cosmic velocity dipole detected in this experiment (Blake & Wall 2002b). The NVSS angular power spectrum decreases with ℓ as (roughly) a power law. The offset due to multiple-component sources is significant. For example, equation (9.60) produces $\Delta C_\ell \approx 1 \times 10^4$ for the 10 mJy threshold.

It is initially surprising that the observed c_ℓ spectrum of Fig. 9.6 concurs so well with the angular correlation function prediction of equation (9.45): c_ℓ depends on $w(\theta)$ at all angles, but $w(\theta)$ is only measurable for $\theta < 10^\circ$ and will deviate from a power law (and become slightly negative) at larger angles. The agreement implies that long-wavelength surface density fluctuations (generated by multipoles at low ℓ) are important in producing angular correlations at small θ. This is not a contradiction: the angular correlation function is the average of the product of the galaxy over-density at any point with the over-density at any other point at fixed angular separation, and positive contributions to this average are readily produced by long-wavelength fluctuations.

Mathematically, agreement arises because the dominant contribution from the integrand of equation (9.45), $\mathrm{d}c_\ell/\mathrm{d}\theta \propto w(\theta)\, P_\ell(\cos\theta) \sin\theta$, originates from small angles. As $\theta \to 0$, $\mathrm{d}c_\ell/\mathrm{d}\theta \to \theta^{-0.8} \times 1 \times \theta \to 0$; but as θ increases, $P_\ell(\cos\theta)$ falls off and a maximum in $\mathrm{d}c_\ell/\mathrm{d}\theta$ occurs at $\theta \approx$ a few degrees. At larger angles, the oscillations in $P_\ell(\cos\theta)$ ensure that subsequent contributions to c_ℓ approximately cancel out.

9.7 Galaxy distribution statistics: interpretation

It is important to emphasize that the picture presented by these three forms of analysis is far from complete. Topology in particular is important and cannot necessarily be deduced from them; it is known to be sponge-like. There are many further statistical approaches in addition to the topological one (Gott *et al.* 1989) – *minimal spanning trees* (Barrow, Bhavsar & Sonada 1985), *percolation theory* (Zeldovich, Einasto & Shandarin 1982; Dekel & West 1985; Einasto & Saar 1987), *nearest-neighbour analysis* (Bogart & Wagoner 1973), *higher-order correlation functions* (Peebles & Groth 1975), and *fractal analysis* (Martínez *et al.* 1990). Further detail on these approaches together with cosmological

interpretation may be found in the comprehensive textbooks of Peacock (1999) and Saslaw (2000).

Exercises

In the exercises denoted by (D), datasets are provided on the book's website; or create your own.

9.1 Why should the test statistic for **Rayleigh's test** be asymptotically chi-square? Compute the statistic for small numbers, say < 10; see Section 3.3.3.

9.2 **Variance of estimators for $w(\theta)$ (D).** Generate 20 000 data points randomly in the region $0^\circ < \alpha < 5^\circ$, $0^\circ < \delta < 5^\circ$. Estimate $w(\theta)$ using the natural estimator w_1, the Peebles estimator w_2, the Landy–Szalay estimator w_3 and the Hamilton estimator w_4. (Average DR and RR over say 10 comparison sets each of 20 000 random points.) Plot the results as a function of δ showing Poisson error bars $1/\sqrt{DD}$. Comment on the results. Which estimator is best?

9.3 **Integral constraint on $w(\theta)$.** (a) Show that the factor C in equation (9.27) is $1/(1+W)$ where $W = \int w(\theta)\, \mathrm{d}G_p$. (b) Derive an approximate expression for W, assuming a power-law form for $w(\theta) = (\theta/\theta_0)^{-b}$.

9.4 **The effect of surface density changes on $w(\theta)$ (D).** (a) Estimate the magnitude of the offset in $w(\theta)$ taking a simple model in which a survey is divided into two equal areas between which there is a fractional surface density shift ϵ (equation 9.29). Find the expected step in $w(\theta)$ as a function of ϵ; verify that a step of 20 per cent results in $\Delta w = 0.01$. (b) Confirm this prediction with a toy-model simulation, putting say 100 000 random points in the region $0^\circ < \alpha < 60^\circ$, $-20^\circ < \delta < +20^\circ$ with a 20 per cent step at $\delta = 0^\circ$. Then calculate the $w(\theta)$ using say a Landy–Szalay $w(\theta)_4$ estimator over the small angular-scale range $\theta < 1^\circ$, checking that $w(\theta)$ agrees within errors with the prediction from equation (9.29).

9.5 **The effect of surface-density changes on c-in-c (D).** (a) Use the 100 000 random points generated in the region $0^\circ < \alpha < 60^\circ$, $-20^\circ < \delta < +20^\circ$ for Exercise (4). Generate a set of 10 grid patterns for circular non-overlapping cells over the area, with diameter $\theta = 0.03^\circ$ to 3°, evenly spaced in $\log \theta$. Compile

$P(N)$ for each of these and show that the means and variances are as expected for Poissonian distributions. Calculate and plot the variance statistic $y(L)$ (equation 9.31) as a function of cell size; verify that there is no significant offset from zero. (b) Put in a 20 per cent step in surface density, dividing the field in half at $\delta = 0°$. Recalculate the $y(L)$ and verify that the apparent offset in $y(L)$ is of the expected magnitude $\Delta y = 0.01$ (equation 9.41).

9.6 $w(\theta)$ **and the angular power spectrum (D).** Simulate a square piece of sky $10° \times 10°$, using 10 000 points placed at random. (a) Verify that there is no significant signal either in $w(\theta)$ and in the angular power spectrum. (b) Build a hierarchy of galaxy clusters and clusters of clusters using perhaps another 10 000 points, adopting Gaussian shapes for clusters, cluster-clusters, etc. (c) Show that with a few adjustments to the parameters (see Fig. 9.1), it is possible to produce an approximate power law of slope ~ -1 for a single hierarchy of clustering. Relate the resultant form of the angular power spectrum and its information content to this $w(\theta)$.

Appendix 1
The literature

There is a vast literature. Here we point to a few works which we have found useful, binning these into five types: popular, the basic text, the rigorous text, the data analysis manual, and the books of specialist interest to astronomers.

(1) The classic popular books have legendary titles: How to Lie with Statistics (Huff 1973), Facts from Figures (Moroney 1965), Statistics in Action (Sprent 1977) and Statistics without Tears (Rowntree 1981). They are all fun. A modern version with a twist in the title is Seeing through Statistics (Utts 1996), which entertains, serves as a statistics primer, and is almost a member of the next group.

(2) Textbooks come in types (a) and (b), both of which cover similar material for the first two-thirds of each book. They start with descriptive or summarizing statistics (mean, standard deviation), the distributions of these statistics, then moving to the concept of probability and hence statistical inference and hypothesis testing, including correlation of two variables. They then diverge, choosing from a menu including analysis of variance (ANOVA), regression analysis, non-parametric statistics, etc. Modern versions come in bright colours and flavours, perhaps to help presentation to undergraduates of a subject with which excitement is not always associated. The value of many such books is exceptional because of the sales they generate. They are complete with tables, ready summaries of tests and formulae inside covers or in coloured insets, and frequently arrive with CDs and floppy disks including test datasets. Those of type (a) are essentially

devoid of any calculus but with much arithmetic in the form of worked examples, and are statistics primers for undergraduates in non-scientific disciplines. Type (b) has basic mathematics which may run as far as simple calculus. A wonderfully readable example of the former is *Statistics* by Freedman et al. (1995), in which a non-conventional approach is adopted, very successfully. Another which gets substantially further, for example to ANOVA and to non-parametric tests, is *Introductory Statistics* by Weiss (1995), entertaining through inclusion of short biographical sketches of the founding fathers of statistical science. Of type (b), moreappropriate in the present context but not necessarily so entertaining, an outstanding example is *Mathematical Statistics and Data Analysis* by Rice (1995), basic but erudite and thorough; it goes so far as to discuss covariance matrices, Bayesian inference, moment generating functions, multiple linear regression, and computer-intensive methods such as the bootstrap; it includes a floppy disk with examples; and all at a bargain price for a hard-back book. Unfortunately non-parametric tests do not get a mention. They do in other basic texts of type (b), such as that by Hogg & Tanis (1993): *Probability and Statistical Inference*, a tried-and-true serious textbook with excellent presentation, now in its fourth edition.

(3) The serious books which go beyond the undergraduate level include *Statistics: Concepts and Applications* by Frank & Altheon (1994), a thorough and well-set out description of classical general statistics; and *Statistical Inference* by Casella & Berger (2002), where the theory is presented in a highly accessible manner. *Kendall's Advanced Theory of Statistics*, the three volumes being *Distribution Theory* (Stuart & Ord 1994), *Classical Inference and Relationship* (Stuart & Ord 1991), and *Bayesian Inference* (O'Hagan 1994), is a complete reference; no easy going, though. Another very useful classic is *Probability, Random Variables and Stochastic Processes* by Papoulis & Unnikrishna Pillai (2002), strong mathematically and biased towards classic real-time signal processing issues. Various works by Jaynes (1968; 1976; 1983; 1986; 2003) are indispensable reading on the concepts of probability. There is an archive of his writings at `bayes.wustl.edu`.

(4) The data analysis books are led by the highly practical Bevington & Robinson (2002), *Data Reduction and Error Analysis for the Physical Sciences*. A useful little monograph is *A Practical Guide to Data Analysis for Physical Science Students* by Lyons (1991). Lyons has also written *Statistics for Nuclear and Particle Physicists* (1986), an outstandingly practical guide, and very strong on parameter fitting, hypothesis testing and Monte Carlo methods. Another useful book, with a strong Bayesian emphasis, is *Data Analysis: a Bayesian Tutorial* by Sivia (1996). Carlin & Louis (2000) *Bayes and Empirical Bayes Methods for Data Analysis* gives a very thorough treatment of Bayesian techniques in data reduction and is excellent on Bayesian integration problems.

The monographs which simply discuss applying statistical tests might also be considered in this class, and among these *100 Statistical Tests* by Kanji (1993) stands out for the sheer baldness with which the tests are presented, one page plus a page for the worked example. A classic in simplicity it may be, but the lethal nature of the availability of a large number of unconsidered tests must be emphasized. With regard to applying non-parametric statistical tests, the books by Conover (1999) *Practical Nonparametric Statistics*, and Siegel & Castellan (1988) *Nonparametric Statistics for the Behavioural Sciences* are very straightforward, the latter particularly recommended. Manuals of the now highly developed statistics program packages, e.g. MINITAB, SPSS, GENSTAT, S-PLUS, contain much practical advice.

The dominant force in physical analysis books is, however, *Numerical Recipes* (Press *et al.* 1992), which contains unparalled breadth, much common sense, and subroutines in our favourite computer languages which invariably work. No scientist should be without access to this book; it is superb.

Finally note the two books by Tufte, *The Visual Display of Quantitative Information* (1983) and *Envisaging Information* (1990), magnificent in presentation and representing essential browsing for anybody wishing to present data in graphical form.

(5) The growth of interest by astronomers in statistical methods, perhaps driven by the data explosion, is demonstrated by a series of specialist conferences which have resulted in the collection of much useful information. The first of these, *Statistical Methods*

in Astronomy (Rolfe 1983), contains useful background bibliographies in time-series analysis and in non-parametric statistics. The two later conferences, Errors, Bias and Uncertainties in Astronomy (Jaschek & Murtagh 1990) and Statistical Challenges in Modern Astronomy (Feigelson & Babu 1992a) reflect the dramatic change in what we consider to be the important datasets over a 15-year period, and are instructive reading for this alone. The impressive growth in rigorous statistical methods for astronomy is reflected in Astrostatistics (Babu & Feigelson 1996).

Appendix 2
Statistical tables

Table A2.1. Area under the Normal (Gaussian) distribution

$\int_0^z \exp\left(-\frac{1}{2}z^2\right) \mathrm{d}z$, with $z = (x - \mu)/\sigma$

z +	0.00	0.01	0.02	0.03	0.04	0.05	0.06	0.07	0.08	0.09
0.0	0.0000	0.0040	0.0080	0.0120	0.0160	0.0199	0.0239	0.0279	0.0319	0.0359
0.1	0.0398	0.0438	0.0478	0.0517	0.0557	0.0596	0.0636	0.0675	0.0714	0.0754
0.2	0.0793	0.0832	0.0871	0.0910	0.0948	0.0987	0.1026	0.1064	0.1103	0.1141
0.3	0.1179	0.1217	0.1255	0.1293	0.1331	0.1368	0.1406	0.1443	0.1480	0.1517
0.4	0.1554	0.1591	0.1628	0.1664	0.1700	0.1736	0.1772	0.1808	0.1844	0.1879
0.5	0.1915	0.1950	0.1985	0.2019	0.2054	0.2088	0.2123	0.2157	0.2190	0.2224
0.6	0.2258	0.2291	0.2324	0.2357	0.2389	0.2422	0.2454	0.2486	0.2518	0.2549
0.7	0.2580	0.2612	0.2642	0.2673	0.2704	0.2734	0.2764	0.2794	0.2823	0.2852
0.8	0.2881	0.2910	0.2939	0.2967	0.2996	0.3023	0.3051	0.3079	0.3106	0.3133
0.9	0.3159	0.3186	0.3212	0.3238	0.3264	0.3289	0.3315	0.3340	0.3365	0.3389
1.0	0.3413	0.3438	0.3461	0.3485	0.3508	0.3531	0.3554	0.3577	0.3599	0.3621
1.1	0.3643	0.3665	0.3686	0.3708	0.3729	0.3749	0.3770	0.3790	0.3810	0.3830
1.2	0.3849	0.3869	0.3888	0.3907	0.3925	0.3944	0.3962	0.3980	0.3997	0.4015
1.3	0.4032	0.4049	0.4066	0.4082	0.4099	0.4115	0.4131	0.4147	0.4162	0.4177
1.4	0.4192	0.4207	0.4222	0.4236	0.4251	0.4265	0.4279	0.4292	0.4306	0.4319
1.5	0.4332	0.4345	0.4357	0.4370	0.4382	0.4394	0.4406	0.4418	0.4430	0.4441
1.6	0.4452	0.4463	0.4474	0.4485	0.4495	0.4505	0.4515	0.4525	0.4535	0.4545
1.7	0.4554	0.4564	0.4573	0.4582	0.4591	0.4599	0.4608	0.4616	0.4625	0.4633
1.8	0.4641	0.4649	0.4656	0.4664	0.4671	0.4678	0.4686	0.4693	0.4700	0.4706
1.9	0.4713	0.4719	0.4726	0.4732	0.4738	0.4744	0.4750	0.4756	0.4762	0.4767
2.0	0.4773	0.4778	0.4783	0.4788	0.4793	0.4798	0.4803	0.4808	0.4812	0.4817
2.1	0.4821	0.4826	0.4830	0.4834	0.4838	0.4842	0.4846	0.4850	0.4854	0.4857
2.2	0.4861	0.4865	0.4868	0.4871	0.4875	0.4878	0.4881	0.4884	0.4887	0.4890
2.3	0.4893	0.4896	0.4898	0.4901	0.4904	0.4906	0.4909	0.4911	0.4913	0.4916
2.4	0.4918	0.4920	0.4922	0.4925	0.4927	0.4929	0.4931	0.4932	0.4934	0.4936
2.5	0.4938	0.4940	0.4941	0.4943	0.4945	0.4946	0.4948	0.4949	0.4951	0.4952
2.6	0.4953	0.4955	0.4956	0.4957	0.4959	0.4960	0.4961	0.4962	0.4963	0.4964
2.7	0.4965	0.4966	0.4967	0.4968	0.4969	0.4970	0.4971	0.4972	0.4973	0.4974
2.8	0.4974	0.4975	0.4976	0.4977	0.4977	0.4978	0.4979	0.4980	0.4980	0.4981
2.9	0.4981	0.4982	0.4983	0.4983	0.4984	0.4984	0.4985	0.4985	0.4986	0.4986
3.0	0.4987	0.4987	0.4987	0.4988	0.4988	0.4989	0.4989	0.4989	0.4990	0.4990
3.1	0.4990	0.4991	0.4991	0.4991	0.4992	0.4992	0.4992	0.4992	0.4993	0.4993
3.2	0.4993	0.4993	0.4994	0.4994	0.4994	0.4994	0.4994	0.4995	0.4995	0.4995
3.3	0.4995	0.4995	0.4996	0.4996	0.4996	0.4996	0.4996	0.4996	0.4996	0.4997
3.4	0.4997	0.4997	0.4997	0.4997	0.4997	0.4997	0.4997	0.4997	0.4998	0.4998

Table A2.2. The tails of the Gaussian distribution

	Percentage area under the Gaussian curve in region:		
m	$> m\sigma$ (one tail)	$< -m\sigma, > m\sigma$ (both tails)	$-m\sigma < m\sigma$ (between tails)
0.0	50.0	100.00	0.00
0.5	30.85	61.71	38.29
1.0	15.87	31.73	68.27
1.5	6.681	13.36	86.64
2.0	2.275	4.550	95.45
2.5	0.621	1.24	98.76
3.0	0.135	0.270	99.73
3.5	0.0233	0.0465	99.954
4.0	0.00317	0.00633	99.9937
4.5	0.000340	0.000680	99.99932
5.0	0.0000287	0.0000573	99.999943

Table A2.3. Critical values of 'Student's' t distribution

	Level of significance for one-tailed test					
	0.100	0.050	0.025	0.010	0.005	0.0005
	Level of significance for two-tailed test					
	0.200	0.100	0.050	0.020	0.010	0.001
$\nu = 1$	3.078	6.314	12.706	31.821	63.657	636.619
2	1.886	2.920	4.303	6.965	9.925	31.598
3	1.638	2.353	3.182	4.541	5.841	12.941
4	1.533	2.132	2.776	3.747	4.604	8.610
5	1.476	2.015	2.571	3.365	4.032	6.859
6	1.440	1.943	2.447	3.143	3.707	5.959
7	1.415	1.895	2.365	2.998	3.499	5.405
8	1.397	1.860	2.306	2.896	3.355	5.041
9	1.383	1.833	2.262	2.821	3.250	4.781
10	1.372	1.812	2.228	2.764	3.169	4.587
11	1.363	1.796	2.201	2.718	3.106	4.437
12	1.356	1.782	2.179	2.681	3.055	4.318
13	1.350	1.771	2.160	2.650	3.012	4.221
14	1.345	1.761	2.145	2.624	2.977	4.140
15	1.341	1.753	2.131	2.602	2.947	4.073
16	1.337	1.746	2.120	2.583	2.921	4.015
17	1.333	1.740	2.110	2.567	2.898	3.965
18	1.330	1.734	2.101	2.552	2.878	3.922
19	1.328	1.729	2.093	2.539	2.861	3.883
20	1.325	1.725	2.086	2.528	2.845	3.850
21	1.323	1.721	2.080	2.518	2.831	3.819
22	1.321	1.717	2.074	2.508	2.819	3.792
23	1.319	1.714	2.069	2.500	2.807	3.767
24	1.318	1.711	2.064	2.492	2.797	3.745
25	1.316	1.708	2.060	2.485	2.787	3.725
26	1.315	1.706	2.056	2.479	2.779	3.707
27	1.314	1.703	2.052	2.473	2.771	3.690
28	1.313	1.701	2.048	2.467	2.763	3.674
29	1.311	1.699	2.045	2.462	2.756	3.659
30	1.310	1.697	2.042	2.457	2.750	3.646
40	1.303	1.684	2.021	2.423	2.704	3.551
60	1.296	1.671	2.000	2.390	2.660	3.460
120	1.289	1.658	1.980	2.358	2.617	3.373
∞	1.282	1.645	1.960	2.326	2.576	3.291

Table A2.4. Critical values of the F distribution

Level of significance = 0.90

n	m = 5	10	15	20	25	30	35	40	45	50
5	3.45	2.52	2.27	2.16	2.09	2.05	2.02	2.00	1.98	1.97
10	3.30	2.32	2.06	1.94	1.87	1.82	1.79	1.76	1.74	1.73
15	3.24	2.24	1.97	1.84	1.77	1.72	1.69	1.66	1.64	1.63
20	3.21	2.20	1.92	1.79	1.72	1.67	1.63	1.61	1.58	1.57
25	3.19	2.17	1.89	1.76	1.68	1.63	1.60	1.57	1.55	1.53
30	3.17	2.16	1.87	1.74	1.66	1.61	1.57	1.54	1.52	1.50
35	3.16	2.14	1.86	1.72	1.64	1.59	1.55	1.52	1.50	1.48
40	3.16	2.13	1.85	1.71	1.63	1.57	1.53	1.51	1.48	1.46
45	3.15	2.12	1.84	1.70	1.62	1.56	1.52	1.49	1.47	1.45
50	3.15	2.12	1.83	1.69	1.61	1.55	1.51	1.48	1.46	1.44

Level of significance = 0.95

n	m = 5	10	15	20	25	30	35	40	45	50
5	5.05	3.33	2.90	2.71	2.60	2.53	2.49	2.45	2.42	2.40
10	4.74	2.98	2.54	2.35	2.24	2.16	2.11	2.08	2.05	2.03
15	4.62	2.85	2.40	2.20	2.09	2.01	1.96	1.92	1.89	1.87
20	4.56	2.77	2.33	2.12	2.01	1.93	1.88	1.84	1.81	1.78
25	4.52	2.73	2.28	2.07	1.96	1.88	1.82	1.78	1.75	1.73
30	4.50	2.70	2.25	2.04	1.92	1.84	1.79	1.74	1.71	1.69
35	4.48	2.68	2.22	2.01	1.89	1.81	1.76	1.72	1.68	1.66
40	4.46	2.66	2.20	1.99	1.87	1.79	1.74	1.69	1.66	1.63
45	4.45	2.65	2.19	1.98	1.86	1.77	1.72	1.67	1.64	1.61
50	4.44	2.64	2.18	1.97	1.84	1.76	1.70	1.66	1.63	1.60

Level of significance = 0.99

n	m = 5	10	15	20	25	30	35	40	45	50
5	10.97	5.64	4.56	4.10	3.85	3.70	3.59	3.51	3.45	3.41
10	10.05	4.85	3.80	3.37	3.13	2.98	2.88	2.80	2.74	2.70
15	9.72	4.56	3.52	3.09	2.85	2.70	2.60	2.52	2.46	2.42
20	9.55	4.41	3.37	2.94	2.70	2.55	2.44	2.37	2.31	2.27
25	9.45	4.31	3.28	2.84	2.60	2.45	2.35	2.27	2.21	2.17
30	9.38	4.25	3.21	2.78	2.54	2.39	2.28	2.20	2.14	2.10
35	9.33	4.20	3.17	2.73	2.49	2.34	2.23	2.15	2.09	2.05
40	9.29	4.17	3.13	2.69	2.45	2.30	2.19	2.11	2.05	2.01
45	9.26	4.14	3.10	2.67	2.42	2.27	2.16	2.08	2.02	1.97
50	9.24	4.12	3.08	2.64	2.40	2.25	2.14	2.06	2.00	1.95

Table A2.5. Critical values of r_s, the Spearman rank correlation coefficient

	Level of significance for one-tailed test								
	0.250	0.100	0.050	0.025	0.010	0.005	0.0025	0.0010	0.0005
	Level of significance for two-tailed test								
	0.500	0.200	0.100	0.050	0.020	0.010	0.005	0.002	0.001
$N = 4$	0.600	1.000	1.000	–	–	–	–	–	–
5	0.500	0.800	0.900	1.000	1.000	–	–	–	–
6	0.371	0.657	0.829	0.886	0.943	1.000	1.000	–	–
7	0.321	0.571	0.714	0.786	0.893	0.929	0.964	1.000	1.000
8	0.310	0.524	0.643	0.738	0.833	0.881	0.905	0.952	0.976
9	0.267	0.483	0.600	0.700	0.783	0.833	0.867	0.917	0.933
10	0.248	0.455	0.564	0.648	0.745	0.794	0.830	0.879	0.903
11	0.236	0.427	0.536	0.618	0.709	0.755	0.800	0.845	0.873
12	0.224	0.406	0.503	0.587	0.671	0.727	0.776	0.825	0.860
13	0.209	0.385	0.484	0.560	0.648	0.703	0.747	0.802	0.835
14	0.200	0.367	0.464	0.538	0.622	0.675	0.723	0.776	0.811
15	0.189	0.354	0.443	0.521	0.604	0.654	0.700	0.754	0.786
16	0.182	0.341	0.429	0.503	0.582	0.635	0.679	0.732	0.765
17	0.176	0.328	0.414	0.485	0.566	0.615	0.662	0.713	0.748
18	0.170	0.317	0.401	0.472	0.550	0.600	0.643	0.695	0.728
19	0.165	0.309	0.391	0.460	0.535	0.584	0.628	0.677	0.712
20	0.161	0.299	0.380	0.447	0.520	0.570	0.612	0.662	0.696
21	0.156	0.292	0.370	0.435	0.508	0.556	0.599	0.648	0.681
22	0.152	0.284	0.361	0.425	0.496	0.544	0.586	0.634	0.667
23	0.148	0.278	0.353	0.415	0.486	0.532	0.573	0.622	0.654
24	0.144	0.271	0.344	0.406	0.476	0.521	0.562	0.610	0.642
25	0.142	0.265	0.337	0.398	0.466	0.511	0.551	0.598	0.630
26	0.138	0.259	0.331	0.390	0.457	0.501	0.541	0.587	0.619
27	0.136	0.255	0.324	0.382	0.448	0.491	0.531	0.577	0.608
28	0.133	0.250	0.317	0.375	0.440	0.483	0.522	0.567	0.598
29	0.130	0.245	0.312	0.368	0.433	0.475	0.513	0.558	0.589
30	0.128	0.240	0.306	0.362	0.425	0.467	0.504	0.549	0.580
31	0.126	0.236	0.301	0.356	0.418	0.459	0.496	0.541	0.571
32	0.124	0.232	0.296	0.350	0.412	0.452	0.489	0.533	0.563
33	0.121	0.229	0.291	0.345	0.405	0.446	0.482	0.525	0.554
34	0.120	0.225	0.287	0.340	0.399	0.439	0.475	0.517	0.547
35	0.118	0.222	0.283	0.335	0.394	0.433	0.468	0.510	0.539
36	0.116	0.219	0.279	0.330	0.388	0.427	0.462	0.504	0.533
37	0.114	0.216	0.275	0.325	0.383	0.421	0.456	0.497	0.526
38	0.113	0.212	0.271	0.321	0.378	0.415	0.450	0.491	0.519
39	0.111	0.210	0.267	0.317	0.373	0.410	0.444	0.485	0.513
40	0.110	0.207	0.264	0.313	0.368	0.405	0.439	0.479	0.507
41	0.108	0.204	0.261	0.309	0.364	0.400	0.433	0.473	0.501
42	0.107	0.202	0.257	0.305	0.359	0.395	0.428	0.468	0.495
43	0.105	0.199	0.254	0.301	0.355	0.391	0.423	0.463	0.490
44	0.104	0.197	0.251	0.298	0.351	0.386	0.419	0.458	0.484
45	0.103	0.194	0.248	0.294	0.347	0.382	0.414	0.453	0.479
46	0.102	0.192	0.246	0.291	0.343	0.378	0.410	0.448	0.474
47	0.101	0.190	0.243	0.288	0.340	0.374	0.405	0.443	0.469
48	0.100	0.188	0.240	0.285	0.336	0.370	0.401	0.439	0.465
49	0.098	0.186	0.238	0.282	0.333	0.366	0.397	0.434	0.460
50	0.097	0.184	0.235	0.279	0.329	0.363	0.393	0.430	0.456

Table A2.6. Critical values of the chi-square distribution for ν degrees of freedom

	Probability under H_0 that χ^2 exceeds listed value												
	0.99	0.98	0.95	0.90	0.80	0.50	0.30	0.20	0.10	0.05	0.02	0.01	0.001
ν =1	0.00016	0.00063	0.0039	0.016	0.15	0.46	1.07	1.64	2.71	3.84	5.41	6.64	10.83
2	0.02	0.04	0.10	0.21	0.71	1.39	2.41	3.22	4.60	5.99	7.82	9.21	13.82
3	0.12	0.18	0.35	0.58	1.42	2.37	3.66	4.64	6.25	7.82	9.84	11.34	16.27
4	0.30	0.43	0.71	1.06	2.20	3.36	4.88	5.99	7.78	9.49	11.67	13.28	18.46
5	0.55	0.75	1.14	1.61	3.00	4.35	6.06	7.29	9.24	11.07	13.39	15.09	20.52
6	0.87	1.13	1.64	2.20	3.83	5.35	7.23	8.56	10.64	12.59	15.03	16.81	22.46
7	1.24	1.56	2.17	2.83	4.67	6.35	8.38	9.80	12.02	14.07	16.62	18.48	24.32
8	1.65	2.03	2.73	3.49	5.53	7.34	9.52	11.03	13.36	15.51	18.17	20.09	26.12
9	2.09	2.53	3.32	4.17	6.39	8.34	10.66	12.24	14.68	16.92	19.68	21.67	27.88
10	2.56	3.06	3.94	4.86	7.27	9.34	11.78	13.44	15.99	18.31	21.16	23.21	29.59
11	3.05	3.61	4.58	5.85	8.15	10.34	12.90	14.63	17.28	19.68	22.62	24.72	31.26
12	3.57	4.18	5.23	6.30	9.03	11.34	14.01	15.81	18.55	21.03	24.05	26.22	32.91
13	4.11	4.76	5.89	7.04	9.93	12.34	15.12	16.98	19.81	22.36	25.47	27.69	34.53
14	4.66	5.37	6.57	7.79	10.82	13.34	16.22	18.15	21.06	23.68	26.87	29.14	36.12
15	5.23	5.98	7.26	8.55	11.72	14.34	17.32	19.30	22.31	25.00	28.26	30.58	37.70
16	5.81	6.61	7.96	9.31	12.62	15.34	18.42	20.46	23.54	26.30	29.63	32.00	39.29
17	6.41	7.26	8.67	10.08	13.53	16.34	19.51	21.62	24.77	27.59	31.00	33.41	40.75
18	7.02	7.91	9.39	10.86	14.44	17.34	20.60	22.76	25.99	28.87	32.35	34.80	42.31
19	7.63	8.57	10.12	11.65	15.35	18.34	21.69	23.90	27.20	30.14	33.69	36.19	43.82
20	8.26	9.24	10.85	12.44	16.27	19.34	22.78	25.04	28.41	31.41	35.02	37.57	45.32
21	8.90	9.92	11.59	13.24	17.18	20.34	23.86	26.17	29.62	32.67	36.34	38.93	46.80
22	9.54	10.60	12.34	14.04	18.10	21.24	24.94	27.30	30.81	33.92	37.66	40.29	48.27
23	10.20	11.29	13.09	14.85	19.02	22.34	26.02	28.43	32.01	35.17	38.97	41.64	49.73
24	10.86	11.99	13.85	15.66	19.94	23.34	27.10	29.55	33.20	36.42	40.27	42.98	51.18
25	11.52	12.70	14.61	16.47	20.87	24.34	28.17	30.68	34.38	37.65	41.57	44.31	52.62
26	12.20	15.38	15.38	17.29	21.79	25.34	29.25	31.80	35.56	38.88	42.86	45.64	54.05
27	12.88	16.15	16.15	18.11	22.72	26.34	30.32	32.91	36.74	40.11	44.14	46.96	55.48
28	13.56	16.93	16.93	18.94	23.65	27.34	31.39	34.03	37.92	41.34	45.42	48.28	56.89
29	14.26	17.71	17.71	19.77	24.58	28.34	32.46	35.14	39.09	42.56	46.69	49.59	58.30
30	14.95	18.49	18.49	20.60	25.51	29.34	33.53	36.25	40.26	43.77	47.96	50.89	59.70

Table A2.7. Critical values of D, the Kolmogorov–Smirnov one-sample test

	Level of significance for $D = \max[F_0(X) - S_N(X)]$				
	0.200	0.150	0.100	0.050	0.010
$N = 1$	0.900	0.925	0.950	0.975	0.995
2	0.684	0.726	0.776	0.842	0.929
3	0.565	0.597	0.642	0.708	0.828
4	0.494	0.525	0.564	0.624	0.733
5	0.446	0.474	0.510	0.565	0.669
6	0.410	0.436	0.470	0.521	0.618
7	0.381	0.405	0.498	0.466	0.577
8	0.358	0.381	0.411	0.457	0.543
9	0.339	0.360	0.388	0.432	0.514
10	0.322	0.342	0.368	0.410	0.490
11	0.307	0.326	0.352	0.391	0.468
12	0.295	0.313	0.338	0.375	0.450
13	0.284	0.302	0.325	0.361	0.433
14	0.274	0.292	0.314	0.349	0.418
15	0.266	0.283	0.304	0.338	0.404
16	0.258	0.274	0.295	0.328	0.392
17	0.250	0.266	0.286	0.318	0.381
18	0.244	0.259	0.278	0.309	0.371
19	0.237	0.252	0.272	0.301	0.363
20	0.231	0.246	0.264	0.294	0.356
25	0.210	0.220	0.240	0.270	0.320
30	0.190	0.200	0.220	0.240	0.290
35	0.180	0.190	0.210	0.230	0.270
>35	$1.07/\sqrt{N}$	$1.14/\sqrt{N}$	$1.22/\sqrt{N}$	$1.36/\sqrt{N}$	$1.63/\sqrt{N}$

Table A2.8. Critical values of r in the one-sample runs test

$r \leq$ (smaller value) or $\geq$ (larger value) indicates significance at $\alpha = 0.05$

	$n=2$	3	4	5	6	7	8	9	10	11	12	13	14	15	16	17	18	19	20
$m=2$	–	–	–	–	–	–	–	–	–	–	2	2	2	2	2	2	2	2	2
	–	–	–	–	–	–	–	–	–	–	–	–	–	–	–	–	–	–	
3	–	–	–	–	2	2	2	2	2	2	2	2	2	3	3	3	3	3	3
	–	–	–	–	–	–	–	–	–	–	–	–	–	–	–	–	–	–	
4	–	–	–	2	2	2	3	3	3	3	3	3	3	3	4	4	4	4	4
	–	–	–	9	9	–	–	–	–	–	–	–	–	–	–	–	–	–	–
5	–	–	2	2	3	3	3	3	3	4	4	4	4	4	4	4	5	5	5
	–	–	9	10	10	11	11	–	–	–	–	–	–	–	–	–	–	–	–
6	–	2	2	3	3	3	3	4	4	4	4	5	5	5	5	5	5	6	6
	–	–	9	10	11	12	12	13	13	13	13	–	–	–	–	–	–	–	–
7	–	2	2	3	3	3	4	4	5	5	5	5	5	6	6	6	6	6	6
	–	–	–	11	12	13	13	14	14	14	14	15	15	15	–	–	–	–	–
8	–	2	3	3	3	4	4	5	5	5	6	6	6	6	6	7	7	7	7
	–	–	–	11	12	13	14	14	15	15	16	16	16	16	17	17	17	17	17
9	–	2	3	3	4	4	5	5	5	6	6	6	7	7	7	7	8	8	8
	–	–	–	–	13	14	14	15	16	16	16	17	17	18	18	18	18	18	18
10	–	2	3	3	4	5	5	5	6	6	7	7	7	7	8	8	8	8	9
	–	–	–	–	13	14	15	16	16	17	17	18	18	18	19	19	19	20	20
11	–	2	3	4	4	5	5	6	6	7	7	7	8	8	8	9	9	9	9
	–	–	–	–	13	14	15	16	17	17	18	19	19	19	20	20	20	21	21
12	2	2	3	4	4	5	6	6	7	7	7	8	8	8	9	9	9	10	10
	–	–	–	–	13	14	16	16	17	18	19	19	20	20	21	21	21	22	22
13	2	2	3	4	5	5	6	6	7	7	8	8	9	9	9	10	10	10	10
	–	–	–	–	–	15	16	17	18	19	19	20	20	21	21	22	22	23	23
14	2	2	3	4	5	5	6	7	7	8	8	9	9	9	10	10	10	11	11
	–	–	–	–	–	15	16	17	18	19	19	20	20	21	21	22	22	23	23
15	2	3	3	4	5	6	6	7	7	8	8	9	9	10	10	11	11	11	12
	–	–	–	–	–	15	16	18	18	19	20	21	22	22	23	23	24	24	25
16	2	3	4	4	5	6	6	7	8	8	9	9	10	10	11	11	11	12	12
	–	–	–	–	–	–	17	18	19	20	21	21	22	23	23	24	25	25	25
17	2	3	4	4	5	6	7	7	8	9	9	10	10	11	11	11	12	12	13
	–	–	–	–	–	–	17	18	19	20	21	22	23	23	24	25	25	26	26
18	2	3	4	5	5	6	7	8	8	9	9	10	10	11	11	12	12	13	13
	–	–	–	–	–	–	17	18	19	20	21	22	23	24	25	25	26	26	27
19	2	3	4	5	6	6	7	8	8	9	10	10	11	11	12	12	13	13	13
	–	–	–	–	–	–	17	18	20	21	22	23	23	24	25	25	26	26	27
20	2	3	4	5	6	6	7	8	9	9	10	10	11	12	12	13	13	13	14
	–	–	–	–	–	–	17	18	20	21	22	23	24	25	25	26	27	27	28

Table A2.9. Lower- and upper-tail probabilities for U, the Wilcoxon–Mann–Whitney rank-sum statistic

Entries are $P(U < c_l)$ and $P(U > c_u)$. U is the rank sum for the smaller group.

$m = 3$

c_l	$n = 3$	c_u	$n = 4$	c_u	$n = 5$	C_u	$n = 6$	c_u	$n = 7$	c_u	$n = 8$	c_u	$n = 9$	c_u	$n = 10$	c_u
6	0.0500	15	0.0286	18	0.0179	21	0.0119	24	0.0083	27	0.0061	30	0.0045	33	0.0035	36
7	0.1000	14	0.0571	17	0.0357	20	0.0238	23	0.0167	26	0.0121	29	0.0091	32	0.0070	35
8	0.2000	13	0.1143	16	0.0714	19	0.0476	22	0.0333	25	0.0242	28	0.0182	31	0.0140	34
9	0.3500	12	0.2000	15	0.1250	18	0.0833	21	0.0583	24	0.0424	27	0.0318	30	0.0245	33
10	0.5000	11	0.3143	14	0.1964	17	0.1310	20	0.0917	23	0.0667	26	0.0500	29	0.0385	32
11	0.6500	10	0.4286	13	0.2857	16	0.1905	19	0.1333	22	0.0970	25	0.0727	28	0.0559	31
12	0.8000	9	0.5714	12	0.3929	15	0.2738	18	0.1917	21	0.1394	24	0.1045	27	0.0804	30
13	0.9000	8	0.6857	11	0.5000	14	0.3571	17	0.2583	20	0.1879	23	0.1409	26	0.1084	29
14	0.9500	7	0.8000	10	0.6071	13	0.4524	16	0.3333	19	0.2485	22	0.1864	25	0.1434	28
15	1.0000	6	0.8857	9	0.7143	12	0.5476	15	0.4167	18	0.3152	21	0.2409	24	0.1853	27
16	–	–	0.9429	8	0.8036	11	0.6429	14	0.5000	17	0.3879	20	0.3000	23	0.2343	26
17	–	–	0.9714	7	0.8750	10	0.7262	13	0.5833	16	0.4606	19	0.3636	22	0.2867	25
18	–	–	1.0000	6	0.9286	9	0.8095	12	0.6667	15	0.5394	18	0.4318	21	0.3462	24
19	–	–	–	–	0.9643	8	0.8690	11	0.7417	14	0.6121	17	0.5000	20	0.4056	23
20	–	–	–	–	0.9821	7	0.9167	10	0.8083	13	0.6848	16	0.8682	19	0.4685	22
21	–	–	–	–	1.0000	6	0.9524	9	0.8667	12	01515	15	0.6364	18	0.5315	21
22	–	–	–	–	–	–	0.9762	8	0.9083	11	0.8121	14	0.7000	17	0.5944	20
23	–	–	–	–	–	–	0.9881	7	0.9417	10	0.8606	13	0.7591	16	0.6538	19
24	–	–	–	–	–	–	1.0000	6	0.9667	9	0.9030	12	0.8136	15	0.7133	18

$m = 4$

c_l	$n = 4$	c_u	$n = 5$	C_u	$n = 6$	c_u	$n = 7$	c_u	$n = 8$	c_u	$n = 9$	c_u	$n = 10$	c_u
10	0.0143	26	0.0079	30	0.0048	34	0.0030	38	0.0020	42	0.0014	46	0.0010	50
11	0.0286	25	0.O159	29	0.0095	33	0.0061	37	0.0040	41	0.0028	45	0.0020	49
12	0.0571	24	0.0317	28	0.0190	32	0.0121	36	0.0081	40	0.0056	44	0.0040	48
13	0.1000	23	0.0556	27	0.0333	31	0.0212	35	0.0141	39	0.0098	43	0.0070	47
14	0.1714	22	0.0952	26	0.0571	30	0.0364	34	0.0242	38	0.0168	42	0.0120	46
15	0.2429	21	0.1429	25	0.0857	29	0.0545	33	0.0364	37	0.0252	41	0.0180	45
16	0.3429	20	0.2063	24	0.1286	28	0.0818	32	0.0545	36	0.0378	40	0.0270	44
17	0.4429	19	0.2778	23	0.1762	27	0.1152	31	0.0768	35	0.0531	39	0.0380	43
18	0.5571	18	0.3651	22	0.2381	26	0.1576	30	0.1071	34	0.0741	38	0.0529	42
19	0.6571	17	0.4524	21	0.3048	25	0.2061	29	0.1414	33	0.0993	37	0.0709	41
20	0.7571	16	0.5476	20	0.3810	24	0.2636	28	0.1838	32	0.1301	36	0.0939	40
21	0.8286	15	0.6349	19	0.4571	23	0.3242	27	0.2303	31	0.1650	35	0.1199	39
22	0.9000	14	0.7222	18	0.5429	22	0.3939	26	0.2848	30	0.2070	34	0.1518	38
23	0.9429	13	0.7937	17	0.6190	21	0.4636	25	0.3414	29	0.2517	33	0.1868	37
24	0.9714	12	0.8571	16	0.6952	20	0.5364	24	0.4040	28	0.3021	32	0.2268	36
25	0.9857	11	0.9048	15	0.7619	19	0.6061	23	0.4667	27	0.3552	31	0.2697	35

Table A2.10. Kolmogorov–Smirnov two-sample test

Critical values for one-tailed rejection region $mnD_{m,n} \geq c$.
The upper, middle and lower values are $c_{0.10}$, $c_{0.05}$ and $c_{0.01}$ for each (m, n)

m =	3	4	5	6	7	8	9	10	11	12	13	14	15	16	17	18	19	20
n = 3	9	10	11	15	15	16	21	19	22	24	25	26	30	30	32	36	36	37
	9	10	13	15	16	19	21	22	25	27	28	31	33	34	35	39	40	41
	**	**	**	**	19	22	27	28	31	33	34	37	42	43	43	48	49	52
4	10	16	13	16	18	24	21	24	26	32	29	32	34	40	37	40	41	48
	10	16	16	18	21	24	25	28	29	36	33	38	38	44	44	46	49	52
	**	**	17	22	25	32	29	34	37	40	41	46	46	52	53	56	57	64
5	11	13	20	19	21	23	26	30	30	32	35	37	45	41	44	46	47	55
	13	16	20	21	24	26	28	35	35	36	40	42	50	46	49	51	56	60
	**	17	25	26	29	33	36	40	41	46	48	51	60	56	61	63	67	75
6	15	16	19	24	24	26	30	32	33	42	37	42	45	48	49	54	54	56
	15	18	21	30	25	30	33	36	38	48	43	48	51	54	56	66	61	66
	**	22	26	36	31	38	42	44	49	54	54	60	63	66	68	78	77	80
7	15	18	21	24	35	28	32	34	38	40	44	49	48	51	54	56	59	61
	16	21	24	25	35	34	36	40	43	45	50	56	56	58	61	64	68	72
	19	25	29	31	42	42	46	50	53	57	59	70	70	71	75	81	85	87
8	16	24	23	26	28	40	33	40	41	48	47	50	52	64	57	62	64	72
	19	24	26	30	34	40	40	44	48	52	53	58	60	72	65	72	73	80
	22	32	33	38	42	48	49	56	59	64	66	72	75	88	81	88	91	100
9	21	21	26	30	32	33	45	43	45	51	51	54	60	61	65	72	70	73
	21	25	28	33	36	40	54	46	51	57	57	63	69	68	74	81	80	83
	27	29	36	42	46	49	63	61	62	69	73	77	84	86	92	99	99	103
10	19	24	30	32	34	40	43	50	48	52	55	60	65	66	69	72	74	90
	22	28	35	36	40	44	46	60	57	60	62	68	75	76	77	82	85	100
	28	34	40	44	50	56	61	70	69	74	78	84	90	94	97	104	104	120
11	22	26	30	33	38	41	45	48	66	54	59	63	66	69	72	76	79	84
	25	29	35	38	43	48	51	57	66	64	67	72	76	80	83	87	92	95
	31	37	41	49	53	59	62	69	88	77	85	89	95	100	104	108	114	117
12	24	32	32	42	40	48	51	52	54	72	61	68	72	76	77	84	85	92
	27	36	36	48	45	52	57	60	64	72	71	78	84	88	89	96	98	104
	33	40	46	54	57	64	69	74	77	96	92	94	102	108	111	120	121	128
13	25	29	35	37	44	47	51	55	59	61	78	72	75	79	81	87	89	95
	28	33	40	43	50	53	57	62	67	71	91	78	86	90	94	98	102	108
	34	41	48	54	59	66	73	78	85	92	104	102	106	112	118	121	127	135
14	26	32	37	42	49	50	54	60	63	68	72	84	80	84	87	92	94	100
	31	38	42	48	56	58	63	68	72	78	78	98	92	96	99	104	108	114
	37	46	51	60	70	72	77	84	89	94	102	112	111	120	124	130	135	142
15	30	34	45	45	48	52	60	65	66	72	75	80	90	87	91	99	100	110
	33	38	50	51	56	60	69	75	76	84	86	92	105	101	105	111	113	125
	42	46	60	63	70	75	84	90	95	102	106	111	135	120	130	138	142	150

** Statistic cannot achieve this significance level.

Table A2.11. Kolmogorov–Smirnov two-sample test

Critical values for two-tailed rejection region $mnD_{m,n} \geq c$.
The upper, middle and lower values are $c_{0.10}$, $c_{0.05}$ and $c_{0.01}$ for each (m, n)

$m =$	2	3	4	5	6	7	8	9	10	11	12	13	14	15	16	17	18	19	20
$n = 1$	–	–	–	–	–	–	–	–	–	–	–	–	–	–	–	–	–	19	20
2	–	–	–	10	12	14	16	18	18	20	22	24	24	26	28	30	32	32	34
	–	–	–	–	–	–	16	18	20	22	24	26	26	28	30	32	34	36	38
	–	–	–	–	–	–	–	–	–	–	–	–	–	–	–	–	–	38	40
3	–	9	12	15	15	18	21	21	24	27	27	30	33	33	36	36	39	42	42
	–	–	–	15	18	21	21	24	27	30	30	33	36	36	39	42	45	45	48
	–	–	–	–	–	–	–	27	30	33	36	39	42	42	45	48	51	54	57
4	–	12	16	16	18	21	24	27	28	29	36	35	38	40	44	44	46	49	52
	–	–	16	20	20	24	28	28	30	33	36	39	42	44	48	48	50	53	60
	–	–	–	–	24	28	32	36	36	40	44	48	48	52	56	60	60	64	68
5	10	15	16	20	24	25	27	30	35	35	36	40	42	50	48	50	52	56	60
	–	15	20	25	24	28	30	35	40	39	43	45	46	55	54	55	60	61	65
	–	–	–	25	30	35	35	40	45	45	50	52	56	60	64	68	70	71	80
6	12	15	18	24	30	28	30	33	36	38	48	46	48	51	54	56	66	64	66
	–	18	20	24	30	30	34	39	40	43	48	52	54	57	60	62	72	70	72
	–	–	24	30	36	36	40	45	48	54	60	60	64	69	70	73	84	83	88
7	14	18	21	25	28	38	34	36	40	44	46	50	56	56	59	61	65	69	72
	–	21	24	28	30	42	40	42	46	48	53	56	63	62	64	68	70	76	79
	–	–	28	35	36	42	48	49	53	59	60	65	77	75	77	84	87	91	93
8	16	21	24	27	30	34	40	40	44	48	52	54	58	60	72	68	72	74	80
	16	21	28	30	34	40	48	46	48	53	60	62	64	67	80	77	80	82	88
	–	–	32	35	40	48	56	55	60	64	68	72	76	81	88	88	94	98	104
9	18	21	27	30	33	36	40	54	5o	52	57	59	63	69	69	74	81	80	84
	18	24	28	35	39	42	46	54	53	59	63	65	70	75	78	82	92	89	93
	–	27	36	40	45	49	55	63	63	70	75	78	84	90	94	99	108	107	111
10	18	24	28	35	36	40	44	50	60	57	60	64	68	75	76	79	82	85	100
	20	27	30	40	40	46	48	53	70	60	66	70	74	80	84	89	92	94	110
	–	30	36	45	48	53	60	63	80	77	80	84	90	100	100	106	108	113	130
11	20	27	29	35	38	44	48	52	57	66	64	67	73	76	80	85	88	92	96
	22	30	33	39	43	48	53	59	60	77	72	75	8	84	89	93	97	102	107
	–	33	40	45	54	59	64	70	77	88	86	91	96	102	106	110	118	122	127
12	22	27	36	36	48	46	52	57	60	64	72	71	78	84	88	90	96	99	104
	24	30	36	43	48	53	60	63	66	72	84	81	86	93	96	100	108	108	116
	–	36	44	50	60	60	68	75	80	86	96	95	104	108	116	119	126	130	140
13	24	30	35	40	46	50	54	59	64	67	71	91	78	87	91	96	99	104	108
	26	33	39	45	52	56	62	65	70	75	81	91	89	96	101	105	110	114	120
	–	39	48	52	60	65	72	78	84	91	95	117	104	115	121	127	131	138	143
14	24	33	38	42	48	56	58	63	68	73	78	78	98	92	96	100	104	110	114
	26	36	42	46	54	63	64	70	74	82	86	89	112	98	106	111	116	121	126
	–	47	48	56	64	77	76	84	90	96	104	104	126	123	126	134	140	148	152
15	26	33	40	50	51	56	60	69	75	76	84	87	92	105	101	105	111	114	125
	28	36	44	55	57	62	67	75	80	84	93	96	98	120	114	116	123	127	135
	–	42	52	60	69	75	81	90	100	102	108	115	123	135	133	142	147	152	160

Table A2.12. Critical values of D for the Kolmogorov–Smirnov two-sample test: large samples, two-tailed

Level of significance	Value of D so large as to require rejection of H_0 at the indicated significance, where $D = \max[S_m(X) - S_n(X)]$
0.100	$1.22\sqrt{\frac{m+n}{mn}}$
0.050	$1.36\sqrt{\frac{m+n}{mn}}$
0.025	$1.48\sqrt{\frac{m+n}{mn}}$
0.010	$1.63\sqrt{\frac{m+n}{mn}}$
0.005	$1.73\sqrt{\frac{m+n}{mn}}$
0.001	$1.95\sqrt{\frac{m+n}{mn}}$

Table A2.13. Critical values of R in the Rayleigh test

Percentiles of the resultant length R in samples of size n from the uniform distribution on the sphere; H_0 is rejected at significance level α for the values tabulated (Fisher, Lewis & Embleton 1987).

n	$\alpha = 10\%$	5%	2%	1%
4	2.85	3.10	3.35	3.49
5	3.19	3.50	3.83	4.02
6	3.50	3.85	4.24	4.48
7	3.78	4.18	4.61	4.89
8	4.05	4.48	4.96	5.26
9	4.30	4.76	5.28	5.61
10	4.54	5.03	5.58	5.94
11	4.76	5.28	5.87	6.25
12	4.97	5.52	6.14	6.55
13	5.18	5.75	6.40	6.83
14	5.38	5.98	6.65	7.10
15	5.57	6.19	6.90	7.37
16	5.75	6.40	7.13	7.62
17	5.93	6.60	7.36	7.86
18	6.10	6.79	7.58	8.10
19	6.27	6.98	7.79	8.33
20	6.44	7.17	8.00	8.55
21	6.60	7.35	8.20	8.77
22	6.75	7.52	8.40	8.99
23	6.90	7.69	8.59	9.19
24	7.05	7.86	8.78	9.40
25	7.20	8.02	8.96	9.60

Table A2.14. The eigenvalue test; critical values of E_3

Percentiles of E_3 for a uniform distribution on the sphere; H_0 is rejected at significance level α for the values tabulated (Fisher, Lewis & Embleton 1987).

n	$\alpha = 10.0\%$	5.0%	2.5%	1.0%
5	0.714	0.751	0.784	0.821
6	0.678	0.712	0.743	0.779
7	0.651	0.685	0.712	0.746
8	0.630	0.662	0.687	0.718
9	0.610	0.641	0.667	0.694
10	0.590	0.625	0.650	0.677
12	0.574	0.598	0.621	0.648
14	0.554	0.578	0.599	0.623
16	0.538	0.559	0.581	0.604
18	0.525	0.544	0.566	0.587
20	0.515	0.535	0.553	0.575
25	0.496	0.512	0.530	0.550
30	0.479	0.495	0.510	0.528
40	0.459	0.473	0.487	0.501
50	0.447	0.460	0.471	0.484
60	0.438	0.449	0.458	0.470
70	0.429	0.438	0.448	0.461
80	0.423	0.432	0.441	0.452
100	0.413	0.422	0.430	0.440

Table A2.15. The eigenvalue test; critical values of S

Percentiles of S for a uniform distribution on the sphere; H_0 is rejected at significance level α for the values tabulated (Fisher, Lewis & Embleton 1987).

n	$\alpha = 10.0\%$	5.0%	2.5%	1.0%	0.5%
3	0.569	0.639	0.697	0.761	0.801
4	0.534	0.594	0.641	0.703	0.740
5	0.512	0.565	0.611	0.663	0.697
6	0.495	0.544	0.585	0.633	0.665
7	0.483	0.527	0.566	0.610	0.640
8	0.472	0.514	0.550	0.592	0.620
9	0.464	0.503	0.537	0.577	0.603
10	0.457	0.494	0.526	0.564	0.589
12	0.446	0.480	0.509	0.543	0.566
14	0.438	0.468	0.495	0.527	0.548
16	0.431	0.459	0.485	0.514	0.534
18	0.425	0.452	0.476	0.503	0.522
20	0.420	0.446	0.468	0.494	0.512
25	0.411	0.434	0.454	0.477	0.493
30	0.404	0.425	0.443	0.464	0.479
35	0.399	0.418	0.435	0.454	0.467
40	0.394	0.412	0.428	0.446	0.459
45	0.391	0.408	0.422	0.440	0.451
50	0.388	0.404	0.418	0.434	0.445
60	0.383	0.398	0.410	0.425	0.435
70	0.379	0.393	0.404	0.418	0.427
80	0.376	0.389	0.400	0.412	0.421
90	0.374	0.386	0.396	0.408	0.416
100	0.372	0.383	0.393	0.404	0.412

References

Akritas, M. G. & Siebert, J., 1996, *Mon. Not. R. Astr. Soc.*, 278, 919
Andrews L. C., 1985, *Special Functions for Engineers and Applied Mathematicians.* MacMillan
Anscombe F. J., 1973, *The American Statistician*, 27, 17
Avni Y., 1976, *Astrophys. J.*, 210, 642
1978, *Astron. Astrophys.*, 66, 307
Avni Y., Soltan A., Tananbaum H. & Zamorani G., 1980, *Astrophys. J.*, 238, 800
Babu G. J. & Feigelson E. D., 1992, *Comm. Stat. Comp. Simul.*, 22, 533
1996, *Astrostatistics.* Chapman & Hall
Barlow R. J., 1989, *A Guide to the Use of Statistical Methods.* Wiley
Barrow J. D., Bhavsar S. P. & Sonada D. H., 1985, *Mon. Not. R. Astr. Soc.*, 216, 17
Bendat J. S. & Piersol A. G., 1971, *Measurement and Analysis of Random Data.* Wiley
Bevington P. R. & Robinson D. K., 2002, *Data Reduction and Error Analysis for the Physical Sciences*, 3rd Ed. McGraw-Hill
Bhavsar S. 1990, In *Errors, Bias and Uncertainties in Astronomy*, eds. Jaschek, C, and Murtagh, F., Cambridge University Press p. 107
Birnbaum Z. W. & Tingey F. H., 1951, *Ann. Math. Statistics*, 22, 592
Blake C. & Wall J., 2002a, *Mon. Not. R. Astr. Soc.*, 329, L37
2002b, *Nature*, 416, 150
2002c, *Mon. Not. R. Astr. Soc.*, 337, 993
Blake C., 2002, D.Phil. thesis, University of Oxford
Bogart R. S. & Wagoner R. V., 1973, *Astrophys. J.*, 181, 609
Bracewell R. N., 1986, *The Hartley Transform.* Oxford University Press
Bracewell R. N., 1999, *The Fourier Transform and its Applications*, 3rd ed. McGraw-Hill
Bruce A., Donoho D. & Gao H.-Y., 1996, *IEEE Spectrum*, October, 26
Carlin B. P. & Louis T. A., 2000, *Bayes and Empirical Bayes Methods for Data Analysis.* Chapman & Hall
Casella G. & Berger R. L., 2002, *Statistical Inference*, 2nd Ed. Duxbury Press
Chib, S., and Greenberg, E., 1995. *Am Statistician*, 49, 327
Chołoniewski J., 1987, *Mon. Not. R. Astr. Soc.*, 226, 273

Cline D. & Lesser P. M. S., 1970, *Nuclear Inst. and Methods*, 82, 291
Cochran W. G., 1952, *Ann. Math. Statistics*, 23, 315
Coles P. & Frenk C. S., 1991, *Mon. Not. R. Astr. Soc.*, 253, 727
Condon J. J., 1974, *Astrophys. J.*, 188, 279
Conover W. J., 1999, *Practical Nonparametric Statistics*, 3rd Ed. Wiley
Cooley O. W. & Tukey J. W., 1965, *Math. Comput.*, 19, 297
Cox R. T., 1946, *Amer. J. Phys.*, 14, 1
Cress C. M., Helfand D. J., Becker R. H., Gregg M. D. & White R. L., 1996, *Astrophys. J.*, 473, 7
Daubechies I., 1992, *Ten Lectures on Wavelets*. SIAM Press
Davis M. & Peebles P. J. E., 1983, *Astrophys. J.*, 267, 465
Davison A. C. & Hinkley D. V., 1997, *Bootstrap Methods and their Applications*. Cambridge University Press
De Jager O. C., Swanepoel J. W. H. & Raubenheimer B. C., 1989, *Astron. Astrophys.*, 221, 180
Dekel A. & West M. J., 1985, *Astrophys. J.*, 288, 11
Diaconis P. & Efron B., 1983, *Sci. Am.*, 100, 96
Disney M. J., Sparks W. B. & Wall J. V., 1984, *Mon. Not. R. Astr. Soc.*, 206, 899
Disney, M. J. & Wall, J. V., 1977, *Mon. Not. R. Astron. Soc.*, 179, 235
Dixon, R. S. & Kraus J. D., 1968, *Astron. J.*, 73, 381
Dunlop J. S. & Peacock J., 1990, *Mon. Not. R. Astr. Soc.*, 247, 19
Edmunds M. G. & George G. H., 1985, *Mon. Not. R. Astr. Soc.*, 213, 905
Efron B., 1979, *Ann. Statistics*, 7, 1
Efron B., Tibshirani R., 1986, *Stat. Sci.*, 1, 54
1993, *An Introduction to the Bootstrap*. Chapman & Hall
Efstathiou G. & Moody S. J., 2001, *Mon. Not. R. Astr. Soc.*, 325, 1603
Einasto J. & Saar E., 1987, In *Observational Cosmology*, Proc IAU Symp. 124. Reidel p. 349
Evans, M. and Swartz, T. B., 1995, *Statistical Sci.* 10, 245
Feigelson E. D. & Babu G. J., 1992a, *Statistical Challenges in Modern Astronomy*. Springer-Verlag
Feigelson E. D. & Babu G. J., 1992b, *Astrophys. J.*, 397, 55
Feigelson E. D. & Nelson P. I., 1985, *Astrophys. J.*, 293, 192
Fisher N. I., Lewis T. & Embleton B. J. J., 1987, *Statistical Analysis of Spherical Data*. Cambridge University Press
Fisher R. A., 1944, *Statistical Methods for Research Workers*. Oliver & Boyd
Folkes S., *et al.*, 1999, *Mon. Not. R. Astr. Soc.*, 308, 459
Francis P. J. & Wills B. J., 1999, In ASP Conf. Ser. 162: *Quasars and Cosmology*. p. 363
Francis P. J., Hewett P. C., Foltz C. B. & Chaffee F. H., 1992, *Astrophys. J.*, 398, 476
Frank H. & Altheon S. C., 1994, *Statistics: Concepts and Applications*. Cambridge University Press
Freedman D., Pisani R., Purves R. & Adhikari A., 1995, *Statistics*, 2nd Ed. Norton
Galton F., 1889, *Natural Inheritance*. MacMillan
Gaskill J. D., 1978, *Linear Systems, Fourier Transforms and Optics*. Wiley
Goodman L. A., 1954, *Psychol. Bull.*, 51, 160
Gott J. R., *et al.*, 1989, *Astrophys. J.*, 340, 625

Gull S. F. & Fielden J. 1986, In *Maximum Entropy and Bayesian Methods in Applied Statistics*, ed. Justice, J.H., Cambridge University Press
Haigh J., 1999, *Taking Chances.* Oxford
Hald A., 1990, *A History of Probability and Statistics and their Applications before 1750.* Wiley
Hald A., 1998, *A History of Mathematical Statistics from 1750 to 1930.* Wiley
Hamilton A. J. S., 1993, *Astrophys. J.*, 417, 19
Hauser M. G. & Peebles P. J. E., 1973, *Astrophys. J.*, 185, 757
Hewish A., Bell S. J., Pilkington J. D. H., Scott P. F. & Collins R. A., 1968, *Nature*, 217, 709
Hobson M. P. & McLachlan C., 2003, *Mon. Not. R. Astr. Soc.*, 338, 765
Hobson M. P., Bridle S. L. & Lahav O., 2002, *Mon. Not. R. Astr. Soc.*, 335, 377
Hogg R. V. & Tanis E. A., 1993, *Probability and Statistical Inference*, 4th Ed. MacMillan
Horne J. H. & Baliunas S. L., 1986, *Astrophys. J.*, 302, 757
Hoyle F., 1958, *The Black Cloud.* Cambridge University Press
Hubble E., 1936, *The Realm of the Nebulae.* Yale University Press
Huff D., 1973, *How to Lie with Statistics.* Penguin
Huterer D., Knox L. & Nichol R., 2001, *Astrophys. J.*, 555, 547
Isobe T., Feigelson E. D. & Nelson P. I., 1986, *Astrophys. J.*, 306, 490
Isobe T., Feigelson E. D. & Akritas M. J., Babu G. J., 1990, *Astrophys. J.*, 364, 104
James J. F., 1995, *A Student's Guide to Fourier Transforms.* Cambridge University Press
Jaschek C. & Murtagh F., 1990, *Errors, Bias and Uncertainties in Astronomy.* Cambridge University Press
Jauncey D. L., 1967, *Nature*, 216, 877
Jaynes E. T., 1983, *Papers on Probability Theory, Statistics and Statistical Physics*, ed. Rosenkrantz, R. D. ESO Garching
Jaynes E. T., 1986, In *Maximum Entropy and Bayesian Methods in Applied Statistics.* Cambridge University Press
Jaynes E. T., 2003, *Probability Theory: the Logic of Science.* Cambridge University Press
Jeffreys H., 1961, *Theory of Probability.* Clarendon Press
Jenkins C. R., 1987, *Mon. Not. R. Astr. Soc.*, 226, 341
1989, *The Observatory*, 109, 69
Jenkins C. R. & Reid I. N., 1991, *Astron. J.*, 101, 1595
Joliffe I. T., 2002, *Principal Component Analysis*, 2nd Ed. Springer-Verlag
Kalbfleish J. D. & Prentice R. L., 2002, *The Statistical Analysis of Failure Time Data*, 2nd Ed. Wiley
Kanji G. K., 1993, *100 Statistical Tests.* Sage
Kendall M. G., 1980, *Multivariate Analysis*, 2nd Ed. Charles Griffin & Co.
Kennicut R., 1992, *Astrophys. J. Suppl.*, 79, 255
Koornwinder T. H., 1993, *Wavelets: An Elementary Treatment in Theory and Applications.* World Scientific
Laing, R. A., Jenkins, C. R., Wall, J. V. and Unger, S. W., 1994. In *The Physics of Active Galaxies*, ASP Conf. Ser., eds. G. V. Bicknell, M. A. Dopita, and P. J. Quinn, Vol. 54, p. 201

Landy S. D. & Szalay A. S., 1993, *Astrophys. J.*, 412, 64
Lange A. E., *et al.*, 2001, *Phys. Rev. D.*, 63, 042001
Lee P. M., 1997, *Bayesian Statistics: an Introduction*, 2nd Ed. Arnold
LePage R. & Billiard L., 1993, *Exploring the Limits of the Bootstrap.* Wiley
Linnik Y. V., 1961, *Methods of Least-Squares and Principles of the Theory of Observations.* Pergammon Press
Lomb N. R., 1976, *Astrophys. Space Sci.*, 39, 447
Lynden-Bell D., 1971, *Mon. Not. R. Astr. Soc.*, 155, 95
Lyons L., 1986, *Statistics for Nuclear and Particle Physicists.* Cambridge University Press
1991, *A Practical Guide to Data Analysis for Physical Science Students.* Cambridge University Press
Lyons R. G., 1997, *Understanding Digital Signal Processing.* Addison Wesley
Macklin J. T., 1982, *Mon. Not. R. Astr. Soc.*, 199, 1119
Magliocchetti M., Maddox S. J., Lahav O. & Wall J. V., 1998, *Mon. Not. R. Astr. Soc.*, 300, 257
Manly B. J. F., 1994, *Multivariate Statistical Methods – A Primer*, 2nd Ed. Chapman & Hall
Marshall H. L., Avni Y., Tananbaum H. & Zamorani G., 1983, *Astrophys. J.*, 269, 35
Martin B. R., 1971, *Statistics for Physicists.* Academic Press
Martínez V. J., Jones B. J. T., Dominguez-Tenreiro R. & van de Weygaert R., 1990, *Astrophys. J.*, 357, 50
Masson C. R. & Wall J. V., 1977, *Mon. Not. R. Astr. Soc.*, 180, 193
Maxted, P. F. L., Hill, G. and Hilditch, R. W., 1994, *Astron. Astrophys*, 282, 821
Mittaz J. P. D., Penston M. V. & Snijders M. A. J., 1990, *Mon. Not. R. Astr. Soc.*, 242, 370
Montgomery D. C. & Peck E. A., 1992, *Introduction to Linear Regression Analysis*, 2nd Ed. Wiley
Mood A. M., Graybill F. A. & Boes D. B., 1974, *Introduction to the Theory of Statistics*, 3rd Ed. McGraw-Hill
Moroney M. J., 1965, *Facts from Figures.* Penguin
Murray C. A., 1983, *Vectorial Astrometry.* Adam Hilger
Newman W. I., Haynes M. P. & Terzian Y., 1992, In *Statistical Challenges in Modern Astronomy*, eds. Feigelson, E. D. and Babu, G. J. Springer-Verlag, p. 137
Neyman J., Scott E. L. & Shane C. D., 1953, *Astrophys. J.*, 117, 92
O'Hagan A., 1994, *Kendall's Advanced Theory of Statistics*, Volume 2b: Bayesian Inference. Arnold
O'Ruanaidh, J. J. K. and Fitzgerald, W. J., 1996, *Numerical Bayesian Methods Applied to Signal Processing*, Springer
Papoulis A. & Unnikrishna Pillai S., 2002, *Probability, Random Variables and Stochastic Processes*, 4th Ed. McGraw-Hill
Peacock J. A., 1983, *Mon. Not. R. Astr. Soc.*, 202, 615
1985, *Mon. Not. R. Astr. Soc.*, 217, 601
1999, *Cosmological Physics.* Cambridge University Press
Pearson K., 1900, *Phil. Mag. Series 5*, 50, 157
Peebles P. J. E., 1973, *Astrophys. J.*, 185, 413
1980, *The Large-Scale Structure of the Universe.* Princeton University Press

Peebles P. J. E. & Groth E. J., 1975, *Astrophys. J.*, 196, 1
Peebles P. J. E. & Hauser M. G., 1974, *Astrophys. J. Suppl.*, 28, 19
Phillips M. M., Jenkins C. R., Dopita M. A., Sadler E. M. & Binette L., 1986, *Astron. J.*, 91, 1062
Press W. H., Teukolsky S. A., Vetterling W. T. & Flannery B. P., 1992, *Numerical Recipes: the Art of Scientific Computing*, 2nd Ed. Cambridge University Press
Press W. H., 1978, *Comments Astrophys.*, 7, 103
Reinking J. T., 2002, *The Mathematica Journal*, 8, 473
Rice J. R., 1995, *Mathematical Statistics and Data Analysis*. Duxbury Press
Rolfe E., 1983, *Statistical Methods in Astronomy*. ESA Scientific and Technical Publications
Rowan-Robinson M., 1968, *Mon. Not. R. Astr. Soc.*, 138, 445
Rowntree D., 1981, *Statistics Without Tears*. Penguin
Sadler E. M., Jenkins C. R. & Kotanyi C. G., 1989, *Mon. Not. R. Astr. Soc.*, 240, 591
Saha P., 1995, *Astron. J.*, 110, 916
Sandage A., 1972, *Astrophys. J.*, 178, 25
Sargent W. L. W., Schechter P. L., Boksenberg A. & Shortridge K., 1977, *Astrophys. J.*, 212, 326
Saslaw W. C., 2000, *The Distribution of the Galaxies: Gravitational Clustering in Cosmology*. Cambridge University Press
Scargle J. D., 1982, *Astrophys. J.*, 263, 835
Scheuer P. A. G., 1957, *Proc. Cambridge Phil. Soc.*, 53, 764
1974, *Mon. Not. R. Astr. Soc.*, 166, 329
1991, In *Modern Cosmology in Retrospect*, eds Bertotti, B. *et al.* Cambridge University Press, p. 331
Schmidt M., 1968, *Astrophys. J.*, 151, 393
Schmitt J. H. M. M., 1985, *Astrophys. J.*, 293, 178
Shane C. D. & Wirtanen C. A., 1954, *Astron. J.*, 59, 285
Shannon C. E., 1949, *Proc. IRE*, 37, 10
Siegel S. & Castellan N. J., 1988, *Nonparametric Statistics for the Behavioural Sciences*. McGraw-Hill
Sivia D. S., 1996, *Data Analysis: a Bayesian Tutorial*. Oxford University Press
Sivia D. S. & Carlile C. J., 1992, *J. Chem. Phys.*, 96, 170
Sprent P., 1977, *Statistics in Action*. Penguin
Strang G., 1994, *Amer. Scientist*, 82, 250
Stuart A. & Ord J. K., 1991, *Kendall's Advanced Theory of Statistics*, Volume 2a: Classical Inference and Relationship, 5th Ed. Arnold
Stuart A. & Ord J. K., 1994, *Kendall's Advanced Theory of Statistics*, Volume 1: Distribution Theory, 6th Ed. Arnold
Szapudi I., 1998, *Astrophys. J.*, 497, 16
Tegmark M., *et al.*, 2002, *Astrophys. J.*, 571, 191
Thompson A. R., Moran J. M. & Swenson, Jr. G. W., 2001, *Interferometry and Synthesis in Radio Astronomy*. Wiley
Tonry J. & Davis M., 1979, *Astron. J.*, 84, 1511
Tufte E. R., 1983, *The Visual Display of Quantitative Information*. Graphics Press
1990, *Envisaging Information*. Graphics Press

Turler M. & Courvoisier T. J.-L., 1998, *Astron. Astrophys.*, 329, 863
Utts J. M., 1996, *Seeing through Statistics.* Duxbury Press
Walker J. S., 1999, *A Primer on Wavelets and their Scientific Applications.* Chapman & Hall
Wall J. V., 1997, *Astron. Astrophys.*, 122, 371
Wall J. V. & Cooke D. J., 1975, *Mon. Not. R. Astr. Soc.*, 171, 9
Wall J. V., Rixon G. T. & Benn C. R. 1993, In *Observational Cosmology*, eds. Chincarini, G. *et al.* ASP Conf. Ser., Vol. 51, p. 576
Wall J. V., Scheuer P. A. G., Pauliny-Toth I. I. K. & Witzel A., 1982, *Mon. Not. R. Astr. Soc.*, 198, 221
Webb J. K., Barcons X., Carswell R. F. & Parnell H. C., 1992, *Mon. Not. R. Astr. Soc.*, 255, 319
Webster A. S., 1976, *Mon. Not. R. Astr. Soc.*, 175, 61
Weiss N. A., 1995, *Introductory Statistics*, 4th Ed. Addison Wesley
Wilkinson J. H. 1978, In *Numerical Software – Needs and Availability*, ed. Jacobs, D. A. H. Academic Press
Williams E. J., 1959, *Regression Analysis.* Wiley
Willmer C. N. A., 1997, *Astron. J.*, 114, 898
Wills B. J., *et al.*, 1997, In *Emission Lines in Active Galaxies: New Methods and Techniques*, Proc IAU Colloq. 159. ASP Conf. Ser, Vol. 113, p. 104
Windhorst R. A., Fomalont E. B., Partridge R. B. & Lowenthal J. D., 1993, *Astrophys. J.*, 405, 498
Wittaker E. T., 1915, *Proc. Roy. Soc. Edinburgh A.*, 35
Yu J. T. & Peebles P. J. E., 1969, *Astrophys. J.*, 158, 103
Zeldovich Y. B., Einasto J. & Shandarin S. F., 1982, *Nature*, 300, 407

Index